# ANTI-CANCER DRUG DISPOSITION

*In vitro* and *in vivo* functions of

ABC efflux and OATP uptake transporters

ISBN/EAN: 978-94-6182-469-1

Layout, cover and printing: Off Page, Amsterdam,
www.offpage.nl

The research described in this thesis was performed at the Divisions of Molecular Biology and Molecular Oncology of the Netherlands Cancer Institute, Amsterdam, The Netherlands.

Printing of this thesis was financially supported by Netherlands Cancer Institute and Boehringer Ingelheim BV.

# Anti-cancer drug disposition:

## *In vitro* and *in vivo* functions of ABC efflux and OATP uptake transporters

Dispositie van anti-kankermiddelen:

*In vitro* en *in vivo* functies van ABC efflux en OATP opname transporters

(met een samenvatting in het Nederlands)

**Proefschrift**

ter verkrijging van de graad van doctor aan de Universiteit Utrecht op gezag van de rector magnificus, prof.dr. G.J. van der Zwaan, ingevolge het besluit van het college voor promoties in het openbaar te verdedigen op vrijdag 5 september 2014 des middags te 2.30 uur

door

*Selvi Durmus Erim*

geboren op *6 september 1985 te Ankara, Turkey*

Promotor: Prof.dr. J.H. Beijnen

Copromotor: Dr. A.H. Schinkel

"Bad times have a scientific value. These are occasions a good learner would not miss."

*Ralph Waldo Emerson*

Aileme,

To my family,

## TABLE OF CONTENTS

# CHAPTER 1

## INTRODUCTION

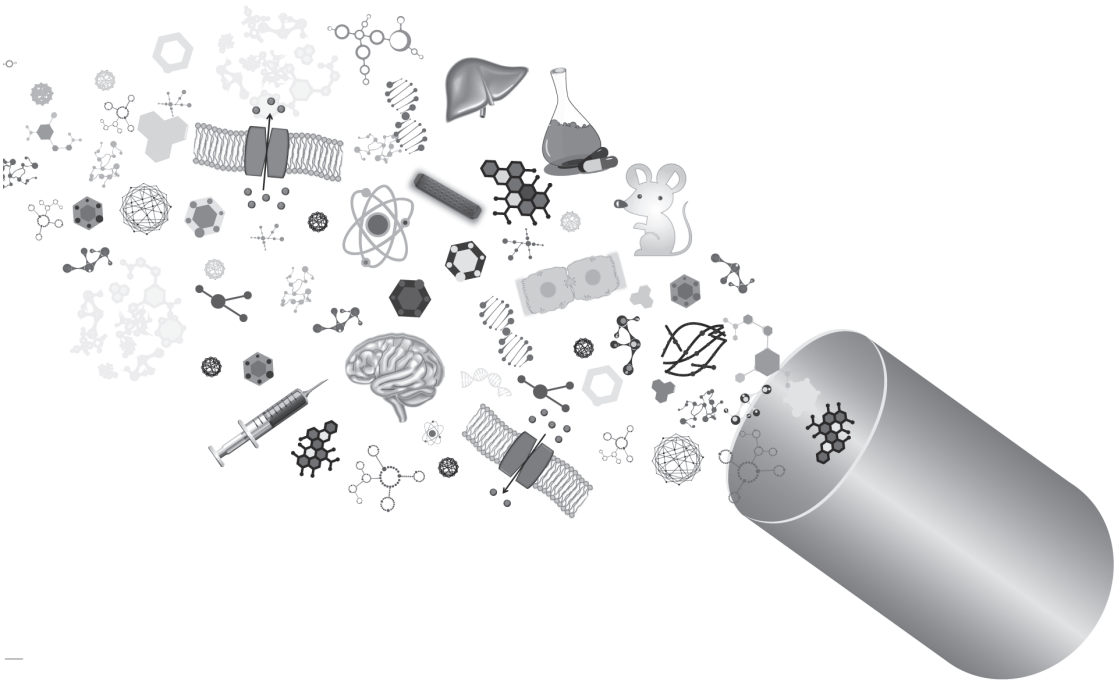

# CHAPTER 1.1

## APICAL ABC TRANSPORTERS AND CANCER: CHEMOTHERAPEUTIC DRUG DISPOSITION

S. Durmus[a], Jeroen J.M.A. Hendrikx[b], Alfred H. Schinkel[a]

[a] Division of Molecular Oncology, The Netherlands Cancer Institute, Plesmanlaan 121, 1066 CX Amsterdam, The Netherlands.
[b] Department of Pharmacy & Pharmacology, The Netherlands Cancer Institute/ Slotervaart Hospital Louwesweg 6, 1066 EC Amsterdam, The Netherlands.

*To be submitted in modified form to Advances in Cancer Research*

## ABSTRACT

ATP-binding cassette (ABC) transporters are transmembrane efflux transporters that mediate cellular extrusion of a broad range of substrates ranging from amino acids, lipids, and ions to xenobiotics including many anti-cancer drugs. ABCB1 (P-GP) and ABCG2 (BCRP) are the most extensively studied ABC drug efflux transporters. They are widely expressed in apical membranes of pharmacokinetically relevant tissues such as epithelial cells of the small intestine and endothelial cells of the brain. In these tissues, they have a protective function as they efflux their substrates back to the intestinal lumen and the blood and thus restrict the intestinal uptake and brain disposition of many compounds. This presents a major challenge for the use of many (anti-cancer) drugs, as the majority of anti-cancer drugs was found to be substrates of these transporters. Here, we review the latest findings on the role of ABC transporters in the disposition of anti-cancer drugs. We show that many new anti-cancer drugs, especially targeted drugs that have been recently developed, are substrates of these transporters and that their oral availability and/or brain disposition are affected by this interaction. We also summarize studies that investigate the improvement of oral availability and brain disposition of many cytotoxic (e.g. taxanes) and targeted (e.g. tyrosine kinase inhibitor) anti-cancer drugs by chemical inhibition of these transporters. These findings provide a better understanding of the importance of ABC transporters in chemotherapy and may therefore bring more relevant translation possibilities to clinical studies closer by.

## INTRODUCTION TO ABC TRANSPORTERS

ATP-binding cassette (ABC) transporters are active multispanning transmembrane proteins that are widely expressed in a broad range of membranes of tissues. Forming one of the largest protein families, these proteins are highly preserved across living organisms with different complexity, from bacteria to humans, indicating their essential functionality [1]. ABC transporters utilize the energy of ATP hydrolysis to translocate a broad range of endogenous and exogenous substrates across the membranes, often against a strong concentration gradient. Typical substrates include amino acids, lipids, sterols, bile salts, peptides, nucleotides, ions, toxins and (anti-cancer) drugs in man and rodents [2]. A detailed background on the ABC transporters was presented recently by Klaassen *et al.* [2]. In the present review, we will focus on three members of the ABC superfamily, ABCB1 (P-GP, MDR1), ABCC2 (MRP2) and ABCG2 (BCRP) that are potentially important in the pharmacokinetics of a wide range of substrate drugs, including chemotherapeutics.

ABCB1, ABCC2, and ABCG2 are the most extensively studied apical ABC transporters in relation to chemotherapeutic drug disposition. They are localized at the apical membranes of intestinal and renal proximal tubule epithelial cells and at the bile canalicular membranes of hepatocytes, where they efflux their substrates into intestinal lumen or feces, urine and bile to protect the organism (Figure 1) [2]. They are also expressed at the apical membranes of blood-brain, blood-testis and blood-placenta barriers, where they extrude endogenous or exogenous substrates, including drugs, carcinogens and toxins into the main circulation in order to protect those tissue sanctuaries (Figure 1) [2, 3]. Indeed, interactions of many chemotherapeutics with these ABC efflux transporters are known to affect their intestinal uptake (oral availability), hepatic and renal elimination, plasma exposure and tissue disposition [4]. Interestingly, there is a large overlap in the substrate specifities of these ABC transporters; therefore the absence or decreased activity of one of these transporters is often compensated by one or more other members. Consequently, it has at times been difficult to understand the contribution of each transporter in drug disposition [2, 5].

To experimentally study the *in vivo* impact of each ABC transporter on for example drug disposition, studies often made use of the single and combination transporter-deficient mouse models that have been generated in the last decades and could thus unravel interactions between these transporters and many drugs [5, 6]. In this review, we will focus on recent data showing interaction of chemotherapeutic drugs with ABC transporters and on how ABC transporters affect their pharmacokinetics such as oral availability and brain penetration.

In the clinic, several studies have assessed polymorphisms in the genes encoding ABC transporters and tried to correlate these with drug pharmacokinetics and sometimes with the outcomes of anti-cancer drug treatments. These studies are very useful to understand the clinical use of ABC transporters as predictive markers for therapy response [7, 8]; however, assessment of their role in anti-cancer disposition in the patients remains a challenge.

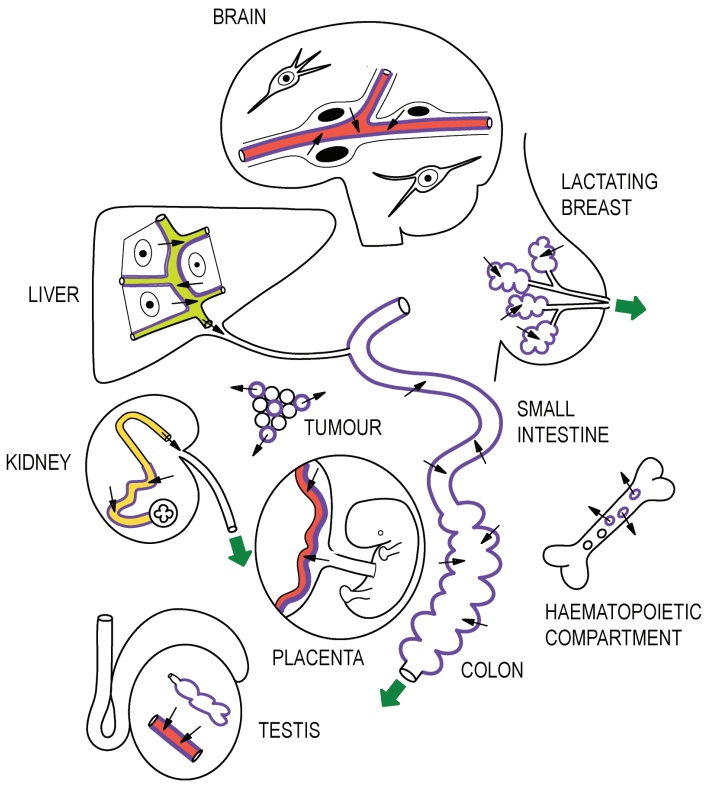


**Figure 1. Generalized overview of tissue expression of the human ATP-binding cassette (ABC) transporters ABCB1 (P-GP), ABCG2 (BCRP) and ABCC2 (MRP2).** Purple (or grey) bold lines indicate the functionally relevant locations of one or more of these transporters. Black arrows indicate the direction of transport of substrates at all expression sites. Wide arrows indicate net body excretion of the substrates of these transporters. For lactating breast, only the expression of ABCG2 has been demonstrated. For testis the situation in humans is depicted, where ABCB1, ABCG2 and ABCC2 are expressed at the blood-testis barrier. This figure was modified from van Herwaarden and Schinkel, Trends Pharmacol Sci. 2006 Jan; 27(1):10-6 and Vlaming et al., Adv Drug Deliv Rev. 2009 Jan 31; 61(1):14-25.

## IMPACT OF APICAL ABC TRANSPORTERS ON INTESTINAL ABSORPTION OF ORAL CHEMOTHERAPEUTIC DRUGS

Oral administration of drugs, including cancer chemotherapeutics, is strongly preferred for a number of reasons including convenience, safety and cost-effectiveness. However, the percentage of orally administered chemotherapeutic drugs still remains limited, which is often because of their poor bioavailability and high interindividual variation in exposure [9]. Several factors are known to contribute to the rate and extent of oral drug absorption including physiological conditions of the gastrointestinal tract (e.g. pH and emptying rate of gastrointestinal tract, activity of metabolic enzymes and food-drug and drug-drug interactions), physicochemical properties of the drug (e.g. molecular weight, structure, solubility and

lipophilicity) and formulation design [9, 10]. Other important players in bioavailability of orally administered drugs are the ABC and solute carrier (SLC) drug transporters and drug-metabolizing enzymes [11, 12]. Focusing on ABC transporters, there are two functional barriers at the gastrointestinal tract and liver that limit oral bioavailability of drugs, primarily via the apical ABC transporters ABCB1, ABCC2, and ABCG2 [13, 14]. These transporters can restrict the systemic availability of orally administered drugs and other xenotoxins such as the dietary phototoxin pheophorbide A and the dietary carcinogen 2-amino-1-methyl-6-phenylimidazo[4,5-b]pyridine (PhIP), by effluxing those substrates that are taken up into the enterocytes back into the lumen and mediating the excretion of drugs and their metabolites from the liver into the bile [15-18]. Increased bioavailability therefore can be obtained when ABC transporters are absent or inhibited, which has been experimentally shown for several drugs [9, 10]. In the intestine, absence of apical ABC transporter activity leads to increased net drug uptake by the intestinal cells and increased portal vein drug concentrations, leading to higher systemic levels eventually. In the liver, absence of apical ABC transporter activity might lead to increased hepatic tissue drug levels due to impaired biliary excretion [19] and/or mostly basolateral secretion of drugs and drug metabolites from hepatocytes into the systemic circulation [14]. In this section, we will focus on the most recent findings on the interaction of apical ABC transporters and chemotherapeutic drugs, with a special focus on taxanes and targeted anti-cancer drugs.

Since knockout mouse models lacking one or more ABC transporters have been generated, they have been widely used as tools to experimentally assess the contribution of ABC transporters to (limiting) oral availability of drug substrates [5, 6, 20-22]. Indeed, several studies have clearly shown the *in vivo* impact of apical ABC efflux transporters on the oral uptake of many anti-cancer drugs including cytotoxic drugs such as paclitaxel, docetaxel, topotecan and etoposide and new generation targeted anti-cancer drugs such as dasatinib [23-28]. A detailed list of drugs whose oral availability is affected by apical ABC transporters was presented by Lagas *et al.* [5], whereas a recent review by Tang *et al.* [6] addressed the impact of other transporters. Thus, we here focus on the most recent studies assessing the effect of apical ABC transporters on chemotherapeutic drug absorption.

**Apical ABC transporters in the oral bioavailability of taxanes**

The taxanes paclitaxel and docetaxel are routinely applied as intravenous (i.v.) formulations to treat several types of cancer, e.g. non-small cell lung cancer (NSCLC), breast, prostate, gastric and head and neck cancer [29, 30]. Although paclitaxel and docetaxel are effective as anticancer agents, their use is limited by side effects such as hypersensitivity reactions and peripheral neuropathy. Hypersensitivity reactions are related to pharmaceutical additives used in the i.v. formulations of paclitaxel and docetaxel (Cremophor EL and polysorbate 80, respectively) [31]. As a result, there has been increasing interest in the development of Cremophor EL- and polysorbate 80-free taxane formulations. One of the strategies considered is the development of an oral formulation. However, a major limitation in oral administration of taxanes is their limited oral biovailability, partly the result of a low aqueous solubility of the taxanes, but also of their handling by taxane-transporting and -metabolizing enzymes in the gastrointestinal tract and liver [32].

The most important ABC transporter involved in the limited bioavailability of orally administered taxanes is ABCB1 (Abcb1a in mice). The impact of Abcb1a on the intestinal uptake of paclitaxel was first studied in Abcb1a (Mdr1a) knockout mice [33]. Oral administration of paclitaxel (10 mg/kg) to these mice resulted in a 6-fold higher plasma $AUC_{0-8}$ than oral administration to wild-type mice. As a result of increased intestinal uptake, oral bioavailability of paclitaxel increased from 11.2% to 35.2% in the absence of Abcb1a. Similar results were observed in rats, were knockout of Mdr1a resulted in an 8.4-fold increase in plasma $AUC_{0-inf}$ after oral administration of 5 mg/kg paclitaxel [34]. Docetaxel is also a good substrate for Abcb1a, although Abcb1a-mediated transport is even more efficient for paclitaxel [35]. Similar to paclitaxel, after an oral dosage of 10 mg/kg docetaxel, oral bioavailability ($AUC_{oral}/AUC_{iv}$) was increased by 6.3-fold in Abcb1a/1b knockout mice compared to wild-type mice [35], whereas this increase was 2.8-fold in oral availability ($AUC_{oral}$) [36]. In contrast to early suggestions, Abcb1a/1b is usually not acting synergistically with Cyp3a to prevent docetaxel or paclitaxel reaching the systemic circulation, but rather additively [36, 37].

More recently, the role of the ABC transporter Abcc2 was studied for taxanes. Although *in vitro* experiments showed that docetaxel is a good substrate for both human and mouse ABCC2/Abcc2, van Waterschoot *et al*. [38] showed that complete gene knockout of Abcc2 in mice did not result in altered plasma exposure after oral or i.v. administration of docetaxel. For paclitaxel, the absence of Abcc2 resulted in a 1.3-fold increase in plasma $AUC_{0-8}$ after i.v. administration, but the plasma $AUC_{0-8}$ was not changed after oral administration [24]. In a Cyp3a- and Abcb1a/1b-deficient background, the loss of Abcc2 increased the AUC of docetaxel and paclitaxel after both oral and i.v. administration [24, 38]. Obviously, Cyp3a and Abcb1a/1b can mostly compensate for the loss of Abcc2, making its function of less importance for the oral bioavailability of taxanes. Moreover, intraperitoneal (i.p.) administration of paclitaxel in Cyp3a/Abcb1a/1b knockout mice resulted in a similar plasma $AUC_{0-inf}$ as oral administration [37]. Since i.p. administration circumvents the intestinal uptake step, these results indicate that taxane-transporting or -metabolizing enzymes other than Abcb1a/1b and Cyp3a are not that relevant in the intestinal uptake of paclitaxel. Most likely, therefore, the absence of hepatic Abcc2 - rather than intestinal Abcc2 - was primarily responsible for the increased paclitaxel AUC after oral administration in a Cyp3a- and Abcb1a/1b-deficient background.

Since Abcb1a/1b plays such a dominant role in the limited bioavailability of taxanes, Abcb1a/1b inhibition might result in increased plasma exposure to orally administered taxanes. For this concept of boosting taxanes, both chemically developed entities and substances derived from herbal extracts are studied in preclinical models. Herbal extracts such as curcumin, resveratrol, and silibinin are often used as Complementary and Alternative Medicines (CAMs) in cancer [39, 40]. Although their anticancer efficacy is not well established in randomized clinical trials, it is well known that herbal extracts can interfere with Abcb1a/1b activity [41, 42]. These extracts and their active substances are therefore often combined with orally administered taxanes in preclinical studies to inhibit (intestinal) Abcb1a/1b and to boost oral availability of taxanes. Oral bioavailability of paclitaxel in rats is around 3.1 - 3.5%, but reported to be increased by co-administration of Schisandrol B [43], naringin (up to 6.8%) [44] and flavones (up to 6.4%) [45]. Plasma exposure of paclitaxel in terms of AUC is also increased in rats after oral co-

administration with genistein [46], Biochanin A [47], 20(s)-Ginsenoside Rg3 [48], silymarin [49], and its main component silibinin [50]. Single oral co-administration of docetaxel with curcumin showed no effect on plasma exposure of docetaxel in rats, but pretreatment with curcumin for four consecutive days resulted in increased docetaxel absorption [51]. It was therefore suggested that curcumin decreased protein expression of Abcb1a/1b and Cyp3a.

For the development of oral formulations of taxanes, specially developed ABCB1 inhibitors and FDA-approved drugs were tested to boost availability of oral taxanes. Oral co-administration of paclitaxel and the immunosuppressive drug cyclosporine A increased biovailability of paclitaxel in mice from 9.3% up to 25.7% [52]. Indirect comparison with Abcb1a knockout mice showed that bioavailability of paclitaxel was lower when boosted with cyclosporin A than after complete gene knockout [33, 52]. The compounds valspodar and elacridar were specifically developed as ABCB1 inhibitors to decrease multidrug resistance. Co-administration of oral paclitaxel with valspodar resulted in a similar increase in bioavailability as co-administration with cyclosporine A [53]. However, oral co-administration with elacridar to mice increased oral bioavailability of paclitaxel from 8.5% to 40.2% [54]. This was a similar oral bioavailability as observed in Abcb1a/1b knockout mice in the same experiment. These experiments thus show that elacridar is an effective *in vivo* Abcb1a/1b inhibitor and results in almost complete uptake of paclitaxel from the intestinal tract. Cyclosporin A and valspodar are more modest inhibitors, resulting in lower uptake rates [55]. As with paclitaxel, oral co-administration of docetaxel and elacridar to mice expressing human CYP3A4 resulted in apparently complete intestinal Abcb1a/1b inhibition by elacridar and thus increased plasma exposure to docetaxel [56]. Elacridar boosting was not only studied in mice, but also in rats. Orally administered paclitaxel resulted in a bioavailability of 3.4%, while oral co-administration of paclitaxel and elacridar increased bioavailability to 41.3% and resulted in a 12.2-fold increase in $AUC_{0\text{-}24}$ [57]. The boosting effect of elacridar is much more pronounced compared to bioavailability after oral co-administration of paclitaxel with herbal extracts (~6-9%). Thus, oral co-administration of taxanes with the Abcb1a/1b inhibitor elacridar seems feasible to increase oral bioavailability of taxanes. But since brain penetration of intravenously administered taxanes is increased in mice after co-administration with orally administered elacridar, oral co-administration of taxanes and elacridar potentially increases brain penetration of the orally administered taxanes as well [58, 59]. This may result in an increase in the relative risk of CNS toxicity in clinical practice. Recently, we studied brain penetration of paclitaxel and docetaxel in mice after oral co-administration with elacridar and/or ritonavir, an inhibitor of Cyp3a, to examine wether it would be feasible and safe to substantially increase the oral availability of taxanes by simultaneous inhibition of ABCB1 and CYP3A [56]. Even at the highly increased plasma concentrations of taxanes after boosting with both elacridar and ritonavir, relative brain accumulation was still similar as seen after oral single administration of paclitaxel or docetaxel. It thus appears that oral taxane bioavailability can be boosted with ritonavir and elacridar, without compromising the protective action of ABCB1 in the blood-brain barrier (BBB) in helping the potentially neurotoxic taxanes out of the brain.

As shown above, safely boosting availability of orally administered taxanes with Abcb1a/1b inhibitors in mice is feasible. But also tumor efficacy of orally administered taxanes was evaluated

when co-administered with Abcb1a/1b inhibitors. Co-administration of paclitaxel and the Abcb1a/1b inhibitor dofequidar to mice showed that dofequidar increased paclitaxel absorption [60]. But in the same experiment, it was also shown that oral co-administration of paclitaxel (50 mg/kg or 100 mg/kg) and dofequidar resulted in comparable anti-tumor efficacy as single intravenously administered paclitaxel (20 mg/kg). Yang *et al.* [48] showed that antitumor efficacy of orally co-administered paclitaxel and 20(s)-Ginsenoside Rg3 against MCF-7 tumours in BALB/c mice was similar as intravenously administered paclitaxel at the same dose. Similar findings were observed when the antitumor efficacy of intravenously administered paclitaxel was compared to efficacy after oral co-administration of paclitaxel and elacridar [57]. However, since plasma and tumor concentrations of paclitaxel were not measured during these tumor growth experiments, it remains unclear if inhibition of Abcb1a/1b takes place only in intestinal tissue or also in tumor tissue. Further experimentation will be needed to resolve this matter.

**Role of apical ABC transporters in the oral bioavailability of targeted anti-cancer drugs**

In contrast to the traditional cytotoxic drugs, which usually work against all actively dividing cells, targeted anti-cancer drugs are designed to interfere with specific molecules involved in cancer cell growth and survival. These drugs are relatively new and could be developed due to our better understanding of genetics, the cell cycle and molecular signaling pathways. Targeted anti-cancer therapy aims to change the cancer treatment from general to specific target molecules. In principle, therefore the risk of damage to healthy cells is decreased and treatment success is generally increased. There are two groups of targeted anti-cancer drugs: small molecule and antibodies. As the latter are not directly affected by apical ABC transporters, we will not discuss those here.

Tyrosine kinase inhibitors (TKIs) are a class of small-molecule, targeted anti-cancer drugs that have been recently generated to inhibit or block activity of tyrosine kinase enzymes. These enzymes can phosphorylate many proteins in the cell and activate signal transduction cascades, triggering many cellular functions involving cell growth. Several TKIs have been developed to date, including imatinib and dasatinib (inhibit BCR-ABL), gefinitinib and erlotinib (inhibit EGFR), sunitinib (inhibits receptors for the FGF, PDGF and VEGF), vemurafenib (inhibits BRAF) and many others [61-63]. Many of these TKIs have been tested for their interactions with ABC transporters and a majority were proven to be transported substrates of ABC transporters including ABCB1 and ABCG2 [5, 64]. Making use of various *in vitro* and *in vivo* models, we have recently shown that several different TKIs, axitinib, vemurafenib and crizotinib, were transported substrates of Abcb1a/1b and/or Abcg2/ABCG2 and that their oral availability was limited by either Abcb1a/1b and/or Abcg2 [65-67]. For axitinib, an inhibitor of VEGF receptor, c-KIT and PDGF receptor, absence of Abcb1a/1b did not change oral availability, but absence of Abcg2 increased the systemic levels by 1.7-fold compared to wild-type mice, which means that oral uptake of axitinib is restricted by Abcg2, and not by Abcb1a/1b [65]. However, Abcb1a/1b and Abcg2 showed additive roles in limiting oral absorption of the TKI vemurafenib, a $BRAF^{V600E}$ inhibitor [66]. Absence of Abcb1a/1b increased the oral availability of vemurafenib by 1.6-fold, that of Abcg2 by 2.3-fold and that of both transporters by 6.6-fold compared to WT mice. On the other hand, oral availability of the ALK inhibitor crizotinib was about 2-fold increased in the

knockout mice for either Abcb1a/1b or Abcb1a/1b;Abcg2 at 5 mg/kg dose, but this difference disappeared at 50 mg/kg dose [67]. This indicates that oral uptake of crizotinib was restricted only by Abcb1a/1b and that this process was saturable. Using combination knockout mice, it was recently shown that the absence of Abcb1a/1b and Abcg2 together led to a ~2-fold increase in the plasma exposure of dabrafenib, another $BRAF^{V600E}$ inhibitor, suggesting that one or both of these transporters can restrict the oral absorption of this TKI as well [68].

Another class of targeted anti-cancer drugs are the pharmacological inhibitors of Poly (ADP-ribose) polymerase (PARP). PARP enzymes are important players in the single-strand break repair of DNA [69]. If these DNA breaks cannot be repaired, they lead to double-strand breaks, which can then still be repaired by homologous recombination. However, in cells that are deficient in homologous recombination such as in BRCA1- and BRCA2-mutated cancers, these DNA breaks lead to cell death, unless they are repaired. Inhibitors of PARP enzymes were developed to exploit this process in BRCA-mutated cancer cells with the idea that combination of two or more deficiencies in tumor cells, one genetic and one environmental (e.g., drug-induced), would become lethal for the tumor cells (so-called synthetic lethality) [70, 71]. There are a number of PARP inhibitors that are under clinical investigation for the treatment of mainly BRCA-mutated breast and ovarian cancers, but also lately for the treatment of other cancers defective in DNA damage repair pathways [72]; however, data about the interaction of PARP inhibitors with ABC transporters are limited to only few studies. Rottenberg *et al*. [73] found that expression of Abcb1a/1b in BRCA-1 deficient mouse mammary tumors caused resistance to olaparib (AZD2281) treatment in mice, which could be reversed by coadministration of the P-glycoprotein inhibitor tariquidar. In those tumor models, tumor-specific genetic deletion of Abcb1a/1b increased the long-term response to olaparib treatment [74]. In colon cancer cells, chemical inhibition of ABCB1 by verapamil increased the cellular toxicity after treatment with the PARP inhibitor KU 58948 [75]. The impact of ABC transporters on the general disposition of PARP inhibitors is even less studied. Oral absorption of the PARP inhibitor veliparib (ABT-888) was not affected by Abcb1a/1b and Abcg2 in mice. Nevertheless, inhibition of these transporters by elacridar improved temozolomide and veliparib combination treatment in a spontaneous glioblastoma model in mice [76]. Very recently, we have shown that oral absorption of rucaparib is restricted by Abcb1a/1b and Abcg2 in mice [77].

In several preclinical studies, chemical inhibition of ABC transporters has been shown to improve oral availability of (targeted) anti-cancer drugs. For instance, co-administration of the EGFR-inhibitor gefitinib has been shown to increase oral availability of the anti-cancer drug irinotecan via inhibition of ABCG2 and maybe also via inhibition of intestinal metabolism of irinotecan [78]. Abcb1a/1b and Abcg2 have also been shown to affect the bioavailability of imatinib moderately after their inhibition by elacridar [10]. The studies with vemurafenib and crizotinib showed that oral availability of both drugs could be increased in WT mice when elacridar was used [66, 67]. Very likely the information gained from these preclinical studies can be used for translation to the clinical use of inhibitors to improve the oral bioavailability of chemotherapeutic agents. Several clinical investigations have been conducted for this reason, some of which, but not all, have been promising. For example, the apparent bioavailability of oral topotecan could be increased from 40% to 97.1% when elacridar was coadministered to

patients, likely due to inhibition of ABCG2 restricting topotecan intestinal absorption and, probably to a lesser extent, inhibition of ABCG2-mediated systemic clearance [79]. It will be of interest to further extend such studies.

## IMPACT OF APICAL ABC TRANSPORTERS ON BRAIN DISPOSITION OF ORAL CHEMOTHERAPEUTIC DRUGS

Central nervous system (CNS) delivery of drugs is a major challenge in chemotherapy due to the presence of the blood-brain barrier (BBB). The BBB is formed by a layer of endothelial cells that separates brain and blood circulation, and protects the CNS from exposure to potentially toxic molecules, including drugs [80]. Thus, it is both important and difficult for chemotherapeutic agents to reach the CNS for the treatment of primary or metastatic brain tumors that are behind this protective barrier. On the other hand, when the targeted tumor is located in another organ, drug delivery to the CNS may not be desired because of the possible toxic side effects in brain. In order to achieve a properly targeted and successful therapy, we need to better understand the mechanisms of drug delivery to the CNS.

One of the discussion points on the protective function of the BBB during chemotherapy is its integrity in the presence of a brain tumor. One point of view is that integrity of the BBB is not complete when there is a tumor in the brain; thus any drug that is in the systemic circulation might be able to reach the tumor cells in the CNS without any barrier protection. This, of course, would lead to the idea that there is no point in targeting the protective mechanisms of the BBB for chemotherapy. However, recent studies indicate that in brains that harbor tumor(s), the integrity of BBB is not the same through the whole brain and tumor, but shows a heterogeneous pattern [81]. Usually, this barrier around the large tumor is disrupted; however there are nearly always substantial areas around and in the tumor where this barrier is intact and thus part of primary or metastatic tumors can be located behind it [81]. Chemotherapy is only effective if virtually all tumor cells can be hit. Even a partially intact BBB will severely compromise this aim. Therefore, optimal CNS delivery of chemotherapeutic drugs is still critical for eradication of those tumors and tumor parts that are located behind an intact BBB.

Several ABC transporters such as ABCB1 and ABCG2 are expressed at the apical (blood luminal) side of brain endothelial cells and proven important players in CNS protection [5, 22]. ABCB1 is one of the first ABC transporters found to be expressed at the BBB [82] and to restrict the CNS delivery of many substrate drugs using knockout mice [83]. ABCG2 is another prominent transporter expressed at the BBB [84, 85]. ABCB1 and ABCG2 are the main players at the BBB, where they usually work together to restrict the brain disposition of a wide range of chemotherapeutic drugs by extruding them back to the systemic circulation [15, 86]. Membrane transporter expression of Abcb1a at the mouse BBB was found to be approximately 5-fold higher compared than that of Abcg2 protein as assessed by mass spectrometry, whereas Abcb1b was undetectable [87, 88]; therefore Abcb1a often appears to dominate the efflux activity at the BBB of dual Abcb1a and Abcg2 substrates with similar affinities for both transporters. This has been confirmed for many anti-cancer drugs, with the exception of a few drugs that display a clearly more efficient transport by Abcg2 than by Abcb1a [15]. For example, Abcg2 is the major contributor to the brain efflux of sorafenib and Abcb1a can only to a limited extent take over

this efflux activity at the BBB as assessed in Abcg2 or Abcb1a/1b;Abcg2 knockout mice [5]. A few years ago, Agarwal *et al*. [15] extensively reviewed the literature on the individual and combined contribution of Abcb1a and Abcg2 to the brain disposition of many anti-cancer drugs including topotecan, mitoxantrone and several TKIs (dasatinib, gefitinib, imatinib, erlotinib, sorafenib, tandutinib and lapatinib), and the approaches that are taken to improve their brain delivery. Since then, more drugs, especially TKIs, whose brain disposition is restricted by Abcb1a/1b and/or Abcg2 have been added to this list.

For a few of those new drugs, the impact of Abcb1a was predominant in restricting the brain disposition, and the contribution of Abcg2 became only apparent when Abcb1 was absent. Tang *et al*. [89] showed that the brain accumulation of the TKI sunitinib was significantly increased in the absence of Abcb1a/1b, but not in the absence of Abcg2, whereas combination knockout mice lacking both Abcb1 and Abcg2 showed a further increase of brain accumulation of sunitinib by 10-fold compared to the Abcb1a/1b knockout mice. Similar results were found with another TKI, vemurafenib, where brain-to-plasma ratios of Abcb1a/1b, but not Abcg2 knockout mice, were significantly increased compared to WT mice [66]. Moreover, combinational deletion of both transporters led to a further increase in brain-to-plasma ratio of vemurafenib by ~12.5-fold compared to the Abcb1a/1b knockout mice. Interestingly, brain accumulation of the PARP inhibitor rucaparib was also restricted by both Abcb1a/1b and Abcg2, but the impact of Abcb1a/1b was somewhat higher than that of Abcg2 [77].

For a few other drugs, Abcb1a seems to be the only contributor to brain efflux at the BBB. Brain distribution of the TKI cediranib was found to be limited only by Abcb1a/1b, based on findings that there was no difference in brain AUC to plasma AUC of cediranib between Abcb1a/1b and Abcb1a/1b;Abcg2 knockout mice, whereas these were significantly higher than in WT and Abcg2 knockout mice [48]. Also, the brain disposition of another TKI, crizotinib, was substantially and similarly increased in Abcb1a/1b and Abcb1a/1b;Abcg2 knockout mice, whereas no effect was observed of deletion of Abcg2 alone [67]. Similar results were found with the mTOR inhibitor everolimus, where brain concentrations and brain-to-liver ratios were substantially increased in Abcb1a/1b and Abcb1a/1b;Abcg2 knockout, but not Abcg2 knockout mice [90].

Being one of only a few drugs, the JAK1/2 inhibitor CYT387 seems to be a slightly better substrate of Abcg2 than of Abcb1a at the BBB, as the brain accumulation of CYT387 was more substantially increased in the absence of Abcg2 than in the absence of Abcb1 [91]. Other studies showed that the brain dispositions of dabrafenib, of an active sunitinib metabolite, N-desethyl sunitinib, and of veliparib are effectively restricted by both Abcb1 and Abcg2 [68, 76, 92].

We note here that it is quite remarkable that the great majority of modern TKIs still turn out to be fairly good substrates of ABCB1 or ABCG2, or both. No doubt all major pharmaceutical companies currently screen their candidate drugs as potential ABCB1 and ABCG2 substrates, so they must be aware of these properties.

Being a good ABCB1 or ABCG2 substrate carries the risk of potentially low and variable oral availability, and especially limited penetration into sanctuary tissues such as brain and testis. This could limit therapeutic efficacy of these drugs against primary tumors or (micro-) metastases residing in part behind the blood-tissue barriers in these tissues. Also tumors that

are, or have become multi-drug resistant due to overexpression of ABCB1 and/or ABCG2 will be less sensitive to such drugs. We therefore assume that it is still extremely difficult for drug developers to design efficacious targeted drugs that are not at all transported by ABCB1 and ABCG2. However, we do note that there are recent examples of targeted drugs that are not substantially transported by ABCB1 and ABCG2 (e.g., the PI3K/mTOR inhibitor GNE-317) [93]. It is therefore in principle possible to obtain such compounds.

It is very common that for shared Abcb1 and Abcg2 substrates, there is often little or no detectable effect on brain accumulation upon single deletion of Abcb1a/1b or Abcg2 in mice, whereas a dramatic increase in the brain accumulation occurs upon combined deletion of these two transporters [28, 66, 94-98]. Some groups have proposed that this behavior might be perhaps caused by upregulation in the BBB of Abcb1a in Abcg2 knockout mice, and of Abcg2 in Abcb1a/1b knockout mice. However, Agarwal *et al*. [88] convincingly showed that this is not the case using mass spectrometric detection of the proteins. In fact, these seemingly counterintuitive findings can be explained by a simple pharmacokinetic model developed by Kodaira *et al*. [95]. This describes that the disproportionate effect on drug accumulation observed in the Abcb1a/1b;Abcg2 knockout mice can result from the sum of the separate contributions of each transporter to the net efflux at the BBB, without invoking the need for any direct or indirect interaction between Abcb1 and Abcg2. This model assumes that the intrinsic efflux transport activity of each of the transporters is considerably larger than the remaining (passive, or lowly active) efflux activity at the BBB in the absence of both transporters. There are more sophisticated pharmacokinetic models developed by Kalvass and Pollack [99] and Zamek-Gliszczynski *et al*. [100], which make similar predictions on transepithelial active transport. These models can also resolve complications as identified by Bentz *et al*. [101]. The concept of the various models is illustrated in Figure 2 in a highly simplified manner and we refer to the primary publications for further details.

Predictions by these theoretical models also indicate that halving the amount of active transporter-mediated drug efflux activity at the BBB, which could be due to decreased expression or activity inhibition, should result in only a minor increase of drug accumulation into the brain (never more than 2-fold), whereas there could be a disproportionate increase in the brain accumulation upon complete removal of the active transporter-mediated efflux. We have experimentally tested these models using heterozygous *Abcb1a/1b*(+/-);*Abcg2*(+/-) mice, which showed ~2-fold decreased expression of both Abcb1a and Abcg2 in the brain [66, 102]. In line with the predictions of the pharmacokinetic models, we found that brain accumulation of the TKIs vemurafenib, sunitinib, dasatinib and sorafenib were increased by 21.5- to 36-fold in the mice with complete knockout of the transporters, whereas they were increased only 1.3- to 1.9-fold in the heterozygous mice compared to wild-type strains [66, 102]. Our findings thus provide strong support for the validity of the pharmacokinetic models for a wider range of drugs. As other blood-tissue barriers, such as the blood-testis barrier and fetal-maternal placental barrier can be described with the same pharmacokinetic models, the same principles very likely apply there as well.

It should still be noted that the *in vivo* functional effect of ABC transporters can be context-dependent and that their apparent activity at different tissues may not always be the same.

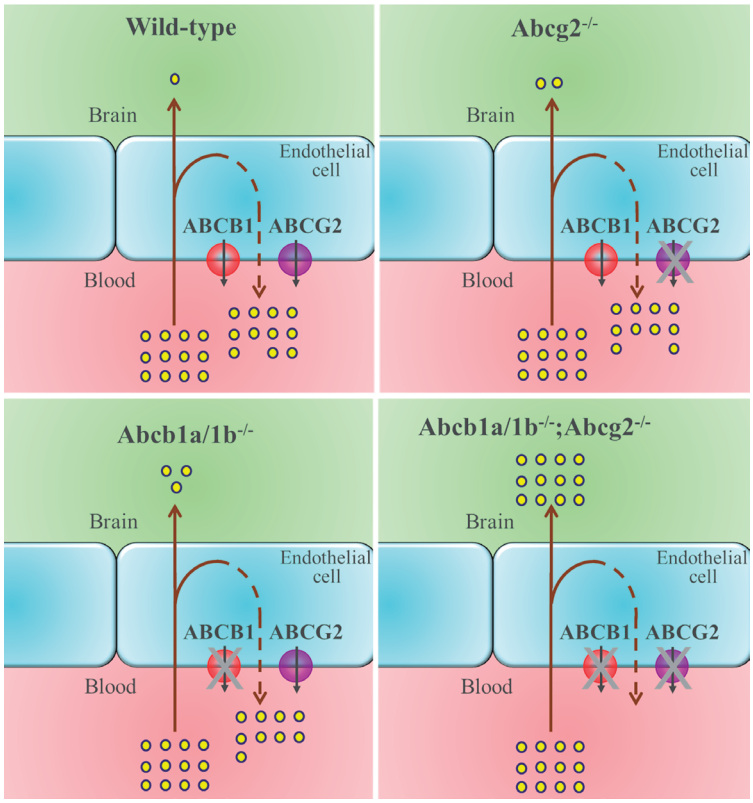


**Figure 2. Simplified illustration of the pharmacokinetic models for the disproportionate impact of complete removal of ABCB1 and ABCG2 at the BBB on brain accumulation of drugs.** ABCB1 and ABCG2, expressed at the apical membrane of brain endothelial cells, restrict the brain disposition of many substrate drugs by effluxing them out to the blood. Removal of either ABCB1 or ABCG2 does not lead to a major change in this restriction function at the BBB, as intrinsic efflux transport activity of the remaining single transporter is still substantially larger than the remaining (passive, or lowly active) efflux activity. However, complete removal of ABCB1 and ABCG2 at the BBB leads to a disproportionately large increase in the brain accumulation of the substrates, which is simply due to the separate contributions of each transporter being large relative to the net passive efflux activity at the BBB.

For example, Abcb1a/1b and/or Abcg2 may not noticeably restrict the oral absorption of their substrate drugs at the intestinal barrier, whereas the same transporters can drastically limit brain disposition of the same drug substrates. To illustrate this, the systemic exposures of the orally administered TKIs sunitinib and CYT387 were not changed in the absence of Abcb1a/1b and/or Abcg2, but their brain dispositions were markedly increased [89, 91]. It may be that the overall uptake capacity of the small intestine is far higher than that of the BBB, which makes it much harder for Abcb1a and Abcg2 to make a noticeable impact in the gut.

Pharmacological inhibition of ABCB1 and ABG2 at the BBB has been successfully tried by several studies aiming to improve the brain distribution of many substrate drugs. These include

several TKIs such as sunitinib, N-desethyl sunitinib, vemurafenib and crizotinib, and the PARP inhibitor veliparib, whose brain penetrations were improved mostly to the knockout levels by administration of elacridar [66, 67, 76, 89, 92]. Together with older findings reviewed by Agarwal *et al*. [15], these studies further confirmed that the use of elacridar in preclinical studies can significantly increase the brain penetration of anti-cancer drugs that are dual ABCB1 and ABCG2 substrates, often to levels equivalent to those in Abcb1a/1b;Abcg2 knockout mice. Nowadays, several groups consider applying this principle also in clinical trials in humans.

## CONCLUDING REMARKS

Recent studies demonstrating the interactions between apical ABC transporters and many new anti-cancer drugs have further confirmed their importance in cancer chemotherapy. ABC transporters, expressed in many tissues, certainly have key roles in the disposition of a broad range of anti-cancer drugs to the plasma (oral availability) and tissues (especially brain), and thus are important players in clinical efficacy. ABCB1 and ABCG2 have been shown to restrict the oral availability and brain accumulation of many new anti-cancer drugs, especially TKIs and PARP inhibitors, which underpins the idea of using pharmacological inhibition of these transporters to further improve efficacy of these drugs. Elacridar is widely used in preclinical studies as a dual inhibitor of these transporters and has been shown to improve oral availability and/or brain disposition of several of those substrate drugs. Moreover, it has been safely used in several clinical trials to treat multidrug resistant tumors. Yet, the feasibility and efficacy of applying this principle in the clinic remains to be investigated properly.

## REFERENCE LIST

1. Glavinas H, Krajcsi P, Cserepes J, Sarkadi B. The role of ABC transporters in drug resistance, metabolism and toxicity. Curr Drug Deliv 2004;1:27-42.
2. Klaassen CD, Aleksunes LM. Xenobiotic, bile acid, and cholesterol transporters: function and regulation. Pharmacol Rev 2010;62:1-96.
3. Borst P, Elferink RO. Mammalian ABC transporters in health and disease. Annu Rev Biochem 2002;71:537-92.
4. Szakacs G, Varadi A, Ozvegy-Laczka C, Sarkadi B. The role of ABC transporters in drug absorption, distribution, metabolism, excretion and toxicity (ADME-Tox). Drug Discov Today 2008;13:379-93.
5. Lagas JS, Vlaming ML, Schinkel AH. Pharmacokinetic assessment of multiple ATP-binding cassette transporters: the power of combination knockout mice. Mol Interv 2009;9:136-45.
6. Tang SC, Hendrikx JJ, Beijnen JH, Schinkel AH. Genetically modified mouse models for oral drug absorption and disposition. Curr Opin Pharmacol 2013;13:853-8.
7. Pander J, Guchelaar HJ, Gelderblom H. Pharmacogenetics of small-molecule tyrosine kinase inhibitors: Optimizing the magic bullet. Curr Opin Mol Ther 2010;12:654-61.
8. Erdem L, Giovannetti E, Leon LG, Honeywell R, Peters GJ. Polymorphisms to predict outcome to the tyrosine kinase inhibitors gefitinib, erlotinib, sorafenib and sunitinib. Curr Top Med Chem 2012;12:1649-59.
9. Oostendorp RL, Beijnen JH, Schellens JH. The biological and clinical role of drug transporters at the intestinal barrier. Cancer Treat Rev 2009;35:137-47.
10. Oostendorp RL, Buckle T, Beijnen JH, van TO, Schellens JH. The effect of P-gp (Mdr1a/1b), BCRP (Bcrp1) and P-gp/BCRP inhibitors on the in vivo absorption, distribution, metabolism and excretion of imatinib. Invest New Drugs 2009;27:31-40.
11. Giacomini KM, Huang SM, Tweedie DJ, *et al*. Membrane transporters in drug development. Nat Rev Drug Discov 2010;9:215-36.
12. Suzuki H, Sugiyama Y. Role of metabolic enzymes and efflux transporters in the absorption of

drugs from the small intestine. Eur J Pharm Sci 2000;12:3-12.

13. Misaka S, Muller F, Fromm MF. Clinical relevance of drug efflux pumps in the gut. Curr Opin Pharmacol 2013;13:847-52.
14. Dietrich CG, Geier A, Oude Elferink RP. ABC of oral bioavailability: transporters as gatekeepers in the gut. Gut 2003;52:1788-95.
15. Agarwal S, Hartz AM, Elmquist WF, Bauer B. Breast cancer resistance protein and P-glycoprotein in brain cancer: two gatekeepers team up. Curr Pharm Des 2011;17:2793-802.
16. Jonker JW, Buitelaar M, Wagenaar E, *et al*. The breast cancer resistance protein protects against a major chlorophyll-derived dietary phototoxin and protoporphyria. Proc Natl Acad Sci U S A 2002;99:15649-54.
17. Dietrich CG, de Waart DR, Ottenhoff R, Schoots IG, Elferink RP. Increased bioavailability of the food-derived carcinogen 2-amino-1-methyl-6-phenylimidazo[4,5-b]pyridine in MRP2-deficient rats. Mol Pharmacol 2001;59:974-80.
18. Vlaming ML, Teunissen SF, van de Steeg E, *et al*. Bcrp1;Mdr1a/b;Mrp2 combination knockout mice: altered disposition of the dietary carcinogen PhIP (2-amino-1-methyl-6-phenylimidazo[4,5-b]pyridine) and its genotoxic metabolites. Mol Pharmacol 2014;85:520-30.
19. Watanabe T, Kusuhara H, Maeda K, Shitara Y, Sugiyama Y. Physiologically based pharmacokinetic modeling to predict transporter-mediated clearance and distribution of pravastatin in humans. J Pharmacol Exp Ther 2009;328:652-62.
20. Schinkel AH, Mol CA, Wagenaar E, van DL, Smit JJ, Borst P. Multidrug resistance and the role of P-glycoprotein knockout mice. Eur J Cancer 1995;31A:1295-8.
21. van Herwaarden AE, Schinkel AH. The function of breast cancer resistance protein in epithelial barriers, stem cells and milk secretion of drugs and xenotoxins. Trends Pharmacol Sci 2006;27:10-6.
22. Vlaming ML, Lagas JS, Schinkel AH. Physiological and pharmacological roles of ABCG2 (BCRP): recent findings in Abcg2 knockout mice. Adv Drug Deliv Rev 2009;61:14-25.
23. Sparreboom A, van TO, Nooijen WJ, Beijnen JH. Preclinical pharmacokinetics of paclitaxel and docetaxel. Anticancer Drugs 1998;9:1-17.
24. Lagas JS, Vlaming ML, van TO, *et al*. Multidrug resistance protein 2 is an important determinant of paclitaxel pharmacokinetics. Clin Cancer Res 2006;12:6125-32.
25. Jonker JW, Smit JW, Brinkhuis RF, *et al*. Role of breast cancer resistance protein in the bioavailability and fetal penetration of topotecan. J Natl Cancer Inst 2000;92:1651-6.
26. Allen JD, Van Dort SC, Buitelaar M, van TO, Schinkel AH. Mouse breast cancer resistance protein (Bcrp1/Abcg2) mediates etoposide resistance and transport, but etoposide oral availability is limited primarily by P-glycoprotein. Cancer Res 2003;63:1339-44.
27. Lagas JS, Fan L, Wagenaar E, *et al*. P-glycoprotein (P-gp/Abcb1), Abcc2, and Abcc3 determine the pharmacokinetics of etoposide. Clin Cancer Res 2010;16:130-40.
28. Lagas JS, van Waterschoot RA, van Tilburg VA, *et al*. Brain accumulation of dasatinib is restricted by P-glycoprotein (ABCB1) and breast cancer resistance protein (ABCG2) and can be enhanced by elacridar treatment. Clin Cancer Res 2009;15:2344-51.
29. Gligorov J, Lotz JP. Preclinical pharmacology of the taxanes: implications of the differences. Oncologist 2004;9 Suppl 2:3-8.
30. Schellens JH, Malingre MM, Kruijtzer CM, *et al*. Modulation of oral bioavailability of anticancer drugs: from mouse to man. Eur J Pharm Sci 2000;12:103-10.
31. Ten Tije AJ, Verweij J, Loos WJ, Sparreboom A. Pharmacological effects of formulation vehicles: implications for cancer chemotherapy. Clin Pharmacokinet 2003;42:665-85.
32. Stuurman FE, Nuijen B, Beijnen JH, Schellens JH. Oral anticancer drugs: mechanisms of low bioavailability and strategies for improvement. Clin Pharmacokinet 2013;52:399-414.
33. Sparreboom A, van AJ, Mayer U, *et al*. Limited oral bioavailability and active epithelial excretion of paclitaxel (Taxol) caused by P-glycoprotein in the intestine. Proc Natl Acad Sci U S A 1997;94:2031-5.
34. Zamek-Gliszczynski MJ, Bedwell DW, Bao JQ, Higgins JW. Characterization of SAGE Mdr1a (P-gp), Bcrp, and Mrp2 knockout rats using loperamide, paclitaxel, sulfasalazine, and carboxydichlorofluorescein pharmacokinetics. Drug Metab Dispos 2012;40:1825-33.
35. Bardelmeijer HA, Ouwehand M, Buckle T, *et al*. Low systemic exposure of oral docetaxel in mice resulting from extensive first-pass metabolism is boosted by ritonavir. Cancer Res 2002;62:6158-64.
36. van Waterschoot RA, Lagas JS, Wagenaar E, *et al*. Absence of both cytochrome P450 3A and P-glycoprotein dramatically increases docetaxel oral bioavailability and risk of intestinal toxicity. Cancer Res 2009;69:8996-9002.

37. Hendrikx JJ, Lagas JS, Rosing H, Schellens JH, Beijnen JH, Schinkel AH. P-glycoprotein and cytochrome P450 3A act together in restricting the oral bioavailability of paclitaxel. Int J Cancer 2013;132:2439-47.
38. van Waterschoot RA, Lagas JS, Wagenaar E, Rosing H, Beijnen JH, Schinkel AH. Individual and combined roles of CYP3A, P-glycoprotein (MDR1/ABCB1) and MRP2 (ABCC2) in the pharmacokinetics of docetaxel. Int J Cancer 2010;127:2959-64.
39. Klempner SJ, Bubley G. Complementary and alternative medicines in prostate cancer: from bench to bedside? Oncologist 2012;17:830-7.
40. Philippou Y, Hadjipavlou M, Khan S, Rane A. Complementary and alternative medicine (CAM) in prostate and bladder cancer. BJU Int 2013;112:1073-9.
41. Kumar YS, Adukondalu D, Sathish D, *et al*. P-Glycoprotein- and cytochrome P-450-mediated herbal drug interactions. Drug Metabol Drug Interact 2010;25:3-16.
42. Li Y, Paxton JW. The effects of flavonoids on the ABC transporters: consequences for the pharmacokinetics of substrate drugs. Expert Opin Drug Metab Toxicol 2013;9:267-85.
43. Jin J, Bi H, Hu J, *et al*. Enhancement of oral bioavailability of paclitaxel after oral administration of Schisandrol B in rats. Biopharm Drug Dispos 2010;31:264-8.
44. Choi JS, Shin SC. Enhanced paclitaxel bioavailability after oral coadministration of paclitaxel prodrug with naringin to rats. Int J Pharm 2005;292:149-56.
45. Choi JS, Choi HK, Shin SC. Enhanced bioavailability of paclitaxel after oral coadministration with flavone in rats. Int J Pharm 2004;275:165-70.
46. Li X, Choi JS. Effect of genistein on the pharmacokinetics of paclitaxel administered orally or intravenously in rats. Int J Pharm 2007;337:188-93.
47. Peng SX, Ritchie DM, Cousineau M, Danser E, Dewire R, Floden J. Altered oral bioavailability and pharmacokinetics of P-glycoprotein substrates by coadministration of biochanin A. J Pharm Sci 2006;95:1984-93.
48. Yang LQ, Wang B, Gan H, *et al*. Enhanced oral bioavailability and anti-tumour effect of paclitaxel by 20(s)-ginsenoside Rg3 in vivo. Biopharm Drug Dispos 2012;33:425-36.
49. Park JH, Park JH, Hur HJ, Woo JS, Lee HJ. Effects of silymarin and formulation on the oral bioavailability of paclitaxel in rats. Eur J Pharm Sci 2012;45:296-301.
50. Lee CK, Choi JS. Effects of silibinin, inhibitor of CYP3A4 and P-glycoprotein in vitro, on the pharmacokinetics of paclitaxel after oral and intravenous administration in rats. Pharmacology 2010;85:350-6.
51. Yan YD, Kim DH, Sung JH, Yong CS, Choi HG. Enhanced oral bioavailability of docetaxel in rats by four consecutive days of pre-treatment with curcumin. Int J Pharm 2010;399:116-20.
52. van AJ, van TO, van der Valk MA, Rozenhart M, Beijnen JH. Enhanced oral absorption and decreased elimination of paclitaxel in mice cotreated with cyclosporin A. Clin Cancer Res 1998;4:2293-7.
53. van AJ, van TO, Sparreboom A, *et al*. Enhanced oral bioavailability of paclitaxel in mice treated with the P-glycoprotein blocker SDZ PSC 833. Br J Cancer 1997;76:1181-3.
54. Bardelmeijer HA, Beijnen JH, Brouwer KR, *et al*. Increased oral bioavailability of paclitaxel by GF120918 in mice through selective modulation of P-glycoprotein. Clin Cancer Res 2000;6:4416-21.
55. Bardelmeijer HA, Ouwehand M, Beijnen JH, Schellens JH, van TO. Efficacy of novel P-glycoprotein inhibitors to increase the oral uptake of paclitaxel in mice. Invest New Drugs 2004;22:219-29.
56. Hendrikx JJ, Lagas JS, Wagenaar E, *et al*. Oral co-administration of elacridar and ritonavir enhances plasma levels of oral paclitaxel and docetaxel without affecting relative brain accumulation. Br J Cancer 2014;110:2669-76.
57. Kwak JO, Lee SH, Lee GS, *et al*. Selective inhibition of MDR1 (ABCB1) by HM30181 increases oral bioavailability and therapeutic efficacy of paclitaxel. Eur J Pharmacol 2010;627:92-8.
58. Kemper EM, van Zandbergen AE, Cleypool C, *et al*. Increased penetration of paclitaxel into the brain by inhibition of P-Glycoprotein. Clin Cancer Res 2003;9:2849-55.
59. Kemper EM, Verheij M, Boogerd W, Beijnen JH, van TO. Improved penetration of docetaxel into the brain by co-administration of inhibitors of P-glycoprotein. Eur J Cancer 2004;40:1269-74.
60. Kimura Y, Aoki J, Kohno M, Ooka H, Tsuruo T, Nakanishi O. P-glycoprotein inhibition by the multidrug resistance-reversing agent MS-209 enhances bioavailability and antitumor efficacy of orally administered paclitaxel. Cancer Chemother Pharmacol 2002;49:322-8.
61. Hartmann JT, Haap M, Kopp HG, Lipp HP. Tyrosine kinase inhibitors - a review on pharmacology, metabolism and side effects. Curr Drug Metab 2009;10:470-81.

62. Eckstein N, Roper L, Haas B, *et al*. Clinical pharmacology of tyrosine kinase inhibitors becoming generic drugs: the regulatory perspective. J Exp Clin Cancer Res 2014;33:15.
63. Jackson SE, Chester JD. Personalised cancer medicine. Int J Cancer 2014.
64. Eadie LN, Hughes TP, White DL. Interaction of the efflux transporters ABCB1 and ABCG2 with imatinib, nilotinib, and dasatinib. Clin Pharmacol Ther 2014;95:294-306.
65. Poller B, Iusuf D, Sparidans RW, Wagenaar E, Beijnen JH, Schinkel AH. Differential impact of P-glycoprotein (ABCB1) and breast cancer resistance protein (ABCG2) on axitinib brain accumulation and oral plasma pharmacokinetics. Drug Metab Dispos 2011;39:729-35.
66. Durmus S, Sparidans RW, Wagenaar E, Beijnen JH, Schinkel AH. Oral availability and brain penetration of the B-RAFV600E inhibitor vemurafenib can be enhanced by the P-GLYCOprotein (ABCB1) and breast cancer resistance protein (ABCG2) inhibitor elacridar. Mol Pharm 2012;9:3236-45.
67. Chuan TS, Nguyen LN, Sparidans RW, Wagenaar E, Beijnen JH, Schinkel AH. Increased oral availability and brain accumulation of the ALK inhibitor crizotinib by coadministration of the P-glycoprotein (ABCB1) and breast cancer resistance protein (ABCG2) inhibitor elacridar. Int J Cancer 2014;134:1484-94.
68. Mittapalli RK, Vaidhyanathan S, Dudek AZ, Elmquist WF. Mechanisms limiting distribution of the threonine-protein kinase B-RaF(V600E) inhibitor dabrafenib to the brain: implications for the treatment of melanoma brain metastases. J Pharmacol Exp Ther 2013;344:655-64.
69. Rouleau M, Patel A, Hendzel MJ, Kaufmann SH, Poirier GG. PARP inhibition: PARP1 and beyond. Nat Rev Cancer 2010;10:293-301.
70. Farmer H, McCabe N, Lord CJ, *et al*. Targeting the DNA repair defect in BRCA mutant cells as a therapeutic strategy. Nature 2005;434:917-21.
71. Chalmers AJ, Lakshman M, Chan N, Bristow RG. Poly(ADP-ribose) polymerase inhibition as a model for synthetic lethality in developing radiation oncology targets. Semin Radiat Oncol 2010;20:274-81.
72. O'Sullivan CC, Moon DH, Kohn EC, Lee JM. Beyond Breast and Ovarian Cancers: PARP Inhibitors for BRCA Mutation-Associated and BRCA-Like Solid Tumors. Front Oncol 2014;4:42.
73. Rottenberg S, Jaspers JE, Kersbergen A, *et al*. High sensitivity of BRCA1-deficient mammary tumors to the PARP inhibitor AZD2281 alone and in combination with platinum drugs. Proc Natl Acad Sci U S A 2008;105:17079-84.
74. Jaspers JE, Kersbergen A, Boon U, *et al*. Loss of 53BP1 causes PARP inhibitor resistance in Brca1-mutated mouse mammary tumors. Cancer Discov 2013;3:68-81.
75. Oplustilova L, Wolanin K, Mistrik M, *et al*. Evaluation of candidate biomarkers to predict cancer cell sensitivity or resistance to PARP-1 inhibitor treatment. Cell Cycle 2012;11:3837-50.
76. Lin F, de Gooijer MC, Roig EM, *et al*. ABCB1, ABCG2, and PTEN determine the response of glioblastoma to temozolomide and ABT-888 therapy. Clin Cancer Res 2014;20:2703-13.
77. Durmus S, Sparidans RW, van EA, Wagenaar E, Beijnen JH, Schinkel AH. Breast Cancer Resistance Protein (BCRP/ABCG2) and P-glycoprotein (P-GP/ABCB1) Restrict Oral Availability and Brain Accumulation of the PARP Inhibitor Rucaparib (AG-014699). Pharm Res 2014.
78. Stewart CF, Leggas M, Schuetz JD, *et al*. Gefitinib enhances the antitumor activity and oral bioavailability of irinotecan in mice. Cancer Res 2004;64:7491-9.
79. Kruijtzer CM, Beijnen JH, Rosing H, *et al*. Increased oral bioavailability of topotecan in combination with the breast cancer resistance protein and P-glycoprotein inhibitor GF120918. J Clin Oncol 2002;20:2943-50.
80. Hagenbuch B, Gao B, Meier PJ. Transport of xenobiotics across the blood-brain barrier. News Physiol Sci 2002;17:231-4.
81. Lockman PR, Mittapalli RK, Taskar KS, *et al*. Heterogeneous blood-tumor barrier permeability determines drug efficacy in experimental brain metastases of breast cancer. Clin Cancer Res 2010;16:5664-78.
82. Cordon-Cardo C, O'Brien JP, Casals D, *et al*. Multidrug-resistance gene (P-glycoprotein) is expressed by endothelial cells at blood-brain barrier sites. Proc Natl Acad Sci U S A 1989;86:695-8.
83. Schinkel AH, Wagenaar E, Mol CA, van DL. P-glycoprotein in the blood-brain barrier of mice influences the brain penetration and pharmacological activity of many drugs. J Clin Invest 1996;97:2517-24.
84. Eisenblatter T, Galla HJ. A new multidrug resistance protein at the blood-brain barrier. Biochem Biophys Res Commun 2002;293:1273-8.
85. Cooray HC, Blackmore CG, Maskell L, Barrand MA. Localisation of breast cancer resistance protein in microvessel endothelium of human brain. Neuroreport 2002;13:2059-63.
86. de Vries NA, Beijnen JH, Boogerd W, van TO. Blood-brain barrier and chemotherapeutic

treatment of brain tumors. Expert Rev Neurother 2006;6:1199-209.

87. Kamiie J, Ohtsuki S, Iwase R, *et al*. Quantitative atlas of membrane transporter proteins: development and application of a highly sensitive simultaneous LC/MS/MS method combined with novel in-silico peptide selection criteria. Pharm Res 2008;25:1469-83.

88. Agarwal S, Uchida Y, Mittapalli RK, Sane R, Terasaki T, Elmquist WF. Quantitative proteomics of transporter expression in brain capillary endothelial cells isolated from P-glycoprotein (P-gp), breast cancer resistance protein (Bcrp), and P-gp/Bcrp knockout mice. Drug Metab Dispos 2012;40:1164-9.

89. Tang SC, Lagas JS, Lankheet NA, *et al*. Brain accumulation of sunitinib is restricted by P-glycoprotein (ABCB1) and breast cancer resistance protein (ABCG2) and can be enhanced by oral elacridar and sunitinib coadministration. Int J Cancer 2012;130:223-33.

90. Tang SC, Sparidans RW, Cheung KL, *et al*. P-Glycoprotein, CYP3A, and Plasma Carboxylesterase Determine Brain and Blood Disposition of the mTOR Inhibitor Everolimus (Afinitor) in Mice. Clin Cancer Res 2014;20:3133-45.

91. Durmus S, Xu N, Sparidans RW, Wagenaar E, Beijnen JH, Schinkel AH. P-glycoprotein (MDR1/ABCB1) and breast cancer resistance protein (BCRP/ABCG2) restrict brain accumulation of the JAK1/2 inhibitor, CYT387. Pharmacol Res 2013;76:9-16.

92. Tang SC, Lankheet NA, Poller B, Wagenaar E, Beijnen JH, Schinkel AH. P-glycoprotein (ABCB1) and breast cancer resistance protein (ABCG2) restrict brain accumulation of the active sunitinib metabolite N-desethyl sunitinib. J Pharmacol Exp Ther 2012;341:164-73.

93. Salphati L, Heffron TP, Alicke B, *et al*. Targeting the PI3K pathway in the brain--efficacy of a PI3K inhibitor optimized to cross the blood-brain barrier. Clin Cancer Res 2012;18:6239-48.

94. Agarwal S, Sane R, Gallardo JL, Ohlfest JR, Elmquist WF. Distribution of gefitinib to the brain is limited by P-glycoprotein (ABCB1) and breast cancer resistance protein (ABCG2)-mediated active efflux. J Pharmacol Exp Ther 2010;334:147-55.

95. Kodaira H, Kusuhara H, Ushiki J, Fuse E, Sugiyama Y. Kinetic analysis of the cooperation of P-glycoprotein (P-gp/Abcb1) and breast cancer resistance protein (Bcrp/Abcg2) in limiting the brain and testis penetration of erlotinib, flavopiridol, and mitoxantrone. J Pharmacol Exp Ther 2010;333:788-96.

96. Lagas JS, van Waterschoot RA, Sparidans RW, Wagenaar E, Beijnen JH, Schinkel AH. Breast cancer resistance protein and P-glycoprotein limit sorafenib brain accumulation. Mol Cancer Ther 2010;9:319-26.

97. Polli JW, Olson KL, Chism JP, *et al*. An unexpected synergist role of P-glycoprotein and breast cancer resistance protein on the central nervous system penetration of the tyrosine kinase inhibitor lapatinib (N-{3-chloro-4-[(3-fluorobenzyl) oxy]phenyl}-6-[5-({[2-(methylsulfonyl)ethyl] amino }methyl)-2-furyl]-4-quinazolinamine; GW572016). Drug Metab Dispos 2009;37:439-42.

98. Zhou L, Schmidt K, Nelson FR, Zelesky V, Troutman MD, Feng B. The effect of breast cancer resistance protein and P-glycoprotein on the brain penetration of flavopiridol, imatinib mesylate (Gleevec), prazosin, and 2-methoxy-3-(4-(2-(5-methyl-2-phenyloxazol-4-yl)ethoxy) phenyl)propanoic acid (PF-407288) in mice. Drug Metab Dispos 2009;37:946-55.

99. Kalvass JC, Pollack GM. Kinetic considerations for the quantitative assessment of efflux activity and inhibition: implications for understanding and predicting the effects of efflux inhibition. Pharm Res 2007;24:265-76.

100. Zamek-Gliszczynski MJ, Kalvass JC, Pollack GM, Brouwer KL. Relationship between drug/metabolite exposure and impairment of excretory transport function. Drug Metab Dispos 2009;37:386-90.

101. Bentz J, Tran TT, Polli JW, Ayrton A, Ellens H. The steady-state Michaelis-Menten analysis of P-glycoprotein mediated transport through a confluent cell monolayer cannot predict the correct Michaelis constant Km. Pharm Res 2005;22:1667-77.

102. Tang SC, de VN, Sparidans RW, Wagenaar E, Beijnen JH, Schinkel AH. Impact of P-glycoprotein (ABCB1) and breast cancer resistance protein (ABCG2) gene dosage on plasma pharmacokinetics and brain accumulation of dasatinib, sorafenib, and sunitinib. J Pharmacol Exp Ther 2013;346:486-94.

# CHAPTER 1.2

## PHYSIOLOGICAL AND PHARMACOLOGICAL FUNCTIONS OF MOUSE AND HUMAN OATP1A/1B TRANSPORTERS

Selvi Durmus[a] and Alfred H. Schinkel[a]

[a] Division of Molecular Oncology, The Netherlands Cancer Institute, Amsterdam, the Netherlands

Organic anion-transporting polypeptides (OATP/Oatp; gene: SLCO/Slco) are important sodium-independent uptake transporters that mediate cellular uptake of many endogenous and exogenous compounds. OATP transporters belong to a large superfamily of transmembrane proteins, consisting of six families (OATP1-6) sharing more than 40% amino acid identity between members. Of these families, there are several subfamilies such as OATP1A or OATP1B, that share more than 60% amino acid identity within the subfamily [1]. Based on the sequence homology and localization, there are not always straightforward orthologs of the OATPs between human and mouse. For example, the OATP1A subfamily contains one human member (OATP1A2), but at least four mouse members (Oatp1a1, Oatp1a4, Oatp1a5, Oatp1a6). Similarly, there are two human members (OATP1B1 and OATP1B3) of the OATP1B subfamily, whereas there is only one mouse member (Oatp1b2) [1].

OATP1A/1B transporters are thought to have profound effects on absorption, distribution and elimination of their substrates, because they are mainly expressed in pharmacokinetically important organs (e.g. liver, small intestine and kidney) and have broad substrate specificity [2, 3]. Mouse Oatp1a1, -1a4 and -1b2, and human OATP1B1 and -1B3 transporters are prominently expressed in the sinusoidal (basolateral) membrane of the hepatocytes [4, 5]. Human OATP1A2 is expressed in the apical membrane of several other tissues, such as intestinal epithelium, distal nephron cells, cholangiocytes (cells lining the bile ducts) and endothelial cells of brain capillaries at the blood-brain barrier [6, 7]. Up till now, the functional impact of OATP1A2 on the disposition of substrates has not clearly been shown and needs to be further investigated.

In addition to their physiologic expression, OATPs are also expressed in several cancer tissues and cell lines. Expression of OATP1A2 was detected in breast cancer tissue, several breast and prostate cancer cell lines, bone metastases from kidney cancer and malignant osteosarcoma, that of OATP1B1 in neoplastic colon tissue, human ovarian cancer and in ovarian cancer cell lines and that of OATP1B3 in several gastrointestinal, colon and ovarian cancers and cell lines, and pancreatic cancer [4, 5, 8-12]. OATPs in these cells may well be involved in the uptake of anticancer drugs which makes them a potential target for therapy modulation.

OATPs can transport a wide range of substrates of endogenous origin, such as bile acids, steroid and thyroid hormones and bilirubin glucuronide, but also of exogenous origin such as drugs, toxins and their conjugates [1-3, 13-16]. Many studies showed that OATP1A/1B transporters have key roles in hepatic uptake and/or plasma clearance of several drug substrates including statins, cardiac glycosides, antibiotics, and many chemotherapeutics with highly diverse structures [14-21].

The substrate specifity of OATP transporters was initially thought to include primarily polar and anionic compounds; however this perception has changed by many recent findings showing a highly diverse structural range in the substrates of OATPs. As an example of structural diversity, we have previously shown that methotrexate (anion), paclitaxel (bulky hydrophobic) and fexofenadine (zwitterion) were substrates of OATP1A/1B transporters [16, 18, 19]. In this thesis, we have added another unexpected drug substrate of OATPs by showing that plasma disposition and hepatic uptake of doxorubicin, a fairly hydrophobic weak base, was affected by mouse Oatp1a/1b and human OATP1A/1B transporters.

In liver, OATPs contribute to the hepatic elimination of drugs largely by mediating uptake of their wide range of substrates. Recently, we described a novel and efficient liver detoxification

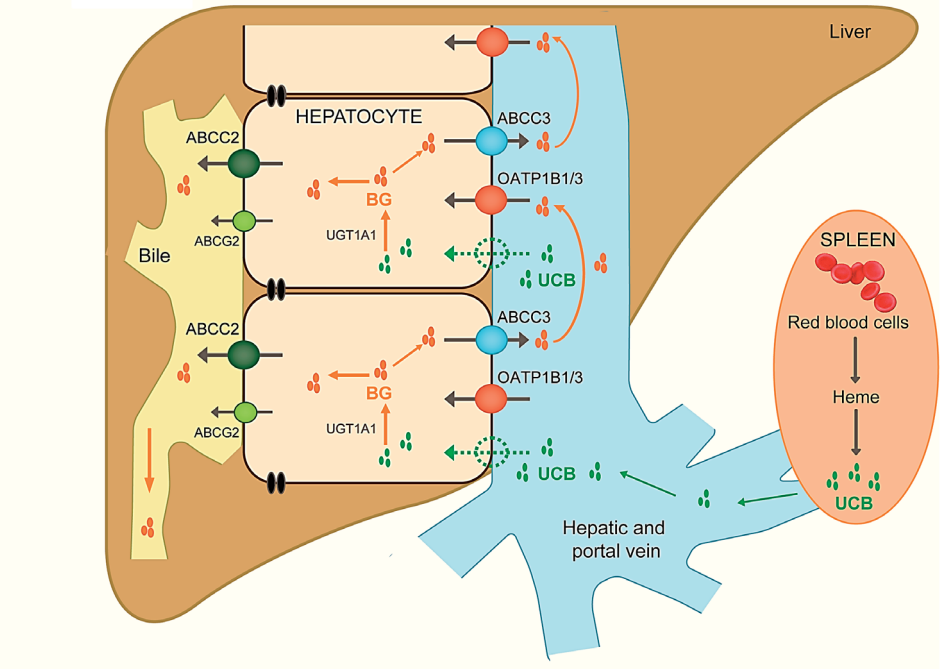


**Figure 1. Hepatocyte hopping of bilirubin glucuronide.** Unconjugated bilirubin (UCB) is formed in the spleen as a degradation product of heme resulting from spent red blood cells, and then travels (tightly bound to albumin) to the liver via the hepatic artery and portal vein. In the liver, UCB enters the hepatocytes via passive diffusion and/or incompletely defined transporters. After conjugation with glucuronic acid by (UDP)-glucuronosyltransferase 1A1 to bilirubin glucuronides (BGs), BGs are secreted into the bile. This secretion is mediated mainly by ATP binding cassette (ABC) transporter ABCC2, although ABCG2 can also contribute to this process. Under physiological conditions, a substantial fraction of the intracellular BGs is secreted by ABCC3 to the blood, from where they can be taken up again into downstream hepatocytes via organic anion–transporting polypeptides (OATP)1B1 and OATP1B3 (Oatp1a and Oatp1b in mice). This secretion-and-reuptake loop may prevent the saturation of biliary excretion in the upstream hepatocytes, thereby ensuring efficient biliary elimination and hepatocyte detoxification. It is likely that an analogous process applies for many of the drugs conjugated in the liver. The figure and the explanation is taken from Iusuf *et al.*, Clinical Pharmacology & Therapeutics (2012); 92 5, 559–562.

process, 'hepatocyte hopping', based on experimental data showing a liver-to-blood shuttling of the endogenous substrate bilirubin glucuronide (BG). We demonstrated that Oatp1a/1b transporters work together with the basolaterally located efflux drug efflux transporter, Abcc3, to mediate substantial hepatic secretion and subsequent reuptake of BG into hepatocytes (Figure 1) [22, 23]. Hepatocyte hopping is an efficient and robust way for hepatic elimination of an important amount of BG that is not immediately excreted into the bile, not only under pathological, but also normal physiological conditions. This can happen when the biliary excretion in upstream hepatocytes is saturated, for example by bilirubin overload or accidental Abcc2 inhibition. In these situations, BG that is secreted into the blood circulation by Abcc3 is then efficiently taken up again in downstream hepatocytes by Slco1a/1b activity, leaving another

possibility for a safe biliary excretion, instead of being trapped in the upstream hepatocytes. This process leads to a more evenly distributed biliary excretion of substrates over all the liver, allowing a more flexible, efficient and safe liver detoxification of the substrates. We recently showed that there are people with full deficiency in the OATP1B1 and OATP1B3 genes who suffer from conjugated hyperbilirubinemia due to interrupted hepatic reuptake of BG. This disorder is called Rotor syndrome [22]. Considering the strong phenotypic similarity between Oatp1a/1b knockout mice and people with Rotor syndrome, we think that ABCC3 is likely to be involved in this process also in humans. We therefore think that hepatocyte hopping is of broad relevance and occurs in humans just as it does in mice. Given the broad substrate specificity of OATPs, we expect that in addition to the endogenous substrates, hepatocyte hopping also applies to many drugs and drug conjugates. In one study in this thesis, we assessed whether this hypothesis could be experimentally tested using the glucuronidated conjugate of the anti-cancer drug sorafenib, which has been shown to be a substrate of Oatp1b2 [24].

Importance of OATPs in pharmacology is increasingly recognized, not only because they are expressed in many tissues and even in a number of tumors, and can transport a wide range of compounds, but also because there are several polymorphisms found in the world's population. Many of these polymorphisms found in the genes encoding OATP1A2, OATP1B1 and OATP1B3 lead to decreased function and are associated with clinically important outcomes [25-28]. For example, significant alterations in the clearance of the anti-cancer drug imatinib in chronic myeloid leukemia patients were associated with two different polymorphisms in the OATP1A2 genes [29]. Also, several other polymorphisms found in the OATP1B1 gene were associated with a reduced transport activity and hence altered plasma and tissue distribution of a wide range of drug substrates (pravastatin, valsartan, methotrexate and SN-38), leading to various degrees of toxicities [25, 30-32].

OATPs can also be involved in drug-drug interactions (DDIs) that lead to clinically important alterations in pharmacokinetic, pharmacodynamic and toxicological risks [33]. Our knowledge on OATP-mediated DDIs is currently limited, but increasing rapidly. Pharmacological inhibition or genetic variations causing reduced OATP activity poses a risk for DDIs when OATP substrate drugs are coadministered. In this respect, investigation of potential DDIs mediated by OATP1B1 and -1B3 during drug development is now strongly recommended by FDA and EMA for new molecular entities (NMEs) [34]. Up till now, the majority of the studies have focused on *in vitro* or *in silico* tools for predicting possible risks of DDIs between many OATP substrate drugs [35-40]. Few studies also used preclinical wild-type or Oatp-knockout mouse models to assess the risk of DDIs mediated by OATPs [41, 42]. However, the limitation of these studies is that translational relevance is often suboptimal. To achieve predictions that lead to better extrapolations to human, "humanized" mouse models expressing human OATP1B1 or -1B3 that we have generated [19] might be useful tools to assess clinically relevant DDIs. Hu *et al*. [43] very recently published a study where they used Oatp1b2 knockout and human OATP1B1-expressing transgenic mice to assess the OATP1B1-mediated interactions between two anti-cancer drugs, sorafenib and docetaxel *in vivo*. Although their *in vivo* results did not reproduce the interactions that they have observed *in vitro*, this study was important as they assessed OATP-mediated DDI involving

anti-cancer drugs on which the current knowledge is very restricted. Moreover, their findings also demonstrated the limitations of making predictions just from *in vitro* studies.

In conclusion, mouse Oatp1a/1b and human OATP1A/1B proteins are important drug uptake transporters, involved especially in the plasma and hepatic disposition of many substrate drugs and drug conjugates, with surprisingly diverse structures. Moreover, DDIs mediated by human hepatic OATP1B1 and -1B3 transporters are of high interest, as they can be clinically relevant. In three studies described in this thesis, we focused on assessing the functions of OATPs alone or together with other efflux transporters in the disposition of drugs (doxorubicin; chapter 2) or drug conjugates (sorafenib glucuronide; chapter 3), and in DDIs (rifampicin/telmisartan and methotrexate; chapter 4).

## REFERENCE LIST

1. Hagenbuch B, Meier PJ. Organic anion transporting polypeptides of the OATP/ SLC21 family: phylogenetic classification as OATP/ SLCO superfamily, new nomenclature and molecular/functional properties. *Pflügers Arch 2004;* 447:653-665.
2. Cheng X, Maher J, Chen C, Klaassen CD. Tissue distribution and ontogeny of mouse organic anion transporting polypeptides (Oatps). *Drug Metab Dispos 2005*; 33:1062-1073.
3. Cheng X, Klaassen CD. Tissue distribution, ontogeny, and hormonal regulation of xenobiotic transporters in mouse kidneys. *Drug Metab Dispos 2009*; 37:2178-2185.
4. Konig J, Cui Y, Nies AT, Keppler D. A novel human organic anion transporting polypeptide localized to the basolateral hepatocyte membrane. *Am J Physiol Gastrointest Liver Physiol 2000*; 278:G156-G164.
5. Konig J, Cui Y, Nies AT, Keppler D. Localization and genomic organization of a new hepatocellular organic anion transporting polypeptide. J Biol *Chem 2000*; 275:23161-23168.
6. Gao B, Hagenbuch B, Kullak-Ublick GA, Benke D, Aguzzi A, Meier PJ. Organic anion-transporting polypeptides mediate transport of opioid peptides across blood-brain barrier. *J Pharmacol Exp Ther 2000*; 294:73-79.
7. Glaeser H, Bailey DG, Dresser GK, Gregor JC, Schwarz UI, McGrath JS *et al. Int*estinal drug transporter expression and the impact of grapefruit juice in humans. Clin *Pharmacol Ther 2007*; 81:362-370.
8. Abe T, Unno M, Onogawa T, Tokui T, Kondo TN, Nakagomi R *et al. LST-2*, a human liver-specific organic anion transporter, determines methotrexate sensitivity in gastrointestinal cancers. *Gastroenterology 2001*; 120:1689-1699.
9. Ballestero MR, Monte MJ, Briz O, Jimenez F, Gonzalez-San Martin F, Marin JJ. Expression of transporters potentially involved in the targeting of cytostatic bile acid derivatives to colon cancer and polyps. *Biochem Pharmacol 2006*; 72:729-738.
10. Svoboda M, Wlcek K, Taferner B, Hering S, Stieger B, Tong D *et al. Expr*ession of organic anion-transporting polypeptides 1B1 and 1B3 in ovarian cancer cells: relevance for paclitaxel transport. *Biomed Pharmacother 2011*; 65:417-426.
11. Tamai I, Nezu J, Uchino H, Sai Y, Oku A, Shimane M *et al.* Molecular identification and characterization of novel members of the human organic anion transporter (OATP) family. *Biochem Biophys Res Commun 2000*; 273:251-260.
12. Meyer zu Schwabedissen HE, Tirona RG, Yip CS, Ho RH, Kim RB. Interplay between the nuclear receptor pregnane X receptor and the uptake transporter organic anion transporter polypeptide 1A2 selectively enhances estrogen effects in breast cancer. *Cancer Res 2008*; 68:9338-9347.
13. Hagenbuch B, Gui C. Xenobiotic transporters of the human organic anion transporting polypeptides (OATP) family. *Xenobiotica 2008*; 38:778-801.
14. Klaassen CD, Aleksunes LM. Xenobiotic, bile acid, and cholesterol transporters: function and regulation. *Pharmacol Rev 2010*; 62:1-96.
15. Shitara Y, Maeda K, Ikejiri K, Yoshida K, Horie T, Sugiyama Y. Clinical significance of organic anion transporting polypeptides (OATPs) in drug disposition: their roles in the hepatic clearance and intestinal absorption. *Biopharm Drug Dispos 2012*.
16. van de Steeg E, Wagenaar E, van der Kruijssen CM, Burggraaff JE, de Waart DR, Elferink RP *et al.*

*Organi*c anion transporting polypeptide 1a/1b-knockout mice provide insights into hepatic handling of bilirubin, bile acids, and drugs. *J Clin Invest 2010*; 120:2942-2952.

17. Iusuf D, Sparidans RW, van Esch A, Hobbs M, Kenworthy KE, van de Steeg E *et al*. *Organi*c anion-transporting polypeptides 1a/1b control the hepatic uptake of pravastatin in mice. *Mol Pharm 2012*; 9:2497-2504.
18. van de Steeg E, van Esch A, Wagenaar E, van der Kruijssen CM, van Tellingen O, Kenworthy KE *et al*. High impact of Oatp1a/1b transporters on in vivo disposition of the hydrophobic anticancer drug paclitaxel. *Clin Cancer Res 2011*; 17:294-301.
19. van de Steeg E, van Esch A, Wagenaar E, Kenworthy KE, Schinkel AH. Influence of human OATP1B1, OATP1B3, and OATP1A2 on the pharmacokinetics of methotrexate and paclitaxel in humanized transgenic mice. *Clin Cancer Res 2013*; 19:821-832.
20. Iusuf D, Ludwig M, Elbatsh A, van EA, van de Steeg E, Wagenaar E *et al*. OATP1A/1B transporters affect irinotecan and SN-38 pharmacokinetics and carboxylesterase expression in knockout and humanized transgenic mice. *Mol Cancer Ther 2014*; 13:492-503.
21. Iusuf D, Hendrikx JJ, van EA, van de Steeg E, Wagenaar E, Rosing H *et al*. Human OATP1B1, OATP1B3 and OATP1A2 can mediate the in vivo uptake and clearance of docetaxel. *Int J Cancer 2014*.
22. van de Steeg E, Stranecky V, Hartmannova H, Noskova L, Hrebicek M, Wagenaar E *et al*. Complete OATP1B1 and OATP1B3 deficiency causes human Rotor syndrome by interrupting conjugated bilirubin reuptake into the liver. *J Clin Invest 2012*; 122:519-528.
23. Iusuf D, van de Steeg E, Schinkel AH. Hepatocyte hopping of OATP1B substrates contributes to efficient hepatic detoxification. *Clin Pharmacol Ther 2012*; 92:559-562.
24. Zimmerman EI, Hu S, Roberts JL, Gibson AA, Orwick SJ, Li L *et al*. *Contri*bution of OATP1B1 and OATP1B3 to the disposition of sorafenib and sorafenib-glucuronide. *Clin Cancer Res 2013*; 19:1458-1466.
25. Konig J, Seithel A, Gradhand U, Fromm MF. Pharmacogenomics of human OATP transporters. *Naunyn Schmiedebergs Arch Pharmacol 2006*; 372:432-443.
26. Laitinen A, Niemi M. Frequencies of single-nucleotide polymorphisms of SLCO1A2, SLCO1B3 and SLCO2B1 genes in a Finnish population. *Basic Clin Pharmacol Toxicol 2011*; 108:9-13.
27. Pasanen MK, Neuvonen PJ, Niemi M. Global analysis of genetic variation in SLCO1B1. *Pharmacogenomics 2008*; 9:19-33.
28. Maeda K, Sugiyama Y. Impact of genetic polymorphisms of transporters on the pharmacokinetic, pharmacodynamic and toxicological properties of anionic drugs. *Drug Metab Pharmacokinet 2008*; 23:223-235.
29. Yamakawa Y, Hamada A, Shuto T, Yuki M, Uchida T, Kai H *et al*. Pharmacokinetic impact of SLCO1A2 polymorphisms on imatinib disposition in patients with chronic myeloid leukemia. *Clin Pharmacol Ther 2011*; 90:157-163.
30. Trevino LR, Shimasaki N, Yang W, Panetta JC, Cheng C, Pei D *et al*. Germline genetic variation in an organic anion transporter polypeptide associated with methotrexate pharmacokinetics and clinical effects. *J Clin Oncol 2009*; 27:5972-5978.
31. Takane H, Kawamoto K, Sasaki T, Moriki K, Moriki K, Kitano H *et al*. Life-threatening toxicities in a patient with UGT1A1*6/*28 and SLCO1B1*15/*15 genotypes after irinotecan-based chemotherapy. *Cancer Chemother Pharmacol 2009*; 63:1165-1169.
32. Kalliokoski A, Niemi M. Impact of OATP transporters on pharmacokinetics. *Br J Pharmacol 2009*; 158:693-705.
33. Giacomini KM, Huang SM, Tweedie DJ, Benet LZ, Brouwer KL, Chu X *et al*. Membrane transporters in drug development. *Nat Rev Drug Discov 2010*; 9:215-236.
34. Prueksaritanont T, Chu X, Gibson C, Cui D, Yee KL, Ballard J *et al*. Drug-drug interaction studies: regulatory guidance and an industry perspective. *AAPS J 2013*; 15:629-645.
35. Hirano M, Maeda K, Shitara Y, Sugiyama Y. Drug-drug interaction between pitavastatin and various drugs via OATP1B1. *Drug Metab Dispos 2006*; 34:1229-1236.
36. Karlgren M, Ahlin G, Bergstrom CA, Svensson R, Palm J, Artursson P. In vitro and in silico strategies to identify OATP1B1 inhibitors and predict clinical drug-drug interactions. *Pharm Res 2012*; 29:411-426.
37. Kindla J, Muller F, Mieth M, Fromm MF, Konig J. Influence of non-steroidal anti-inflammatory drugs on organic anion transporting polypeptide (OATP) 1B1- and OATP1B3-mediated drug transport. *Drug Metab Dispos 2011*; 39:1047-1053.
38. Yoshida K, Maeda K, Sugiyama Y. Transporter-mediated drug-drug interactions involving OATP substrates: predictions based on in vitro inhibition studies. *Clin Pharmacol Ther 2012*; 91:1053-1064.

39. Yoshida K, Maeda K, Sugiyama Y. Transporter-mediated drug--drug interactions involving OATP substrates: predictions based on in vitro inhibition studies. *Clin Pharmacol Ther 2012*; 91:1053-1064.

40. Noe J, Portmann R, Brun ME, Funk C. Substrate-dependent drug-drug interactions between gemfibrozil, fluvastatin and other organic anion-transporting peptide (OATP) substrates on OATP1B1, OATP2B1, and OATP1B3. *Drug Metab Dispos 2007*; 35:1308-1314.

41. Chang JH, Ly J, Plise E, Zhang X, Messick K, Wright M *et al*. Differential Effects of Rifampin and Ketoconazole on the Blood and Liver Concentration of Atorvastatin in Wild-Type and Cyp3a and Oatp1a/b Knockout Mice. *Drug Metab Dispos 2014*; 42:1067-1073.

42. Shitara Y, Hirano M, Adachi Y, Itoh T, Sato H, Sugiyama Y. In vitro and in vivo correlation of the inhibitory effect of cyclosporin A on the transporter-mediated hepatic uptake of cerivastatin in rats. *Drug Metab Dispos 2004*; 32:1468-1475.

43. Hu S, Mathijssen RH, de BP, Baker SD, Sparreboom A. Inhibition of OATP1B1 by tyrosine kinase inhibitors: in vitro-in vivo correlations. *Br J Cancer 2014*; 110:894-898.

# CHAPTER 2

## IMPACT OF ABC TRANSPORTERS ON PHARMACOKINETICS OF TARGETED ANTI-CANCER DRUGS

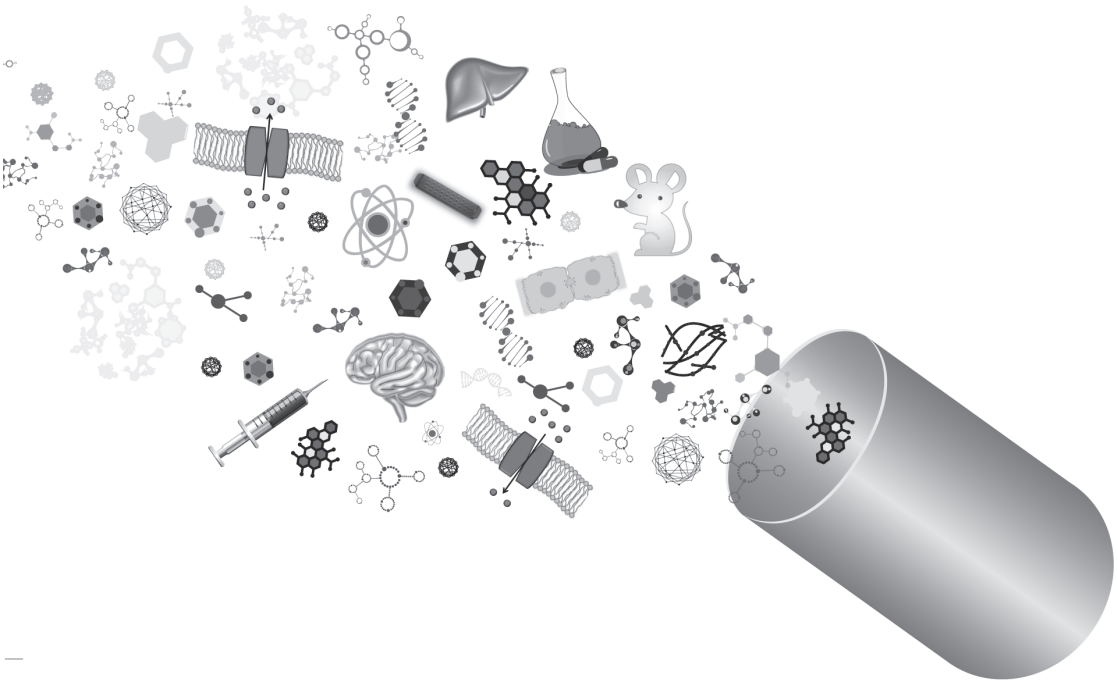

# CHAPTER 2.1

## ORAL AVAILABILITY AND BRAIN PENETRATION OF THE B-RAF$^{V600E}$ INHIBITOR VEMURAFENIB CAN BE ENHANCED BY THE P-GLYCOPROTEIN (ABCB1) AND BREAST CANCER RESISTANCE PROTEIN (ABCG2) INHIBITOR ELACRIDAR

Selvi Durmus[a], Rolf W. Sparidans[b], Els Wagenaar[a], Jos H. Beijnen[c] and Alfred H. Schinkel[a]

[a] The Netherlands Cancer Institute, Division of Molecular Oncology, Plesmanlaan 121, 1066 CX Amsterdam, The Netherlands.
[b]Utrecht University, Faculty of Science, Department of Pharmaceutical Sciences, Division of Pharmacoepidemiology & Clinical Pharmacology, Universiteitsweg 99, 3584 CG Utrecht, The Netherlands.
[c]Slotervaart Hospital, Department of Pharmacy & Pharmacology, Louwesweg 6, 1066 EC Amsterdam, The Netherlands.

*Mol Pharm. 2012 Nov 5;9(11):3236-45*

## ABSTRACT

Vemurafenib (PLX4032) is a novel tyrosine kinase inhibitor that has clinical efficacy against metastatic melanoma harboring a $BRAF^{V600E}$ mutation. We aimed to establish whether the multidrug efflux transporters P-glycoprotein (P-gp/ABCB1) and Breast Cancer Resistance Protein (BCRP/ABCG2) could restrict oral availability and brain penetration of vemurafenib, as these might limit therapeutic efficacy, especially against brain metastases. *In vitro*, vemurafenib was efficiently transported by both human ABCB1 and ABCG2, and very efficiently by mouse Abcg2, but not by mouse Abcc2. Upon oral administration of vemurafenib (5 mg/kg), *Abcb1a/1b*$^{-/-}$ mice had a 1.6-fold increased, *Abcg2*$^{-/-}$ mice a 2.3-fold increased, and *Abcb1a/1b*$^{-/-}$*;Abcg2*$^{-/-}$ mice a 6.6-fold increased plasma AUC, respectively, compared to wild-type (WT) mice, indicating a marked and additive role of these transporters in limiting vemurafenib oral availability. Brain-to-plasma ratios of vemurafenib (oral, 25 mg/kg) were not increased in *Abcg2*$^{-/-}$ mice, only 1.7-fold in *Abcb1a/1b*$^{-/-}$ mice, but 21.4-fold in *Abcb1a/1b*$^{-/-}$*;Abcg2*$^{-/-}$ mice, indicating pronounced overlapping functions of these transporters in reducing vemurafenib brain accumulation. Oral coadministration of the dual ABCB1 and ABCG2 inhibitor elacridar almost completely eliminated the roles of Abcb1 and Abcg2 in restricting oral availability and brain accumulation of vemurafenib. As predicted by previously described pharmacokinetic modelling, halving the amount of active efflux transport at the WT blood-brain barrier by testing heterozygous *Abcb1a/1b*$^{+/-}$*;Abcg2*$^{+/-}$ mice had little impact on vemurafenib brain accumulation. Our data suggest that elacridar coadministration may be considered to improve the therapeutic efficacy of vemurafenib, especially for brain metastases located behind a functional blood-brain barrier.

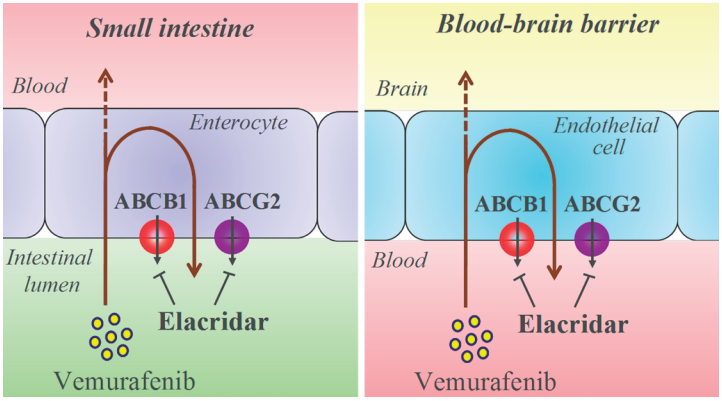

## INTRODUCTION

Melanoma is one of the deadliest form of skin cancer, metastasizing to the brain, liver and bone [1]. Until recently, treatment regimens for advanced melanoma were limited and virtually ineffective, resulting in very poor prognosis for stage IV metastatic melanoma patients with an estimated median survival time of less than a year [2]. However, there have been dramatic changes in the treatment strategies in the past years [3-5]. Recently, a small-molecule inhibitor of the cytoplasmic BRAF serine threonine kinase, vemurafenib (PLX4032 or RG7204) was developed to specifically inhibit B-Raf protein carrying a V600E mutation, which is present in ~66 % of malignant melanomas as well as other cancer types [6]. Clinical trials with this drug on $BRAF^{V600E}$-positive, brain metastasis-negative and previously untreated metastatic melanoma patients yielded promising results on survival benefit (84% vs. 64%) and overall response rate (48% vs. 5%) compared to the conventional chemotherapy [7-9]. However, brain metastases are one of the most common reasons for death in melanoma patients (20-54%) [10] and among those with brain metastases, up to 95% die from these lesions [11]. A clinical study has been started to evaluate the efficacy of vemurafenib in brain metastases (ClinicalTrials.gov identifier: NCT01378975). Therefore, it is highly relevant to investigate the mechanisms behind the brain penetration of vemurafenib and ways to improve the efficacy of vemurafenib in those patients as early as possible. Vemurafenib is also being tested on patients with other advanced or metastatic cancers and BRAF mutations (ClinicalTrials.gov identifiers: NCT01531361 and NCT00405587).

Multidrug efflux transporters of the ATP-binding cassette (ABC) protein family, such as P-glycoprotein (P-gp; ABCB1), Breast Cancer Resistance Protein (BCRP; ABCG2) and multidrug resistance protein 2 (MRP2; ABCC2) can have important roles in the efficacy of chemotherapy. These transporters are present in the apical membranes of several pharmacokinetically important tissues (e.g. small intestine) and pharmacological sanctuary site barriers such as the blood-brain barrier (BBB). Consequently, they affect oral uptake and tissue distribution of wide range of substrate drugs, for example by restricting their intestinal uptake, thus reducing oral bioavailability, and by restricting their brain penetration. Many chemotherapeutic agents, including several tyrosine kinase inhibitors (TKIs), are transported substrates of ABCB1 and ABCG2 and consequently show a restricted brain penetration [12-18]. These interactions with ABC transporters may affect the overall drug exposure and efficacy against tumor (micro-) metastases situated behind a functionally intact BBB. As recently demonstrated by Lockman et al., also parts of many larger brain metastases may be protected by the BBB and efflux transporters situated therein [19].

Vemurafenib, like most other TKIs, is administered orally in the clinic. Thus, depending on its interactions with ABC transporters, these might have a significant impact on oral bioavailability and tissue distribution of vemurafenib and determine the therapeutic efficacy on both primary tumors (if not completely surgically removed) and metastatic sites. In this study, we aimed to assess vemurafenib transport by human (h) hABCB1 (P-gp), hABCG2, and mouse (m) mAbcg2 and mAbcc2 *in vitro* and to establish their individual and combined effects on oral bioavailability and brain penetration of vemurafenib *in vivo*. We used two different vemurafenib dosages to cover different clinically relevant exposure levels. Furthermore, we investigated the possibility of increasing systemic exposure and brain accumulation of vemurafenib using the

clinically most plausible oral coadministration with elacridar, a dual inhibitor of P-gp and ABCG2, since this principle might be used to improve therapeutic efficacy, especially for metastases positioned behind the BBB.



## MATERIALS & METHODS

### Chemicals

Vemurafenib (PLX4032) and Elacridar hydrochloride were obtained from Sequoia Research Products (Pangbourne, UK). [14C]Inulin (5.6 Ci/mol) was from GE Healthcare (Little Chalfont, Buckinghamshire, UK). Zosuquidar (Eli Lilly; Indianapolis, USA) was a kind gift from Dr. O. van Tellingen (The Netherlands Cancer Institute, Amsterdam, NL) and Ko143 was obtained from Tocris Bioscience (Bristol, UK). All other chemicals used in the vemurafenib detection assay were described before [20].

### Transport assays

Polarized canine kidney MDCKII cell lines and subclones transduced with hABCB1, hABCG2, and mAbcg2 or mAbcc2 cDNA were used and cultured as described previously [21-25]. Transport assays were performed using 12-well Transwell® plates (Corning Inc., USA). The parental cells and variant subclones were seeded at a density of 3.5 or 2.5 x $10^5$ per well, respectively, and cultured for 3 days to form an intact monolayer. Membrane tightness was assessed by measurement of transepithelial electrical resistance (TEER). In parallel, monolayer tightness for all cell types except MDCKII-hABCB1 cells was validated by analyzing transepithelial [14C] inulin leakage using the same cells seeded on the same day and at the same density. Leakage had to remain <1% of the total added radioactivity per hour.

Preceding the transport experiment, cells were washed twice with PBS and pre-incubated with fresh DMEM medium (Invitrogen, USA) including 10% FBS (Sigma-Aldrich, USA), and with relevant inhibitors for 1 hour, if required. The transepithelial transport experiment was started (t = 0) by replacing the incubation medium with medium containing 5 μM vemurafenib in the donor compartment. In the inhibition experiments, 5 μM zosuquidar (P-gp inhibitor), 5 μM Ko143 (ABCG2/Abcg2 inhibitor) or 1 μM elacridar (dual P-gp and ABCG2/Abcg2 inhibitor) were added to both apical and basolateral compartments. Plates were kept at 37°C in 5% CO2 during the experiment, and 50 μL aliquots were taken from the acceptor compartment at 1, 2, 4, 8 and 24 h. Vemurafenib concentration was measured by LC-MS/MS. Total amount of drug transported to the acceptor compartment was calculated after correction for volume loss for each time point. Experiments were performed in triplicate and the mean amount of transport is shown in the graphs.

Active transport was expressed by the relative transport ratio (r), defined as r = apically directed amount of transport divided by basolaterally directed amount of translocation, at a defined time point.

### Animals

Mice were housed and handled according to institutional guidelines complying with Dutch legislation. Animals used were female WT, *Abcb1a/1b*$^{-/-}$, *Abcg2*$^{-/-}$, *Abcb1a/1b*$^{-/-}$*;Abcg2*$^{-/-}$ and

*Abcb1a/1b*$^{+/-}$;*Abcg2*$^{+/-}$ mice of a >99% FVB genetic background, between 8 and 13 weeks of age. Animals were kept in a temperature-controlled environment with a 12 h light / 12 h dark cycle and received a standard diet (AM-II, Hope Farms) and acidified water *ad libitum*.

**Drug solutions**

Vemurafenib was dissolved in DMSO (25 mg/ml) and further diluted with a mixture of Polysorbate 80, ethanol and $H_2O$ (20:13:67) to yield a concentration of 2.5 or 0.5 mg/ml. Vemurafenib was administered orally at 25 or 5 mg/kg body weight, using a volume of 10 ml/kg body weight. All working solutions were prepared freshly on the day of experiment.

**Plasma and brain pharmacokinetics**

Mice were fasted about 2-2.5 h before vemurafenib was orally administered in order to minimize the variation in absorption. For plasma pharmacokinetic studies, multiple blood samples (60 µl) were collected from the tail vein at 30 min and 1, 2, 4 and 8 h using heparinized capillary tubes (Sarstedt, Germany). At 4 (in a separate experiment) or 24 h, mice were anesthetized with isoflurane and blood was drawn by cardiac puncture. Immediately thereafter, mice were sacrificed by cervical dislocation and brains and a set of organs were rapidly removed. Organs were homogenized on ice in 1% bovine serum albumin, and stored at -20°C until analysis. Blood samples were centrifuged at 2,100 g for 6 min at 4°C immediately after collection; the plasma fraction was collected and stored at -20°C until analysis.

**Brain accumulation of vemurafenib in combination with elacridar**

Elacridar hydrochloride was dissolved in DMSO (106 mg/ml) in order to get 100 mg pure elacridar in 1 ml of DMSO. The stock solution was further diluted with a mixture of Polysorbate 80, ethanol and $H_2O$ (20:13:67) to yield a concentration of 10 mg/ml pure elacridar and orally administered at a dose of 100 mg/kg body weight (10 ml/kg). Vemurafenib was prepared as explained above and administered orally 90 minutes after oral administration of elacridar or vehicle. Blood and brains were isolated 4 h after vemurafenib administration, and processed and stored as described above.

**Relative brain accumulation**

Relative brain accumulation after oral administration of vemurafenib was calculated by determining the vemurafenib brain concentration relative to the plasma AUC from 0-4 or 0-24 h. Brain concentrations at 24 h were not corrected for the plasma levels in the brain vasculature since the plasma levels were usually negligible at 24 h. In order to keep the results comparable between all experiments, brain concentrations are used without correction for vascular content in all the figures and relevant calculations. In the brain accumulation study with a 4 h end-point, blood was collected only at the end of the experiment. Therefore, only brain-to-plasma ratios were calculated for this experiment (Figure 5B). Relative brain accumulation in this experiment was not likely to be very different from relative brain-to-plasma ratios since the difference in plasma AUC was quite well reflected by the plasma concentrations at 4 h, which is around $T_{max}$ (Figure 5A).

### Drug analysis

Vemurafenib concentrations in cell culture medium, plasma samples and brain homogenates were determined using a sensitive and specific liquid chromatography coupled with tandem mass spectrometry (LC-MS/MS) assay [20]. In order to quantify the vemurafenib in mouse samples, plasma and organ homogenates were pre-treated with water-acetonitrile (1/3, v/v) for protein precipitation. Sorafenib was used as internal standard due to its similar retention time with vemurafenib. The extract was directly injected into the chromatographic system that consisted of a sub-2 µm particle, trifunctional bonded octadecyl silica column with isocratic elution using 0.01% (v/v) of formic acid in a mixture of water and methanol. The eluate was then transferred into the electrospray interface with positive ionization and the analyte was detected in the selected reaction monitoring mode of a triple quadrupole mass spectrometer. Lower limit of quantification (LLQ) for vemurafenib was either 0.1 or 0.01 µg/ml in different experiments of this study.

### Pharmacokinetic calculations and statistical analysis

Pharmacokinetic parameters were calculated by non-compartmental methods using the software package PK Solutions 2.0.2 (Summit Research Services, Ashland, OH). The area under the plasma concentration-time curve was calculated using the trapezoidal rule, without extrapolating to infinity. The maximum drug concentration in plasma ($C_{max}$) and the time to reach maximum drug concentration in plasma ($T_{max}$) were determined directly from individual concentration-time data. One-way analysis of variance (ANOVA) was used to determine significance of differences between groups, after which post-hoc tests with Tukey correction were performed for comparison between individual groups. When variances were not homogeneous, data were log-transformed before statistical tests were applied. Differences were considered statistically significant when $P < 0.05$. Data are presented as means ± SD.

## RESULTS

### *In vitro* transport of vemurafenib by ABCB1 and ABCG2

In order to assess the transepithelial transport of vemurafenib, we used monolayers of MDCKII cells and its subclones overexpressing hABCB1, hABCG2, mAbcg2 or mAbcc2. In the MDCKII parental cell line, there was a modest apically directed transport of vemurafenib (r = 2.1, Figure 1A), which was completely inhibited with the ABCB1 (P-gp) inhibitor zosuquidar (Figure 1B), indicating modest transport by endogenous canine ABCB1. Zosuquidar was therefore added in subsequent experiments with hABCG2, mAbcg2, and mAbcc2 to suppress this background transport activity. In hABCB1- and hABCG2-overexpressing cells, there was a clearly increased apically directed transport of vemurafenib (r = 9.0 and 5.5, respectively, Figure 1C and E). In mAbcg2-overexpressing cells, apically directed transport was very efficient (r > 23.5), leading to undetectable drug levels in the basolateral compartment up till 8 h (Figure 1G). Transport specificity in these cell lines was confirmed by complete inhibition by either the ABCB1 inhibitor zosuquidar or the ABCG2/Abcg2 inhibitor Ko143 (Figure 1D, F and H). In cells overexpressing mAbcc2, there was no active transport of vemurafenib (Supplementary Figure 1). Thus, *in vitro* vemurafenib appears to be an extremely good substrate of mouse Abcg2 and a good substrate of human ABCB1 and ABCG2, but not of mouse Abcc2.

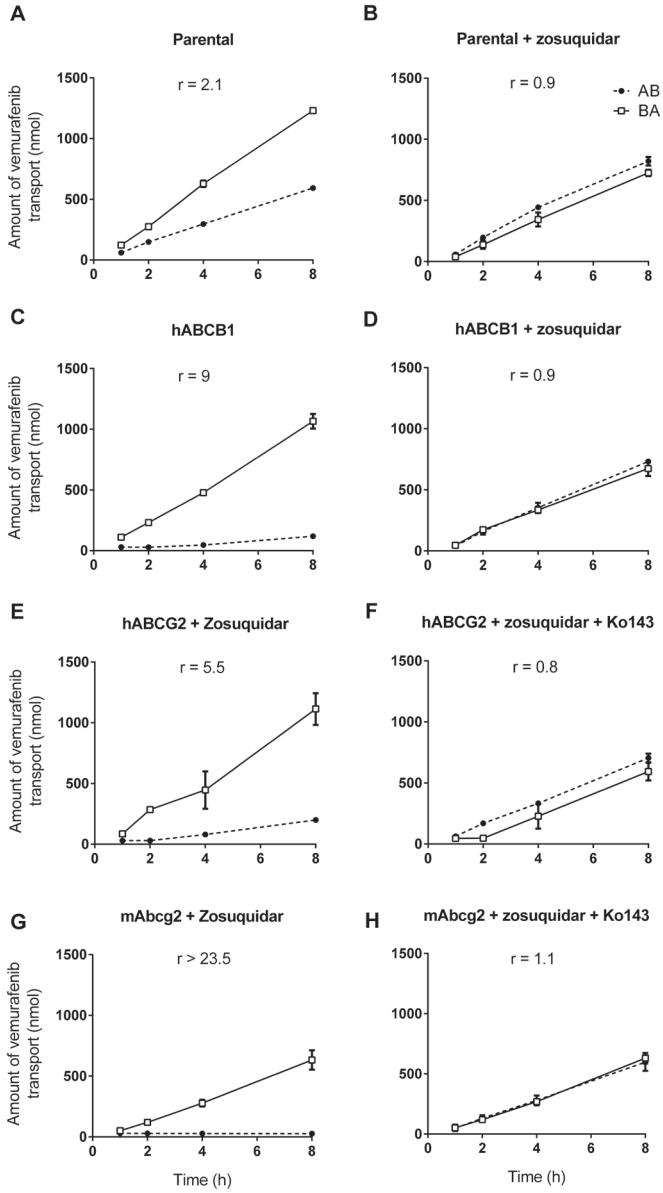


**Figure 1. Transepithelial transport of vemurafenib (5 μM) assessed in MDCK-II cells either nontransduced (A, B) or transduced with human ABCB1 (C, D), human ABCG2 (E, F) or murine Abcg2 (G,H) cDNA.** At t = 0 h, vemurafenib was applied in the donor compartment and the concentration in the acceptor compartment at t = 1, 2, 4, and 8 h was measured and plotted as total amount of transport (nmol) in the graphs (n = 3). B, D, E, F, G and H; Zosuquidar (5 μM) and/or Ko143 (5 μM) were applied to inhibit ABCB1, ABCG2 or Abcg2, respectively. r, relative transport ratio. ○, translocation from the basolateral to the apical compartment; ●, translocation from the apical to the basolateral compartment. Points, mean; bars, SD. 1000 nmol transport at t = 8 h corresponds to an apparent permeability coefficient ($P_{app}$) of 5.3 x $10^{-6}$ cm/s.

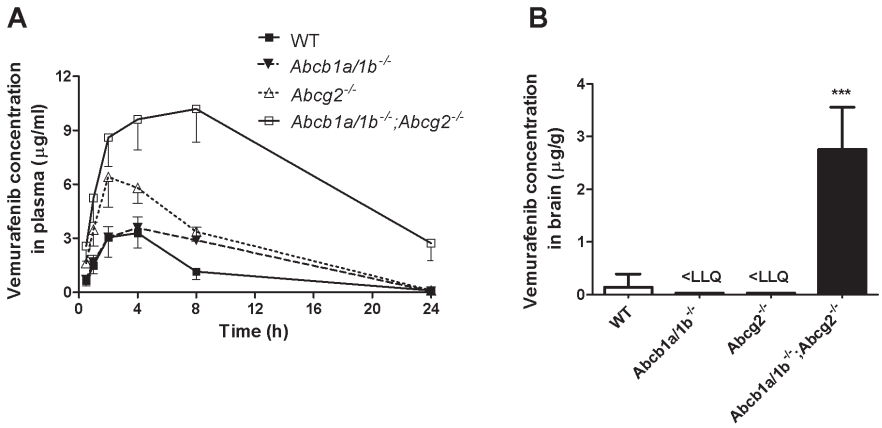


**Figure 2. Plasma concentration-time curve (A) and brain concentration at 24 h (B) of vemurafenib in female WT, *Abcb1a/1b*$^{-/-}$, *Abcg2*$^{-/-}$, and *Abcb1a/1b*$^{-/-}$;*Abcg2*$^{-/-}$ mice after oral administration of 5 mg/kg vemurafenib.** Correction for the significant plasma levels in the brains of *Abcb1a/1b*$^{-/-}$;*Abcg2*$^{-/-}$ mice yielded a 14.7-fold difference instead of 19.2-fold compared to the WT group; however significance levels still remained the same ($P < 0.001$). Points, mean (n = 3-10); bars, SD. 4/5 WT and all *Abcb1a/1b*$^{-/-}$ and *Abcg2*$^{-/-}$ brain concentrations were < LLQ and therefore for calculation purposes replaced with the LLQ value (0.03 µg/g).

### Abcb1a/1b and Abcg2 restrict plasma and brain accumulation of oral vemurafenib (5 mg/kg)

We further investigated the separate and combined effect of Abcb1a/1b and Abcg2 on the disposition of vemurafenib *in vivo*. Vemurafenib is administered to patients orally, so we studied plasma exposure of vemurafenib after oral administration of a dose of 5 mg/kg, which results in similar plasma levels in WT mice (Figure 2A) as seen in patients after a single administration of 960 mg vemurafenib [8]. Absence of Abcg2 resulted in a 2.3-fold higher plasma $AUC_{0\text{-}24h}$ ($P < 0.001$) and absence of Abcb1a/1b in a 1.6-fold ($P < 0.05$) higher plasma $AUC_{0\text{-}24h}$ compared to WT mice (Figure 2A, Table 1). The increase in plasma levels in *Abcg2*$^{-/-}$ mice was apparent from very early on (30 min), and lasted up till at least 8 h, whereas in *Abcb1a/1b*$^{-/-}$ mice the increase was only apparent after 4 h. This suggests that Abcg2 may be particularly important in reducing early intestinal uptake of vemurafenib, whereas Abcb1a/1b may be more important at later stages of the vemurafenib disposition. The combined deficiency of Abcb1a/1b and Abcg2 led to a pronounced, 6.6-fold higher plasma $AUC_{0\text{-}24h}$ compared to WT mice ($P < 0.001$), apparently caused by both more rapid drug uptake and delayed elimination, resulting in a $T_{max}$ of 8 h (Figure 2A, Table 1). In addition, brain concentrations of *Abcb1a/1b*$^{-/-}$;*Abcg2*$^{-/-}$ mice at 24 h were at least 19.7-fold higher than those in WT mice ($P < 0.001$, Figure 2B and Table 1). These results indicate that both Abcb1a/1b and Abcg2 restrict the oral availability and possibly the brain accumulation of vemurafenib at a dose of 5 mg/kg.

**Table 1.** Plasma pharmacokinetic parameters and brain concentrations 24 h after oral administration of 5 or 25 mg/kg vemurafenib to female WT, *Abcb1a/1b*$^{-/-}$, *Abcg2*$^{-/-}$ and *Abcb1a/1b*$^{-/-}$;*Abcg2*$^{-/-}$ mice.

| | | Genotype | | | |
|---|---|---|---|---|---|
| **Dose** | **Parameter** | **WT** | ***Abcb1a/1b*$^{-/-}$** | ***Abcg2*$^{-/-}$** | ***Abcb1a/1b*$^{-/-}$;*Abcg2*$^{-/-}$** |
| 5 mg/kg | $AUC_{0\text{-}24h}$ (µg/ml.h) | 28.2 ± 8.2 | 46.2 ± 10.3* | 64.9 ± 9.1*** | 186.7 ± 7.6*** |
| | $C_{max}$ (µg/ml) | 3.46 ± 0.98 | 3.58 ± 0.61 | 6.75 ± 1.45 | 11.87 ± 1.02 |
| | $T_{max}$ (h) | 4 | 4 | 2 | 8 |
| | $C_{brain}$ (µg/g) | 0.14 ± 0.25 | < LLQ | < LLQ | 2.76 ± 0.80*** |
| 25 mg/kg | $AUC_{0\text{-}24h}$ (µg/ml.h) | 288.9 ± 181.4 | 533.4 ± 68.1* | 335.7 ± 78.7 | 535.5 ± 155.9* |
| | $C_{max}$ (µg/ml) | 24.2 ± 11.4 | 38.2 ± 5.6 | 27.4 ± 6.4 | 35.6 ± 9.1 |
| | $T_{max}$ (h) | 4 | 4 | 4 | 4 |
| | $C_{brain}$ (µg/g) | < LLQ | < LLQ | < LLQ | 7.85 ± 1.97*** |

Abbreviations: $C_{brain}$, brain concentration. LLQ in 5 mg/kg and 25 mg/kg experiments were 0.03 and 0.14 µg/g, respectively. * P < 0.05; *** P < 0.001 compared to WT mice

### The dual Abcb1a/1b and Abcg2 inhibitor elacridar markedly enhances vemurafenib plasma and brain accumulation

Based on our findings that the combination of Abcb1a/1b and Abcg2 activity markedly restricted the plasma and brain concentrations of vemurafenib *in vivo*, we investigated the effect of coadministration of the efficient dual Abcb1a/1b and Abcg2 inhibitor elacridar on the disposition of vemurafenib in WT and *Abcb1a/1b*$^{-/-}$;*Abcg2*$^{-/-}$ mice. Elacridar (100 mg/kg) and vemurafenib (5 mg/kg) were both administered orally, as this would be the clinically most plausible administration route. To properly assess plasma and brain concentrations, we measured at t = 4 hour, i.e. not far from the vemurafenib $C_{max}$ and $T_{max}$ in each strain (Figure 2A).

Elacridar coadministration increased the plasma $AUC_{0\text{-}4h}$ of vemurafenib 2.5-fold in WT mice ($P < 0.05$, Table 2), to levels virtually indistinguishable from those in elacridar-treated *Abcb1a/1b*$^{-/-}$;*Abcg2*$^{-/-}$ mice (Figure 3A). In the absence of elacridar, the plasma $AUC_{0\text{-}4h}$ of vemurafenib was 3.3-fold higher in *Abcb1a/1b*$^{-/-}$;*Abcg2*$^{-/-}$ compared with WT mice ($P < 0.001$, Figure 3A, Table 2). With elacridar coadministration, plasma exposure of vemurafenib was not significantly different between *Abcb1a/1b*$^{-/-}$;*Abcg2*$^{-/-}$ and WT mice (Table 2). These findings indicate that elacridar substantially improved the oral availability of vemurafenib via Abcb1a/1b and Abcg2 inhibition.

Elacridar coadministration resulted in an even more pronounced increase in brain concentration and accumulation of vemurafenib. The brain concentrations (Figure 3B) and accumulations (Figure 3C) in each strain showed very similar trends. Vemurafenib accumulation in WT brain was increased 9.4-fold upon coadministration of elacridar ($P < 0.001$, Figure 3C). This was, however, not as high as the brain levels in vehicle- or elacridar-treated *Abcb1a/1b*$^{-/-}$;*Abcg2*$^{-/-}$ mice, which were both another 1.7-fold higher ($P < 0.05$, Figure 3C). Collectively, these data indicate that elacridar could extensively inhibit Abcb1a/1b and Abcg2 in the BBB, albeit not

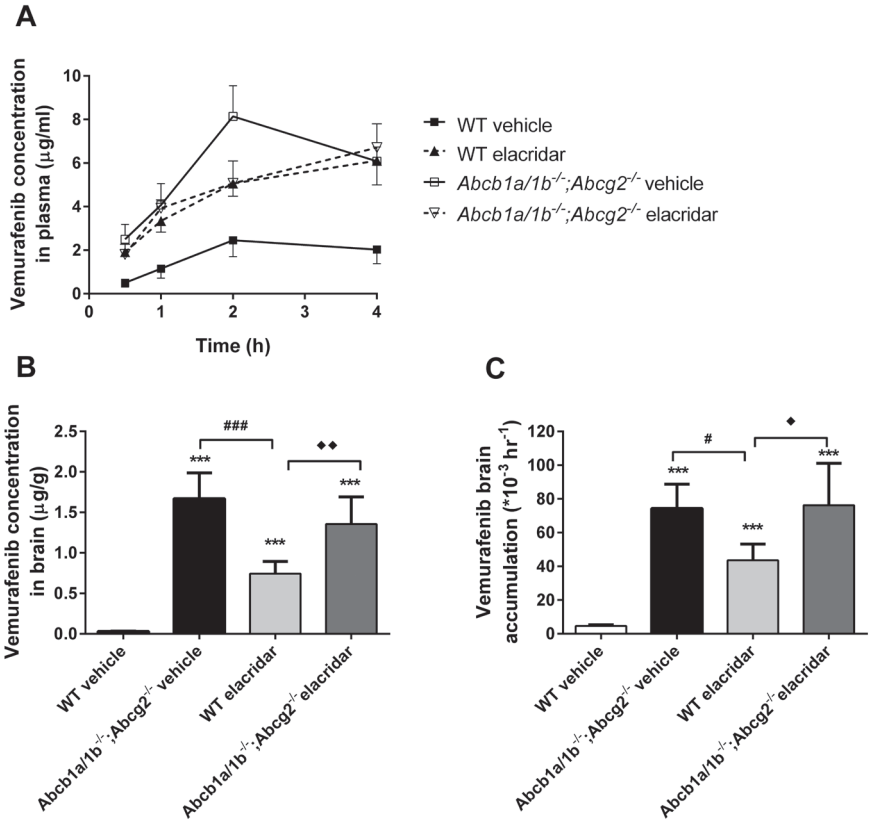


**Figure 3. Effect of elacridar coadministration on plasma exposure (A), brain concentration (B), and relative brain accumulation (C) of vemurafenib in female WT and *Abcb1a/1b*$^{-/-}$;*Abcg2*$^{-/-}$ mice 4 h after oral administration of 5 mg/kg vemurafenib.** Vemurafenib was administered 90 min after oral administration of vehicle or 100 mg/kg elacridar. Columns, mean (n = 5); bars, SD. ***, $P < 0.001$, compared with WT mice treated with vehicle. #, $P < 0.05$ and ###, $P < 0.001$, compared with *Abcb1a/1b*$^{-/-}$;*Abcg2*$^{-/-}$ mice treated with vehicle. ♦, $P < 0.05$ and ♦♦, $P < 0.01$, compared with WT mice treated with elacridar.

completely, resulting in a pronounced increase in brain accumulation of vemurafenib in WT mice. The lack of effect of elacridar on brain accumulation in the *Abcb1a/1b*$^{-/-}$;*Abcg2*$^{-/-}$ mice further suggests that no other efflux or uptake systems for vemurafenib across the BBB were affected by elacridar at this dose (Table 2).

### Effect of Abcb1a/1b and Abcg2 on plasma pharmacokinetics of oral vemurafenib (25 mg/kg)

In order to obtain plasma levels of vemurafenib in mice similar to steady-state therapeutic plasma concentrations in patients [8], we increased the dosage 5-fold to 25 mg/kg, which was the highest oral dose feasible due to solubility limitations of vemurafenib. The plasma levels (24.2 µg/ml) that we could thus reach in WT mice with a single oral bolus administration were

**Table 2.** Effect of elacridar on plasma pharmacokinetic parameters, brain concentrations and relative brain accumulations 4 h after oral administration of 5 mg/kg vemurafenib to female WT and *Abcb1a/1b*$^{-/-}$;*Abcg2*$^{-/-}$ mice.

| Dose | Parameter | Genotype and type of pre-treatment | | | |
|---|---|---|---|---|---|
| | | **WT** | ***Abcb1a/1b*$^{-/-}$;*Abcg2*$^{-/-}$** | **WT** | ***Abcb1a/1b*$^{-/-}$;*Abcg2*$^{-/-}$** |
| | | **Vehicle** | **Vehicle** | **Elacridar** | **Elacridar** |
| 5 mg/kg | $AUC_{0\text{-}4h}$ (µg/ml.h) | 6.84 ± 1.84 | 22.58± 1.96*** | 17.16± 1.93*** | 18.18 ± 2.29*** |
| | $C_{max}$ (µg/ml) | 2.46 ± 0.75 | 8.26 ± 1.24 | 6.11 ± 1.11 | 6.71 ± 1.09 |
| | $T_{max}$ (h) | 2 | 2 | 4 | 4 |
| | $C_{brain}$ (µg/g) | 0.03 ± 0.00 | 1.67 ± 0.32*** | 0.74 ± 0.15*** | 1.36 ± 0.33*** |
| | $P_{brain}$ (*$10^{-3}$ $h^{-1}$) | 4.64 ± 0.70 | 74.34 ± 14.45*** | 43.60 ± 9.60*** | 76.30 ± 24.89*** |

Abbreviations: $C_{brain}$, brain concentration; $P_{brain}$, relative brain accumulation, calculated by determining brain concentration relative to $AUC_{0\text{-}4h}$. *** P < 0.001 compared to WT mice treated with vehicle.

not far from the steady-state plasma levels in patients (~40 µg/ml). An interesting difference was observed with the oral plasma AUCs obtained at 5 mg/kg: Deficiency of only Abcg2 did not affect plasma pharmacokinetics after oral administration at 25 mg/kg, whereas *Abcb1a/1b*$^{-/-}$ mice displayed a 1.8-fold higher $AUC_{0\text{-}24}$ compared to WT mice ($P$ < 0.05, Figure 4, Table 1). *Abcb1a/1b*$^{-/-}$;*Abcg2*$^{-/-}$ mice had a 1.9-fold higher plasma exposure compared to WT mice ($P$ < 0.05, Figure 4, Table 1), which was not significantly different from that in *Abcb1a/1b*$^{-/-}$ mice. These results indicate that Abcb1a/1b, but not Abcg2, restricted the oral availability of vemurafenib at 25 mg/kg.

### Effect of Abcb1a/1b and Abcg2 on brain accumulation of oral vemurafenib (25 mg/kg)

Brain distribution of vemurafenib was analyzed 4 and 24 h after oral administration of 25 mg/kg vemurafenib. The brain concentration and brain-to-plasma ratio of vemurafenib were not increased in *Abcg2*$^{-/-}$ mice at 4 h post-dose (Figure 5A), whereas *Abcb1a/1b*$^{-/-}$ mice had 2.3-fold higher brain concentrations ($P$ < 0.01, Figure 5A), and a 1.7-fold higher brain-to-plasma ratio compared to WT mice ($P$ < 0.001, Figure 5B). At 24 h, brain and plasma levels of WT mice and the brain levels in most of the *Abc1a/1b*$^{-/-}$ and *Abcg2*$^{-/-}$ mice were below the detection limit, preventing reliable calculation of brain-to-plasma ratios (Figure 5C).

When both Abcb1a/1b and Abcg2 transporters were deleted, brain levels of vemurafenib were again highly increased at both 4 and 24 h, indicating the impact of these transporters also at therapeutically relevant plasma concentrations. Vemurafenib concentrations in brain were increased 42.6-fold ($P$ < 0.001, Figure 5A) at 4 h and further to at least 51-fold ($P$ < 0.001, Figure 5C) at 24 h in *Abcb1a/1b*$^{-/-}$;*Abcg2*$^{-/-}$mice compared to WT mice. At 4 h, brain-to-plasma ratios of *Abcb1a/1b*$^{-/-}$;*Abcg2*$^{-/-}$ mice were 21.4-fold higher than in WT mice ($P$ < 0.001, Figure 5B). However, single Abcb1a/1b deficiency resulted in only a modest but significant increase in brain-to-plasma ratios (1.7-fold, $P$ < 0.001), whereas single Abcg2 deficiency did not (Figure 5B). These results show that Abcb1a/1b and Abcg2 each individually had a major impact on the vemurafenib

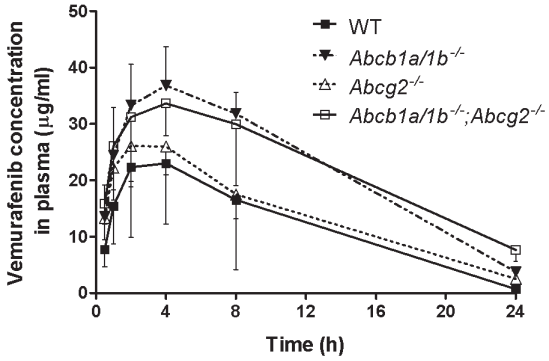


**Figure 4. Plasma concentration-time curve of vemurafenib in female WT, *Abcb1a/1b*$^{-/-}$, *Abcg2*$^{-/-}$, and *Abcb1a/1b*$^{-/-}$;*Abcg2*$^{-/-}$ mice after oral administration of 25 mg/kg vemurafenib.** Points, mean (n = 6); bars, SD.

brain accumulation, and that both Abcb1a/1b and Abcg2 could largely take over each other's function in restricting vemurafenib brain accumulation across the BBB. Nonetheless, there does appear to be a somewhat larger contribution of Abcb1a/1b compared to Abcg2 in the BBB.

### Effect of the dual Abcb1a/1b and Abcg2 inhibitor elacridar on vemurafenib brain accumulation at 25 mg/kg

Analogous to the elacridar experiment at 5 mg/kg vemurafenib, we also tested the impact of coadministration of oral elacridar (100 mg/kg) with 25 mg/kg oral vemurafenib in WT and *Abcb1a/1b*$^{-/-}$;*Abcg2*$^{-/-}$ mice. As expected, in this experiment brain concentrations of vemurafenib at t = 4 h were about 3-5-fold higher, but the overall qualitative impact of elacridar on improving brain accumulation of vemurafenib in the WT strain was quite similar as observed with 5 mg/kg vemurafenib (See Supplemental Figure 2A and B, and compare with Figure 3B and C). Thus, also at vemurafenib plasma levels close to the therapeutically relevant concentrations, elacridar coadministration was effective in greatly improving vemurafenib brain penetration.

### Plasma and brain disposition of vemurafenib in heterozygous *Abcb1a/1b*$^{+/-}$;*Abcg2*$^{+/-}$ mice

The disproportionate effect of removing both Abcb1a/1b and Abcg2 from the BBB on brain penetration of vemurafenib relative to the effect of removing only one of these transporters is surprising at first sight. Yet, similar behavior has been observed for a number of other drugs, including TKIs, that are shared substrates of Abcb1 and Abcg2 [14, 15, 17, 18]**.** Kodaira *et al*. [12] have developed a straightforward pharmacokinetic model that describes that such a disproportionate effect is expected in cases where the passive (or non-Abcb1/non-Abcg2-mediated) clearance of drugs from the brain is small compared to the active efflux clearances by Abcb1 or Abcg2 at the BBB. This situation appears to apply to vemurafenib. An immediate experimental prediction of this theoretical model is that halving the amount of active efflux clearance for vemurafenib at the BBB from the WT situation should have only a very small impact on vemurafenib brain penetration, whereas complete removal of the active efflux

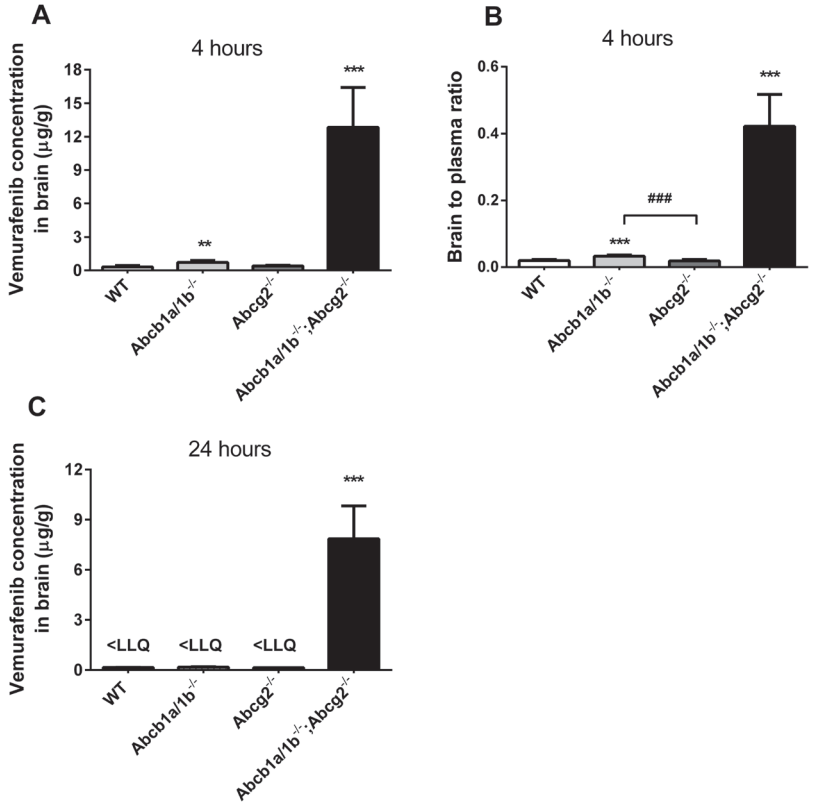


**Figure 5. Vemurafenib brain concentration (A) and brain-to-plasma ratio at 4 h (B) and brain concentration at 24 h (C) in female WT, *Abcb1a/1b*$^{-/-}$, *Abcg2*$^{-/-}$ and *Abcb1a/1b*$^{-/-}$;*Abcg2*$^{-/-}$ mice 4 and 24 h after oral administration of 25 mg/kg vemurafenib.** Columns, mean (n = 5-6); bars, SD. **, P < 0.05; *** and ###, P < 0.001, compared with WT and Abcg2-/- mice, respectively.

clearance should have a big impact. Halving the amount of active efflux clearance by Abcb1 and Abcg2 at the BBB can be easily achieved by generating mice heterozygous for the Abcb1a/1b and Abcg2 knockout alleles. We thus generated these *Abcb1a/1b*$^{+/-}$;*Abcg2*$^{+/-}$ mice, which were, as expected, physiologically normal.

We then tested plasma exposure and brain accumulation of 25 mg/kg orally administered vemurafenib over 4 h in WT, *Abcb1a/1b*$^{+/-}$;*Abcg2*$^{+/-}$, and *Abcb1a/1b*$^{-/-}$;*Abcg2*$^{-/-}$ mice (Figure 6). The plasma $AUC_{0\text{-}4h}$ was again modestly increased in *Abcb1a/1b*$^{-/-}$;*Abcg2*$^{-/-}$ mice (1.4-fold, $P < 0.05$), but also in *Abcb1a/1b*$^{+/-}$;*Abcg2*$^{+/-}$ mice (1.3-fold, $P < 0.05$) compared to WT mice (Figure 6A). The brain accumulation at 4 h was, however, not significantly increased in the heterozygous *Abcb1a/1b*$^{+/-}$;*Abcg2*$^{+/-}$ mice (by 1.3-fold), whereas it was dramatically increased (by 21.5-fold, $P < 0.001$) in the *Abcb1a/1b*$^{-/-}$;*Abcg2*$^{-/-}$ mice compared to WT (Figure 6B). These experimental results are fully in line with the theoretical prediction of the pharmacokinetic model of Kodaira *et al.* [12], and thus further support its validity.

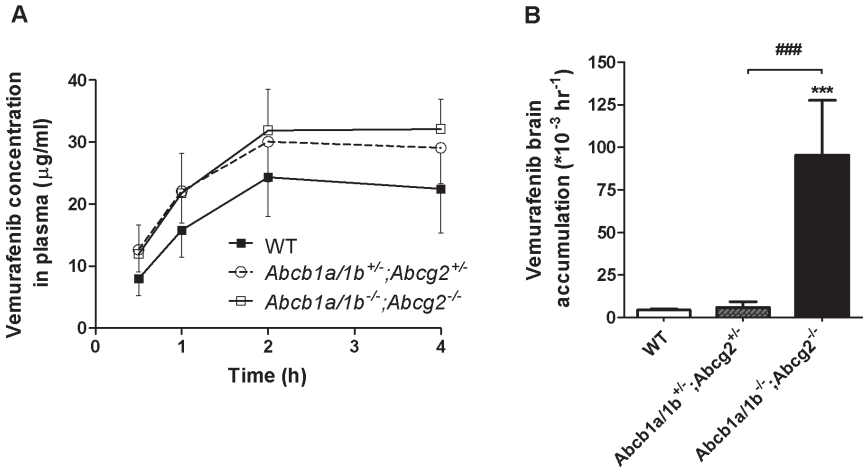


**Figure 6. Plasma concentration-time curve (A) and brain accumulation at t = 4 h (B) of vemurafenib in female WT, *Abcb1a/1b*$^{+/-}$;*Abcg2*$^{+/-}$ and *Abcb1a/1b*$^{-/-}$;*Abcg2*$^{-/-}$ mice after oral administration of 25 mg/kg vemurafenib.** Points, mean (n = 6-7); bars, SD. *** and ###, $P < 0.001$, compared with WT and *Abcb1a/1b*$^{+/-}$;*Abcg2*$^{+/-}$mice, respectively.

## DISCUSSION

Given the therapeutic success of vemurafenib in metastatic melanoma patients and the current clinical trials assessing efficacy against brain metastases, our primary interest in this study was to find ways to improve the oral availability of vemurafenib and its delivery across the BBB. We therefore focused on ABCB1- and ABCG2-mediated restriction of oral availability and brain penetration of vemurafenib. *In vitro*, we found that vemurafenib was very efficiently transported by mAbcg2 and efficiently by both hABCB1 and hABCG2, but not by mAbcc2. *In vivo*, oral availability and especially brain accumulation were clearly restricted by both Abcb1a/1b and Abcg2, albeit to varying extents, and dependent on the dosage of vemurafenib used. Accordingly, when elacridar was orally coadministered with vemurafenib in WT mice, both oral availability and brain accumulation of vemurafenib could be highly increased. Finally, we found that when active efflux transport of vemurafenib at the BBB was halved using heterozygous *Abcb1a/1b*$^{+/-}$;*Abcg2*$^{+/-}$ mice, there was very little impact on vemurafenib brain accumulation, whereas complete removal of Abcb1a/1b and Abcg2 resulted in dramatically increased brain accumulation.

As the present study was nearing completion, Mittapalli *et al*. reported that vemurafenib could be transported by human ABCB1 and mouse Abcg2, and that the simultaneous absence of Abcb1a/1b and Abcg2 in knockout mice, but not the single absence of Abcb1a/1b or Abcg2, resulted in significantly increased brain-to-plasma ratios of vemurafenib [26]. While the brain accumulation data were qualitatively similar to our results, it is worth noting that they were obtained with plasma vemurafenib concentrations in WT mice well below the therapeutically relevant plasma concentrations, or using clinically less relevant (parenteral) administration

routes. Vemurafenib oral availability, *in vivo* inhibition of ABC transporter activity, or mechanistic aspects of BBB transporter interplay were not addressed by Mittapalli *et al.* [26].

Our *in vitro* experiments showed that in addition to hABCB1 and mAbcg2, hABCG2 is also an efficient transporter of vemurafenib. We then investigated the *in vivo* disposition of vemurafenib in Abcb1a/1b and Abcg2 knockout mice at two different oral dosages. Interestingly, we observed a dose-dependent effect of Abcg2 on the oral availability of vemurafenib. At 5 mg/kg, both Abcg2 and Abcb1a/1b restricted the oral availability of vemurafenib, with Abcg2 appearing more important in reducing the early intestinal uptake of vemurafenib, and Abcb1a/1b in reducing plasma levels at later stages of the vemurafenib disposition. Surprisingly, at 25 mg/kg the impact of Abcg2 was no longer noticeable and oral availability of vemurafenib was restricted only by Abcb1a/1b. This suggests that intestinal Abcg2, but not Abcb1a/1b, may have been saturated at this high oral dose. To our knowledge, this is the first study showing that oral availability of a drug is restricted primarily by Abcg2 at a low dose and by Abcb1a/1b at a high dose. It is further worth noting that the combined impact of Abcg2 and Abcb1a/1b on reducing vemurafenib oral availability (at 5 mg/kg) was surprisingly large (nearly 7-fold) when compared to other TKIs analyzed to date, which would rarely display more than a 2-fold effect.

In contrast to the intestinal barrier, Abcg2 (and Abcb1a/1b) vemurafenib transport activity at the BBB was not saturated upon an oral dose of 25 mg/kg, presumably reflecting a lower local vemurafenib concentration in blood than in the intestinal lumen. Consequently, brain vemurafenib accumulation was strongly reduced by both Abcg2 and Abcb1a/1b (>20-fold), although loss of Abcb1a/1b alone also caused a 1.7-fold increase in brain accumulation whereas single Abcg2 loss had no detectable effect (Figure 5B). This suggests that, even though Abcb1a/1b and Abcg2 can nearly completely take over each other's function at the BBB, Abcb1a/1b still has a somewhat larger role than Abcg2. This might reflect beginning saturation of Abcg2, but also the 5-fold higher abundance of Abcb1a at the mouse BBB [27], or other intrinsic differences in efficacy of vemurafenib transport by each transporter. Nonetheless, the typical disproportionate, or "synergistic" effect of combined loss of Abcb1a and Abcg2, resulting in very highly increased brain penetration of many TKIs and some other drugs in *Abcb1a/1b*$^{-/-}$*;Abcg2*$^{-/-}$ mice compared to the single knockout strains [12, 14, 15, 17, 18, 28-30] is also clearly apparent for vemurafenib.

It was initially considered that these disproportionate effects might be caused by compensatory upregulation of Abcb1a in the BBB of *Abcg2*$^{-/-}$ mice, and of Abcg2 in *Abcb1a/1b*$^{-/-}$ mice. However, a range of analyses of brain RNA levels by RT-PCR, of brain or brain capillary protein levels by western blot and quantitative proteomics, and functional brain uptake analyses using transporter-specific drug substrates, have clearly established that such upregulation does not occur in the FVB genetic background knockout strains used by most investigators including us [12, 15, 27, 31, 32]. In addition, also levels of a range of other transporters and receptor proteins were found to be unchanged in the BBB of these knockout strains, revealing a remarkable stability upon these genotypic modifications. The pharmacokinetic model of Kodaira *et al.* [12] provides a straightforward theoretical explanation for the observed disproportionate effects. It predicts that in cases where the remaining brain efflux in the combination knockout mice is small

compared to the active efflux of either Abcb1a or Abcg2 alone, a small or even experimentally negligible effect on brain accumulation is expected of single removal of each transporter, and a pronounced effect of the combined removal of both transporters. The results we obtained with vemurafenib brain accumulation upon exactly halving the total amount of active efflux transport at the BBB using heterozygous *Abcb1a/1b*$^{+/-}$*;Abcg2*$^{+/-}$ mice (Figure 6B) provide strong experimental support for this model.

Considering the very limited brain penetration of vemurafenib observed in WT mice at both 5 and 25 mg/kg doses, and its potential relevance for limiting therapeutic efficacy against brain metastases, we focused on ways to improve the brain concentration of vemurafenib. We could show that oral coadministration of elacridar strongly increased oral availability and brain penetration of vemurafenib in WT mice. Especially at the clinically more relevant higher vemurafenib dose (25 mg/kg), the brain penetration in elacridar-treated WT mice approached that of vehicle-treated combination knockout mice. Still, while very extensive, the inhibition of Abcb1a and Abcg2 at the BBB may not have been complete, as illustrated by the approximately 2-fold higher brain accumulations in elacridar-treated *Abcb1a/1b*$^{-/-}$*;Abcg2*$^{-/-}$ versus elacridar-treated WT mice (Figure 3C and Supplemental Figure 2B). Even so, we demonstrated that nearly complete inhibition can be achieved using a clinically realistic coadministration schedule. After further preclinical and clinical assessments, our findings can therefore provide a rationale for a clinically realistic improved treatment for brain (micro-)metastases of BRAF$^{V600E}$–positive melanoma by enhancing oral availability and especially brain penetration of vemurafenib using oral coadministration of elacridar and vemurafenib.

## ACKNOWLEDGEMENTS

We thank Dilek Iusuf and Seng Chuan Tang for critical reading of the manuscript.

## REFERENCE LIST

1. Lee SM, Betticher DC, Thatcher N. Melanoma: chemotherapy. Br Med *Bull 1995*; 51:609-630.
2. Garbe C, Eigentler TK, Keilholz U, Hauschild A, Kirkwood JM. Systematic review of medical treatment in melanoma: current status and future prospects. *Oncologist 2011*; 16:5-24.
3. Ascierto PA, Kirkwood JM, Grob JJ, Simeone E, Grimaldi AM, Maio M et al. *The r*ole of BRAF V600 mutation in melanoma. *J Transl Med 2012*; 10:85.
4. Lemech C, Arkenau HT. Novel treatments for metastatic cutaneous melanoma and the management of emergent toxicities. *Clin Med Insights Oncol 2012*; 6:53-66.
5. Verschraegen C. The monoclonal antibody to cytotoxic T lymphocyte antigen 4, ipilimumab, in the treatment of melanoma. *Cancer Manag Res 2012*; 4:1-8.
6. Davies H, Bignell GR, Cox C, Stephens P, Edkins S, Clegg S et al. *Muta*tions of the BRAF gene in human cancer. *Nature 2002*; 417:949-954.
7. FDA approves vemurafenib for treatment of metastatic melanoma. *Oncology (Williston Park) 2011*; 25:906.
8. Chapman PB, Hauschild A, Robert C, Haanen JB, Ascierto P, Larkin J et al. *Impro*ved survival with vemurafenib in melanoma with BRAF V600E mutation. *N Engl J Med 2011*; 364:2507-2516.
9. Flaherty KT, Puzanov I, Kim KB, Ribas A, McArthur GA, Sosman JA et al. *Inhib*ition of mutated, activated BRAF in metastatic melanoma. *N Engl J Med 2010*; 363:809-819.
10. Skibber JM, Soong SJ, Austin L, Balch CM, Sawaya RE. Cranial irradiation after surgical excision of brain metastases in melanoma patients. *Ann Surg Oncol 1996*; 3:118-123.
11. Sampson JH, Carter JH, Jr., Friedman AH, Seigler HF. Demographics, prognosis, and therapy in 702 patients with brain metastases from malignant melanoma. *J Neurosurg 1998*; 88:11-20.

12. Kodaira H, Kusuhara H, Ushiki J, Fuse E, Sugiyama Y. Kinetic analysis of the cooperation of P-glycoprotein (P-gp/Abcb1) and breast cancer resistance protein (Bcrp/Abcg2) in limiting the brain and testis penetration of erlotinib, flavopiridol, and mitoxantrone. *J Pharmacol Exp Ther 2010*; 333:788-796.
13. Lagas JS, Sparidans RW, van Waterschoot RA, Wagenaar E, Beijnen JH, Schinkel AH. P-glycoprotein limits oral availability, brain penetration, and toxicity of an anionic drug, the antibiotic salinomycin. *Antimicrob Agents Chemother 2008*; 52:1034-1039.
14. Lagas JS, van Waterschoot RA, van Tilburg VA, Hillebrand MJ, Lankheet N, Rosing H et al. *Brain* accumulation of dasatinib is restricted by P-glycoprotein (ABCB1) and breast cancer resistance protein (ABCG2) and can be enhanced by elacridar treatment. *Clin Cancer Res 2009*; 15:2344-2351.
15. Lagas JS, van Waterschoot RA, Sparidans RW, Wagenaar E, Beijnen JH, Schinkel AH. Breast cancer resistance protein and P-glycoprotein limit sorafenib brain accumulation. *Mol Cancer Ther 2010*; 9:319-326.
16. Shukla S, Chen ZS, Ambudkar SV. Tyrosine kinase inhibitors as modulators of ABC transporter-mediated drug resistance. *Drug Resist Updat 2012*; 15:70-80.
17. Tang SC, Lagas JS, Lankheet NA, Poller B, Hillebrand MJ, Rosing H et al. *Brain* accumulation of sunitinib is restricted by P-glycoprotein (ABCB1) and breast cancer resistance protein (ABCG2) and can be enhanced by oral elacridar and sunitinib coadministration. *Int J Cancer 2012*; 130:223-233.
18. Tang SC, Lankheet NA, Poller B, Wagenaar E, Beijnen JH, Schinkel AH. P-glycoprotein (ABCB1) and breast cancer resistance protein (ABCG2) restrict brain accumulation of the active sunitinib metabolite N-desethyl sunitinib. *J Pharmacol Exp Ther 2012*; 341:164-173.
19. Lockman PR, Mittapalli RK, Taskar KS, Rudraraju V, Gril B, Bohn KA et al. *Hetero*geneous blood-tumor barrier permeability determines drug efficacy in experimental brain metastases of breast cancer. *Clin Cancer Res 2010*; 16:5664-5678.
20. Sparidans RW, Durmus S, Schinkel AH, Schellens JH, Beijnen JH. Liquid chromatography-tandem mass spectrometric assay for the mutated BRAF inhibitor vemurafenib in human and mouse plasma. *J Chromatogr B Analyt Technol Biomed Life Sci 2012;* 889-890:144-147.
21. Bakos E, Evers R, Szakacs G, Tusnady GE, Welker E, Szabo K et al. *Functio*nal multidrug resistance protein (MRP1) lacking the N-terminal transmembrane domain. J Biol *Chem 1998*; 273:32167-32175.
22. Jonker JW, Buitelaar M, Wagenaar E, Van Der Valk MA, Scheffer GL, Scheper RJ et al. *The b*reast cancer resistance protein protects against a major chlorophyll-derived dietary phototoxin and protoporphyria. *Proc Natl Acad Sci U S A 2002*; 99:15649-15654.
23. Pavek P, Merino G, Wagenaar E, Bolscher E, Novotna M, Jonker JW et al. *Human* breast cancer resistance protein: interactions with steroid drugs, hormones, the dietary carcinogen 2-amino-1-methyl-6-phenylimidazo(4,5-b)pyridine, and transport of cimetidine. *J Pharmacol Exp Ther 2005*; 312:144-152.
24. Poller B, Wagenaar E, Tang SC, Schinkel AH. Double-transduced MDCKII cells to study human P-glycoprotein (ABCB1) and breast cancer resistance protein (ABCG2) interplay in drug transport across the blood-brain barrier. *Mol Pharm 2011*; 8:571-582.
25. Zimmermann C, van de Wetering K, van de Steeg E, Wagenaar E, Vens C, Schinkel AH. Species-dependent transport and modulation properties of human and mouse multidrug resistance protein 2 (MRP2/Mrp2, ABCC2/Abcc2). *Drug Metab Dispos 2008*; 36:631-640.
26. Mittapalli RK, Vaidhyanathan S, Sane R, Elmquist WF. Impact of P-glycoprotein (ABCB1) and Breast Cancer Resistance Protein (ABCG2) on the Brain Distribution of a novel B-RAF Inhibitor: Vemurafenib (PLX4032). *J Pharmacol Exp Ther 2012*.
27. Agarwal S, Uchida Y, Mittapalli RK, Sane R, Terasaki T, Elmquist WF. Quantitative Proteomics of Transporter Expression in Brain Capillary Endothelial Cells Isolated from P-Glycoprotein (P-gp), Breast Cancer Resistance Protein (Bcrp), and P-gp/Bcrp Knockout Mice. *Drug Metab Dispos 2012*; 40:1164-1169.
28. Agarwal S, Sane R, Gallardo JL, Ohlfest JR, Elmquist WF. Distribution of gefitinib to the brain is limited by P-glycoprotein (ABCB1) and breast cancer resistance protein (ABCG2)-mediated active efflux. *J Pharmacol Exp Ther 2010*; 334:147-155.
29. Polli JW, Olson KL, Chism JP, John-Williams LS, Yeager RL, Woodard SM et al. *An une*xpected synergist role of P-glycoprotein and breast cancer resistance protein on the central nervous system penetration of the tyrosine kinase inhibitor lapatinib (N-{3-chloro-4-[(3-fluorobenzyl)oxy] phenyl}-6-[5-({[2-(methylsulfonyl)ethyl]amino } methyl)-2-furyl]-4-quinazolinamine; GW572016). *Drug Metab Dispos 2009*; 37:439-442.

30. Zhou L, Schmidt K, Nelson FR, Zelesky V, Troutman MD, Feng B. The effect of breast cancer resistance protein and P-glycoprotein on the brain penetration of flavopiridol, imatinib mesylate (Gleevec), prazosin, and 2-methoxy-3-(4-(2-(5-methyl-2-phenyloxazol-4-yl)ethoxy) phenyl)propanoic acid (PF-407288) in mice. *Drug Metab Dispos 2009*; 37:946-955.

31. Agarwal S, Elmquist WF. Insight into the cooperation of P-glycoprotein (ABCB1) and breast cancer resistance protein (ABCG2) at the blood-brain barrier: a case study examining sorafenib efflux clearance. *Mol Pharm 2012*; 9:678-684.

32. de Vries NA, Zhao J, Kroon E, Buckle T, Beijnen JH, van TO. P-glycoprotein and breast cancer resistance protein: two dominant transporters working together in limiting the brain penetration of topotecan. *Clin Cancer Res 2007*; 13:6440-6449.

## SUPPLEMENTARY MATERIALS

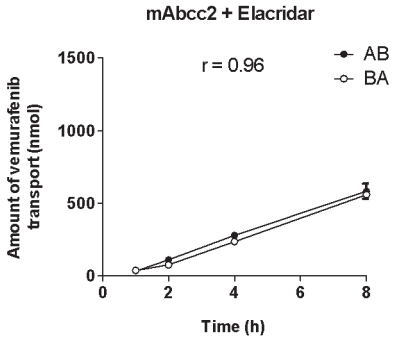


**Supplementary figure 1. Transepithelial transport of vemurafenib (5 µM) was assessed in MDCK-II cells transduced with mAbcc2.** At t = 0 h, vemurafenib was applied in the donor compartment and the concentration in the acceptor compartment at t = 1, 2, 4, and 8 h was measured by LC-MS/MS and plotted as total amount of transport (nmol) in the graphs (n = 3). Elacridar (1 µM) was applied to inhibit endogenous ABCB1 activity. r, relative transport ratio. ○, translocation from the basolateral to the apical compartment; ●, translocation from the apical to the basolateral compartment. Points, mean; bars, SD.

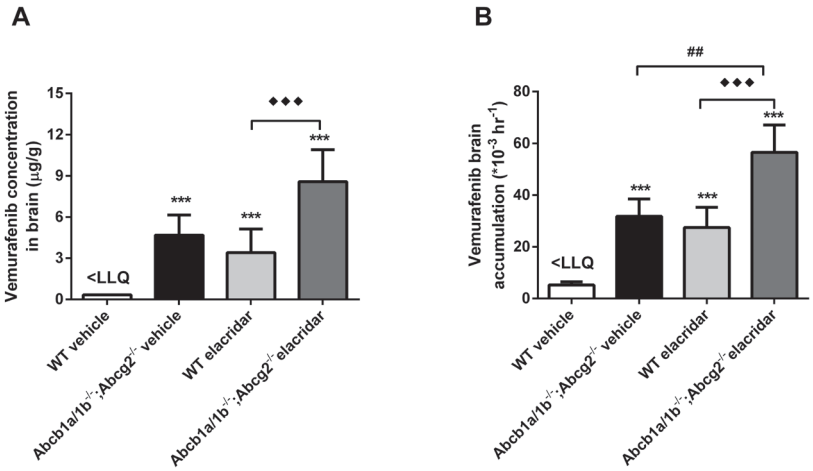


**Supplementary figure 2. Effect of elacridar on brain concentrations (A) and relative brain accumulations (B) of female WT and *Abcb1a/1b*$^{-/-}$*;Abcg2*$^{-/-}$ mice 4 h after oral administration of 25 mg/kg vemurafenib.** Vemurafenib was administered 90 min after oral administration of vehicle or 100 mg/kg elacridar. Brain accumulation of WT mice (panel B) was calculated assuming that WT brain concentrations (panel A) were 0.3 µg/g (LLQ), which is likely an overestimate; therefore actual brain accumulation of WT mice may be considerably lower than what is presented in this graph (panel B). Columns, mean (n = 5-7); bars, SD. ***, $P < 0.001$, compared with WT mice treated with vehicle. ##, $P < 0.01$, compared with *Abcb1a/1b*$^{-/-}$*;Abcg2*$^{-/-}$ mice treated with vehicle. ◆◆◆, $P < 0.001$, compared with WT mice treated with elacridar.

# CHAPTER 2.2

## P-GLYCOPROTEIN (MDR1/ABCB1) AND BREAST CANCER RESISTANCE PROTEIN (BCRP/ABCG2) RESTRICT BRAIN ACCUMULATION OF THE JAK1/2 INHIBITOR, CYT387

S. Durmus[a], N. Xu[a,d], R.W. Sparidans[b], E. Wagenaar[a], J.H. Beijnen[b,c] and A.H. Schinkel[a]

[a] The Netherlands Cancer Institute, Division of Molecular Oncology, Plesmanlaan 121, 1066 CX Amsterdam, The Netherlands.
[b] Utrecht University, Faculty of Science, Department of Pharmaceutical Sciences, Division of Pharmacoepidemiology & Clinical Pharmacology, Universiteitsweg 99, 3584 CG Utrecht, The Netherlands.
[c] Slotervaart Hospital, Department of Pharmacy & Pharmacology, Louwesweg 6, 1066 EC Amsterdam, The Netherlands.
[d] China-Japan Union Hospital of Jilin University, Department of Breast Surgery, Xiantai Street No.126, 130033, Changchun, China

*Pharmacological Research, 2013 Oct;76:9-16.*

## ABSTRACT

CYT387 is an orally bioavailable, small molecule inhibitor of Janus family of tyrosine kinases (JAK) 1 and 2. It is currently undergoing Phase I/II clinical trials for the treatment of myelofibrosis and myeloproliferative neoplasms. We aimed to establish whether the multidrug efflux transporters P-glycoprotein (P-gp; MDR1; ABCB1) and breast cancer resistance protein (BCRP;ABCG2) restrict oral availability and brain penetration of CYT387. In vitro, CYT387 was efficiently transported by both human MDR1 and BCRP, and very efficiently by mouse Bcrp1 and its transport could be inhibited by specific MDR1 inhibitor, zosuquidar and/or specific BCRP inhibitor, Ko143. CYT387 (10 mg/kg) was orally administered to wild-type (WT), Bcrp1-/-, Mdr1a/1b-/- and Bcrp1;Mdr1a/1b-/- mice and plasma and brain concentrations were analyzed. Over 8 h, systemic exposure of CYT387 was similar between all the strains, indicating that these transporters do not substantially limit oral availability of CYT387. Despite the similar systemic exposure, brain accumulation of CYT387 was increased 10.5- and 56-fold in the Bcrp1;Mdr1a/1b-/- mice compared to the WT strain at 2 and 8 h after CYT387 administration, respectively. In single Bcrp1-/- mice, brain accumulation of CYT387 was more substantially increased than in Mdr1a/1b-/- mice, suggesting that CYT387 is a slightly better substrate of Bcrp1 than of Mdr1a at the blood-brain barrier. These results indicate a marked and additive role of Bcrp1 and Mdr1a/1b in restricting brain penetration of CYT387, potentially limiting efficacy of this compound against brain (micro) metastases positioned behind a functional blood-brain barrier.

## INTRODUCTION

ATP-binding cassette (ABC) drug efflux transporters, such as P-glycoprotein (P-gp;MDR1;ABCB1) and breast cancer resistance protein (BCRP;ABCG2) are widely expressed in different tissues (e.g. small intestine, liver, blood-brain barrier) and play important roles in the absorption, distribution, excretion and toxicity of xenobiotics. Many anti-cancer drugs, including several tyrosine kinase inhibitors (TKIs), are substrates of both MDR1 and BCRP, and their interaction with ABC transporters may affect pharmacokinetics, therapeutic efficacy, and toxicity of these drugs in patients. Indeed, several chemotherapeutic agents that are MDR1 and BCRP substrates have restricted brain penetration [1-9]. Improving brain penetration of drugs is of long-standing interest in the clinic, because current systemic therapies are often inefficient in eradicating brain metastases or tumor parts or rims that are behind an intact blood-brain barrier (BBB) [10, 11].

Janus kinases (JAK) 1 and 2 are well-characterized signaling kinases, implicated in various signaling pathways that are exploited by malignant cells. They contribute to the pathogenesis of myeloproliferative neoplasms (MPNs), blood disorders that result from an excess production of hematological cells [12-15]. Therefore, recently several small molecule inhibitors for JAK1 and 2 family kinases have been developed, one of which was an ATP-competitive small molecule inhibitor, CYT387 (Figure 1), with a broad therapeutic activity [16-20].

The inhibitory effect of CYT387 alone or in combination with other conventional drugs on multiple myeloma proliferation has been demonstrated in vitro using human myeloma cell lines and *in vivo* using a murine MPN model [16, 21]. This drug is currently undergoing Phase I/II clinical trials for the targeted treatment of myelofibrosis, a frequently fatal myeloproliferative neoplasm. With the preliminary data showing significant and durable anemia responses and favorable toxicity profile, CYT387 is so far the best candidate among JAK inhibitors for the management of myelofibrosis in patients (http://www.ymbiosciences.net/upload_files/CYT387_poster_ASCO2011.pdf). Besides involvement in MPN pathogenesis, JAKs are implicated in other disorders including inflammatory and immune-mediated diseases. Therefore, several JAK inhibitors are being investigated for therapeutic activity in other neoplastic and rheumatological disorders, and allograft rejection [17, 22]. CYT387 is one of these inhibitors, regarded to have potential for treating other myeloproliferative neoplasms, solid and hematological malignancies, and inflammatory conditions.

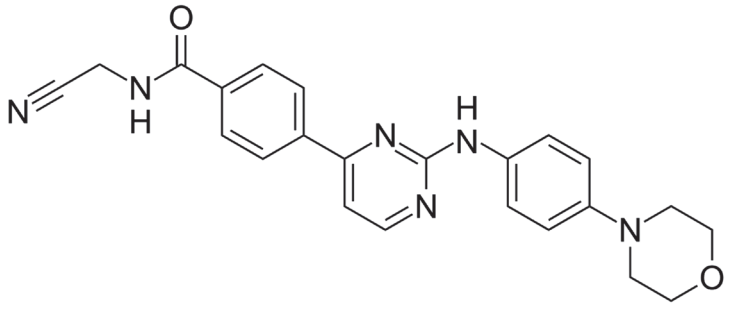


**Figure 1. Chemical Structure of CYT387.**

CYT387 is administered orally in the clinic. Thus, depending on its interactions with ABC transporters, these might have a significant impact on oral bioavailability and tissue or tumor distribution of CYT387 and thus determine the therapeutic efficacy on both primary tumors and metastases. In this study, we investigated the effect of MDR1 and BCRP on the in vitro transport and in vivo disposition of CYT387.





## MATERIALS AND METHODS

### Chemicals

CYT387 ($H_2SO_4$, sulfuric acid salt) was obtained from Sequoia Research Products (Pangbourne, UK). Zosuquidar (Eli Lilly; Indianapolis, USA) was a kind gift from Dr. O. van Tellingen (The Netherlands Cancer Institute, Amsterdam, NL) and Ko143 was obtained from Tocris Bioscience (Bristol, UK). All chemicals used in the chromatographic CYT387 assay were described before [23].

### Transport assays

Polarized canine kidney MDCKII cell lines and subclones transduced with hMDR1, hBCRP, and mBcrp1 cDNA were used and cultured as described previously [7]. Transport assays were performed using 12-well Transwell® plates (Corning Inc., USA). The parental cells and variant subclones were seeded at a density of 3.5 and 2.5 x $10^5$ cells per well, respectively, and cultured for 3 days to form an intact monolayer. Membrane tightness was assessed by measurement of transepithelial electrical resistance (TEER). Preceding the transport experiment, cells were washed twice with PBS and pre-incubated with fresh DMEM medium (Invitrogen, USA) including 10% FBS (Sigma-Aldrich, USA), and with relevant inhibitors for 1 h, if required. The transepithelial transport experiment was started (t = 0) by replacing the incubation medium with medium containing 5 µM CYT387 in the donor compartment. In the inhibition experiments, 5 µM zosuquidar (MDR1 inhibitor), 5 µM Ko143 (BCRP/Bcrp1 inhibitor) or 1 µM elacridar (dual MDR1 and BCRP/Bcrp1 inhibitor) were added to both apical and basolateral compartments. Plates were kept at 37°C in 5% $CO_2$ during the experiment, and 50 µl aliquots were taken from the acceptor compartment at 2, 4, 8 and 24 h. CYT387 concentrations were measured by LC-MS/MS. Total amount of drug transported to the acceptor compartment was calculated after correction for volume loss for each time point. Experiments were performed in triplicate and the mean amount of transport is shown in the graphs. Active transport was expressed by the relative transport ratio (r), defined as r = apically directed amount of transport divided by basolaterally directed amount of translocation, at a defined time point.

### Animals

Mice were housed and handled according to institutional guidelines complying with Dutch legislation. Animals used were female WT, Mdr1a/1b-/-, Bcrp1-/- and Mdr1a/1b-/-;Bcrp1-/- mice of a >99% FVB genetic background, between 8 and 10 weeks of age. Animals were kept in a temperature-controlled environment with a 12 h light / 12 h dark cycle and received a standard diet (AM-II, Hope Farms) and acidified water *ad libitum*.

**Drug solutions**

1 mg/ml CYT387 solution was obtained by dissolving the drug in dimethylsulfoxide (20 mg/ml), followed by 20-fold dilution in 20% Polysorbate 80, 13% ethanol and 67% $H_2O$ vehicle mix and 5% glucose in a ratio of 1:1 (v/v). Mice received a bolus injection, using a blunt-ended needle, of 10 mg/kg CYT387 orally, using a volume of 10 ml/kg body weight. All working solutions were prepared freshly on the day of experiment.

**Plasma and brain pharmacokinetics**

Mice were fasted about 2 h before CYT387 was orally administered in order to minimize the variation in absorption. For plasma pharmacokinetic studies, multiple blood samples (60 µl) were collected from the tail vein at 15 and 30 min and 1, 2 and 4 h using heparinized capillary tubes (Sarstedt, Germany). At 2 (in a separate experiment) or 8 h, mice were anesthetized with isoflurane and blood was collected by cardiac puncture. Immediately thereafter, mice were sacrificed by cervical dislocation and brains and a set of organs were rapidly removed. Organs were homogenized on ice in 1% (w/v) bovine serum albumin, and stored at -20°C until analysis. Blood samples were centrifuged at 2100 g for 6 min at 4°C immediately after collection; the plasma fraction was collected and stored at -20°C until analysis.

**Relative brain accumulation**

Relative brain accumulation after oral administration of CYT387 was calculated by determining the CYT387 brain concentration relative to the plasma AUC from 0 to 2 or 0 to 8 h. Brain concentrations at 2 and 8 h were corrected for the amount of drug present in plasma volume (1.4 %) in the brain vasculature.

**Drug analysis**

CYT387 concentrations in cell culture medium, plasma samples and brain homogenates were determined using liquid chromatography-electrospray-tandem mass spectrometry (LC-MS/MS) based on an assay reported for human plasma [23]. Shortly, samples were pre-treated using protein precipitation with acetonitrile containing cediranib as internal standard. Water diluted extracts were injected onto a sub-2 µm particle, trifunctional bonded octadecyl silica column;a gradient using 0.005% (v/v) of formic acid in a mixture of water and methanol was used. Positive ionization selected reaction monitoring mass transitions were 415.15>244.1; 245.1; 286.1 and 451.2>84.1; 112.1 for CYT387 and cediranib, respectively. The lower limit of quantification (LLoQ) for CYT387 was set at 1 ng/ml.

**Pharmacokinetic calculations and statistical analysis**

Pharmacokinetic parameters were calculated by non-compartmental methods using the software package PK Solutions 2.0.2 (Summit Research Services, Ashland, OH). The area under the plasma concentration-time curve was calculated using the trapezoidal rule, without extrapolating to infinity. The maximum drug concentration in plasma (Cmax) and the time to reach maximum drug concentration in plasma (Tmax) were determined directly from individual concentration-time data. One-way analysis of variance (ANOVA) was used to determine significance of differences between groups, after which post hoc tests with Tukey

correction were performed for comparison between individual groups. When variances were not homogeneous, data were log-transformed before statistical tests were applied. Differences were considered statistically significant when $P < 0.05$. Data are presented as mean ± SD.

## RESULTS

### *In vitro* transport of CYT387 by MDR1 and BCRP





In order to assess the interaction between CYT387 and ABC transporters *in vitro*, we analyzed CYT387 translocation through polarized monolayers of the MDCKII parental cell line and subclones overexpressing human (h)MDR1 or (h)BCRP or mouse (m)Bcrp1. In the MDCKII parental cell line, there was a modest apically directed transport of CYT387 (transport ratio r = 1.2), which was abrogated with the MDR1-specific inhibitor zosuquidar (Figure 2A and B), suggesting that this background transport was mediated by endogenous canine MDR1 present in the MDCKII cells. Zosuquidar was therefore added in subsequent experiments with hBCRP and mBcrp1 to suppress this background transport activity. In MDCKII cells overexpressing hMDR1, there was an active apically directed transport with r = 3.2, which was completely blocked by zosuquidar, indicating that CYT387 is a clear transport substrate of hMDR1 (Figure 2C and D). Further transport experiments in MDCKII cells overexpressing hBCRP showed good transport efficiency with r = 4.5, which could be completely inhibited with the BCRP-specific inhibitor Ko143 (Figure 2E and F). Transport efficiency in mouse Bcrp1-overexpressing MDCKII cells was very high with r = 21.2, and addition of Ko143 could completely abrogate this transport (Figure 2G and H). These results indicate that CYT387 is a very good substrate of mouse Bcrp1. Low but significant basolaterally directed transport in MDCKII parental (r = 0.7) and hBCRP overexpressing MDCKII cells (r = 0.8) co-treated with zosuquidar (Figure 2 B and F) suggested the (low) presence of an endogenous basolaterally directed CYT387 transporter of unknown identity in these cell lines. To the best of our knowledge, this study is the first to demonstrate active transport of CYT387 by hMDR1, hBCRP and mBcrp1.

### Plasma exposure and brain accumulation of oral CYT387

We further investigated the separate and combined effect of Mdr1a/1b and Bcrp1 on the *in vivo* disposition of CYT387 in mice. Because CYT387 is given orally to patients, we administered CYT387 orally at a dose of 10 mg/kg. Neither absence of Mdr1a/1b nor of Bcrp1 showed a significant effect on the overall plasma exposure between 0 to 8 h (Figure 3 and Table 1). The plasma $AUC_{0\text{-}8\ h}$ was decreased 1.2-fold in Mdr1a/1b-/- mice and increased 1.1-fold in Bcrp1-/- mice compared with that in WT mice. Combined deficiency in Mdr1a/1b or Bcrp1 caused a statistically insignificant decrease in the plasma $AUC_{0\text{-}8h}$ by 1.2-fold compared to WT mice (Figure 3, Table 1). Qualitatively similar results were obtained in CYT387 plasma levels up to 2 h in an independent experiment, with slight, but insignificant increases in $AUC_{0\text{–}2h}$ in Bcrp1-/- and Mdr1a/1b-/- mice (1.1-fold for both), and an insignificant decrease in Bcrp1;Mdr1a/1b-/- mice (1.2-fold) compared to WT mice (Table 1). Overall, these results suggest that there is no substantial impact of Mdr1a/1b or Bcrp1 on oral plasma pharmacokinetics of CYT387.

However, both Mdr1a/1b and Bcrp1 were quite important in the brain distribution of CYT387 at 2 and 8 h after oral administration of 10 mg/kg CYT387 (Figure 4 and Table 1). At 2 h, brain

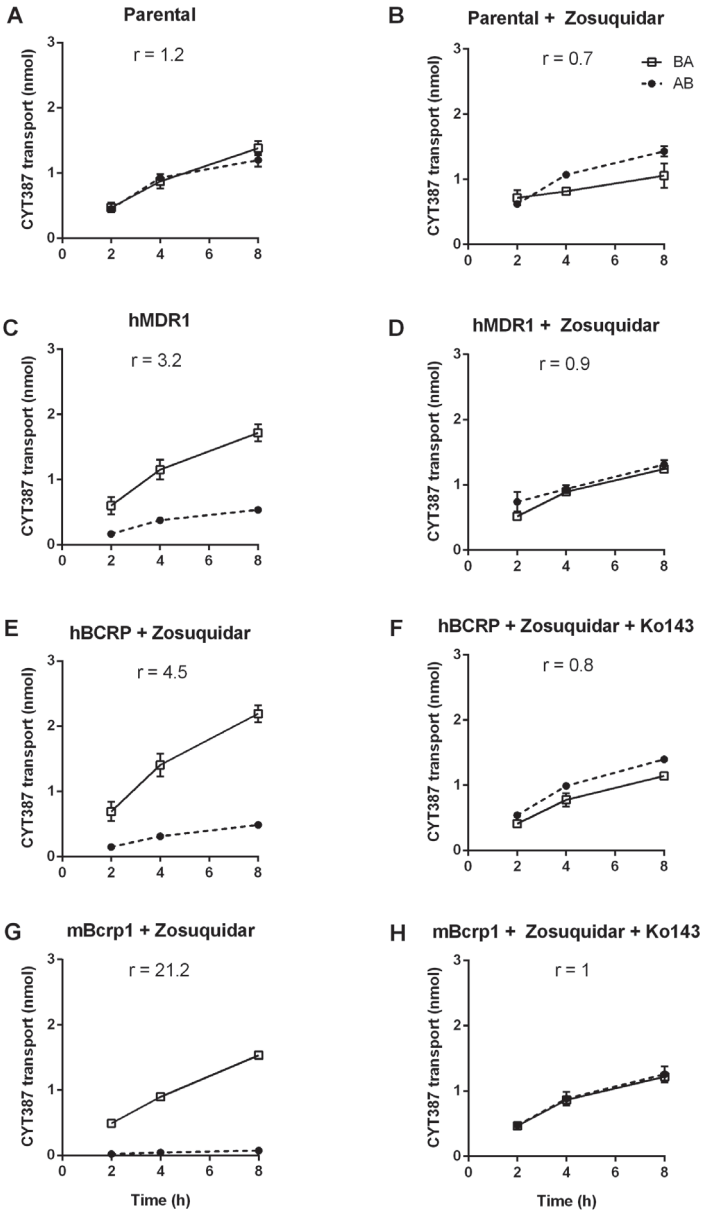


**Figure 2. *In vitro* transport of CYT387.** Transepithelial transport of CYT387 (5 μM) was assessed in MDCK-II cells either nontransduced (A, B) or transduced with hMDR1 (C, D), hBCRP (E, F) or mBcrp1 (G, H) cDNA. At t = 0 h, CYT387 was applied to the donor compartment and the concentrations in the acceptor compartment at t = 2, 4 and 8 h were measured and plotted as total amount of transport (nmol) in the graphs (n = 3). B-H: Zosuquidar (5 μM) and/or Ko143 (5 μM) were applied to inhibit MDR1 and hBCRP or mBcrp1, respectively. r, relative transport ratio. BA (□), translocation from the basolateral to the apical compartment; AB (●), translocation from the apical to the basolateral compartment. Points, mean; bars, SD. 1 nmol transport at t = 8 h corresponds to an apparent permeability coefficient (Papp) of $6.2 \times 10^{-6}$ cm/s.

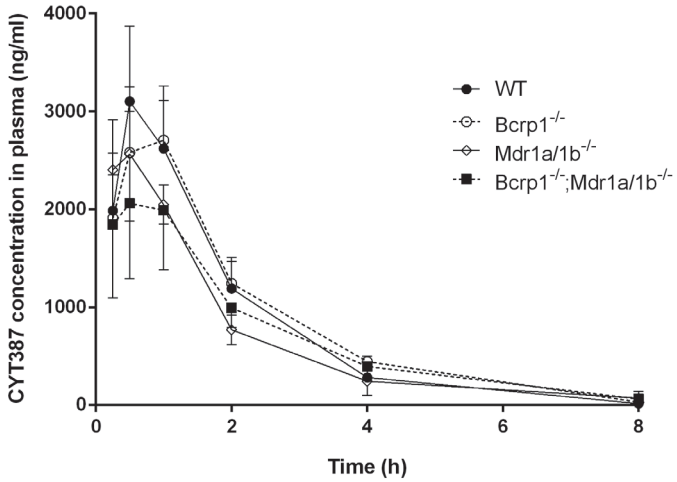


**Figure 3. Plasma concentration-time curves of CYT387.** Plasma levels of CYT387 were detected in female WT (●), Bcrp1-/- (○), Mdr1a/1b-/- (◊), and Bcrp1;Mdr1a/1b-/- (■) mice after oral administration of 10 mg/kg CYT387. Data are given as mean ± S.D. (n = 5 - 6).

**Table 1.** Plasma pharmacokinetic parameters and brain concentrations 2 and 8 h after oral administration of 10 mg/kg CYT387 to female WT, Bcrp1-/-, Mdr1a/1b-/- and Bcrp1;Mdr1a/1b-/- mice (n = 5 - 6).

| | | Genotype | | | |
|---|---|---|---|---|---|
| | **Time (h)** | **WT** | ***Bcrp1*$^{-/-}$** | ***Mdr1a/1b*$^{-/-}$** | ***Bcrp1*$^{-/-}$*;Mdr1a/1b*$^{-/-}$** |
| $AUC_{0\text{-}2\,h}$ (ng/ml.h) | 2 h | 3998 ± 797 | 4231 ± 208 | 4253 ± 1010 | 3224 ± 1537 |
| $C_{max}$ (ng/ml) | | 2782 ± 599 | 3265 ± 227 | 3298 ± 892 | 2307 ± 1158 |
| $T_{max}$ (h) | | 0.5 | 0.5 | 0.5 | 1 |
| $C_{brain}$ 2 h (ng/g) | | 72.7 ± 20.8 | 225.1 ± 69.5*** | 181.0 ± 33.7*** | 585.6 ± 229.6*** |
| $P_{brain}$ (*$10^{-3}$ $hr^{-1}$) | | 18.7 ± 5.7 | 47.1 ± 10.3*** | 44.9 ± 13.6*** | 197.0 ± 55.0*** |
| $AUC_{0\text{-}8\,h}$ (ng/ml.h) | 8 h | 6288 ± 1097 | 6734 ± 829 | 5057 ± 832 | 5467 ± 1186 |
| $C_{max}$ (ng/ml) | | 3162 ± 701 | 2861 ± 389 | 2806 ± 443 | 2177 ± 722 |
| $T_{max}$ (h) | | 0.5 | 1 | 0.5 | 0.5 |
| $C_{brain}$ 8 h (ng/g) | | 3.3 ± 2.0 | 21.4 ± 9.6*** | 10.2 ± 7.4* | 159.6 ± 72.5*** |
| $P_{brain}$ (*$10^{-3}$ $hr^{-1}$) | | 0.6 ± 0.4 | 3.2 ± 1.6** | 2.1 ± 1.5* | 32.2 ± 19.6*** |

*Cmax, maximum concentration in plasma; Tmax, time point (h) that maximum plasma concentration is observed; Cbrain, brain concentration; Pbrain, brain accumulation. LLQ was 1 ng/ml. * P < 0.05; *** P < 0.001 compared to WT mice.*

concentrations in Bcrp1-/- and Mdr1a/1b-/- mice were similarly increased by 3.1- and 2.5-fold compared with that in WT animals (Figure 4A). In Bcrp1;Mdr1a/1b-/- mice, brain concentrations at 2 h were 8.1-fold increased compared to WT mice. Similar increases were observed in brain-to-plasma ratios of all strains, with only a slightly lower increase (2x) in Bcrp1-/- mice, due to their plasma levels at 2 h (Figure 4C). Correcting the CYT387 brain concentrations for the corresponding plasma AUCs also revealed increased CYT387 accumulation in brains of Bcrp1-/- (2.5-fold), Mdr1a/1b-/- (2.4-fold) and Bcrp1;Mdr1a/1b-/- (10.5-fold) mice compared to WT animals (Figure 4E). These results suggest that both Bcrp1 and Mdr1a/1b are equally important in restricting brain entry of CYT387 at 2 h and that both transporters cooperate efficiently at the BBB for transporting this drug.

Interestingly, at 8 h, the role of Bcrp1 in brain concentration of CYT387 appeared to be somewhat more prominent than that of Mdr1a/1b. At 8 h, brain concentrations were increased 6.4-fold in Bcrp1-/- mice, but only 3.1-fold in Mdr1a/1b-/- mice and 47.8-fold in Bcrp1;Mdr1a/1b-/- mice (Figure 4B). Moreover, brain-to-plasma ratios in Bcrp1-/- and Bcrp1;Mdr1a/1b-/- mice were significantly higher than that of WT mice (5- and 17-fold, respectively; $P < 0.001$), whereas brain-to-plasma ratios of Mdr1a/1b-/- mice remained similar to WT mice (Figure 4D). Brain concentrations corrected for the corresponding plasma AUCs also showed significant increases in brain accumulation of CYT387 in all of the strains at 5.6-fold in Bcrp1-/-, 3.6-fold in Mdr1a/1b-/- and a marked 56-fold in Bcrp1;Mdr1a/1b-/- compared to WT mice (Figure 4F). Overall, these results suggest that at the earlier time point (2 h), where systemic concentrations are high, Bcrp1 and Mdr1a/1b each individually have a substantial and similar impact on restricting brain accumulation of CYT387 in single knock-out strains, and at a later time point (8 h), where systemic concentrations are low, the impact of Bcrp1 appears to be somewhat higher than that of Mdr1a/1b on CYT387 brain accumulation. This phenomenon suggests that Bcrp1 might become saturated somewhat more easily (i.e., at lower CYT387 concentrations) compared to Mdr1a/1b. Nonetheless, both Mdr1a/1b and Bcrp1 can still take over most of each other's function in restricting CYT387 brain accumulation across the BBB at early and late time points.

## DISCUSSION

We demonstrated that CYT387 is very efficiently transported by mBcrp1 and efficiently by both hMDR1 and hBCRP *in vitro*. *In vivo*, although there were no observable effects of both transporters on the oral availability of CYT387, brain accumulation of CYT387 was increased in all knock-out strains, with disproportionately higher levels in the combination knockout of Mdr1a/1b and Bcrp1 compared to individual knock-outs. To our knowledge, this is the first study showing that CYT387 is efficiently transported by MDR1 and BCRP *in vitro* and that brain accumulation of CYT387 is restricted by both of these transporters in mice.

Even though CYT387 is a good Mdr1a/1b and Bcrp1 substrate *in vivo*, based on the substantial effects on brain accumulation, we observed no significant effect of Mdr1a/1b and Bcrp1 deficiency on CYT387 oral availability. This is a fairly common observation for several other shared Mdr1a/1b and Bcrp1 substrate drugs such as imatinib, sorafenib, gefitinib, lapatinib and sunitinib [3, 4, 9, 24, 25]. It is possible that this lack of effect on oral bioavailability is due to saturation of efflux transporters by the high local intestinal concentration of CYT387

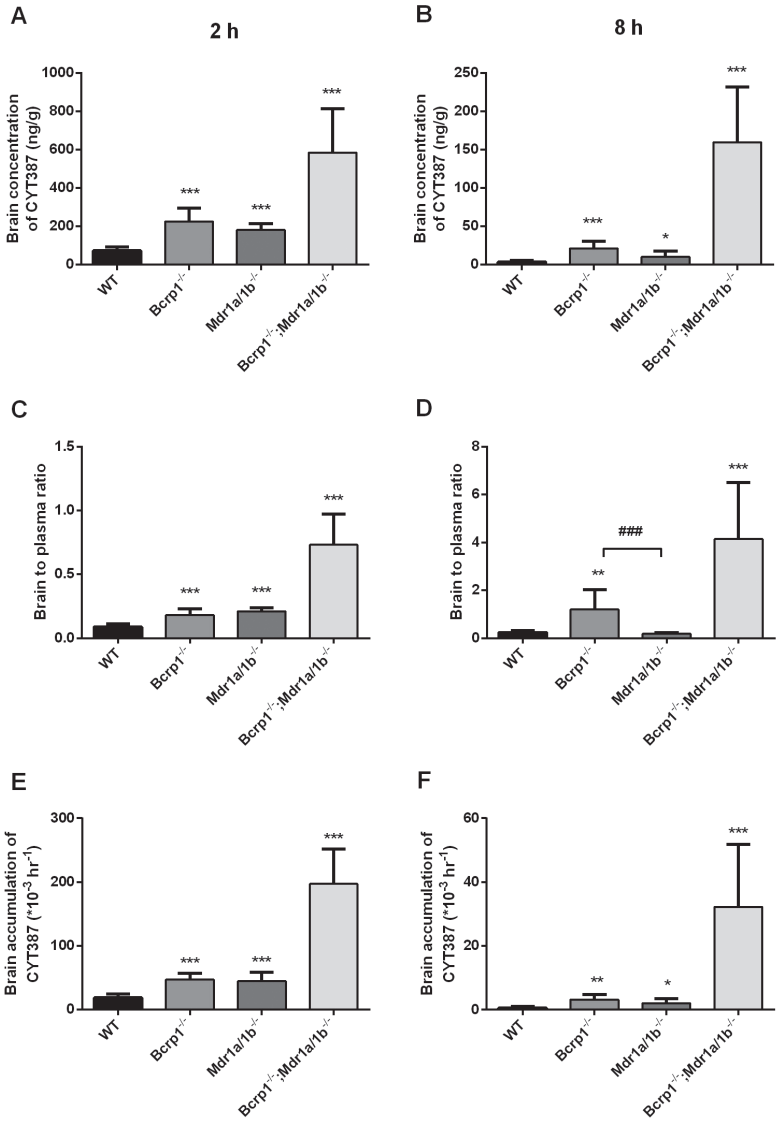


**Figure 4. Levels of CYT387 in brain of female WT, Bcrp1-/-, Mdr1a/1b-/- and Bcrp1;Mdr1a/1b-/- mice.** Brain concentrations (A and B), brain/plasma ratios (C and D), and relative brain accumulation (E and F) of CYT387 were determined at 2 and 8 h after oral administration of 10 mg/kg CYT387. Relative brain accumulation was calculated by dividing brain concentrations by the CYT387 plasma $AUC_{0-2h}$ and $AUC_{0-8h}$, respectively. n = 3 WT and n = 1 Mdr1a/1b CYT387 brain levels at 8 h were lower than LLQ, but detectable, and therefore replaced by extrapolated values below LLQ. Data are mean ± S.D. [n = 4-7]. *, $P < 0.05$; **, $P < 0.01$; ***, $P < 0.001$ compared with WT mice; ###, $P < 0.001$, comparing with Bcrp1-/- and Mdr1a/1b-/- mice, using log-transformed data to normalize the S.D.s between study groups. (n = 5 - 6).

obtained after oral administration, which is much higher than the plasma concentration after oral administration [9]. Other factors responsible for such differences between oral availability and brain accumulation may lie in differences in intrinsic permeability and CYT387 uptake mechanisms between the apical membrane of enterocytes and the BBB endothelial cells

CYT387 does not appear to be tightly bound to brain tissue after it has entered, and we observed a difference in CYT387 clearance from brain of the different strains. The effective brain clearance in mice that are proficient for Bcrp1 and/or Mdr1a/1b was substantially higher between 2 and 8 h after administration than in mice that are deficient for both Bcrp1 and Mdr1a/1b, in spite of lower starting concentrations (Figure 4A and B). Between 2 and 8 h, CYT387 brain levels decreased by 21.8-fold in WT mice, 10.5-fold in Bcrp1-/- mice, 17.7-fold in Mdr1a/1b-/- mice and only 3.7-fold in Bcrp1;Mdr1a/1b-/- mice. Similar qualitative results were obtained for brain accumulation (Supplementary table 1), indicating a much slower CYT387 clearance from the brain of Bcrp1;Mdr1a/1b-/- mice compared to other strains. Clearly, these ABC efflux transporters effect brain clearance of CYT387 strongly. Moreover, our data also suggested a somewhat stronger effect of Bcrp1-mediated brain clearance (17.7-fold decrease in Mdr1a/1b-/- mice), than of Mdr1a-mediated brain clearance (10.5-fold decrease in Bcrp1-/- mice).

Our findings with CYT387 and other TKIs showed that the ability of CYT387 to penetrate the brain was similar to that of sorafenib and dasatinib, but much lower than that of sunitinib. In WT mice, compared at similar plasma clearance phases, brain accumulation of CYT387 at 2 h (18.7 x $10^{-3}$ $hr^{-1}$) was not too different from brain accumulations of sorafenib (5.3 x $10^{-3}$ $hr^{-1}$) and dasatinib (6.4 x $10^{-3}$ $hr^{-1}$) at 6 h, but much lower (8.4-fold) than that of sunitinib (157.9 x $10^{-3}$ $hr^{-1}$) at 6 h [9, 24, 26]. A similar pattern of brain accumulation of the different drugs was observed throughout all the knockout strains as well (Supplementary Figure 1A, B, C). At the same time, however, these drugs have quite different oral availabilities after oral administration of the same dose (10 mg/kg), with sunitinib showing by far the lowest plasma levels, and sorafenib the highest (Supplementary Figure 1D, E, F).

Our findings therefore show that effective plasma levels of a drug after oral administration do not have to correspond at all with the ability of a drug to penetrate the brain. For instance, sunitinib has very low oral availability (plasma $AUC_{0\text{-}6h}$: 287.8 – 445.4 ng $ml^{-1}$ $h^{-1}$), but very high brain accumulation over 6 h in all strains ($P_{brain}$: 160 – 4240 x $10^{-3}$ $h^{-1}$, Supplementary figure 1 A and D) [9]. In contrast, CYT387 has quite good oral availability (plasma $AUC_{0\text{-}8h}$: 3224 – 4253, Figure 3), but low brain penetration ($P_{brain}$ at 8 h: 0.6 – 32.2 x $10^{-3}$ $h^{-1}$, Figure 4 E). Sorafenib has very high, and dasatinib has intermediately low plasma levels (plasma $AUC_{0\text{-}6h}$: 19,600 – 24,000 and 1000 - 2000 ng $ml^{-1}$ $h^{-1}$, respectively, Supplementary figure 1 E and F), whereas both of them have relatively low brain accumulation ($P_{brain}$ at 6 h: 5.3 – 49.4 and 6.4 – 84.3 x $10^{-3}$ $h^{-1}$, respectively, Supplementary figure 1 B and C). These findings illustrate that there are clearly many different factors determining on the one hand oral availability, and on the other hand brain accumulation of TKI drugs. These factors could include differential susceptibility to metabolizing enzymes, transport efficacy by various uptake and efflux systems (in addition to Mdr1a/1b and Bcrp1), capability of passive transmembrane diffusion, differences in membrane (lipid) composition, relative distribution to other tissues, and relative binding to plasma or tissue compartments. Reliable prediction of these parameters for TKIs based on theoretical considerations alone therefore will remain a challenging task for the foreseeable future.

One common finding in the brain accumulation of many TKIs (e.g. vemurafenib, sunitinib, axitinib, imatinib, dasatinib, lapatinib, gefitinib, and erlotinib), including CYT387, is the disproportionate increase in Bcrp1;Mdr1a/1b-/- mice compared to mice deficient for only one transporter [3-7, 9, 25, 26]. This is not unexpected anymore since a straightforward pharmacokinetic model for brain penetration of a wide selection of drugs was developed [5]. The model predicts that when the remaining brain efflux in the combination knockout mice is small compared to the active efflux of either Mdr1a/1b or Bcrp1 alone, only a small effect on brain accumulation is expected of single removal of each transporter due to reduced efflux activity, and a pronounced effect of the combined removal of both transporters due to the pronounced drop in efflux activity. Recently, we performed a limited test of this theoretical explanation in an experimental model for one TKI, where we determined the effect of halving the combined activity of both transporters on brain accumulation of vemurafenib, using heterozygous Bcrp1+/-;Mdr1a/1b+/- mice [7]. The results we obtained were in line with the predictions of the model.

To date, over-expression of MDR1 and BCRP is suggested to limit the efficacy of chemotherapy in several tumors including acute myeloid leukemia (AML) where they confer a particularly poor prognosis [27-30]. Based on this knowledge, we think that resistance to CYT387-mediated chemotherapy in target tumors expressing MDR1 and/or BCRP is likely to occur. In addition, MDR1 and BCRP expression cause poor brain penetration of several anti-cancer drugs due to their efficient efflux capacity at the BBB. This is especially important for cancer patients with central nervous sytem (CNS) involvement. The occurrence or relapse of an isolated CNS metastasis is observed in myeloproliferative diseases such as acute and chronic myeloid leukemia and treating these lesions is considered a big challenge. Therefore lately several studies have focused on optimal treatment strategies that can by-pass the BBB [31-35]. Since our study suggests a poor brain penetration of CYT387 due to MDR1 and BCRP activity, based on previous experience [4, 7, 9, 26], it may be possible to improve the drug levels in brain of patients with CNS involvement when CYT387 is coadministered with elacridar, an efficacious dual inhibitor of MDR1 and BCRP, and possibly other dual inhibitors as well.

## REFERENCE LIST

1. Lagas JS, Sparidans RW, van Waterschoot RA, Wagenaar E, Beijnen JH, Schinkel AH. P-glycoprotein limits oral availability, brain penetration, and toxicity of an anionic drug, the antibiotic salinomycin. *Antimicrob Agents Chemother* 2008; 52:1034-1039.
2. Zhou L, Schmidt K, Nelson FR, Zelesky V, Troutman MD, Feng B. The effect of breast cancer resistance protein and P-glycoprotein on the brain penetration of flavopiridol, imatinib mesylate (Gleevec), prazosin, and 2-methoxy-3-(4-(2-(5-methyl-2-phenyloxazol-4-yl)ethoxy) phenyl)propanoic acid (PF-407288) in mice. *Drug Metab Dispos* 2009; 37:946-955.
3. Polli JW, Olson KL, Chism JP, John-Williams LS, Yeager RL, Woodard SM *et al*. An unexpected synergist role of P-glycoprotein and breast cancer resistance protein on the central nervous system penetration of the tyrosine kinase inhibitor lapatinib (N-{3-chloro-4-[(3-fluorobenzyl) oxy]phenyl}-6-[5-({[2-(methylsulfonyl)ethyl] amino}methyl)-2-furyl]-4-quinazolinamine; GW572016). *Drug Metab Dispos* 2009; 37:439-442.
4. Agarwal S, Sane R, Gallardo JL, Ohlfest JR, Elmquist WF. Distribution of gefitinib to the brain is limited by P-glycoprotein (ABCB1) and breast cancer resistance protein (ABCG2)-mediated active efflux. *J Pharmacol Exp Ther* 2010; 334:147-155.
5. Kodaira H, Kusuhara H, Ushiki J, Fuse E, Sugiyama Y. Kinetic analysis of the cooperation of P-

glycoprotein (P-gp/Abcb1) and breast cancer resistance protein (Bcrp/Abcg2) in limiting the brain and testis penetration of erlotinib, flavopiridol, and mitoxantrone. *J Pharmacol Exp Ther* 2010; 333:788-796.

6. Poller B, Iusuf D, Sparidans RW, Wagenaar E, Beijnen JH, Schinkel AH. Differential impact of P-glycoprotein (ABCB1) and breast cancer resistance protein (ABCG2) on axitinib brain accumulation and oral plasma pharmacokinetics. *Drug Metab Dispos* 2011; 39:729-735.
7. Durmus S, Sparidans RW, Wagenaar E, Beijnen JH, Schinkel AH. Oral availability and brain penetration of the B-RAFV600E inhibitor vemurafenib can be enhanced by the P-GLYCOprotein (ABCB1) and breast cancer resistance protein (ABCG2) inhibitor elacridar. *Mol Pharm* 2012; 9:3236-3245.
8. Mittapalli RK, Vaidhyanathan S, Dudek AZ, Elmquist WF. Mechanisms Limiting Distribution of the BRAFV600E Inhibitor Dabrafenib to the Brain: Implications for the Treatment of Melanoma Brain Metastases. *J Pharmacol Exp Ther* 2012.
9. Tang SC, Lagas JS, Lankheet NA, Poller B, Hillebrand MJ, Rosing H *et al*. Brain accumulation of sunitinib is restricted by P-glycoprotein (ABCB1) and breast cancer resistance protein (ABCG2) and can be enhanced by oral elacridar and sunitinib coadministration. *Int J Cancer* 2012; 130:223-233.
10. Lockman PR, Mittapalli RK, Taskar KS, Rudraraju V, Gril B, Bohn KA *et al*. Heterogeneous blood-tumor barrier permeability determines drug efficacy in experimental brain metastases of breast cancer. *Clin Cancer Res* 2010; 16:5664-5678.
11. Taskar KS, Rudraraju V, Mittapalli RK, Samala R, Thorsheim HR, Lockman J *et al*. Lapatinib distribution in HER2 overexpressing experimental brain metastases of breast cancer. *Pharm Res* 2012; 29:770-781.
12. Kralovics R, Passamonti F, Buser AS, Teo SS, Tiedt R, Passweg JR *et al*. A gain-of-function mutation of JAK2 in myeloproliferative disorders. *N Engl J Med* 2005; 352:1779-1790.
13. Levine RL, Wadleigh M, Cools J, Ebert BL, Wernig G, Huntly BJ *et al*. Activating mutation in the tyrosine kinase JAK2 in polycythemia vera, essential thrombocythemia, and myeloid metaplasia with myelofibrosis. *Cancer Cell* 2005; 7:387-397.
14. Mullighan CG, Zhang J, Harvey RC, Collins-Underwood JR, Schulman BA, Phillips LA *et al*. JAK mutations in high-risk childhood acute lymphoblastic leukemia. *Proc Natl Acad Sci U S A* 2009; 106:9414-9418.
15. Scott LM, Tong W, Levine RL, Scott MA, Beer PA, Stratton MR *et al*. JAK2 exon 12 mutations in polycythemia vera and idiopathic erythrocytosis. *N Engl J Med* 2007; 356:459-468.
16. Tyner JW, Bumm TG, Deininger J, Wood L, Aichberger KJ, Loriaux MM *et al*. CYT387, a novel JAK2 inhibitor, induces hematologic responses and normalizes inflammatory cytokines in murine myeloproliferative neoplasms. *Blood* 2010; 115:5232-5240.
17. Pardanani A, Tefferi A. Targeting myeloproliferative neoplasms with JAK inhibitors. *Curr Opin Hematol* 2011; 18:105-110.
18. Stein BL, Crispino JD, Moliterno AR. Janus kinase inhibitors: an update on the progress and promise of targeted therapy in the myeloproliferative neoplasms. *Curr Opin Oncol* 2011; 23:609-616.
19. Burns CJ, Bourke DG, Andrau L, Bu X, Charman SA, Donohue AC *et al*. Phenylaminopyrimidines as inhibitors of Janus kinases (JAKs). *Bioorg Med Chem Lett* 2009; 19:5887-5892.
20. Pardanani A, Lasho T, Smith G, Burns CJ, Fantino E, Tefferi A. CYT387, a selective JAK1/JAK2 inhibitor: in vitro assessment of kinase selectivity and preclinical studies using cell lines and primary cells from polycythemia vera patients. *Leukemia* 2009; 23:1441-1445.
21. Monaghan KA, Khong T, Burns CJ, Spencer A. The novel JAK inhibitor CYT387 suppresses multiple signalling pathways, prevents proliferation and induces apoptosis in phenotypically diverse myeloma cells. *Leukemia* 2011; 25:1891-1899.
22. Quintas-Cardama A, Kantarjian H, Cortes J, Verstovsek S. Janus kinase inhibitors for the treatment of myeloproliferative neoplasias and beyond. *Nat Rev Drug Discov* 2011; 10:127-140.
23. Sparidans RW, Durmus S, Xu N, Schinkel AH, Schellens JH, Beijnen JH. Liquid chromatography-tandem mass spectrometric assay for the JAK2 inhibitor CYT387 in plasma. *J Chromatogr B Analyt Technol Biomed Life Sci* 2012; 895-896:174-177.
24. Lagas JS, van Waterschoot RA, Sparidans RW, Wagenaar E, Beijnen JH, Schinkel AH. Breast cancer resistance protein and P-glycoprotein limit sorafenib brain accumulation. *Mol Cancer Ther* 2010; 9:319-326.
25. Oostendorp RL, Buckle T, Beijnen JH, van TO, Schellens JH. The effect of P-gp (Mdr1a/1b), BCRP (Bcrp1) and P-gp/BCRP inhibitors on the in vivo absorption, distribution, metabolism and excretion of imatinib. *Invest New Drugs* 2009; 27:31-40.

26. Lagas JS, van Waterschoot RA, van Tilburg VA, Hillebrand MJ, Lankheet N, Rosing H *et al*. Brain accumulation of dasatinib is restricted by P-glycoprotein (ABCB1) and breast cancer resistance protein (ABCG2) and can be enhanced by elacridar treatment. *Clin Cancer Res* 2009; 15:2344-2351.

27. Damiani D, Tiribelli M, Michelutti A, Geromin A, Cavallin M, Fabbro D *et al*. Fludarabine-based induction therapy does not overcome the negative effect of ABCG2 (BCRP) over-expression in adult acute myeloid leukemia patients. *Leuk Res* 2010; 34:942-945.

28. Grundy M, Seedhouse C, Russell NH, Pallis M. P-glycoprotein and breast cancer resistance protein in acute myeloid leukaemia cells treated with the aurora-B kinase inhibitor barasertib-hQPA. *BMC Cancer* 2011; 11:254.

29. Tiribelli M, Geromin A, Michelutti A, Cavallin M, Pianta A, Fabbro D *et al*. Concomitant ABCG2 overexpression and FLT3-ITD mutation identify a subset of acute myeloid leukemia patients at high risk of relapse. *Cancer* 2011; 117:2156-2162.

30. Chauhan PS, Bhushan B, Singh LC, Mishra AK, Saluja S, Mittal V *et al*. Expression of genes related to multiple drug resistance and apoptosis in acute leukemia: response to induction chemotherapy. *Exp Mol Pathol* 2012; 92:44-49.

31. Aichberger KJ, Herndlhofer S, Agis H, Sperr WR, Esterbauer H, Rabitsch W *et al*. Liposomal cytarabine for treatment of myeloid central nervous system relapse in chronic myeloid leukaemia occurring during imatinib therapy. *Eur J Clin Invest* 2007; 37:808-813.

32. Isobe Y, Sugimoto K, Masuda A, Hamano Y, Oshimi K. Central nervous system is a sanctuary site for chronic myelogenous leukaemia treated with imatinib mesylate. *Intern Med J* 2009; 39:408-411.

33. Johnston DL, Alonzo TA, Gerbing RB, Lange BJ, Woods WG. Risk factors and therapy for isolated central nervous system relapse of pediatric acute myeloid leukemia. *J Clin Oncol* 2005; 23:9172-9178.

34. Leis JF, Stepan DE, Curtin PT, Ford JM, Peng B, Schubach S *et al*. Central nervous system failure in patients with chronic myelogenous leukemia lymphoid blast crisis and Philadelphia chromosome positive acute lymphoblastic leukemia treated with imatinib (STI-571). *Leuk Lymphoma* 2004; 45:695-698.

35. Porkka K, Koskenvesa P, Lundan T, Rimpilainen J, Mustjoki S, Smykla R *et al*. Dasatinib crosses the blood-brain barrier and is an efficient therapy for central nervous system Philadelphia chromosome-positive leukemia. *Blood* 2008; 112:1005-1012.

## SUPPLEMENTARY MATERIALS

**Supplementary Table 1.** Fold decrease in the brain concentration and brain accumulation of CYT387 between 2 and 8 h in female WT, Bcrp1-/-, Mdr1a/1b-/- and Bcrp1-/-;Mdr1a/1b-/- mice (n = 5 - 6).

| | Genotype | | | |
|---|---|---|---|---|
| **Relative levels (2 to 8 h)** | **WT** | ***Bcrp1*$^{-/-}$** | ***Mdr1a/1b*$^{-/-}$** | ***Bcrp1*$^{-/-}$*;Mdr1a/1b*$^{-/-}$** |
| **Cbrain** | 21.8 x | 10.5 x | 17.7 x | 3.7 x |
| **Pbrain** | 31.2 x | 14.7 x | 21.4 x | 6.1 x |

*Abbreviations: $C_{brain}$, brain concentration. $P_{brain}$, brain accumulation.*

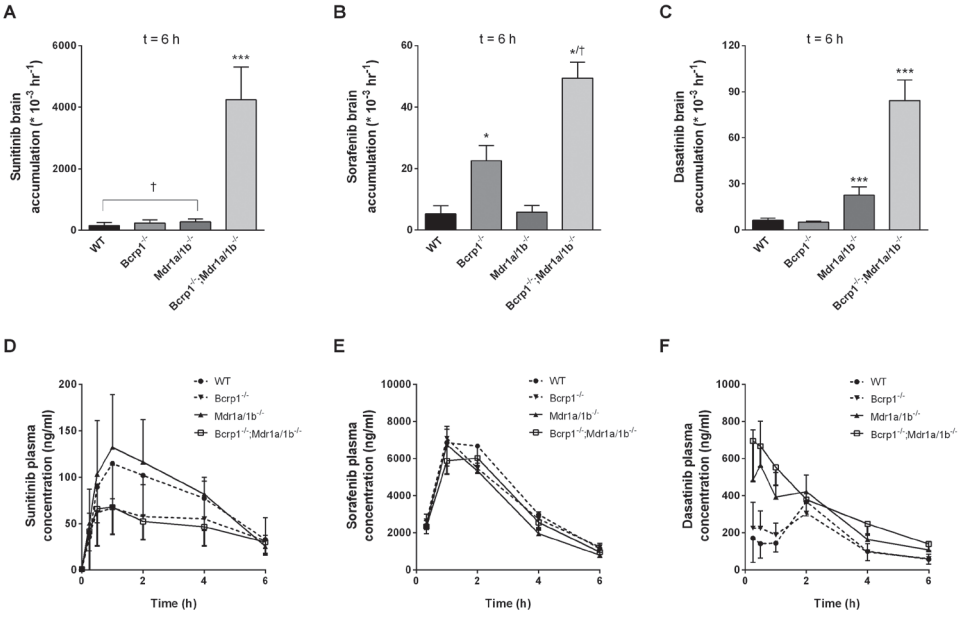


**Supplementary Figure 1. Brain accumulations (A, B, C) and oral exposure (D, E, F) of sunitinib, sorafenib and dasatinib over 6 h after oral administration of 10 mg/kg.** The data in these graphs are taken from previous publications (Lagas, et al., 2009; Lagas et al., 2010; Tang, et al., 2012. The data are being reprinted with permission of the authors).

# CHAPTER 2.3

## BRAIN AND TESTIS ACCUMULATION OF REGORAFENIB IS RESTRICTED BY BREAST CANCER RESISTANCE PROTEIN (BCRP/ABCG2) AND P-GLYCOPROTEIN (P-GP/ABCB1)

Selvi Durmus[a#], Anita Kort[a,c#], Rolf W. Sparidans[b], Els Wagenaar[a], Jos H. Beijnen[b,c,d] and Alfred H. Schinkel[a]

[#]These authors contributed equally
[a] Division of Molecular Oncology, The Netherlands Cancer Institute, Plesmanlaan 121, 1066 CX Amsterdam, The Netherlands.
[b] Division of Pharmacoepidemiology & Clinical Pharmacology, Department of Pharmaceutical Sciences, Faculty of Science, Utrecht University, Universiteitsweg 99, 3584 CG Utrecht, The Netherlands.
[c] Department of Pharmacy & Pharmacology, The Netherlands Cancer Institute/ Slotervaart Hospital, Plesmanlaan 121, 1066 CX Amsterdam, The Netherlands
[d] Department of Clinical Pharmacology, The Netherlands Cancer Institute, Plesmanlaan 121, 1066 CX Amsterdam, The Netherlands

*To be submitted*

## ABSTRACT

### Background

Regorafenib is a novel multikinase inhibitor, currently approved for the treatment of metastasized colorectal cancer and advanced gastrointestinal stromal tumors. We investigated whether regorafenib is a substrate for the multidrug efflux transporter proteins ABCG2 and ABCB1 and whether oral availability, brain and testis accumulation of regorafenib and its active metabolites M2 and M5 are influenced by these transporter proteins.

### Methods

We used *in vitro* transport assays to test whether human (h)ABCB1 or hABCG2 or murine (m) Abcg2 can actively transport high and low concentrations of regorafenib. To study the single and combined roles of ABCG2 and ABCB1 in regorafenib disposition after oral intake and the impact of Cyp3a-mediated metabolism, we used appropriate knockout mouse strains.

### Results

Regorafenib was transported well by mAbcg2 and hABCG2 *in vitro* and modestly by hABCB1. Abcg2 and to a lesser extent Abcb1a/1b limited brain and testis accumulation of regorafenib and M2 in mice. Up till 2 h, M5 was undetectable in plasma and organs.

### Conclusions

Brain and testis accumulation of regorafenib and M2 is restricted by Abcg2 and Abcb1a/1b. Chemical inhibition of these transporters may be of clinical relevance for patients with brain (micro) metastases behind an intact blood-brain barrier.

## INTRODUCTION

Multidrug efflux transporters of the ATP-binding cassette (ABC) protein family can have an important role in drug disposition. This impact is especially relevant for anti-cancer drugs as these drugs are usually administered close to their maximum tolerated dose. ABCB1 (P-glycoprotein) and ABCG2 (BCRP) are expressed on the apical membrane of epithelia in a number of organs which are pivotal for absorption and elimination of drugs like liver, small intestine and kidney, but also on luminal membranes of barriers protecting sanctuary sites like blood-placenta barrier, blood-testis barrier and blood-brain barrier. At these sanctuary sites ABCB1 or ABCG2 substrates are immediately pumped out of the cell back into the blood. As a consequence, only small amounts of drug can accumulate in, for instance, the brain to treat (micro) metastases that are present behind a functionally intact blood-brain-barrier. Many tyrosine kinase inhibitors have been shown to be substrates of either ABCG2 and or ABCB1, resulting in a decreased brain accumulation or a decreased oral availability [1-3].

Regorafenib (BAY 73-4506, Stivarga, Supplementary Figure 1A) is an oral multi-targeted tyrosine kinase inhibitor targeting angiogenic, stromal and oncogenic receptor kinases [4]. In a phase III study in patients with metastasized colorectal carcinoma, regorafenib improved overall survival months compared to placebo [5]. This led to the approval of regorafenib by EMA and FDA in 2012. The latter expanded the indication with advanced gastrointestinal stromal tumors in March 2013, following a placebo-controlled study. Demetri *et al*. showed a significantly improved progression-free survival and disease control rate for regorafenib in patients with advanced GIST whose tumors developed resistance to imatinib and sunitinib [6].

Regorafenib was developed as a more potent RAF-kinase inhibitor than sorafenib. These compounds share an overlap in biochemical activities, however, regorafenib does not only have affinity for a broader range of antiangiogenic kinases (VEGFR1-VEGFR3) compared to sorafenib, it also targets TIE2 (tyrosine kinase with immunoglobulin and epidermal growth factor homology domain 2). Inhibition of both kinases has been shown to act synergistically resulting in a reduced tumor growth in preclinical models [7, 8].

Furthermore, Bruix *et al*. found evidence for regorafenib antitumor activity in hepatocellular carcinoma patients that had previously been treated with sorafenib [9]. Regorafenib was able to delay disease progression in 25 out of 31 patients and one patient exhibited a partial response. A phase III study is currently recruiting to further investigate this effect (ClinicalTrialsGov identifier NCT01774344).

Considering the similarity in chemical structure of regorafenib and sorafenib (Supplementary Figure 1A and 1B, respectively) where regorafenib has an additional fluorine atom attached to the central aromatic ring, regorafenib might be a good substrate of ABCG2 and possibly ABCB1. Sorafenib has been reported by various groups to be a good substrate of ABCG2 and a moderate substrate of ABCB1 *in vitro* as well as *in vivo* [10-13]. Surprisingly, however, according to the manufacturer, regorafenib is not transported by ABCG2 or ABCB1 as tested *in vitro* using transduced and wild-type LLC-MDR1 cells, using clinically relevant concentrations ranging from 0.2 to 10 μM regorafenib [14]. Regorafenib was, however, found to be an inhibitor of transport of digoxin (an ABCB1 substrate) and dipyramidole (an ABCG2 substrate) *in vitro*. For this reason, a clinical phase I study (ClinicalTrialsGov identifier NCT02106845) is planned

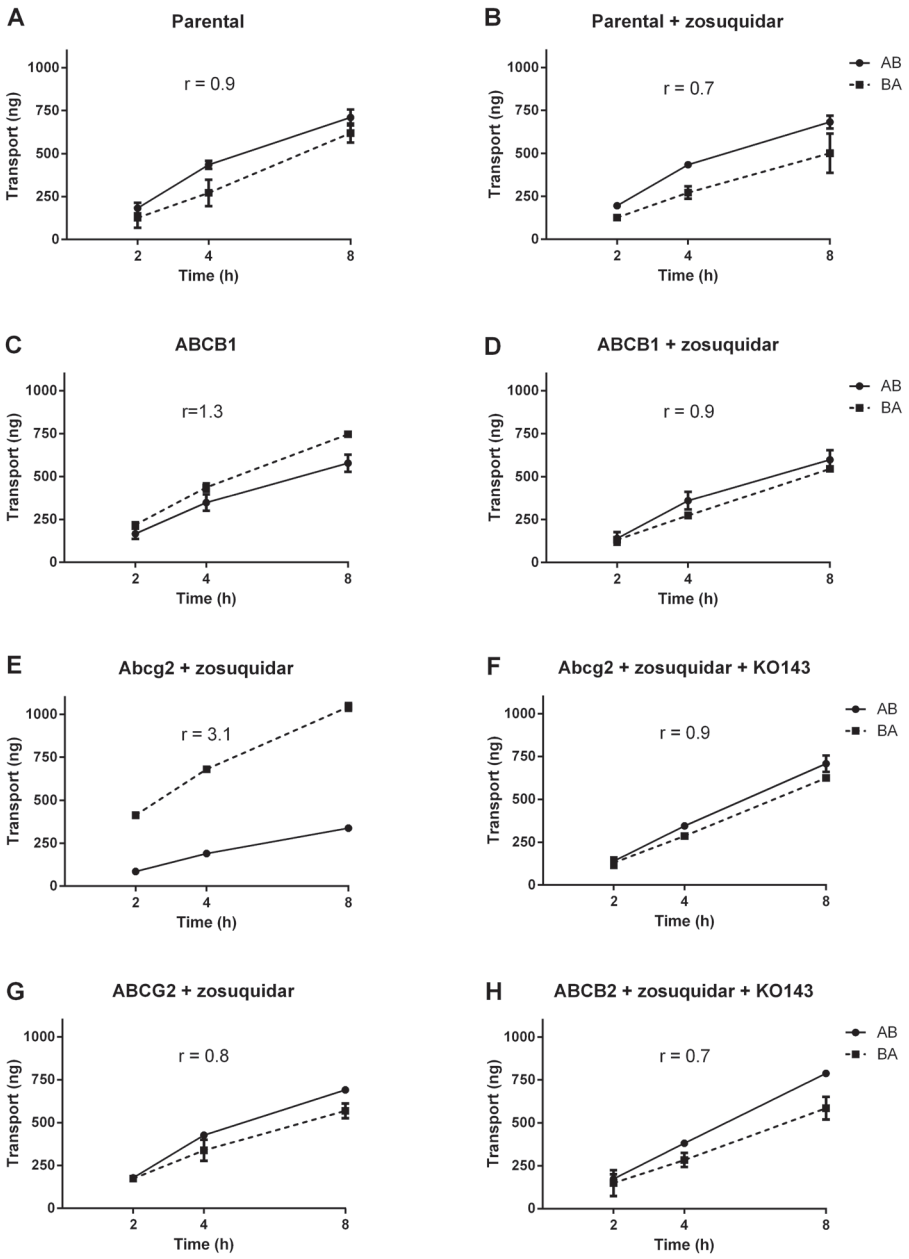


**Figure 1. *In vitro* transport of 5 μM regorafenib.** Transepithelial transport of regorafenib (5 μM) was assessed in MDCK-II cells either nontransduced (A, B) or transduced with hABCB1 (C, D), mAbcg2 (E, F) or hABCG2 (G, H) cDNA. At *t* = 0 h, regorafenib was applied to the donor compartment and concentrations in the acceptor compartment were measured at t = 2, 4 and 8 h and plotted as total amount of transport (ng) in the graphs. B, D-H: zosuquidar (5 μM) and/or Ko143 (5 μM) were applied as indicated to inhibit ABCB1 or ABCG2 and Abcg2, respectively. r, relative transport ratio. BA (■), translocation from basolateral to apical compartment; AB (●), translocation from apical to basolateral compartment. Points, mean (n = 3); bars, S.D.

to investigate the interaction of regorafenib with digoxin and with rosuvastatin (an ABCG2 substrate). CYP3A4 enzymes and UGT1A9 are responsible for the metabolism of regorafenib resulting in two major and six minor metabolites. The formation of the two major circulating metabolites referred to as M2 and M5, is mediated by CYP3A4. Regorafenib and its metabolites can be reabsorbed from the gut lumen and undergo enterohepatic cycling. M2 and M5 are pharmacodynamically active and accumulate to similar plasma levels as regorafenib, once plasma steady state is reached. This accumulation is non-linear and could be a result of the enterohepatic cycling and the long elimination half-life of these metabolites [15]. As a consequence, the metabolites may have a significant impact on the therapeutic efficacy of regorafenib. Interestingly, even though regorafenib was not found to be transported by ABCB1 or ABCG2 *in vitro*, both M2 and M5 were found to be weakly transported by ABCB1 and M5 weakly by ABCG2 [16].

In this study, we investigated the interaction of regorafenib with the ABC transporters ABCB1 and ABCG2 *in vitro* as well as *in vivo*. As the active and main circulating metabolites are formed by Cyp3a enzymes we also studied the drug in Cyp3a$^{-/-}$ mice. We further aimed to investigate to what extent the metabolites are able to cross the BBB.

## MATERIALS AND METHODS

### Chemicals

Regorafenib and zosuquidar were purchased from Sequoia Research Products (Pangbourne, UK). Zosuquidar (Eli Lilly; Indianapolis, USA) used for the 5 μM transwell experiment was a kind gift from Dr. O. van Tellingen (The Netherlands Cancer Institute, Amsterdam, NL) and Ko143 was obtained from Tocris Bioscience (Bristol, UK). Methoxyflurane (Metofane®) was obtained from Medical Developments Australia (Melbourne, Australia). Heparin (5000 IU ml$^{-1}$) was obtained from Leo Pharma BV (Breda, The Netherlands). Bovine Serum Albumin (BSA) Fraction V, was purchased from Roche (Mannheim, Germany). Chemicals used for the bioanalytical assay of regorafenib were described previously [17]. All other chemicals and reagents were obtained from Sigma-Aldrich (Steinheim, Germany).

### Transport assays

Polarized Madin-Darby Canine Kidney (MDCK-II) cell lines transduced with ABCB1, Abcg2 and ABCG2 cDNA were used and cultured as described previously [18]. Transepithelial transport assays were performed in triplicate on 12-well microporous polycarbonate membrane filters (3.0-μm pore size, Transwell 3402, Corning Inc., Lowell, MA) as described previously [19]. In short, cells were allowed to grow an intact monolayer in 3 days. On day 3, cells were pre-incubated with the relevant inhibitors for 1 hour. To inhibit endogenous canine P-gp in the MDCK-II Abcg2 and MDCK-II ABCG2 cell lines, we added 5 μM zosuquidar (P-gp inhibitor) to the culture medium during the entire experiment. The experiment was started by replacing the incubation medium from the donor compartment with fresh drug-containing medium. At 2, 4, 8 and 24 hours, 50 μL samples were collected and stored at -20 °C until analysis. The amount of transported drug was calculated after correction for volume loss due to sampling at each time point. Active transport was expressed by the transport ratio (*r*), which is defined as the amount

of apically directed transport divided by the amount of basolaterally directed transport at a defined time point. Each experiment was performed in triplicate.

**Animals**

Male wild-type, *Abcb1a/1b*$^{-/-}$ [20], *Abcg2*$^{-/-}$ [21], *Abcg2*$^{-/-}$*;Abcb1a/1b*$^{-/-}$ [22] and *Cyp3a*$^{-/-}$ mice [23], all of a >99% FVB genetic background were used. Mice between 9 and 13 weeks of age were used in groups of 5 mice per strain. The mice were kept in a temperature-controlled environment with a 12-h light/dark cycle and received a standard diet (AM-II, Hope Farms B.V., Woerden, the Netherlands) and acidified water *ad libitum*. Animals were housed and handled according to institutional guidelines in compliance with Dutch and European legislation.





**Drug solutions**

Regorafenib was dissolved in DMSO (20 mg/mL) and diluted 20-fold with a vehicle mixture consisting of 2.5% glucose, 10% polysorbate 80, 6.5% ethanol and 33.5% $H_2O$ to obtain a 1 mg/mL solution. Regorafenib was administered orally at 10 mL/kg body weight. All working solutions were prepared freshly on the day of experiment.

**Plasma and tissue pharmacokinetics of regorafenib**

To minimize variation in absorption, mice were fasted for two hours prior to regorafenib administration, using oral gavage with a blunt-ended needle. For the pharmacokinetic experiment, 50 µL blood samples were drawn from the tail vein using heparin-coated capillaries (Sarstedt, Germany) at 0.5, 1, 2, 4 and 8 hours. At 24 hours mice were anesthetized using isoflurane and blood was collected via cardiac puncture. Immediately thereafter, mice where sacrificed by cervical dislocation and a set of organs was rapidly removed, weighed and subsequently frozen as whole organ at -20 degrees. Prior to analysis, organs were allowed to thaw and then homogenized in 1% BSA in water using a FastPrep®-24 device (MP Biomedicals, SA, California, USA). Brain and testis were homogenized in 1 mL of 1% BSA and liver in 3 mL. Blood samples were immediately centrifuged after collection at 2,100 g for 6 min at 4°C, and plasma was collected and stored at -20°C until analysis.

**Relative accumulation of regorafenib in brain, testis, liver and kidney**

Mice were fasted for 2 hours before oral gavage of regorafenib. At 0.25, 0.5 and 1 hour blood was collected by tail vein sampling. At 2 hours, roughly corresponding with the $T_{max}$, mice were anesthetized with isoflurane and blood was collected by cardiac puncture. Immediately thereafter, mice were sacrificed and brain, testis, liver and kidney were removed and processed as described above. Regorafenib concentration in brain tissue was corrected for the presence of plasma in the vascular space (1.4%) [24].

**Drug analysis**

Regorafenib concentration in culture medium was analyzed with a previously reported liquid-chromatography tandem mass spectrometry (LC-MS/MS) assay for regorafenib, with a calibration ranging from 25-25,000 ng/mL [17]. Plasma and tissue homogenates were analyzed with an LC-MS/MS assay where two active metabolites were included to the previously mentioned

regorafenib assay. The calibration range covers 10-10,000 ng/mL with an extrapolated lower limit of detection of 5 ng/mL for both regorafenib and its metabolites (unpublished data).

### Pharmacokinetic calculations and statistical analysis

The area-under the curve (AUC) of the plasma concentration-time curve was calculated using the trapezoidal rule, without extrapolating to infinity. The peak plasma concentration ($C_{max}$) and the time to reach peak plasma concentration ($T_{max}$) were determined from individual concentration-time data. Ordinary one-way analysis of variance (ANOVA) was used to determine significant differences between groups. Post-hoc Tukey's multiple comparison test was used to compare significant differences between individual groups. When variances were not homogeneously distributed, data were log-transformed before applying statistical tests. Differences were considered statistically significant when $P < 0.05$. Data are presented as mean ± SD with each experimental group containing 5 mice.



## RESULTS

### Regorafenib is a modestly transported by ABCB1 and efficiently by Abcg2 and ABCG2 *in vitro*

Polarized MDCK-II cell lines transduced with human (h)ABCB1, murine (m)Abcg2 or human (h) ABCG2 were used to assess active transport of 5 μM regorafenib. We observed a slight amount of basolaterally directed transport in the parental cells which was even more pronounced upon addition of zosuquidar, resulting in a transport ratio of 0.9 and 0.7, respectively. Bearing this in mind, there was a modest transport of regorafenib by ABCB1 counteracting the basolaterally directed transport (r = 1.3) as shown in figure 1C. This transport was completely inhibited by zosuquidar (Fig. 1D, r = 0.9). Regorafenib was a good substrate of mAbcg2 (r = 3.1) and this transport was efficiently inhibited by Ko143. In contrast to mAbcg2, hABCG2 appeared to have no effect on the transport of regorafenib (Fig. 1G, r = 0.8). As 5 μM regorafenib might saturate a possible modest transport activity of hABCG2, we lowered the concentration in the assay to 1 μM. Results similar to the previous experiment were obtained for the parental, hABCB1 and mAbcg2 expressing cells, although the background basolaterally directed transport of regorafenib in the parental cells was even more pronounced, and potentially also inhibited by zosuquidar. However, now hABCG2 showed a clear apically directed transport of regorafenib which was completely inhibited by Ko143 (Fig. 2 E-H).

### Plasma pharmacokinetics of regorafenib in Abcg2$^{-/-}$, Abcb1a/1b$^{-/-}$ and Abcg2$^{-/-}$;Abcb1a/1b$^{-/-}$ mice

As regorafenib is orally administered to patients, the mice received regorafenib by oral gavage into the stomach. The time to reach peak plasma concentrations was about 2 hours in each strain (Fig. 3A). The experimental variation was quite high, and although the AUCs in the single knock-out strains were significantly lower compared to WT, 0.8-fold for Abcg2$^{-/-}$ mice ($P < 0.01$) and 0.5-fold in Abcb1a/1b$^{-/-}$ ($P < 0.001$), the combination Abcg2$^{-/-}$;Abcb1a/1b$^{-/-}$ mice had an AUC close to the WT mice. Collectively, this indicates there is no substantial effect of these transporters on restricting the oral availability of regorafenib.

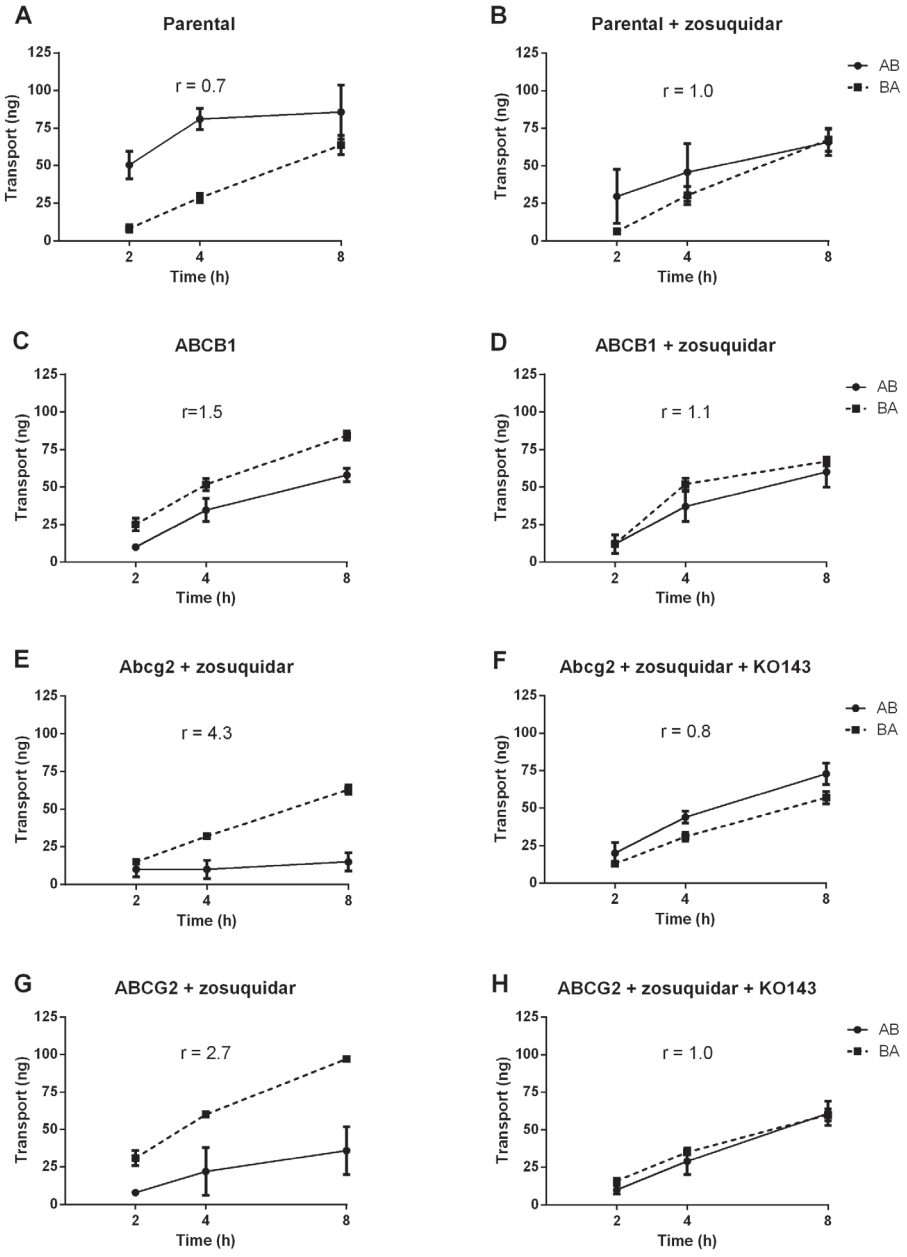


**Figure 2. *In vitro* transport of 1 µM regorafenib.** Transepithelial transport of regorafenib (1 µM) was assessed in MDCK-II cells either nontransduced (A, B) or transduced with hABCB1 (C, D), mAbcg2 (E, F) or hABCG2 (G, H) cDNA. At *t* = 0 h, regorafenib was applied to the donor compartment and concentrations in the acceptor compartment were measured at t = 2, 4 and 8 h and plotted as total amount of transport (ng) in the graphs (n = 3). B, D-H: zosuquidar (5 µM) and/or Ko143 (5 µM) were applied as indicated to inhibit hABCB1 or hABCG2 and mAbcg2, respectively. r, relative transport ratio. BA (■), translocation from basolateral to apical compartment; AB (●), translocation from apical to basolateral compartment. Points, mean (n = 3); bars, S.D.

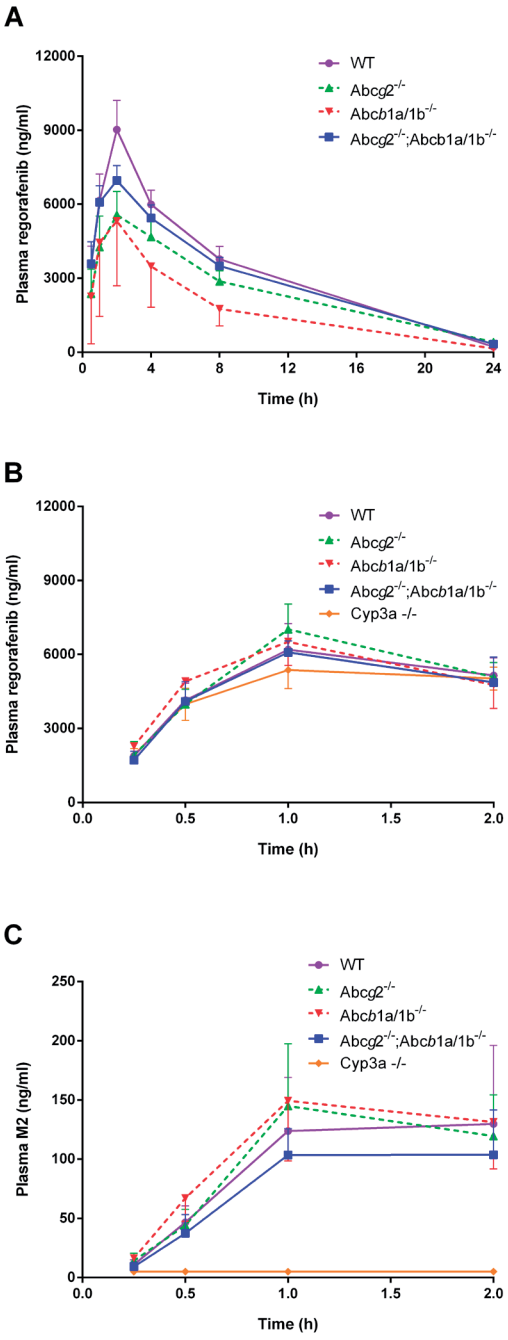


**Figure 3. Plasma concentration-time curves ($AUC_{0-24}$) of regorafenib in male WT (●), Abcg2$^{-/-}$ (▲), Abcb1a/1b$^{-/-}$ (▼), and Abcg2$^{-/-}$;Abcb1a/1b$^{-/-}$ (■) mice over 24 h (A) and plasma concentration-time curves ($AUC_{0-2}$) of regorafenib (B) and metabolite M2 (C) 2 h after oral administration of 10 mg/kg regorafenib.** Points, mean (n=5); bars, SD.

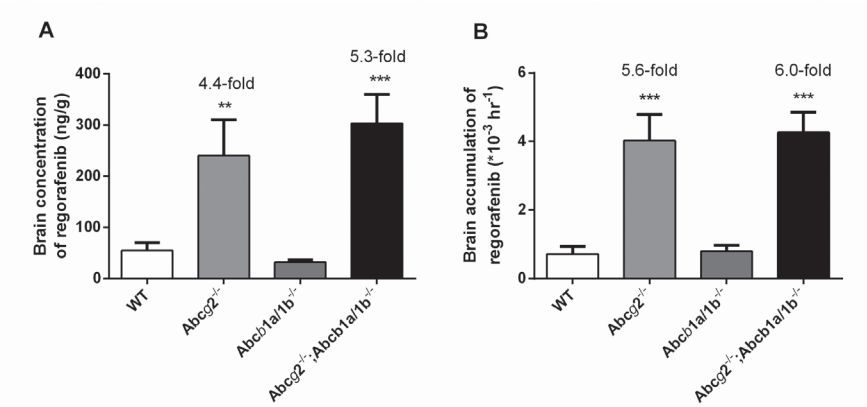


**Figure 4. Brain concentration (A) and relative brain accumulation (B) of regorafenib in male WT, Abcg2$^{-/-}$, Abcb1a/1b$^{-/-}$ and Abcg2$^{-/-}$;Abcb1a/1b$^{-/-}$ mice 24 h after oral administration of 10 mg/kg regorafenib.** **, $P < 0.01$; ***, $P < 0.001$ compared with WT mice. Data are presented as mean ± S.D. Where necessary, data were log-transformed to normalize the S.D.s between study groups (n = 5).

### Abcg2 and Abcb1a/1b limit regorafenib brain and testis accumulation in mice

After completion of the 24-hr pharmacokinetic experiment brains were collected to assess the brain accumulation of regorafenib. Although regorafenib was largely eliminated from the plasma within 24 hours, elevated concentrations were found in the brain of Abcg2$^{-/-}$ mice and Abcg2$^{-/-}$;Abcb1a/1b$^{-/-}$ mice, respectively 4.4-fold and 5.3-fold compared to WT (Fig. 4A). Also after correction for the individual plasma AUCs, comparable effects were seen for Abcg2$^{-/-}$ and Abcg2$^{-/-}$;Abcb1a/1b$^{-/-}$ mice whereas there was no effect of single Abcb1 deficiency on brain accumulation, as shown in Figure 4B.

The impact of transporter proteins may be especially relevant around the maximum plasma concentration. Mice were therefore also sacrificed two hours after oral administration of 10 mg/kg regorafenib and plasma and brains were removed and analyzed. Plasma AUC curves up to 2 hours (Fig. 3B) were similar for all mouse strains, further confirming that the absence of Abcg2 and Abcb1a/1b did not have a strong effect on the plasma AUC. As shown in Table I and Fig. 5A, Abcg2 deficiency resulted in a 3.7-fold increase in regorafenib brain concentration compared to WT mice. Single Abcb1a/1b knockout had no effect on brain concentration but when both Abcg2 and Abcb1a/1b were absent, the brain concentration further increased to a 7.9-fold higher brain concentration compared to WT mice. This was a significant twofold increase compared to the effect of Abcg2 deficiency alone ($P < 0.001$).

As testis resembles the brain with regard to the presence of Abcg2 and Abcb1a/1b in its blood-tissue barrier (blood-testis barrier, BTB), this organ was also analyzed to assess whether regorafenib is kept out by either Abcg2 and/or Abcb1a/1b. As shown in Figure 5C, absence of Abcg2 resulted in a 2.9-fold increase of regorafenib accumulation and a dual knock out with Abcb1a/1b further increased regorafenib accumulation. In contrast to brain data, single knockout of Abcb1a/1b also resulted in a significant, twofold increase of regorafenib accumulation in testis compared to wild type ($P < 0.01$). These results show that

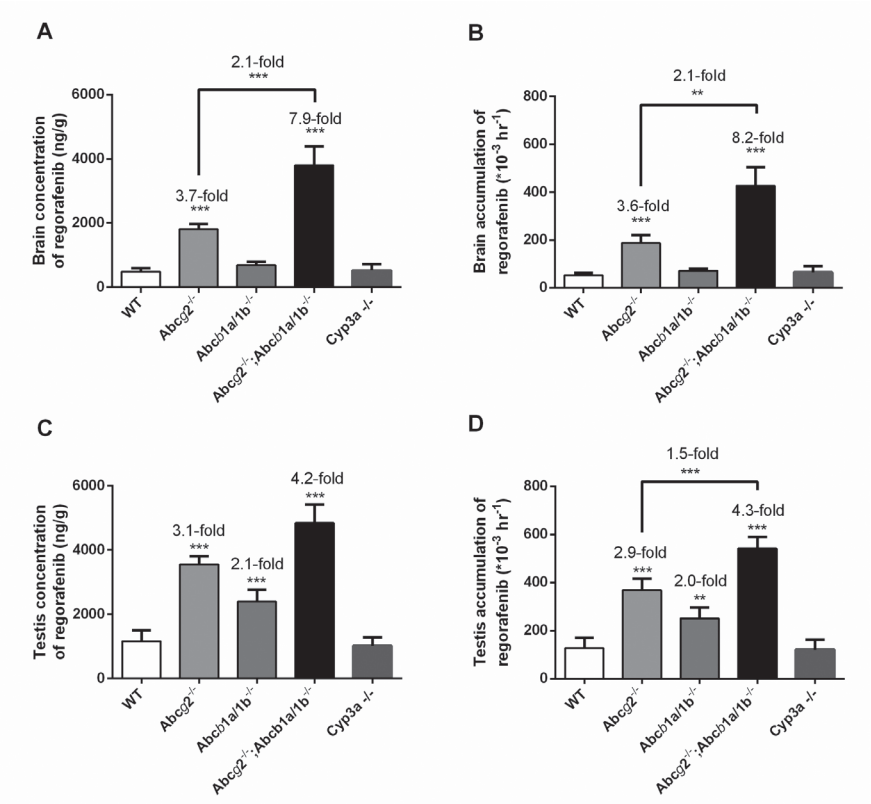


**Figure 5. Brain concentration (A), relative brain accumulation (B), testis concentration (C) and testis accumulation (D) of regorafenib in male WT, Abcg2$^{-/-}$, Abcb1a/1b$^{-/-}$, Abcg2$^{-/-}$;Abcb1a/1b$^{-/-}$ and Cyp3a$^{-/-}$ mice, 2 h after oral administration of 10 mg/kg regorafenib.** **, $P < 0.01$; ***, $P < 0.001$ compared with WT mice. Data are presented as mean ± S.D. Where necessary, data were log-transformed to normalize the S.D.s between study groups (n = 5).

both Abcg2 and Abcb1, single or in combination, contribute to restricting testis accumulation of regorafenib.

Regorafenib concentrations in well perfused organs like liver and kidney did not differ between the strains (Supplementary Fig. 2A-F), indicating that Abcg2 and Abcb1a/1b did not have a strong impact on the regorafenib disposition to these organs. The relative brain penetration of regorafenib in WT mice was about 2% of the liver penetration, whereas brain or testis penetration of regorafenib in the absence of Abcg2 and Abcb1a/1b was increased to 17% to 30% of the liver and kidney penetration.

### Active regorafenib metabolite M2 is able to penetrate the brain in Abcg2$^{-/-}$;Abcb1a/1b$^{-/-}$ mice

To investigate the effect of CYP3A enzymes on metabolite formation, we gave 10 mg/kg regorafenib orally to Cyp3a$^{-/-}$ mice. As shown in Fig. 3C, M2 was already detectable in plasma

**Table 1.** Pharmacokinetic parameters of regorafenib and the metabolite M2, 2h and 24h after oral administration of 10 mg/kg regorafenib to male WT, Abcg2$^{-/-}$, Abcb1a/1b$^{-/-}$, Abcg2$^{-/-}$;Abcb1a/1b$^{-/-}$ and Cyp3a$^{-/-}$ mice (n = 5).

| | | | Genotype | | | | |
|---|---|---|---|---|---|---|---|
| **Parameter** | **Time (h)** | **Compound** | **Wild-type** | ***Abcg2*$^{-/-}$** | ***Abcb1a/1b*$^{-/-}$** | ***Abcb1a/1b;Abcg2*$^{-/-}$** | ***Cyp3a*$^{-/-}$** |
| Plasma AUC(0-2), | 2h | Regorafenib | 9241 ± 1304 | 9780 ± 1177 | 9679 ± 1403 | 8965 ± 1006 | 8505 ± 846 |
| Cmax, ng/mL | | | 6235 ± 1011 | 7021 ± 1029 | 6516 ± 966 | 6086 ± 464 | 5535 ± 541 |
| Tmax, h | | | 1-2 | 1-2 | 1-2 | 1-2 | 1-2 |
| Cbrain, ng/g | | | 482 ± 112 | 1808 ± 161 ***,++ | 689 ± 104 +++ | 3804 ± 585 *** | 522 ± 199 +++ |
| Fold increase Cbrain | | | 1.0 | 3.7 | 1.4 | 7.9 | 1.1 |
| Pbrain (*10-3 h-1) | | | 52 ± 11 | 188 ± 33 ***,++ | 72 ± 10 +++ | 428 ± 78 *** | 66 ± 26 +++ |
| Fold increase Pbrain | | | 1.0 | 3.6 | 1.4 | 8.2 | 1.3 |
| Plasma AUC(0-2), | 2h | M2 | 178 ± 68 | 188 ± 62 | 207 ± 65 | 146 ± 37 | < LOD |
| Cmax, ng/mL | | | 143 ± 61 | 145 ± 53 | 150 ± 51 | 115 ± 27 | < LOD |
| Tmax, h | | | 1-2 | 1-2 | 1-2 | 1-2 | n.a. |
| Cbrain, ng/g | | | < LOD | < LOD | < LOD | 34 ± 14 | < LOD |
| Pbrain (*10-3 h-1) | | | n.a. | n.a. | n.a. | 235 ± 80 | n.a. |
| Plasma AUC(0-24), | 24h | Regorafenib | 77367 ± 7766 | 58780 ± 8418 ** | 41590 ± 10623 *** | 70750 ± 4696 | |
| Cmax, ng/mL | | | 9027 ± 1183 | 4404 ± 2635 | 6477 ± 1705 | 6959 ± 602 | |
| Tmax, h | | | 2 | 2 | 1-4 | 2 | |
| Cbrain, ng/g | | | 55 ± 15 | 240 ± 69 *** | 32 ± 5* | 303 ± 56 *** | |
| Fold increase Cbrain | | | 1.0 | 4.4 | 0.6 | 5.5 | |
| Pbrain (*10-3 h-1) | | | 0.72 | 4.0 *** | 0.80 +++ | 4.3 *** | |
| Fold increase Pbrain | | | 1.0 | 5.6 | 1.1 | 6.0 | |

*AUC, area under the plasma concentration-time curve; $C_{max}$, maximum drug concentration in plasma; $T_{max}$, the time (h) after administration of a drug when the maximum plasma concentration is reached; $C_{brain}$, brain concentration; $P_{brain}$, brain accumulation; LOD, limit of detection.*
*Note that for calculation of M2 concentrations the LOD value of 5 ng/mL was used when the analytical results was below LOD. * P < 0.05; ** P < 0.01; *** P < 0.001 compared to WT mice and + P < 0.05; ++ P < 0.01 ; +++ P < 0.001 compared to Abcg2$^{-/-}$;Abcb1a/1b$^{-/-}$ mice (WT mice were excluded from this last comparison). Data are given as mean ± S.D (n = 5).*

after 15 minutes, with a likely $C_{max}$ at roughly 1-2 hour in WT mice. No detectable amount of M2 was found in plasma of Cyp3a$^{-/-}$ mice up to two hours, while similar AUCs were obtained for WT, Abcg2$^{-/-}$, Abcb1a/1b$^{-/-}$ and Abcg2$^{-/-}$;Abcb1a/1b$^{-/-}$ mice corresponding with roughly 2% of the regorafenib $AUC_{0-2}$. M2 brain concentrations were below the lower limit of quantitation (LLOQ) in all mouse strains and even below the limit of detection (LOD; < 5 ng/mL), with the exception of Abcg2$^{-/-}$;Abcb1a/1b$^{-/-}$ mice. There was therefore a minimally 2.2-fold increase in brain levels of M2 visible after two hours compared to all the other tested mouse strain (Table 1, Supplementary Fig. 3A-B). M5 was not detected within two hours in plasma or in the analyzed tissues.

## DISCUSSION

Our results indicate that regorafenib is a transported substrate of ABCG2 as well as ABCB1. This is evidenced *in vitro* by positive transport ratios and full inhibition of the transport by the respective inhibitors. Furthermore, we were able to extend these findings to the *in vivo* situation using single and dual knockout mice. As shown in Fig. 4 and 5, Abcg2 clearly restricts the brain and testis accumulation of regorafenib in mice. Additional Abcb1a/1b knockout leads to an even bigger increase in brain and testis accumulation of regorafenib and M2. As trace amounts of M2, only slightly above LOD were measured in the absence of both Abcg2 and Abcb1, it is possible that M2 is also a shared substrate of these transporter proteins (Data not shown).

According to the manufacturer, regorafenib is an inhibitor of ABCG2, but not a transported substrate of either ABCG2 or ABCB1 *in vitro*. Transwell membrane experiments in LLC-ABCB1 and MDCK-II-ABCG2 cell lines with concentrations ranging from 0.2-10 μM were used and no evidence of active transport by either transporter was found. Therefore no further *in vivo* and clinical investigations were deemed necessary [14, 16, 25]. We, however, found low but still active transport (r = 1.3) mediated by hABCB1, using the mid-level concentration of 5 μM regorafenib. This transport is inhibited by zosuquidar to similar levels as seen in parental cells. Clear transport by mAbcg2 (r=3.1) was efficiently inhibited by Ko143, but interestingly enough hABCG2 seemed to have no effect on the active transport of regorafenib. To exclude that the lack of transport by hABCG2 was caused by saturation, we chose to repeat the experiment with 1 μM regorafenib to ensure that transported regorafenib would still be detectable by the assay. Similar results are seen for hABCB1 and mAbcg2, but now we clearly observed active transport of regorafenib by hABCG2 which was efficiently inhibited by Ko143. These results are similar to previously published data for sorafenib, where a more pronounced effect of Abcg2 compared to ABCB1 was found on the transepithelial transport of sorafenib [12].

No substantial effect of Abcg2 and Abcb1a/1b transporters on the oral availability of regorafenib and M2 were observed (Fig.3). However, regorafenib brain accumulation was increased 3.6-fold in Abcg2$^{-/-}$ mice compared to WT, where there was no significant effect of Abcb1a/1b deficiency. This indicates that a single Abcb1a/1b knockout had no detectable effect on the brain penetration, presumably as Abcg2 was able to take over the function of Abcb1a/1b. When both transporters were knocked out, the additional contribution of Abcb1a/1b for the brain penetration became apparent. This disproportionate effect is seen more often for tyrosine kinase inhibitors and other drugs that are shared Abcg2 and Abcb1 substrates. Kodaira *et al*. (2010) developed a pharmacokinetic model of the cooperation of ABCG2 and ABCB1 at the

BBB for multiple drugs amongst which imatinib. They found that the disproportionate effect is not due to a direct interaction between ABCG2 and ABCB1, but merely a result of the net efflux activity of the transporters at the BBB and BTB being much higher than the remaining (possibly only) passive efflux activity at these barriers [26]. Also, a previously reported pharmacokinetic model from Kalvass and Pollack in 2007 made very similar predictions [27].

As ABCG2 and ABCB1 are present in the BTB as well, the concentration and accumulation of regorafenib in testis was also investigated. As expected, more or less similar distribution properties of regorafenib in the single and dual knockout mice were seen as in the brain. This provided even more evidence that regorafenib is transported *in vivo* by Abcg2 as well as Abcb1. At the BTB, however, there was also a significant impact of single Abcb1a/1b knockout on the regorafenib accumulation.

The formation of M2 appears to be solely regulated by Cyp3a enzymes. Regorafenib was rapidly oxidized to M2 as we were able to measure the compound already 15 minutes after oral administration of regorafenib in all strains except for the Cyp3a knockout mice. There was a clear increase in passage of M2 across the BBB in Abcg2$^{-/-}$;Abcb1a/1b$^{-/-}$ mice, suggesting that M2 is able to penetrate the BBB, like regorafenib. M5 was not detectable in mouse plasma after two hours but we cannot exclude that M5 will show a similar pattern as M2. The amount of metabolite formed within two hours of regorafenib administration, was too low to observe BTB passage of M2, although small amounts of M2 were already detectable in liver and kidney tissue. Subsequent daily oral administrations of regorafenib in patients appear to play a role in the substantial levels of M2 and M5 that are detected, presumably by gradual (non-linear) accumulation of these metabolites over time.



## CONCLUSIONS

We conclude that the multikinase inhibitor regorafenib is transported *in vitro* by hABCG2, mAbcg2 and hABCB1. This is supported *in vivo* in mice where brain and testis concentrations and relative tissue accumulation is restricted mostly by Abcg2 and additionally by Abcb1. These results indicate that co-administration of ABCG2 and/or ABCB1 inhibitors may increase regorafenib exposure in patients thus providing them an option to treat (micro)metastases behind a functionally intact blood-brain barrier.

## REFERENCE LIST

1. Burger, H. and K. Nooter, *Pharmacokinetic resistance to imatinib mesylate: role of the ABC drug pumps ABCG2 (BCRP) and ABCB1 (MDR1) in the oral bioavailability of imatinib.* Cell Cycle, 2004. 3(12): p. 1502-5.
2. Schinkel, A.H., et al., *P-glycoprotein in the blood-brain barrier of mice influences the brain penetration and pharmacological activity of many drugs.* J Clin Invest, 1996. 97(11): p. 2517-24.
3. Chen, Y., et al., *P-glycoprotein and breast cancer resistance protein influence brain distribution of dasatinib.* J Pharmacol Exp Ther, 2009. 330(3): p. 956-63.
4. Wilhelm, S.M., et al., *Regorafenib (BAY 73-4506): a new oral multikinase inhibitor of angiogenic, stromal and oncogenic receptor tyrosine kinases with potent preclinical antitumor activity.* Int J Cancer, 2011. 129(1): p. 245-55.
5. Grothey, A., et al., *Regorafenib monotherapy for previously treated metastatic colorectal cancer (CORRECT): an international, multicentre, randomised, placebo-controlled, phase 3 trial.* Lancet, 2013. 381(9863): p. 303-12.
6. Demetri, G.D., et al., *Efficacy and safety of regorafenib for advanced gastrointestinal stromal tumours after failure of imatinib and*

*sunitinib (GRID): an international, multicentre, randomised, placebo-controlled, phase 3 trial*. Lancet, 2013. 381(9863): p. 295-302.

7. Sallinen, H., et al., *Cotargeting of VEGFR-1 and -3 and angiopoietin receptor Tie2 reduces the growth of solid human ovarian cancer in mice*. Cancer Gene Ther, 2011. 18(2): p. 100-9.
8. Tsai, J.H. and W.M. Lee, *Tie2 in tumor endothelial signaling and survival: implications for antiangiogenic therapy*. Mol Cancer Res, 2009. 7(3): p. 300-10.
9. Bruix, J., et al., *Regorafenib as second-line therapy for intermediate or advanced hepatocellular carcinoma: multicentre, open-label, phase II safety study*. Eur J Cancer, 2013. 49(16): p. 3412-9.
10. Poller, B., et al., *Differential impact of P-glycoprotein (ABCB1) and breast cancer resistance protein (ABCG2) on axitinib brain accumulation and oral plasma pharmacokinetics*. Drug Metab Dispos, 2011. 39(5): p. 729-35.
11. Agarwal, S., et al., *The role of the breast cancer resistance protein (ABCG2) in the distribution of sorafenib to the brain*. J Pharmacol Exp Ther, 2011. 336(1): p. 223-33.
12. Lagas, J.S., et al., *Breast cancer resistance protein and P-glycoprotein limit sorafenib brain accumulation*. Mol Cancer Ther, 2010. 9(2): p. 319-26.
13. Hu, S., et al., *Interaction of the multikinase inhibitors sorafenib and sunitinib with solute carriers and ATP-binding cassette transporters*. Clin Cancer Res, 2009. 15(19): p. 6062-9.
14. *Center for Drug Evaluation and Research of the US Department of Health and Human Services, Food and Drug Administration. Clinical Pharmacology and Biopharmaceutics Review(s)*. 2012 [cited 2014 June 5]; Available from: http://www.accessdata.fda.gov/drugsatfda_docs/nda/2012/203085Orig1s000ClinPharmR.pdf.
15. Mross, K., et al., *A phase I dose-escalation study of regorafenib (BAY 73-4506), an inhibitor of oncogenic, angiogenic, and stromal kinases, in patients with advanced solid tumors*. Clin Cancer Res, 2012. 18(9): p. 2658-67.
16. European Medicines Agency. *Stivarga Summary of Product Characteristics*. 2013 [cited 2014 June 5]; Available from: http://www.ema.europa.eu/docs/en_GB/document_library/EPAR_-_Product_Information/human/002573/WC500149164.pdf.
17. Luethi, D., et al., *Liquid chromatography-tandem mass spectrometric assay for the multikinase inhibitor regorafenib in plasma*. Biomed Chromatogr, 2014.
18. Evers, R., et al., *Drug export activity of the human canalicular multispecific organic anion transporter in polarized kidney MDCK cells expressing cMOAT (MRP2) cDNA*. J Clin Invest, 1998. 101(7): p. 1310-9.
19. Durmus, S., et al., *Oral availability and brain penetration of the B-RAFV600E inhibitor vemurafenib can be enhanced by the P-glycoprotein (ABCB1) and breast cancer resistance protein (ABCG2) inhibitor elacridar*. Mol Pharm, 2012. 9(11): p. 3236-45.
20. Schinkel, A.H., et al., *Normal viability and altered pharmacokinetics in mice lacking mdr1-type (drug-transporting) P-glycoproteins*. Proc Natl Acad Sci U S A, 1997. 94(8): p. 4028-33.
21. Jonker, J.W., et al., *The breast cancer resistance protein protects against a major chlorophyll-derived dietary phototoxin and protoporphyria*. Proc Natl Acad Sci U S A, 2002. 99(24): p. 15649-54.
22. Jonker, J.W., et al., *The breast cancer resistance protein BCRP (ABCG2) concentrates drugs and carcinogenic xenotoxins into milk*. Nat Med, 2005. 11(2): p. 127-9.
23. van Waterschoot, R.A., et al., *Absence of both cytochrome P450 3A and P-glycoprotein dramatically increases docetaxel oral bioavailability and risk of intestinal toxicity*. Cancer Res, 2009. 69(23): p. 8996-9002.
24. Dai, H., et al., *Distribution of STI-571 to the brain is limited by P-glycoprotein-mediated efflux*. J Pharmacol Exp Ther, 2003. 304(3): p. 1085-92.
25. *Pharmaceuticals and Medical Devices Agency Japan*. Review report, 2013.
26. Kodaira, H., et al., *Kinetic analysis of the cooperation of P-glycoprotein (P-gp/Abcb1) and breast cancer resistance protein (Bcrp/Abcg2) in limiting the brain and testis penetration of erlotinib, flavopiridol, and mitoxantrone*. J Pharmacol Exp Ther, 2010. 333(3): p. 788-96.
27. Kalvass, J.C. and G.M. Pollack, *Kinetic considerations for the quantitative assessment of efflux activity and inhibition: implications for understanding and predicting the effects of efflux inhibition*. Pharm Res, 2007. 24(2): p. 265-76.

## SUPPLEMENTARY MATERIALS

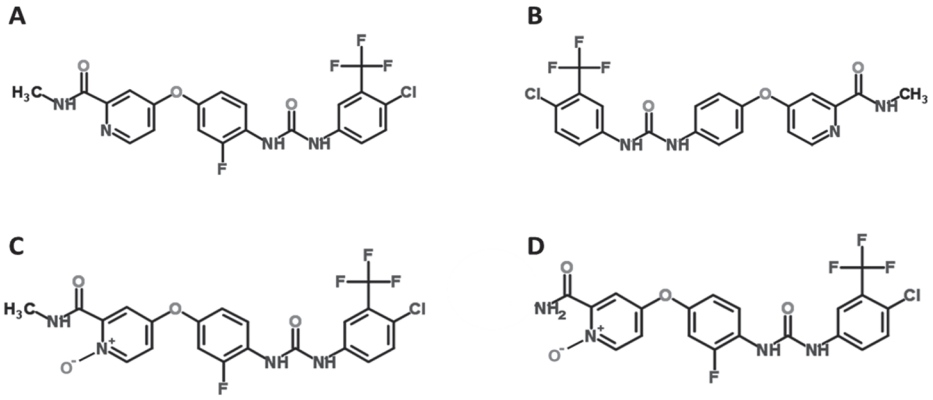


**Supplementary Figure 1. Structural formula of regorafenib (A), sorafenib (B), M2, N-oxidized metabolite of regorafenib (C) and M5, N-oxidized and demethylated metabolite of regorafenib (D).**

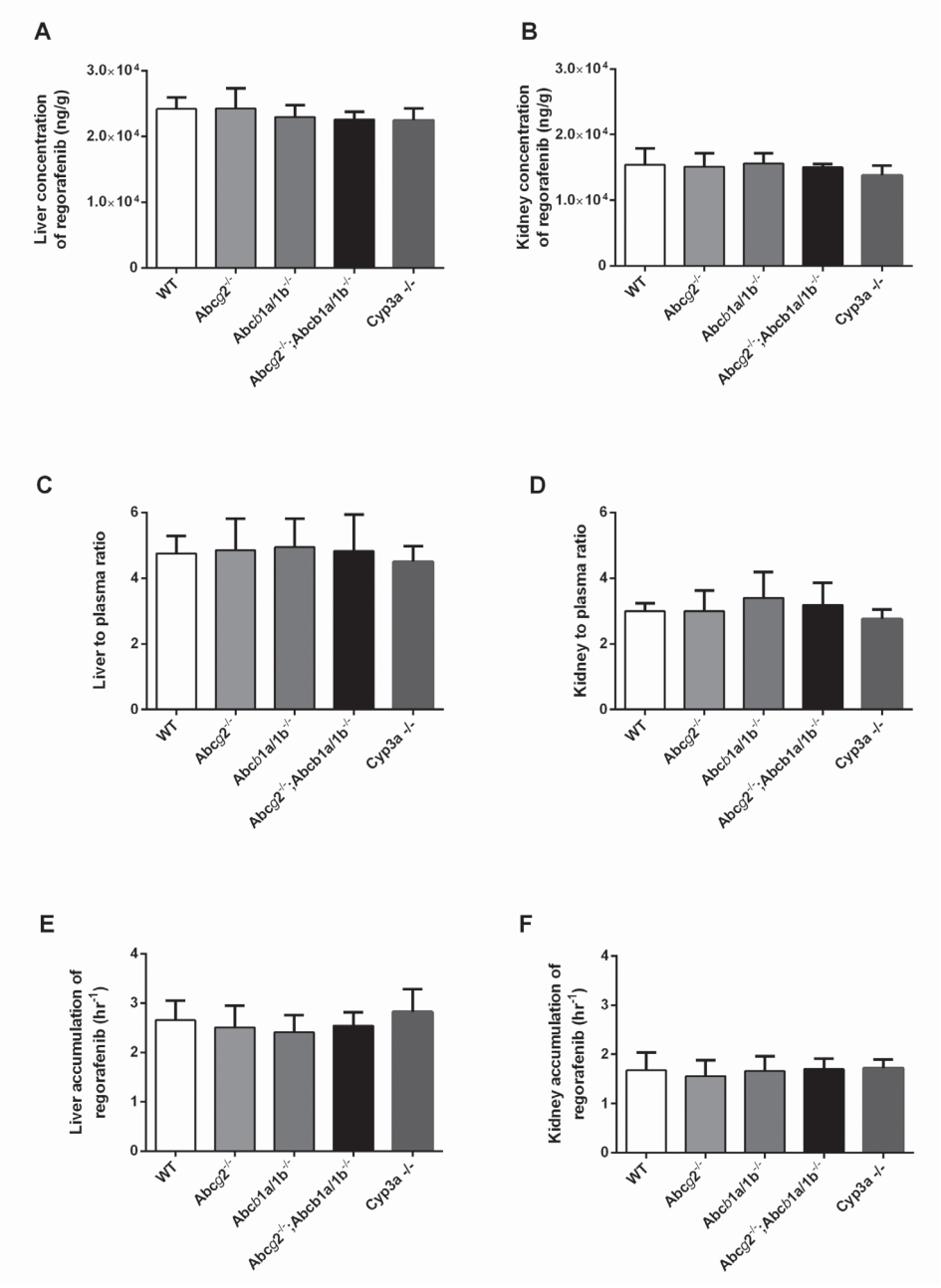


**Supplementary Figure 2. Liver and kidney concentration (A,B), liver and kidney tissue-to-blood ratios (C,D) and relative liver and kidney accumulation (E,F) in male WT, Abcg2$^{-/-}$, Abcb1a/1b$^{-/-}$, Abcg2$^{-/-}$;Abcb1a/1b$^{-/-}$ and Cyp3a$^{-/-}$ mice, 2 h after oral administration of 10 mg/kg regorafenib.** There were no statistically significant differences in concentration or tissue accumulation between the strains. Data are presented as mean ± S.D. Where necessary, data were log-transformed to normalize the S.D.s between study groups. (n = 5).

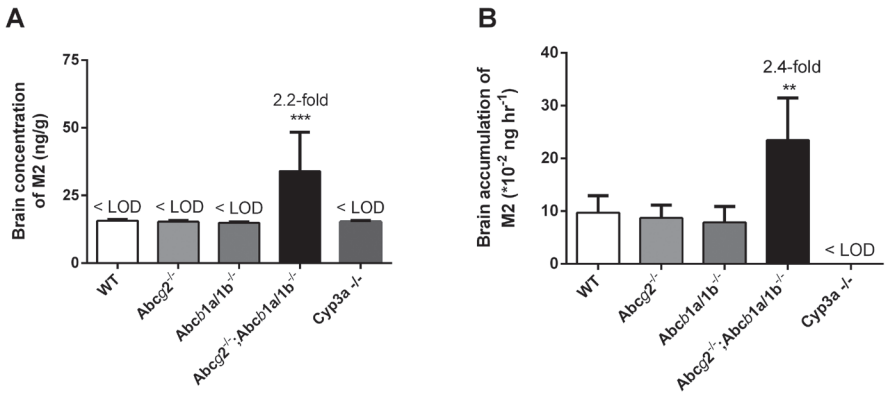


**Supplementary Figure 3. M2 brain concentration (A), relative brain accumulation (B) in male WT, Abcg2$^{-/-}$, Abcb1a/1b$^{-/-}$, Abcg2$^{-/-}$;Abcb1a/1b$^{-/-}$ and Cyp3a$^{-/-}$ mice, 2 h after oral administration of 10 mg/kg regorafenib.** Note that for M2 results below LOD, we used the LOD value (5 ng/mL) to perform calculations. **, $P < 0.01$; ***, $P < 0.001$ compared with WT mice. Data are presented as mean ± S.D. Where necessary, data were log-transformed to normalize the S.D.s between study groups. (n = 5).

# CHAPTER 2.4

## BREAST CANCER RESISTANCE PROTEIN (BCRP/ABCG2) AND P-GLYCOPROTEIN (P-GP/ABCB1) RESTRICT ORAL AVAILABILITY AND BRAIN ACCUMULATION OF THE PARP INHIBITOR RUCAPARIB (AG-014699)

Selvi Durmus[a], Rolf W. Sparidans[b], Anita van Esch[a], Els Wagenaar[a], Jos H. Beijnen[b,c] and Alfred H. Schinkel[a]

[a] The Netherlands Cancer Institute, Division of Molecular Oncology, Plesmanlaan 121, 1066 CX Amsterdam, The Netherlands.
[b]Utrecht University, Faculty of Science, Department of Pharmaceutical Sciences, Division of Pharmacoepidemiology & Clinical Pharmacology, Universiteitsweg 99, 3584 CG Utrecht, The Netherlands.
[c]Slotervaart Hospital, Department of Pharmacy & Pharmacology, Louwesweg 6, 1066 EC Amsterdam, The Netherlands.

*Pharmaceutical Research. 2014 June (Epub ahead of print).*

## ABSTRACT

### Background

Rucaparib is a potent, orally available, small-molecule inhibitor of poly ADP-ribose polymerase (PARP) 1 and 2. Ongoing clinical trials are assessing the efficacy of rucaparib alone or in combination with other cytotoxic drugs, mainly inbreast and ovarian cancer patients with mutations in the breast cancer associated (BRCA) genes.

### Purpose

We aimed to establish whether the multidrug efflux transporters ABCG2 (BCRP) and ABCB1 (P-gp, MDR1) affect the oral availability and brain penetration of rucaparib in mice.

### Results

*In vitro*, rucaparib was efficiently transported by both human ABCB1 and ABCG2, and very efficiently by mouse Abcg2. Transport could be inhibited by the small-molecule ABCB1 and ABCG2 inhibitors zosuquidar and Ko143, respectively. *In vivo*, oral availability (plasma $AUC_{0\text{-}1}$ and $AUC_{0\text{-}24}$) and brain levels of rucaparib at 1 and 24 h were increased by the absence of both Abcg2 and Abcb1a/1b after oral administration of rucaparib at 10 mg/kg.

### Conclusions

Our data show to our knowledge for the first time that oral availability and brain accumulation of a PARP inhibitor are markedly and additively restricted by Abcg2 and Abcb1a/1b. This may have clinical relevance for improvement of rucaparib therapy in PARP inhibitor-resistant tumors with ABCB1 and/or ABCG2 expression and in patients with brain (micro)metastases positioned behind a functional blood-brain barrier.

## INTRODUCTION

ATP-binding cassette (ABC) drug efflux transporters, such as P-glycoprotein (P-gp; ABCB1) and breast cancer resistance protein (BCRP; ABCG2) can have crucial roles in anti-cancer therapy. These transporters are expressed in apical membranes of several pharmacokinetically important tissues (e.g. small intestine, liver, blood-brain barrier) where they can affect the oral absorption, tissue distribution and toxicity of many anti-cancer drugs. Up till now, many (anti-cancer) drugs, and recently especially many tyrosine kinase inhibitors (TKIs) have been shown to be transported substrates of ABCB1 and/or ABCG2. The pharmacokinetics of these drugs are often affected by their interaction with these ABC transporters, resulting in altered tissue distribution (e.g. restricted brain penetration) or reduced oral availability [1-13]. Restriction in brain penetration of drugs by ABC transporters is potentially clinically important, because tumor parts or tumor rims, and (micro)metastases that are behind a functionally intact blood-brain barrier (BBB) cannot be efficiently eradicated by most currently available systemic drug therapies [14, 15]. Brain metastasis is for instance a major and challenging clinical problem in the treatment of advanced breast cancer (stage IV), and thought to be responsible for more than half of the deaths in those patients [16].

Rucaparib (AG-014699, CO-338 or PF-01367338, Supplementary Figure 1) is an orally available, potent small molecule inhibitor of the PARP1 and PARP2 enzymes, and under development for the treatment of advanced breast and ovarian cancers. PARP enzymes play critical roles in DNA repair, especially in the base excision repair (BER) pathway, which is responsible for single-strand break repair [17, 18]. Inhibiting activity of PARP enzymes in cells prevents single-strand break repair mediated via the BER pathway and this might result in double strand breaks. Under normal circumstances other DNA repair pathways such as homologous recombination can take over from BER, but in cells that are deficient in homologous recombination repair such as BRCA1- and BRCA2-mutated cancers, inhibition of PARP enzymes becomes toxic [17]. PARP inhibitors were thus developed to exploit this phenomenon of synthetic lethality which assumes that the combination of two or more deficiencies in tumors, one genetic and one drug-induced, would become lethal for the tumor cells, whereas one defect alone would by itself be bearable [19-21]. Indeed, several studies testing PARP inhibitors showed substantial activity when these were used as monotherapy for tumors with BRCA1 and BRCA2 mutations, whereas additional therapeutic effects were seen when used in combination with other agents that cause DNA damage, such as certain cytotoxic chemotherapy and ionizing radiation [22-25]. Rucaparib has been investigated in multiple clinical studies, largely in combination with DNA-damaging agents (such as carboplatin or the alkylating agent temozolomide). These studies characterized the safety profile and showed promising responses in cancer patients with advanced solid tumors [23, 26, 27]. Currently, there are several phase II and III studies assessing the efficacy of rucaparib as orally administered monotherapy for the treatment of metastatic breast, high-grade epithelial ovarian, primary peritoneal or fallopian tube cancer, mostly with BRCA1 or BRCA2 mutations. Also combinations with several chemotherapeutic regimens are being tested. (U.S. National Institutes of Health ClinicalTrials.gov; Available from: http://clinicaltrials.gov/ct2/results?term=rucaparib&Search=Search). However, as all of the clinical trials to date have excluded patients with CNS metastases, so far nothing is known about the efficacy of rucaparib against these lesions.

Despite the number of completed and ongoing clinical trials, very little work on the interaction of ABC transporters with rucaparib and even with most other PARP inhibitors has been reported. This is surprising since ABC transporters can have substantial effects on the oral availability and tissue distribution of many (anti-cancer) drugs, which might result in alterations in therapeutic activity and toxicity profiles. Regardless of their use in monotherapy or in combination with other DNA-damaging agents, optimal distribution of rucaparib to tumors and into individual tumor cells is very important for its efficacy. Therefore, in this study, we assessed whether the ABC transporters ABCB1 and ABCG2 are important in *in vitro* transport and *in vivo* disposition of rucaparib, with a special emphasis on oral availability and brain distribution.

## MATERIALS AND METHODS



### Chemicals

Rucaparib was obtained from Sequoia Research Products (Pangbourne, UK). Zosuquidar (Eli Lilly; Indianapolis, USA) was a kind gift of Dr. O. van Tellingen (The Netherlands Cancer Institute, Amsterdam, NL) and Ko143 was obtained from Tocris Bioscience (Bristol, UK). All chemicals used in the chromatographic rucaparib assay were described before [28].

### Transport assays

Polarized canine kidney MDCKII cell lines and subclones transduced with hABCB1, hABCG2, and mAbcg2 cDNA were cultured and used in transwell assays as described previously [7]. Transport assays were performed using 12-well Transwell® plates (Corning Inc., USA). Briefly, the parental cells and subclones were seeded at a density of 3.5 and 2.5 x $10^5$ cells per well, respectively and cultured for 3 days to form an intact monolayer. Membrane tightness was assessed by measurement of transepithelial electrical resistance (TEER) using reference values that were previously established and well correlated to <1% transepithelial [14C] inulin leakage per hour [7]. Preceding the transport experiment, cells were washed twice with PBS and pre-incubated with fresh DMEM medium (Invitrogen, USA) including 10% FBS (Sigma-Aldrich, USA), and with relevant inhibitors for 1 hour, if required. The transepithelial transport experiment was started (t = 0) by replacing the incubation medium with medium containing 5 μM rucaparib in the donor compartment. In the inhibition experiments, 5 μM zosuquidar (ABCB1 inhibitor) and/or 5 μM Ko143 (ABCG2/Abcg2 inhibitor) were added to both apical and basolateral compartments. Plates were kept at 37°C in 5% $CO_2$ during the experiment, and 50 μl aliquots were taken from the acceptor compartment at 2, 4 and 8 h for LC-MS/MS measurement of rucaparib concentrations. Total amount of drug transported to the acceptor compartment was calculated after correction for volume loss for each time point. Experiments were performed in triplicate and the mean amount of transport is shown in the graphs. Active transport was expressed by the relative transport ratio (r), defined as r = apically directed amount of transport divided by basolaterally directed amount of translocation, at a defined time point.

### Animals

Mice were housed and handled according to institutional guidelines complying with Dutch legislation. Animals used were female WT, Abcb1a/1b-/-, Abcg2-/- and Abcg2-/-;Abcb1a/1b -/-

mice of a >99% FVB genetic background, between 8 and 14 weeks of age. Animals were kept in a temperature-controlled environment with a 12 h light / 12 h dark cycle and received a standard diet (AM-II, Hope Farms) and acidified water *ad libitum*.

**Drug solutions**

Rucaparib was administered to mice at a dose of 10 mg/kg, using a volume of 10 ml/kg body weight. Stock solution was prepared in DMSO at a concentration of 20 mg/ml. The 1 mg/ml working solution that was administered to mice was obtained by 20-fold dilution of the stock solution with a 1:1 (v/v) mixture of 5 % glucose and a vehicle mix consisting of 20% Polysorbate 80 (v/v), 13% absolute ethanol (v/v) and 67% H2O (v/v). Final concentrations for DMSO, Polysorbate 80 and ethanol were therefore 5%, 9.5%, and 6.2% (v/v), respectively. All working solutions were prepared freshly on the day of the experiment.



**Plasma and brain pharmacokinetics**

Rucaparib (10 mg/kg) was administered to the mice by oral gavage using a blunt ended needle. In order to minimize the variation in absorption, mice were fasted about 2 h before rucaparib was administered. Two separate experiments over 24 h and 1 h were performed to determine the whole plasma curve and the organ concentrations at Cmax (1 h), respectively. For plasma pharmacokinetic studies, multiple blood samples were collected from the tail vein using heparinized capillary tubes (Sarstedt, Germany). Blood samples were withdrawn from the tail vein at 0.5, 1, 2, 4 and 8 h in 24 h experiments and at 7.5, 15 and 30 min in 1 h experiments. 5 mice per group were used in 24 h and 5-8 mice per group were used in 1 h experiments. At the end of the experiments, mice were anesthetized with isoflurane and blood was collected by cardiac puncture. Mice were sacrificed by cervical dislocation immediately thereafter, and brains and a set of organs were removed rapidly. Organs were homogenized on ice in 1% (w/v) bovine serum albumin, and stored at -20°C until analysis. Blood samples were centrifuged at 2,100 g for 6 min at 4°C immediately after collection; the plasma fraction was collected and stored at -30°C until analysis.

**Relative brain accumulation**

Relative brain accumulation after oral administration of rucaparib was calculated by determining the rucaparib brain concentration relative to the plasma AUC from 0 - 1 h. Brain concentrations at 1 h were corrected for the amount of drug present in plasma volume (1.4 %) in the brain vasculature.

**Drug analysis**

Rucaparib concentrations in cell culture medium, plasma samples and brain homogenates were determined using liquid chromatography-electrospray-tandem mass spectrometry (LC-MS/MS) based on an validated assay reported for human and mouse plasma [28]. The original lower limit of quantification (LLQ) for rucaparib, 1.25 ng/ml, could be extrapolated to as low as 0.25 ng/ml (eLLQ). At 24 h, rucaparib concentrations in several samples were below the original LLQ (1.25 ng/ml), part of which could be extrapolated to a value above 0.25 ng/ml (e.g. brain of all Abcg2-/- mice and 2 out of 5 Abcb1a/1b-/- mice). A number of samples were below eLLQ

(e.g. brain in 4 out of 5 WT mice and plasma of all mice). Values below the eLLQ were assumed to be distributed according to 1/2eLLQ ± 1/2eLLQ.

### Pharmacokinetic calculations and statistical analysis

Pharmacokinetic parameters were calculated by non-compartmental methods using the software package PK Solutions 2.0.2 (Summit Research Services, Ashland, OH). The area under the plasma concentration-time curve was calculated using the trapezoidal rule, without extrapolating to infinity. The maximum drug concentration in plasma (Cmax) and the time to reach maximum drug concentration in plasma (Tmax) were determined directly from individual concentration-time data. One-way analysis of variance (ANOVA) was used to determine significance of differences between groups, after which post-hoc tests with Tukey correction were performed for comparison between individual groups. When variances were not homogeneous, data were log-transformed before statistical tests were applied. Differences were considered statistically significant when $P < 0.05$. Data are presented as mean ± SD.



## RESULTS

### Rucaparib is a transported substrate of ABCB1 and ABCG2

We assessed the *in vitro* transepithelial transport of rucaparib by ABC transporters using polarized monolayers of the MDCKII parental cell line and its subclones overexpressing human (h)ABCB1 or (h)ABCG2 or mouse (m)Abcg2. In the MDCKII parental cell line, both apically and basolaterally directed translocation of rucaparib were the same, yielding a transport ratio (r) of 1 (Figure 1A). Treatment of these cells with the ABCB1 inhibitor zosuquidar resulted in a slight decrease in apically directed transport (r = 0.8, Figure 1B), which could be either due to aspecific inhibition of an unidentified rucaparib uptake transporter at the basolateral side, or inhibition of endogenous canine ABCB1 (see below). In hABCB1-overexpressing MDCKII cells, there was an active apically directed transport with r = 4, which was reduced to 0.9 by zosuquidar coincubation, indicating that rucaparib is a clear transport substrate of hABCB1 (Figure 1C and D; see supplemental data for further explanation). Previously, MDCKII parental cells have shown a modest level of background transport with many ABCB1 substrates due to endogenous expression of canine ABCB1 [7, 29, 30], and the same might apply to rucaparib. We therefore included zosuquidar in subsequent experiments with hABCG2 and mAbcg2 to suppress this background transport activity. There was clear apically-directed transport of rucaparib with r = 3 in MDCKII cells overexpressing hABCG2 and this could be completely abrogated with the ABCG2 inhibitor Ko143 (Figure 1E and F). Transport efficiency in mouse Abcg2-overexpressing MDCKII cells was high, with r = 15, and this transport could be completely inhibited by addition of Ko143 (Figure 1G and H). These results indicate that rucaparib is a moderate substrate of hABCB1 and hABCG2 and a good substrate of mAbcg2. Collectively, these experiments demonstrate active transport of rucaparib by hABCB1, hABCG2 and mAbcg2, which can also be effectively inhibited by dedicated pharmacological inhibitors of these transporters. The observed slightly lower apically directed translocation and slightly higher basolaterally directed transport in all cell lines co-treated with zosuquidar and/or Ko143 (r = 0.8 – 0.9; Figure 1 B, D, F and G) may represent low-level activity of an endogenous basolaterally directed rucaparib

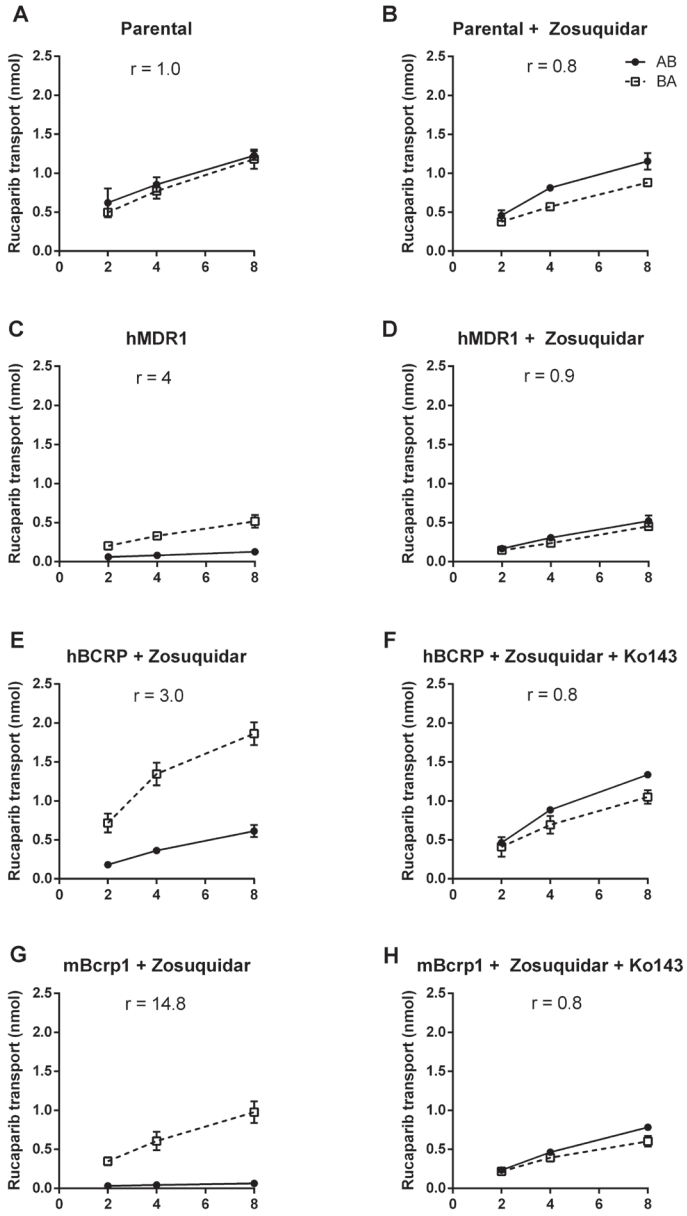


**Figure 1. *In vitro* transport of rucaparib.** Transepithelial transport of rucaparib (5 μM) was assessed in MDCK-II cells either nontransduced (A, B) or transduced with hABCB1 (C, D), hABCG2 (E, F) or mAbcg2 (G, H) cDNA. At t = 0 h, rucaparib was applied to the donor compartment and the concentrations in the acceptor compartment at t = 2, 4 and 8 h were measured and plotted as total amount of transport (nmol) in the graphs (n = 3). B, D-H: zosuquidar (5 μM) and/or Ko143 (5 μM) were applied as indicated to inhibit ABCB1 and hABCG2 or mAbcg2, respectively. r, relative transport ratio. BA (□), translocation from the basolateral to the apical compartment; AB (●), translocation from the apical to the basolateral compartment. Points, mean; bars, S.D. 1 nmol transport at t = 8 h corresponds to an apparent permeability coefficient (Papp) of $6.2 \times 10^{-6}$ cm/s.

efflux transporter of unknown identity, with similar low transport activity as the endogenous canine ABCB1.

**Oral availability of rucaparib is restricted by both Abcg2 and Abcb1**

We next analyzed the separate and combined effect of Abcg2 and Abcb1a/1b activity on the *in vivo* disposition of orally administered rucaparib at a dose of 10 mg/kg in wild-type (WT) and single and combination Abcg2 and Abcb1a/1b knockout mice. A dose of 10 mg/kg was chosen to allow easy comparison with previous related studies on TKIs in mice, but it also resulted in plasma AUC values in the same order of magnitude (160-600 ng/ml·h) as seen in patients receiving a clinically recommended oral dose of 600 mg rucaparib (800-900 ng/ml·h) (see Table 1). Plasma exposure of rucaparib over 24 h ($AUC_{0-24}$) was increased by the absence of Abcg2 by 1.7-fold (P = 0.18), by the absence of Abcb1a/1b by 2.5-fold (P < 0.01) and by the absence of both Abcg2 and Abcb1a/1b by 4-fold (P < 0.001) compared to WT mice (Figure 2, Table I), indicating that each of these transporters can affect the intestinal uptake and/or the systemic elimination of rucaparib. Further supporting the contribution of each of the individual transporters, comparison of the plasma $AUC_{0-24}$ values of the single knockout strains with that of the combination knockout strain also yielded significant differences (Table I). The effect of the single Abcb1a/1b deficiency was somewhat bigger than that of Abcg2 deficiency, mainly due to an apparently delayed elimination of rucaparib beyond 1 h after drug administration (Figure 2).



**Table 1.** Plasma pharmacokinetic parameters and brain concentrations 1 and 24 h after oral administration of 10 mg/kg rucaparib to male WT, Abcg2-/-, Abcb1a/1b-/- and Abcg2-/-;Abcb1a/1b-/- mice (n = 5 - 8).

| Parameter | Time (h) | Genotype | | | |
|---|---|---|---|---|---|
| | | ***WT*** | ***Abcg2$^{-/-}$*** | ***Abcb1a/1b$^{-/-}$*** | ***Abcg2$^{-/-}$;Abcb1a/1b$^{-/-}$*** |
| Plasma $AUC_{0-1}$ (ng/ml·h) | 1 h | 40.1 ± 13.5 | 40.1 ± 12.3 $^{+}$ | 70.3 ± 29.7 | 83.4 ± 29.6 * |
| $C_{max}$ (ng/ml) | | 57.1 ± 23.9 | 56.1 ± 18.1 | 105.6 ± 41.9 | 112.3 ± 38.9 |
| $T_{max}$ (h) | | 0.5 | 0.5 | 1 | 0.5 |
| $C_{brain}$ (ng/g) | | 9.7 ± 5.3 | 20.4 ± 16.1 $^{++}$ | 39.8 ± 27.8 * | 76.7 ± 32.6 *** |
| $P_{brain}$ (*$10^{-3}$ $h^{-1}$) | | 266.9 ± 189.7 | 450.6 ± 277.4 | 549.4 ± 252.6 | 993.0 ± 503.6 ** |
| Plasma $AUC_{0-24}$ (ng/ml·h) | 24 h | 157.6 ± 53.6 | 275.7 ± 64.4 $^{+++}$ | 402.9 ± 128.6 **, $^{++}$ | 626.7 ± 80.2 *** |
| $C_{max}$ (ng/ml) | | 80.6 ± 56.7 | 105.7 ± 27.9 | 91.9 ± 51.8 | 125.4 ± 44.7 |
| $T_{max}$ (h) | | 1 | 1 | 1 | 1 |
| $C_{brain}$ (ng/g) | | 0.7 ± 0.7 | 1.3 ± 0.4 $^{+++}$ | 3.4 ± 0.9 ***, $^{+++}$ | 21.4 ± 3.3 *** |
| $P_{brain}$ (*$10^{-3}$ $h^{-1}$) | | 3.8 ± 3.7 | 4.8 ± 2.0 $^{+++}$ | 8.9 ± 2.4 $^{+++, \#}$ | 34.6 ± 7.8 *** |

*$C_{max}$, maximum concentration in plasma; $T_{max}$, time point (h) that maximum plasma concentration is observed; $C_{brain}$, brain concentration; $P_{brain}$, brain accumulation. LLQ was 1.25 ng/ml and extrapolated LLQ was 0.25 ng/ml. Note that brain concentrations and brain accumulationof WT mice at 24 h are estimated values calculated by assuming 1/2eLLQ ± 1/2eLLQ distribution within those samples. * P < 0.05; ** P < 0.01; *** P < 0.001 compared to WT mice, # P < 0.05 compared to Abcg2-/- mice and $^{+}$ P < 0.05; $^{++}$ P < 0.01 ; $^{+++}$ P < 0.001 compared to Abcg2-/-;Abcb1a/1b-/- mice (WT mice were excluded from this last comparison. Data are given as mean ± S.D. (n = 5 - 8).*

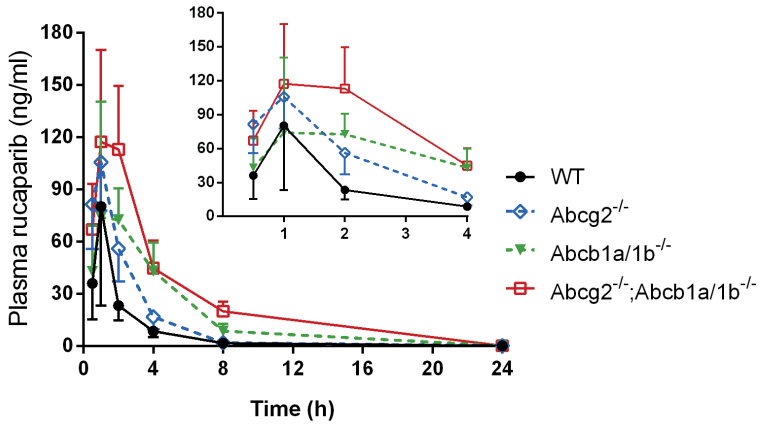


**Figure 2. Plasma concentration-time curves ($AUC_{0-24}$) in male WT (●), Abcg2-/- (◊), Abcb1a/1b-/- (▼), and Abcg2-/-;Abcb1a/1b-/- (□) mice over 24 h after oral administration of 10 mg/kg rucaparib.** Note that at 24 h, plasma levels of rucaparib in all the groups were below the extrapolated LLQ (0.25 ng/ml). The values below eLLQ were assumed to be distributed according to 1/2eLLQ ± 1/2eLLQ for calculations. Inset: same data plotted up to 4 h. Data are given as mean ± S.D. (n = 5).

Experimental variation at earlier time points was too high to assess whether deficiency in either of these transporters directly affected the initial rate of rucaparib uptake. Of note, a recent study on oral rucaparib pharmacokinetics in mice also reported high interindividual variation [31]. However, the effect of the combined deficiency of Abcg2 and Abcb1a/1b on rucaparib plasma concentrations and $AUC_{0-24}$ appeared to be a fairly straightforward additive effect of the single deficiencies (Figure 2, Table I). Overall, these results indicate that both Abcg2 and Abcb1a/1b can restrict the oral availability of rucaparib.

### Brain accumulation of oral rucaparib is restricted by Abcg2 and Abcb1

Drugs that are transported by Abcg2 and/or Abcb1 often display brain acumulation that is strongly restricted by these transporters. We therefore also measured the brain concentrations of rucaparib at 24 h after oral administration of rucaparib at 10 mg/kg. This was increased in Abcg2-/- mice by about 2-fold ($P = 0.79$), in Abcb1a/1b-/- mice by 5.2-fold ($P < 0.001$) and in Abcg2-/-;Abcb1a/1b-/- mice by 32.6-fold ($P < 0.001$) compared to WT mice (Figure 3A). Note that differences between the knockout and WT mice might be underestimated, because the rucaparib levels in brain of 4 out of 5 WT mice were undetectably low (< 0.25 ng/ml, eLLQ) as well as the plasma rucaparib concentrations at 24 h in all strains. The values below eLLQ were assumed to be distributed according to 1/2eLLQ ± 1/2eLLQ for calculations. Thus, estimates of brain accumulation (brain concentration of rucaparib corrected for the rucaparib plasma $AUC_{0-24}$ exposure) could be calculated for all knockout strains (Figure 3B). In this comparison, brain accumulation of rucaparib over 24 h in Abcg2-/-;Abcb1a/1b-/- mice was significantly increased by 9.1-fold compared to WT mice ($P < 0.001$), by 7.2-fold relative to Abcg2-/- mice ($P < 0.001$), and by 3.9-fold relative to Abcb1a/1b-/- mice ($P < 0.001$). Also, the absence of Abcb1a/1b led to 1.8-fold ($P < 0.05$) higher rucaparib accumulation in brain compared to the

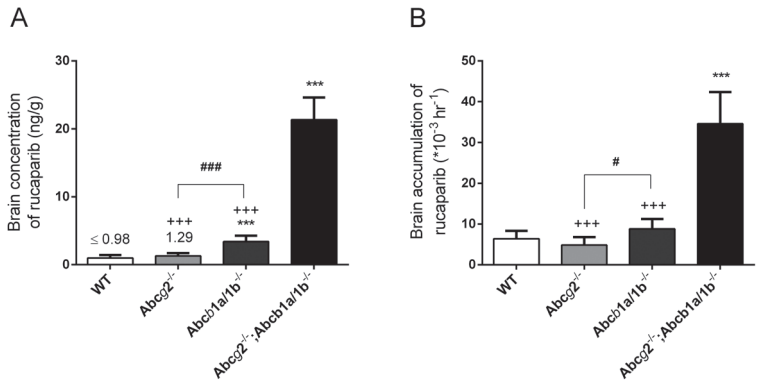






**Figure 3. Brain concentration (A) and relative brain accumulation (B) of rucaparib in male WT, Abcg2-/-, Abcb1a/1b-/- and Abcg2-/-;Abcb1a/1b-/- mice 24 h after oral administration of 10 mg/kg rucaparib.** Note that at 24 h, brain concentrations of rucaparib in 4 of 5 WT mice were below the extrapolated LLQ (0.25 ng/ml). Those values were assumed to be distributed according to 1/2eLLQ ± 1/2eLLQ for calculations. ***, $P < 0.001$ compared with WT mice; #, $P < 0.05$ and ###, $P < 0.001$ compared with Abcg2-/- mice and +++, $P < 0.001$ compared with Abcg2-/-;Abcb1a/1b-/- mice (WT mice were excluded from this last comparison). Data are given as mean ± S.D. (n = 5).

absence of Abcg2. These data suggest a clear contribution of Abcb1a/1b to restricting brain penetration of rucaparib, and a smaller, but still significant contribution of Abcg2.

We next assessed the impact of the transporters on the brain accumulation of rucaparib at an earlier time point, 1 h after oral administration of rucaparib (10 mg/kg). This was close to the peak plasma concentration of rucaparib in most strains, with readily detectable plasma and brain concentrations in all cases (Figure 4). The plasma concentrations up to 1 h (Figure 4A) were not significantly different from those observed in the 24 h experiment, and again quite variable, with the $AUC_{0-1}$ in combination knockout mice significantly higher than in the WT mice and that in Abcg2-/- mice significantly lower than in combination knockout mice (Table I). Fairly high experimental variation was also observed in the brain concentrations. Partly as a consequence of this variation, the brain concentration, brain-to-plasma ratio and brain accumulation of rucaparib 1 h after administration were not significantly increased in Abcg2−/− mice, whereas Abcb1a/1b−/− mice had 4.1-fold higher brain concentrations ($P < 0.05$, Figure 4B), but no significantly higher brain-to-plasma ratios and brain accumulation compared to WT mice (Figure 4C-D). However, when both Abcg2 and Abcb1a/1b transporters were deleted, there was an increase in brain levels by 7.9-fold ($P < 0.001$), brain-to-plasma ratio by 2.9-fold ($P < 0.05$) and brain accumulation of rucaparib by 3.7-fold ($P < 0.01$) relative to WT mice (Figure 4B-D). Collectively, these results suggest that Abcg2 and Abcb1a/1b each individually contributed to restricting rucaparib brain accumulation, and both Abcb1a/1b and Abcg2 could largely take over each other's function in restricting rucaparib brain accumulation across the BBB, albeit with a somewhat more pronounced effect of Abcb1a/1b. Although these effects were apparent at both 1 and 24 h after drug administration, at 1 h the individual and combined contributions of Abcg2 and Abcb1a/1b in restricting the brain accumulation of rucaparib were more modest.

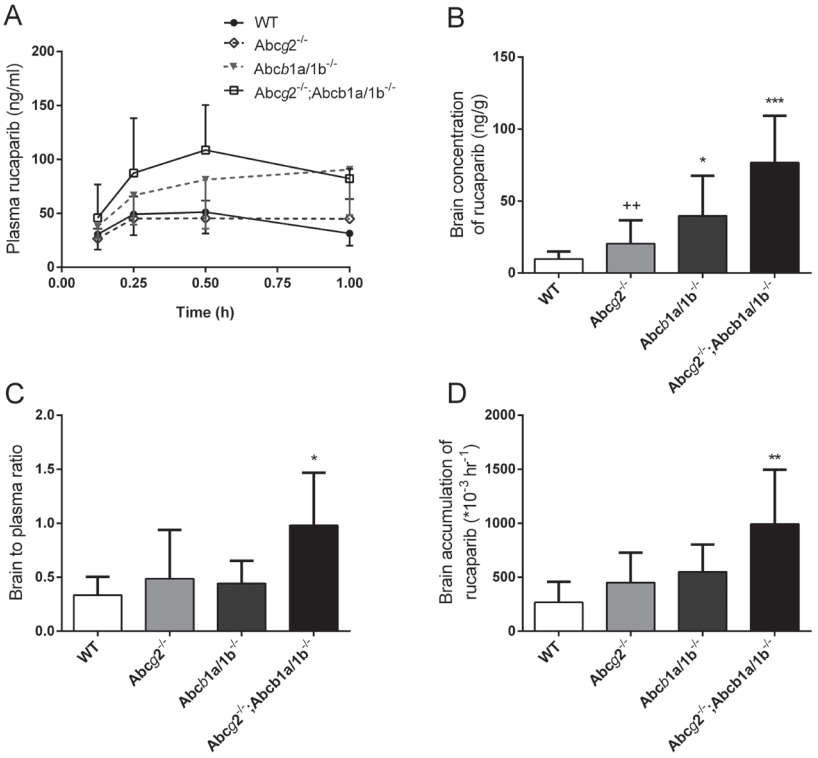


**Figure 4. Plasma concentration-time curves ($AUC_{0-t}$) (A), brain concentration (B), brain-to-plasma ratios (C) and relative brain accumulation (D) of rucaparib in male WT, Abcg2-/-, Abcb1a/1b-/- and Abcg2-/-;Abcb1a/1b-/- mice 1 h after oral administration of 10 mg/kg rucaparib.** *, $P < 0.05$; **, $P < 0.01$; ***, $P < 0.001$ compared with WT mice and ++, $P < 0.01$ compared with Abcg2-/-;Abcb1a/1b-/- mice (WT mice were excluded from this last comparison). Data are mean ± S.D. Where necessary, data were log-transformed to normalize the S.D.s between study groups. (n = 5 - 8).



## DISCUSSION

This study shows that the PARP1/2 inhibitor rucaparib is a transported substrate of the ABC efflux transporters Abcg2 and Abcb1a/1b and that these transporters affect the *in vivo* disposition of rucaparib in mice. *In vitro* rucaparib was transported very efficiently by mAbcg2, and modestly by both hABCB1 and hABCG2. This transport could be completely inhibited by specific small-molecule ABCB1 and ABCG2 inhibitors. *In vivo*, the oral availability and brain accumulation of rucaparib were clearly restricted by both Abcg2 and Abcb1a/1b, but the impact of Abcb1a/1b was somewhat higher than that of Abcg2 for both processes. Moreover, rucaparib seems to have comparatively good intrinsic brain accumulation properties which might be clinically useful. To the best of our knowledge, this study is the first to show that a PARP inhibitor is efficiently transported by both ABCB1 and ABCG2 *in vitro* and that its oral availability and brain accumulation are restricted by both of these transporters *in vivo*.

To date, a number of ABC transporters, including ABCB1 and ABCG2, have been associated with resistance to chemotherapy in several types of cancers, including breast cancer, where they confer resistance to a wide range of drugs [32-35]. Decreased intracellular availability of PARP inhibitor olaparib due to ABCB1 expression was found to be one of the mechanisms responsible for the resistance to this drug in BRCA-deficient mammary tumors, which could be reversed by pharmacological inhibition or deletion of ABCB1 [36, 37]. Based on these findings, it is very likely that target tumors expressing ABCB1 and/or ABCG2 might also demonstrate resistance to rucaparib-based chemotherapy.

The disproportionate increase in brain accumulation of rucaparib in Abcg2;Abcb1a/1b-/- mice compared to mice deficient for only one of the efflux transporters (Figure 3B and 4D) was similar to that found for several TKIs (e.g. lapatinib, gefitinib, erlotinib, axitinib, vemurafenib, sunitinib, dasatinib and imatinib) [3-7, 9, 29, 38]. A recent study by Agarwal *et al.* [39] showed that these disproportionate effects of combination vs. single transporter knockout are not related to compensatory upregulation of other efflux transporter(s) in the absence of either Abcb1a or Abcg2 at the BBB. This was done using extensive quantitative proteomic analyses of transporter expression in brain capillary endothelial cells isolated from single and combination knockout mice for Abcb1a/1b and Abcg2. In fact, the observed disproportionate effects could be readily explained with a pharmacokinetic model developed for brain accumulation of a wide range of drugs that are transported by both Abcb1 and Abcg2 [5]. We recently experimentally tested and further validated some critical predictions of this model using the anti-cancer drugs vemurafenib, dasatinib, sunitinib and sorafenib [7, 40]. Moreover, similar disproportionate effects are observed upon pharmacological inhibition of Abcb1a/1b and Abcg2 in studies of the brain disposition of several anti-cancer drugs such as vemurafenib, sunitinib and ABT-888 [7, 9, 41, 42]. For BBB drug efflux transporters with similar transport activity towards a certain substrate, the model of Kodaira *et al.* [5] predicts only a limited impact on brain accumulation of a drug by removal of a single transporter, and a pronounced impact by removal of both transporters due to the substantial drop in efflux activity. It is important to note that this model assumes that the remaining brain efflux in the combination knockout mice is small compared to the active efflux of either Abcg2 or Abcb1a/1b alone. Our findings therefore suggest that there are no alternative apical efflux transporters for rucaparib in the BBB that have a transport activity in the same order as that seen for Abcg2 and Abcb1a/1b.

Consequently, although it has been shown that some apical multidrug resistance proteins (MRPs) in the BBB, such as MRP2 or MRP4, can contribute to the brain efflux of drugs including phenytoin and topotecan, respectively [43, 44], it is unlikely that they play a role for rucaparib in the BBB that is substantial compared to that of Abcb1a/1b or Abcg2.

Brain clearance of rucaparib also seems to be more efficient in the presence of one or both transporters compared to that in the absence of both Abcg2 and Abcb1a/1b. Between 1 and 24 h, brain levels of rucaparib were decreased by about 13.9-fold in WT mice, 15.7-fold in Abcg2-/- mice, 11.7-fold in Abcb1a/1b-/- mice, but only by 3.6-fold in Abcg2-/-;Abcb1a/1b-/- mice (Table I). Thus, brain clearance of rucaparib seems to be markedly affected by both Abcg2 and Abcb1a/1b. Of interest, a prolonged retention of rucaparib in sanctuary tissues and tumors may be therapeutically beneficial as it allows less frequent dosing of the drug [31].

Given the activity of ABCB1 and ABCG2 in the blood-brain barrier, restricted accumulation of rucaparib into brain tissue may compromise the efficacy of rucaparib against tumors (e.g., micro-metastases) or tumor parts or rims positioned in part behind a functional blood-brain barrier. Yet, it is worth noting that in absolute terms the brain penetration of rucaparib is relatively good even in WT mice. For instance, compared to sunitinib, which is considered a very highly brain-accumulating drug [40], the brain-to-plasma ratio of rucaparib 1 hr after oral administration in WT mice is only about 3-fold lower (Supplemental Figure 2). Further enhancement of this favorable brain accumulation using coadministration of pharmacological ABCB1 and ABCG2 inhibitors might further improve this situation, especially in reducing the brain clearance of rucaparib (see above).

Clinical trials for rucaparib up till now did not assess the effect of rucaparib in central nervous system (CNS) metastases. Our findings showing that ABCB1 and ABCG2 can restrict brain penetration of rucaparib due to their efflux capacity at the BBB can be relevant for future clinical studies of cancer patients with CNS involvement. Brain metastases derived from advanced breast cancers are common and responsible for a large fraction of mortality in these patients [45], whereas those from ovarian cancers are rare, but remain a challenge for treatment [46]. Since our study suggests a relatively good intrinsic brain penetration of rucaparib, it could be that this drug alone can already be efficacious for the treatment of tumors with CNS involvement. However, based on previous knowledge with several anti-cancer drugs [7, 9, 41, 42], it may be possible to further increase rucaparib levels in the brain of patients with CNS involvement for better efficacy when rucaparib is coadministered with an efficacious dual inhibitor of ABCB1 and ABCG2 such as elacridar or other dual inhibitors. Such a coadministration may also enhance the oral availability of rucaparib, which should obviously be taken into account for possible dose adjustment.



## CONCLUSIONS

Our study shows that ABCB1 and ABCG2 together restrict oral availability and brain disposition of the PARP inhibitor rucaparib. These findings may have clinical relevance, since there is additional evidence that ABCB1 contributes to tumor resistance against PARP inhibitors. Moreover, PARP inhibitors have not been tested yet in patients with CNS metastases. We suggest that using pharmacological inhibitors of these transporters along with rucaparib treatment might enhance the therapeutic efficacy of rucaparib in ABCB1- and ABCG2-expressing primary tumors and in CNS metastases that are protected even in part by the BBB.

## ACKNOWLEDGEMENTS

We thank Anita Kort for critical reading and valuable contributions during the development of this manuscript.

## REFERENCE LIST


1. Lagas JS, Sparidans RW, van Waterschoot RA, Wagenaar E, Beijnen JH, Schinkel AH. P-glycoprotein limits oral availability, brain penetration, and toxicity of an anionic drug, the antibiotic salinomycin. Antimic*rob Agents Chemother 2008;* 52:1034-1039.
2. Zhou L, Schmidt K, Nelson FR, Zelesky V, Troutman MD, Feng B. The effect of breast cancer resistance protein and P-glycoprotein on the brain penetration of flavopiridol, imatinib mesylate (Gleevec), prazosin, and 2-methoxy-3-(4-(2-(5-methyl-2-phenyloxazol-4-yl)ethoxy) phenyl)propanoic acid (PF-407288) in mice. Drug M*etab Dispos 2009;* 37:946-955.
3. Polli JW, Olson KL, Chism JP, John-Williams LS, Yeager RL, Woodard SM et al. *An un*expected synergist role of P-glycoprotein and breast cancer resistance protein on the central nervous system penetration of the tyrosine kinase inhibitor lapatinib (N-{3-chloro-4-[(3-fluorobenzyl) oxy]phenyl}-6-[5-({[2-(methylsulfonyl)ethyl] amino}methyl)-2-furyl]-4-quinazolinamine; GW572016). Drug M*etab Dispos 2009;* 37:439-442.
4. Agarwal S, Sane R, Gallardo JL, Ohlfest JR, Elmquist WF. Distribution of gefitinib to the brain is limited by P-glycoprotein (ABCB1) and breast cancer resistance protein (ABCG2)-mediated active efflux. J Phar*macol Exp Ther 2010;* 334:147-155.
5. Kodaira H, Kusuhara H, Ushiki J, Fuse E, Sugiyama Y. Kinetic analysis of the cooperation of P-glycoprotein (P-gp/Abcb1) and breast cancer resistance protein (Bcrp/Abcg2) in limiting the brain and testis penetration of erlotinib, flavopiridol, and mitoxantrone. J Phar*macol Exp Ther 2010;* 333:788-796.
6. Poller B, Iusuf D, Sparidans RW, Wagenaar E, Beijnen JH, Schinkel AH. Differential impact of P-glycoprotein (ABCB1) and breast cancer resistance protein (ABCG2) on axitinib brain accumulation and oral plasma pharmacokinetics. Drug M*etab Dispos 2011;* 39:729-735.
7. Durmus S, Sparidans RW, Wagenaar E, Beijnen JH, Schinkel AH. Oral availability and brain penetration of the B-RAFV600E inhibitor vemurafenib can be enhanced by the P-GLYCOprotein (ABCB1) and breast cancer resistance protein (ABCG2) inhibitor elacridar. Mol Pha*rm 2012;* 9:3236-3245.
8. Mittapalli RK, Vaidhyanathan S, Dudek AZ, Elmquist WF. Mechanisms Limiting Distribution of the BRAFV600E Inhibitor Dabrafenib to the Brain: Implications for the Treatment of Melanoma Brain Metastases. J Phar*macol Exp Ther 2012.*
9. Tang SC, Lagas JS, Lankheet NA, Poller B, Hillebrand MJ, Rosing H et al. *Brain* accumulation of sunitinib is restricted by P-glycoprotein (ABCB1) and breast cancer resistance protein (ABCG2) and can be enhanced by oral elacridar and sunitinib coadministration. Int J *Cancer 2012;* 130:223-233.
10. Iusuf D, Teunissen SF, Wagenaar E, Rosing H, Beijnen JH, Schinkel AH. P-glycoprotein (ABCB1) transports the primary active tamoxifen metabolites endoxifen and 4-hydroxytamoxifen and restricts their brain penetration. J Pharm*acol Exp Ther 2011;* 337:710-717.
11. Lagas JS, Fan L, Wagenaar E, Vlaming ML, van TO, Beijnen JH et al. *P-gly*coprotein (P-gp/Abcb1), Abcc2, and Abcc3 determine the pharmacokinetics of etoposide. Clin C*ancer Res 2010;* 16:130-140.
12. Lagas JS, Sparidans RW, Wagenaar E, Beijnen JH, Schinkel AH. Hepatic clearance of reactive glucuronide metabolites of diclofenac in the mouse is dependent on multiple ATP-binding cassette efflux transporters. Mol Pha*rmacol 2010;* 77:687-694.
13. Lin F, Marchetti S, Pluim D, Iusuf D, Mazzanti R, Schellens JH et al. *Abcc4* together with abcb1 and abcg2 form a robust cooperative drug efflux system that restricts the brain entry of camptothecin analogues. Clin C*ancer Res 2013;* 19:2084-2095.
14. Lockman PR, Mittapalli RK, Taskar KS, Rudraraju V, Gril B, Bohn KA et al. *Hetero*geneous blood-tumor barrier permeability determines drug efficacy in experimental brain metastases of breast cancer. Clin C*ancer Res 2010;* 16:5664-5678.
15. Taskar KS, Rudraraju V, Mittapalli RK, Samala R, Thorsheim HR, Lockman J et al. *Lapati*nib distribution in HER2 overexpressing experimental brain metastases of breast cancer. Pharm R*es 2012;* 29:770-781.
16. Pestalozzi BC, Francis P, Quinaux E, Dolci S, Azambuja E, Gelber RD et al. *Is ri*sk of central nervous system (CNS) relapse related to adjuvant taxane treatment in node-positive breast cancer? Results of the CNS substudy in the intergroup Phase III BIG 02-98 Trial. Ann Onc*ol 2008;* 19:1837-1841.
17. Farmer H, McCabe N, Lord CJ, Tutt AN, Johnson DA, Richardson TB et al. *Target*ing the DNA repair defect in BRCA mutant cells as a therapeutic strategy. Nature *2005;* 434:917-921.

18. Rouleau M, Patel A, Hendzel MJ, Kaufmann SH, Poirier GG. PARP inhibition: PARP1 and beyond. Nat Rev *Cancer 2010;* 10:293-301.
19. Chalmers AJ, Lakshman M, Chan N, Bristow RG. Poly(ADP-ribose) polymerase inhibition as a model for synthetic lethality in developing radiation oncology targets. Semin R*adiat Oncol 2010;* 20:274-281.
20. Helleday T. The underlying mechanism for the PARP and BRCA synthetic lethality: clearing up the misunderstandings. Mol Onco*l 2011;* 5:387-393.
21. Leung M, Rosen D, Fields S, Cesano A, Budman DR. Poly(ADP-ribose) polymerase-1 inhibition: preclinical and clinical development of synthetic lethality. Mol Med *2011;* 17:854-862.
22. Davar D, Beumer JH, Hamieh L, Tawbi H. Role of PARP inhibitors in cancer biology and therapy. Curr M*ed Chem 2012;* 19:3907-3921.
23. Rosen EM, Pishvaian MJ. Targeting the BRCA1/2 Tumor Suppressors. Curr Dr*ug Targets 2014;* 15:17-31.
24. Drew Y, Mulligan EA, Vong WT, Thomas HD, Kahn S, Kyle S et al. *Therap*eutic potential of poly(ADP-ribose) polymerase inhibitor AG014699 in human cancers with mutated or methylated BRCA1 or BRCA2. J Natl *Cancer Inst 2011;* 103:334-346.
25. Drew Y, Plummer R. PARP inhibitors in cancer therapy: two modes of attack on the cancer cell widening the clinical applications. Drug R*esist Updat 2009;* 12:153-156.
26. Plummer R, Jones C, Middleton M, Wilson R, Evans J, Olsen A et al. *Phase* I study of the poly(ADP-ribose) polymerase inhibitor, AG014699, in combination with temozolomide in patients with advanced solid tumors. Clin C*ancer Res 2008;* 14:7917-7923.
27. Plummer R, Lorigan P, Steven N, Scott L, Middleton MR, Wilson RH et al. *A phase* II study of the potent PARP inhibitor, Rucaparib (PF-01367338, AG014699), with temozolomide in patients with metastatic melanoma demonstrating evidence of chemopotentiation. Cancer C*hemother Pharmacol 2013;* 71:1191-1199.
28. Sparidans RW, Durmus S, Schinkel AH, Schellens JH, Beijnen JH. Liquid chromatography-tandem mass spectrometric assay for the PARP inhibitor rucaparib in plasma. J Pharm *Biomed Anal 2014;* 88:626-629.
29. Lagas JS, van Waterschoot RA, van Tilburg VA, Hillebrand MJ, Lankheet N, Rosing H et al. *Brain* accumulation of dasatinib is restricted by P-glycoprotein (ABCB1) and breast cancer resistance protein (ABCG2) and can be enhanced by elacridar treatment. Clin C*ancer Res 2009;* 15:2344-2351.
30. Poller B, Wagenaar E, Tang SC, Schinkel AH. Double-transduced MDCKII cells to study human P-glycoprotein (ABCB1) and breast cancer resistance protein (ABCG2) interplay in drug transport across the blood-brain barrier. Mol Pha*rm 2011;* 8:571-582.
31. Murray J, Thomas H, Berry P, Kyle S, Patterson M, Jones C et al. *Tumour* cell retention of rucaparib, sustained PARP inhibition and efficacy of weekly as well as daily schedules. Br J C*ancer 2014*.
32. Szakacs G, Paterson JK, Ludwig JA, Booth-Genthe C, Gottesman MM. Targeting multidrug resistance in cancer. Nat Rev *Drug Discov 2006;* 5:219-234.
33. Leonessa F, Clarke R. ATP binding cassette transporters and drug resistance in breast cancer. Endocr *Relat Cancer 2003;* 10:43-73.
34. Yamada A, Ishikawa T, Ota I, Kimura M, Shimizu D, Tanabe M et al. *High* expression of ATP-binding cassette transporter ABCC11 in breast tumors is associated with aggressive subtypes and low disease-free survival. Breast *Cancer Res Treat 2013;* 137:773-782.
35. Szakacs G, Annereau JP, Lababidi S, Shankavaram U, Arciello A, Bussey KJ et al. *Predict*ing drug sensitivity and resistance: profiling ABC transporter genes in cancer cells. Cancer *Cell 2004;* 6:129-137.
36. Rottenberg S, Jaspers JE, Kersbergen A, van der Burg E, Nygren AO, Zander SA et al. *High* sensitivity of BRCA1-deficient mammary tumors to the PARP inhibitor AZD2281 alone and in combination with platinum drugs. Proc Na*t Acad Sci U S A 2008;* 105:17079-17084.
37. Jaspers JE, Kersbergen A, Boon U, Sol W, van Deemter L, Zander SA et al. *Loss* of 53BP1 causes PARP inhibitor resistance in Brca1-mutated mouse mammary tumors. Cancer *Discov 2013;* 3:68-81.
38. Oostendorp RL, Buckle T, Beijnen JH, van Tellingen O, Schellens JH. The effect of P-gp (Mdr1a/1b), BCRP (Bcrp1) and P-gp/BCRP inhibitors on the in vivo absorption, distribution, metabolism and excretion of imatinib. Invest *New Drugs 2009;* 27:31-40.
39. Agarwal S, Uchida Y, Mittapalli RK, Sane R, Terasaki T, Elmquist WF. Quantitative proteomics of transporter expression in brain capillary endothelial cells isolated from P-glycoprotein (P-gp), breast cancer resistance protein (Bcrp), and P-gp/Bcrp knockout mice. Drug Me*tab Dispos 2012;* 40:1164-1169.

40. Tang SC, de Vries N, Sparidans RW, Wagenaar E, Beijnen JH, Schinkel AH. Impact of P-glycoprotein (ABCB1) and breast cancer resistance protein (ABCG2) gene dosage on plasma pharmacokinetics and brain accumulation of dasatinib, sorafenib, and sunitinib. J Pharm*acol Exp Ther 2013;* 346:486-494.
41. Lin F, de Gooijer MC, Moreno RE, Buil L, Christner SM, Beumer JH et al. *ABCB1,* ABCG2 and PTEN determine the response of glioblastoma to temozolomide and ABT-888 therapy. Clin C*ancer Res 2014*.
42. Oberoi RK, Mittapalli RK, Elmquist WF. Pharmacokinetic assessment of efflux transport in sunitinib distribution to the brain. J Pharm*acol Exp Ther 2013;* 347:755-764.
43. Leggas M, Adachi M, Scheffer GL, Sun D, Wielinga P, Du G et al. *Mrp4* confers resistance to topotecan and protects the brain from chemotherapy. Mol Cel*l Biol 2004;* 24:7612-7621.
44. Potschka H, Fedrowitz M, Loscher W. Multidrug resistance protein MRP2 contributes to blood-brain barrier function and restricts antiepileptic drug activity. J Pharm*acol Exp Ther 2003;* 306:124-131.
45. Weil RJ, Palmieri DC, Bronder JL, Stark AM, Steeg PS. Breast cancer metastasis to the central nervous system. Am J Pa*thol 2005;* 167:913-920.
46. Piura E, Piura B. Brain metastases from ovarian carcinoma. ISRN Onc*ol 2011;* 2011:527453.



## SUPPLEMENTARY EXPLANATION

This shift was mainly due to a strong increase in the basolaterally directed transport (from 0.12 to 0.52 nmol at 8 h) and only a modest decrease in the apically directed transport of rucaparib (from 0.52 to 0.45 nmol at 8 h) (Figure 1C and D). These results suggest that rucaparib is efficiently transported by MDR1 and that this can be largely inhibited by zosuquidar. The lack of a substantial decrease in B to A transport (from 0.52 to 0.45 nmol at 8 h) of rucaparib by zosuquidar can be explained by a rate-limiting rucaparib influx capacity of the MDCKII-MDR1 cells from the basolateral side, presumably by a low-abundance (unidentified) uptake transporter. This influx capacity was so low that the remaining transport capacity of MDR1 after zosuquidar inhibition only resulted in a minor further reduction in A to B transport. However, the increase in the A to B transport can be explained by a major inhibition of MDR1 activity by zosuquidar, leading to strongly increased intracellular accumulation of rucaparib which primarily drives the A to B directed transport.

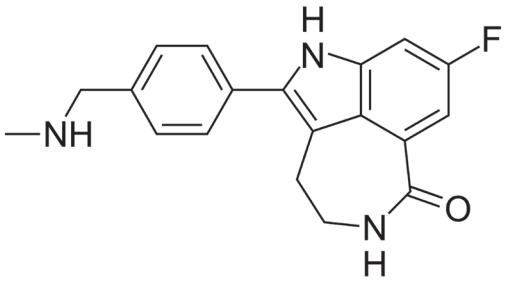


**Supplementary Figure 1. Structural formula of rucaparib**

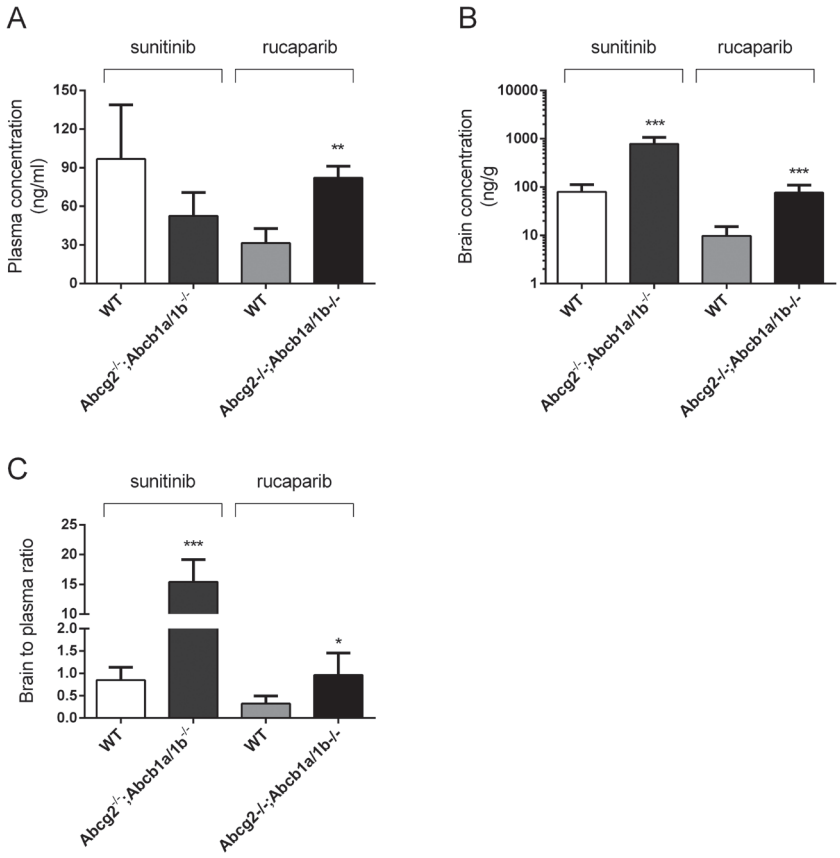


**Supplementary Figure 2. Plasma (ng/ml) (A) and brain (ng/g) (B) concentrations and brain-to-plasma ratios (C) of sunitinib and rucaparib in WT and Abcg2$^{-/-}$;Abcb1a/1b$^{-/-}$ mice 1 h after oral administration of 10 mg/kg of the drug.** ***, $P < 0.001$ compared with WT mice treated with the same drug. Data are mean ± S.D. (n = 5 - 8).

# CHAPTER 3

## IMPACT OF OATP TRANSPORTERS ON PHARMACOKINETICS OF ANTI-CANCER DRUGS

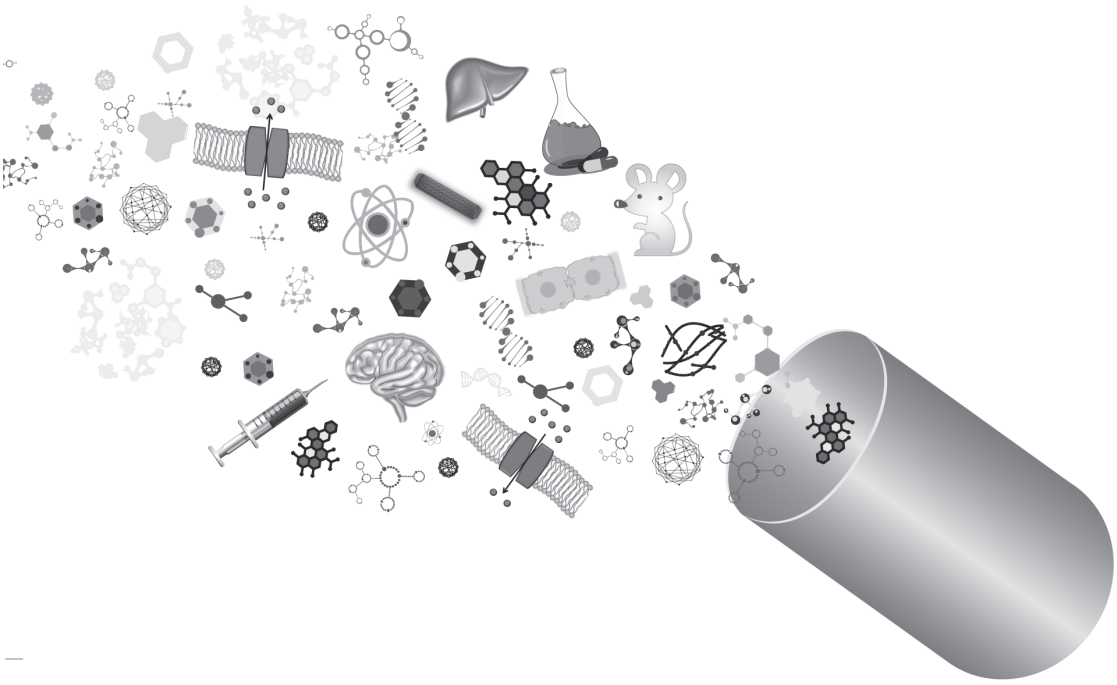

# CHAPTER 3.1

## *IN VIVO* DISPOSITION OF DOXORUBICIN IS AFFECTED BY MOUSE OATP1A/1B AND HUMAN OATP1A/1B TRANSPORTERS

Selvi Durmus[1], Jyoti Naik[1,2], Levi Buil[3], Els Wagenaar[1], Olaf van Tellingen[3], Alfred H. Schinkel[1]

[1]Division of Molecular Oncology, The Netherlands Cancer Institute, Amsterdam, the Netherlands,
[2]Tytgat Institute for Liver and Intestinal Research, Academic Medical Center, University of Amsterdam, the Netherlands,
[3]Department of Clinical Chemistry, The Netherlands Cancer Institute, Amsterdam, the Netherlands

*Int J Cancer. 2014 Feb (Epub ahead of print).*

## ABSTRACT

Organic anion-transporting polypeptides (OATPs) are important drug uptake transporters, mediating distribution of substrates to several pharmacokinetically relevant organs. Doxorubicin is a widely used anti-cancer drug extensively studied for its interactions with various drug transporters, but not OATPs. Here, we investigated the role of OATP1A/1B proteins in the distribution of doxorubicin. *In vitro*, we observed ~2-fold increased doxorubicin uptake in HEK293 cells overexpressing human OATP1A2, but not OATP1B1 or OATP1B3. In mice, absence of Oatp1a/1b transporters led to up to 2-fold higher doxorubicin plasma concentrations and 1.3-fold higher plasma AUC. Conversely, liver AUC and liver-to-plasma ratios of Oatp1a/1b$^{-/-}$ mice were 1.4-fold and up to 4.1-fold lower than in wild-type mice, respectively. Decreased doxorubicin levels in the small intestinal content reflected those in the liver, indicating a reduced biliary excretion of doxorubicin in Oatp1a/1b$^{-/-}$ mice. These results demonstrate important control of doxorubicin plasma clearance and hepatic uptake by mouse Oatp1a/1b transporters. This is unexpected, as the fairly hydrophobic weak base doxorubicin is an atypical OATP1A/1B substrate. Interestingly, transgenic liver-specific expression of human OATP1A2, OATP1B1 or OATP1B3 could partially rescue the increased doxorubicin plasma levels of Oatp1a/1b$^{-/-}$ mice. Hepatic uptake and bile-derived intestinal excretion of doxorubicin were completely reverted to wild-type levels by OATP1A2, and partially by OATP1B1 and OATP1B3. Thus, doxorubicin is transported by hepatocyte-expressed OATP1A2, -1B1 and -1B3 *in vivo*, illustrating an unexpectedly wide substrate specificity. These findings have possible implications for the uptake, disposition, therapy response and toxicity of doxorubicin, also in human tumors and tissues expressing these transporters.



## NOVELTY & IMPACT STATEMENTS

We show that mouse and human OATP1A/1B transporters can mediate the *in vivo* tissue distribution and clearance of doxorubicin, an unexpected OATP1A/1B substrate due to its structure. These results are potentially of high clinical interest as patients with pharmacological inhibition or polymorphic variants of OATP1A/1B proteins might demonstrate toxicity or an altered therapeutic index upon doxorubicin treatment. Moreover, tumors with OATP1A/1B expression might have increased doxorubicin uptake, thus becoming more susceptible to doxorubicin-containing chemotherapy.

## INTRODUCTION

Organic anion-transporting polypeptides (OATP/Oatp; gene name: *SLCO/Slco*) are sodium-independent transmembrane uptake transporters. They form a superfamily consisting of six families (OATP1–6) and several subfamilies (OATP1A, 1B, etc.), sharing more than 40% and 60% amino acid identity, respectively [1]. Members of the human and mouse OATP1A and OATP1B subfamilies do not have straightforward orthologs. The human OATP1A/1B subfamilies encompass OATP1A2, OATP1B1 and OATP1B3 whereas the mouse subfamilies encompass Oatp1a1, Oatp1a4, Oatp1a5, Oatp1a6 and Oatp1b2.

OATP1A/1B transporters are believed to be important in the absorption, distribution and elimination of many (usually anionic or polar) drugs including statins, cardiac glycosides, antibiotics, and anticancer drugs. The OATP1A and 1B subfamilies are expressed mainly in pharmacokinetically relevant tissues like liver, kidney and small intestine in both human and mice [2-4]. OATP1A2 is thought to be substantially expressed in the intestine (apical side of enterocytes), kidney (apical membrane of the distal nephron), cholangiocytes (cells lining the bile ducts) and the blood-brain barrier (apical membrane of the endothelial cells of brain capillaries) [5-7], but its effect on drug absorption, distribution, and elimination needs to be further investigated. OATP1B1 and OATP1B3 are highly expressed in the basolateral membrane of hepatocytes and are thought to play a key role in the hepatic uptake and plasma clearance of substrate drugs and toxins [8-10].

Besides their physiologic expression, many OATPs are expressed in several cancer tissues and cell lines, where they may well be involved in the tumor uptake of anticancer drugs and thus be a candidate target for therapy modulation. For example, OATP1A2 expression was specifically detected in breast cancer tissue, several breast and prostate cancer cell lines, bone metastases from kidney cancer and malignant osteosarcoma [11-13]. Furthermore, expression of OATP1A2 was significantly increased in malignant compared to non-malignant breast tissue and was found to be highest in Stage I and IIA breast cancers [11]. OATP1B1 expression was detected in neoplastic colon tissue, human ovarian cancer and in ovarian cancer cell lines, whereas OATP1B3 expression was detected in several gastrointestinal, colon and ovarian cancers and cell lines, and pancreatic cancer [8, 14, 15].

In recent years, several polymorphic variants of genes encoding OATP1A2, OATP1B1 and OATP1B3 have been identified, some of which are clinically important due to their reduced function [16-19]. Two different polymorphisms detected in the gene encoding OATP1A2 were associated with significantly altered imatinib clearance in chronic myeloid leukemia patients [20]. Several polymorphisms found in the gene encoding OATP1B1 reduce its activity, and cause decreased transport and increased plasma levels of several drug substrates (e.g. pravastatin, valsartan, methotrexate and SN-38) and hence various degrees of toxicities in patients [16, 21-23]. We recently also showed that complete deficiency alleles exist, of OATP1B1 and OATP1B3, resulting in Rotor syndrome, in which patients suffer from conjugated hyperbilirubinemia [24]. These studies indicate that polymorphisms in genes encoding OATP1A/1B transporters can lead to variation in disposition, therapeutic effect and toxicity of drugs between individuals. It is therefore important to understand the relative roles of OATP1A/1B transporters in drug pharmacokinetics *in vivo*.

Doxorubicin (Adriamycin) is an anthracycline antibiotic used as a chemotherapy agent to treat several types of cancers, including leukemias, Hodgkin's lymphoma, breast, lung, ovarian and thyroid cancers [25]. Multiple mechanisms of action have been described for doxorubicin [26]. A major mechanism for preventing proper DNA replication is the intercalation between base pairs of the DNA helix, leading to inhibition of topoisomerase II, an enzyme that relaxes supercoils in DNA resulting from transcription and replication. It may also generate free radicals, leading to DNA and cell membrane damage. There have been extensive investigations on the interaction of several ABC-family drug efflux transporters with doxorubicin, showing that it is a transported substrate of P-gp, BCRP and MRP2, which can affect its distribution in the body [27-30]. Studies on the interactions between drug uptake transporters and doxorubicin, however, have been limited so far. Of drug uptake transporters, OCT6 has been found to transport doxorubicin [31]; however nothing has been reported yet on the interaction of OATP transporters and doxorubicin. *A priori*, doxorubicin did not seem a likely transported substrate, since it is a fairly hydrophobic weak base. On the other hand, more and more drugs of highly diverse structures such as methotrexate (anion), paclitaxel (bulky hydrophobic) and fexofenadine (zwitterion) have been found to be substrates of OATP1A/1B proteins [32, 33]. These findings are of interest, since initially typical OATP substrates were thought to be primarily polar and anionic drugs. In this study, we aimed to elucidate the possible impact of OATP1A and 1B transporters on the disposition of doxorubicin *in vitro* using HEK293 cell-based uptake systems and *in vivo* using knockout and humanized transgenic mouse models.



## MATERIALS AND METHODS

### Chemicals

Doxorubicin hydrochloride (Doxorubicin-HCl) was obtained as a parenteral formulation from Pharmachemie BV, Haarlem, The Netherlands. Estradiol 17B-D-glucuronide [6,7-3H] was from Perkin Elmer, Massachusetts, USA. All of the chemicals used for HPLC analysis were from Merck, Darmstadt, Germany.

### Animals

Mice were housed and handled according to institutional guidelines complying with Dutch legislation. Female WT, *Slco1a/1b*$^{-/-}$, *Slco1a/1b*$^{-/-}$*;1A2*$^{tg}$, *Slco1a/1b*$^{-/-}$*;1B1*$^{tg}$ and *Slco1a/1b*$^{-/-}$*;1B3*$^{tg}$ with liver-specific expression of human *SLCO* genes, all of a >99% FVB genetic background, were used between 8 and 13 weeks of age. Animals were kept in a temperature-controlled environment with a 12 h light / 12 h dark cycle and received a standard diet (AM-II, Hope Farms) and acidified water *ad libitum*.

### Drug solutions

Doxorubicin-HCl solution (2 mg/ml) was diluted two-fold with 0.9% NaCl to yield a concentration of 1 mg/ml. Doxorubicin was administered intravenously at 5 mg/kg body weight, using a volume of 5 µl/g body weight. All working solutions were prepared freshly on the day of experiment.

### Cell Culture

HEK293 cells, transporter-expressing or vector-transfected were grown in Dulbecco's modified Eagle's medium low glucose (Invitrogen) supplemented with 10% fetal bovine serum (Sigma), 100 U/ml penicillin, 100 µg/ml streptomycin, and 0.25 µg/ml amphotericin B at 37°C with 5% CO2 and 95% humidity. For the uptake experiments, cells were seeded in 12-well plates (coated with 50 mg/l poly(l-lysine) and 50 mg/l poly(l-ornithine); Sigma) at a density of 1.0 × $10^5$ cells/well. For the transport study, the cell culture medium was replaced with culture medium supplemented with 5 mM sodium butyrate 24 h before the uptake assay to induce the expression of OATP transporters.

### Cellular uptake assays

HEK293 cells transduced with vector control, human *(h)SLCO1A2, hSLCO1B1* and *hSLCO1B3* cDNAs, a kind gift from Prof. Werner Siegmund and Dr. Markus Keiser, (University of Greifswald, Greifswald, Germany) [34], were used to assess the uptake capacity for estradiol 17β-D-glucuronide and doxorubicin. The uptake transport study was carried out as described previously [35]. After cells had been washed twice and preincubated with Krebs-Henseleit buffer at 37°C for 15 min, uptake was initiated by adding Krebs-Henseleit buffer containing $^3$H-labeled estradiol 17β-D-glucuronide or unlabeled doxorubicin. The Krebs-Henseleit buffer consisted of 118 mM NaCl, 23.8 mM NaHCO3, 4.8 mM KCl, 1.0 mM KH2PO4, 1.2 mM MgSO4, 12.5 mM HEPES, 5.0 mM d-glucose, and 1.5 mM CaCl2 adjusted to pH 7.4 with 1M NaOH. When doxorubicin was used as a substrate, 10% FCS was added to the Krebs-Henseleit buffer in the preincubation and incubation steps to reduce aspecific binding of the drug to the well plates. For inhibition studies, cyclosporin A (CsA) as an OATP inhibitor was added in the incubation buffer. At designated times, the incubation buffer was removed and uptake was terminated by adding 1 ml of ice-cold Krebs-Henseleit buffer, followed by two times washing with 1 ml of ice-cold Krebs-Henseleit buffer. In estradiol 17β-D-glucuronide experiments, cells were lysed with 500 µl of 0.2 N NaOH overnight at 4°C and cell lysates were neutralized with 250 µl of 0.4 N HCl the next day. Aliquots (50 µl) were transferred to scintillation vials and the radioactivity associated with the cells and incubation buffer was measured in a liquid scintillation counter. The cellular protein amount was determined by the Bradford method using 50 µl of the cell lysate with bovine serum albumin as a standard. In doxorubicin experiments, cells were lysed with 250 ul acetonitrile for 10 min at room temperature and aliquots (200 µl) of the lysates were used to analyze doxorubicin levels by HPLC. For determination of the cellular protein levels using the Bradford method, a replicate of the cell plate was used and cells were lysed with NaOH and lysates were neutralized with HCl as described above.

### Western blot analysis

Isolation of crude membrane fractions from livers and Western blot analysis were conducted as described previously [36]. Monoclonal mouse anti-β-actin antibody (AC-74; A5316; Sigma) was used as a loading control for western blot analysis. Human OATP1B1 and OATP1B3 were detected with the rabbit polyclonal antibodies ESL and SKT (dilution 1:10000 for both), provided by D. Keppler (Deutsches Krebsforschungszentrum, Heidelberg, Germany). Human OATP1A2 was detected with antibody OATP1 (sc-18428; dilution 1:1000) from Santa Cruz.

### Plasma and liver pharmacokinetics

Doxorubicin was administered to mice intravenously. For extensive pharmacokinetic analyses, mice were sacrificed at multiple time points: 3, 7.5, 15 and 30 min, and 1, 4, 8, 24 and 72 hours using isoflurane anesthesia. Heparin-blood samples were collected via cardiac puncture, mice were sacrificed immediately thereafter by cervical dislocation, and livers and a set of organs were rapidly removed. Organs were homogenized on ice in 1% bovine serum albumin, and stored at -20°C until analysis. Blood samples were centrifuged at 2,100 g for 6 min at 4°C immediately after collection; the plasma fraction was collected and stored at -20°C until analysis. After HPLC analysis, results are presented as concentrations in the organs (nmol/g), % of the total dose (a 5 mg/kg dose corrected for the body weight of each individual mouse being equivalent to 100%), and/or organ to plasma ratios. Organ to plasma ratios are calculated by dividing organ concentration expressed as nmol/g by plasma concentration expressed as nmol/ml, assuming 1 ml of plasma is roughly equivalent to 1 g of tissue.





### HPLC analysis

To detect the level of doxorubicin in plasma and the various organ homogenates, a reverse phase high performance liquid chromatography (HPLC) method with attached fluorescence detector was used as described previously [37]. The chromatographic system consisted of an Ultimate 3000 pump and Dionex ASI-100 automated injector (Dionex, Sunnyvale, CA, USA). The HPLC column (3 x 150 mm) was packed with 5 µm Lichrosorb 100 RP-8 material (Dr Maisch GMBH, Ammerbuch, Germany). A Jasco intelligent fluorescent detector (FP-1520) was used with excitation and emission wavelengths at 460 nm and 550 nm, respectively, bandwidth 40 nm, gain 100, and response time 5 seconds. Peak area integration was performed with a Chromeleon data system version 6.8 (Dionex). For the preparation of test samples, tissue homogenates were diluted with human blank plasma, when necessary. Daunorubicin was used as internal standard. Borate buffer was used to adjust the pH of the sample to 9, and extraction fluid (80% chloroform and 20% isopropanol) was used to extract doxorubicin from the samples. The organic phase was collected and evaporated in a SpeedVac SC210A (Savant, Farmingdale, NY,USA) and the residues were reconstituted in 100 ul of acetonitrile:terahydrofurane by sonication and further with 400 ul of demineralised water. The mobile phase for the HPLC analysis consisted of 72% demineralised water at pH 2.05, 27% acetonitrile and 0.9% tetrahydrofuran.

### Statistical analysis

Student's t-test or one-way analysis of variance (ANOVA) after which post-hoc tests with Tukey's corrections were used to determine statistical significance between two or multiple groups, respectively. Results are presented as the mean ± standard deviation (SD). Differences were considered to be statistically significant when $P \leq 0.05$. To calculate the area under the plasma concentration time curve (AUC), the linear trapezoidal rule was applied on the mean plasma concentration at each time point from 0 to 72 hours. Results of the AUC measurements are presented as mean ± S.E.M. The other main pharmacokinetic parameters such as AUC extrapolated to infinity (AUC0-∞), clearance, volume of distribution and elimination half-life were calculated by noncompartmental methods using the software package PK Solutions 2.0.2 (Summit Research Services, Ashland, OH).

## RESULTS

### *In vitro* transport of doxorubicin by OATP1A2, OATP1B1 and OATP1B3

We evaluated whether doxorubicin is a substrate of human OATP1A2, OATP1B1 and OATP1B3 *in vitro* using HEK293 cells overexpressing these transporter proteins. The uptake of the common positive control substrate estradiol 17β-D-glucuronide mediated by OATP1A2, OATP1B1 and OATP1B3 was increased 2.1-, 63.9- and 2.7-fold, respectively, compared to that in the vector control cells. This uptake could be effectively inhibited by CsA, an inhibitor of these OATP transporters (Figure 1A). Interestingly, OATP1A2 increased the uptake of doxorubicin (1 μM) by 2.1-fold compared to the vector control cells ($P < 0.001$), and this increase could be significantly inhibited by CsA (Figure 1B). However, we observed no significant increase in the uptake of doxorubicin in OATP1B1- and OATP1B3-expressing cells compared to vector control cells. These results indicate that *in vitro* doxorubicin is a good transport substrate of human OATP1A2, but not of OATP1B1 and OATP1B3 as measured in HEK293 cells. It should be noted, however, that OATP-mediated uptake of certain substrates can be cell-type dependent for as yet unknown reasons [38], so a negative result does not necessarily mean that a substrate cannot be transported under any circumstances.

### *In vivo* roles of Oatp1a/1b transporters in doxorubicin disposition

We next investigated the *in vivo* effect of Oatp1a/1b deficiency in mice on doxorubicin disposition over 72 h upon administration of 5 mg/kg doxorubicin intravenously. We used intravenous administration of doxorubicin as this route of administration is commonly used in the clinic. Systemic exposure of doxorubicin was increased in the Oatp1a/1b$^{-/-}$ mice compared to the WT mice (Figure 2A), leading to a 1.3-fold higher plasma $AUC_{(0\text{-}72)}$ (2056 ± 146 versus 1597 ±

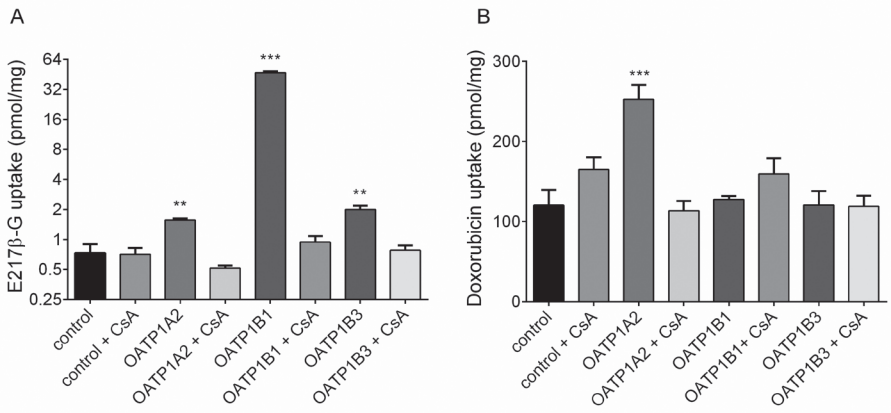


**Figure 1. In vitro uptake of (A) estradiol 17β-D-glucuronide ($E_2$17βG) and (B) doxorubicin by OATP1A2, OATP1B1 and OATP1B3.** Uptake of 1 μM $E_2$17βG and 1 μM doxorubicin was measured after 5 min incubation using vector-transfected (control) or OATP1A2, OATP1B1 or OATP1B3 overexpressing HEK293 cells. Uptake was inhibited by addition of 20 μM Cyclosporin A (CsA), an OATP inhibitor. Note that uptake levels in panel A are presented in log scale. Data are given as mean ± S.D. One-way Anova test was applied to compare all groups to control cells. (n = 3 **, $P < 0.01$; ***, $P < 0.001$ when compared with HEK control cells).

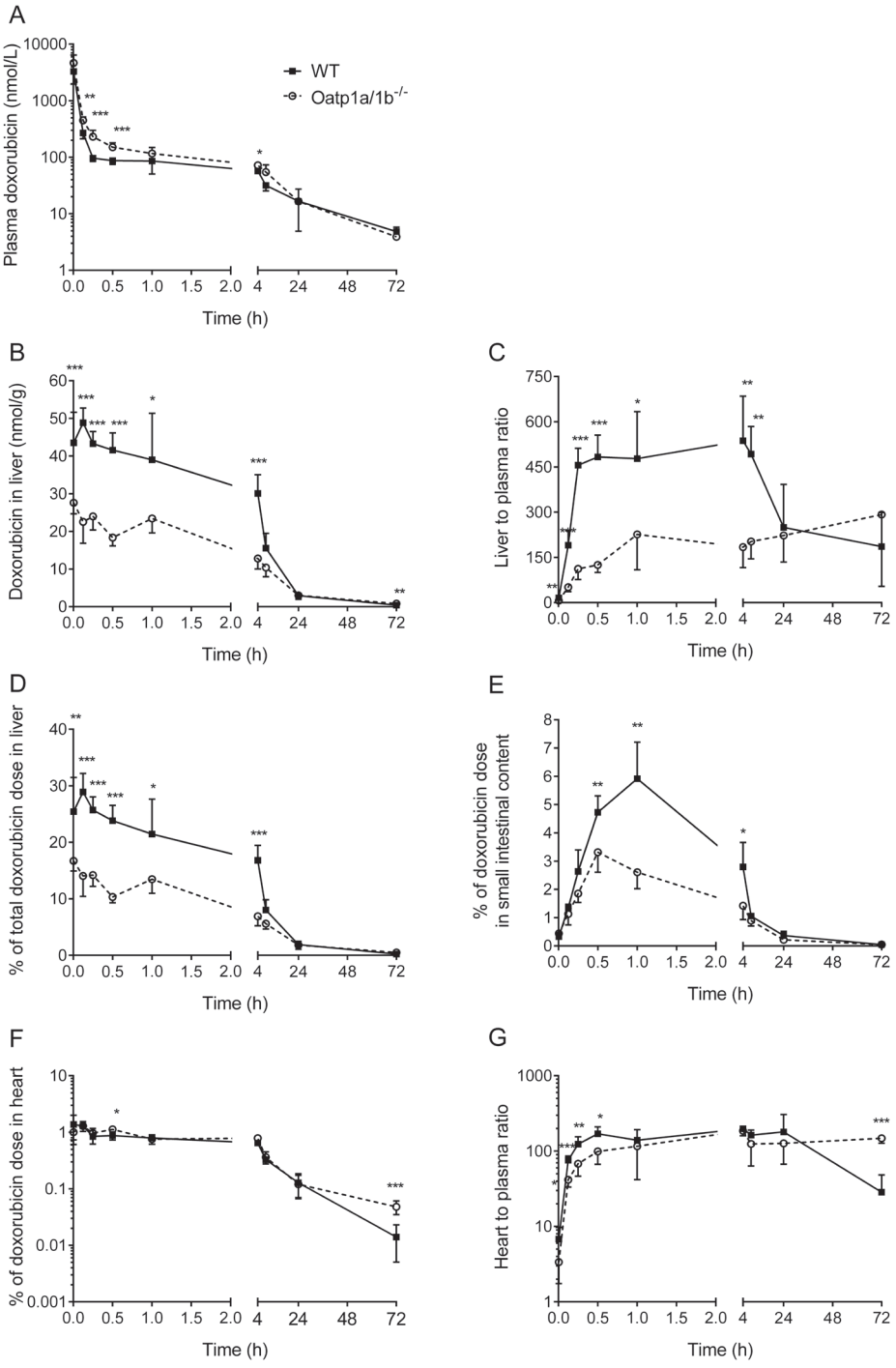
A
Plasma doxorubicin (nmol/L)
WT
Oatp1a/1b-/-
Time (h)
B
Doxorubicin in liver (nmol/g)
Time (h)
C
Liver to plasma ratio
Time (h)
D
% of total doxorubicin dose in liver
Time (h)
E
% of doxorubicin dose in small intestinal content
Time (h)
F
% of doxorubicin dose in heart
Time (h)
G
Heart to plasma ratio
Time (h)

148 nM•h, $P = 0.11$). Especially at early time points such as 7.5, 15 and 30 min after administration, plasma doxorubicin levels were significantly increased by 1.7- ($P < 0.01$), 2.4- ($P < 0.001$) and 1.7-fold ($P < 0.001$) in Oatp1a/1b$^{-/-}$ mice compared to WT. We observed decreases, albeit modest, in the main pharmacokinetic parameters in Oatp1a/1b$^{-/-}$ mice, such as clearance (from 4.8 to 3.9 l/h/kg), elimination half-life (from 26.9 to 23.0 h) and volume of distribution (from 187 to 130.5 l) (Table 1). These findings suggest that Oatp1a/1b transporters play a role in the early systemic disposition and elimination of doxorubicin after intravenous administration.

Conversely, the amount of doxorubicin in the liver (AUC) was markedly and significantly decreased (1.4-fold, $P = 0.009$) over 72 h in the Oatp1a/1b$^{-/-}$ mice compared to WT mice (Figure 2B). Like for the plasma levels, differences were most pronounced during the first 4 h after doxorubicin administration, when plasma and tissue levels were comparatively high. Hepatic uptake of doxorubicin was very rapid, with ~25% of the total doxorubicin dose found in liver of WT mice and ~17% in Oatp1a/1b$^{-/-}$ mice just 3 min after administration (Figure 2D). This is similar to previous findings showing very fast hepatic uptake of paclitaxel and methotrexate [33]. Compared to WT, liver-to-plasma ratios were also significantly and substantially decreased in Oatp1a/1b$^{-/-}$ mice (2.3- to 4.1-fold, $P < 0.01$ to $P < 0.001$, respectively) at all time points up to 8 h (Figure 2C), indicating impaired hepatic uptake of doxorubicin in the absence of Oatp1a/1b transporters.

Corresponding with the reduced liver doxorubicin concentrations, and presumably reduced hepatic throughput, we observed lower doxorubicin levels in the small intestinal content in the Oatp1a/1b$^{-/-}$ compared to WT mice, which was statistically significant between 0.5 and 4 h (Figure 2E). The total amount of doxorubicin retrieved from small intestinal content was maximal in WT mice at 1 h (5.9% of the total dose) and in Oatp1a/1b$^{-/-}$ mice at 30 min (3.3% of the total dose).

Cardiac toxicity is a main dose-limiting factor in the clinical use of doxorubicin, so we also measured cardiac doxorubicin concentrations. However, we observed no markedly altered cardiac doxorubicin levels between the strains, either expressed in nmol/g (Supplementary Figure 1), or as % of the dose (Figure 2F). Heart-to-plasma ratios of doxorubicin did show that absence of Oatp1a/1b resulted in modestly but significantly lower ratios during the first 30 min after administration (Figure 2G), probably mainly reflecting the substantially increased plasma levels over this time period (Figure 2A). Only at 72 h, when most of the doxorubicin was already cleared from the body, Oatp1a/1b$^{-/-}$ mice showed a 5.2-fold higher heart-to-plasma ratio compared to WT mice (Figure 2G, $P < 0.001$). These findings suggest at best a modest, if any, role of OATP1A/1B proteins in the cardiac disposition, and hence toxicity, of doxorubicin.

◀ **Figure 2. Levels of doxorubicin in plasma, liver, small intestinal content and heart of female WT and Oatp1a/1b$^{-/-}$ mice after intravenous administration of 5 mg/kg doxorubicin.** Doxorubicin plasma concentrations as nmol/l (A), liver concentrations as nmol/g (B), % of the total doxorubicin dose in liver, small intestinal content and heart (D, E and F, respectively), and liver- and heart-to-plasma ratios (C and G, respectively) are represented in the graphs. Note the break and scale change in the X-axis. Average liver-to-plasma ratios were calculated from individual mouse data by dividing liver concentration (in nmol/g) by plasma concentration (in nmol/ml), assuming 1 ml of plasma is equivalent to 1 g of liver tissue. Data are given as mean ± S.D. (n = 4-8, *, $P < 0.05$; **, $P < 0.01$; ***, $P < 0.001$ when compared with WT).

**Table 1.** Main pharmacokinetic parameters that are calculated by noncompartmental methods using the software package PK Solutions 2.0.2 (Summit Research Services, Ashland, OH) after intravenous doxorubicin administration to WT, Oatp1a/1b$^{-/-}$ mice.

| Dose | Sample site | PK Parameter | WT | Oatp1a/1b$^{-/-}$ | Fold difference (KO/WT) |
|---|---|---|---|---|---|
| 5 mg/kg i.v. (female) | Systemic blood | $AUC_{(0-\infty)}$, nM•h | 1790.2 | 2196.2 | 1.2 |
| | | Clearance (l/h/kg) | 4.8 | 3.9 | 0.8 |
| | | Elimination half life (h) | 26.9 | 23.0 | |
| | | Volume of distribution (l) | 187.0 | 130.5 | |

### *In vivo* roles of hOATP1A2, hOATP1B1 and hOATP1B3 in the disposition of doxorubicin

To investigate the relevance of our findings for human OATP1A/1B proteins, and hence their clinical implications, we studied doxorubicin disposition in humanized OATP1A2, OATP1B1 and OATP1B3 transgenic mice (*Slco1a/1b*$^{-/-}$*;1A2*$^{tg}$*, Slco1a/1b*$^{-/-}$*;1B1*$^{tg}$ *and Slco1a/1b*$^{-/-}$*;1B3*$^{tg}$; respectively) with hepatocyte-specific expression of each of the transgenic cDNAs in an Oatp1a/1b knockout background. After intravenous administration of 5 mg/kg doxorubicin, we analyzed plasma, liver and small intestinal content levels in these mouse strains and their respective controls at 0.5, 1, and 4 h.

The absence of mouse Oatp1a/1b transporters led to significantly increased plasma levels of doxorubicin by 1.5-, 3.2- and 2.0-fold at 0.5, 1 and 4 h after administration, respectively, compared to WT levels (Figure 3, $P < 0.001$). Compared to the Oatp1a/1b$^{-/-}$ strain, hepatic expression of OATP1A2 in transgenic mice significantly decreased plasma doxorubicin levels at all time points ($P < 0.001$), at 0.5 and 1 h essentially back to WT levels, and at 4 h to even below WT levels ($P < 0.05$). This indicates that hepatic expression of human OATP1A2 in these mice is important in plasma doxorubicin clearance. Despite absence of a clear effect of OATP1B1 or OATP1B3 transgenic transporter expression at 0.5 h, plasma doxorubicin levels in these strains were restored nearly or completely back to WT levels at 1 and 4 h ($P < 0.001$, Figure 3). These results suggest that OATP1B1 and OATP1B3 are important in the plasma clearance of doxorubicin, but their effect only became apparent after 0.5 h after administration. Possibly plasma concentrations before 0.5 h were saturating for these two transporters. The estimated relative plasma elimination rate of doxorubicin from 0.5 h on was rather similar in all transgenic (and WT) mice, but clearly faster than that in Oatp1a/1b$^{-/-}$ mice (Figure 3). This further supports that OATP1A2, -1B1 and -1B3 have roles in the longer-term plasma clearance of doxorubicin.

In the liver of the humanized strains, only hepatic expression of OATP1A2 could markedly reverse the reduced liver concentration of doxorubicin in Oatp1a/1b$^{-/-}$ mice after intravenous administration. The amount of doxorubicin in the liver of Oatp1a/1b$^{-/-}$ mice was markedly decreased (1.4- to 1.7-fold) at all tested time points compared to WT mice (Figure 4A, $P< 0.01$). Among the humanized strains, the OATP1A2 strain could restore the liver doxorubicin back to the WT levels at 0.5 and 1 h, but not at 4 h, whereas liver doxorubicin levels in the OATP1B1 and OATP1B3 strains were similar to those in the Oatp1a/1b$^{-/-}$ strain at all time points (Figure 4A and Supplementary Figure 2). Liver-to-plasma ratios of doxorubicin showed 2.3-, 4.0- and

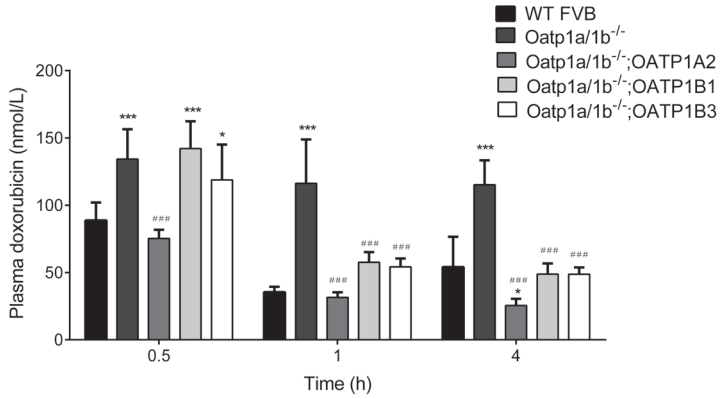


**Figure 3. Plasma levels of doxorubicin (nmol/l) in female WT, Oatp1a/1b$^{-/-}$ and OATP1A2-, OATP1B1-, and OATP1B3-humanized transgenic mice at 0.5, 1 and 4 h after intravenous administration of 5 mg/kg doxorubicin.** Data are given as mean ± S.D. One-way Anova was applied to compare Oatp1a/1b$^{-/-}$ and either of the transgenic strains to WT and Student's t-test was applied to compare either of transgenic strain to Oatp1a/1b$^{-/-}$ mice. (n = 4-9, *, P < 0.05; **, P < 0.01; ***, P < 0.001 when compared with WT, and ###, P < 0.001 when compared with Oatp1a/1b$^{-/-}$ mice).



4.5- fold decreases in Oatp1a/1b$^{-/-}$ mice compared to WT mice at 0.5, 1 and 4 h after injection, respectively (Figure 4B). The OATP1A2 transgenic strain was the only strain that could restore the liver-to-plasma ratios of doxorubicin back to WT levels at all time points, but both the OATP1B1- and OATP1B3-humanized strains showed significant increases in the liver-to-plasma ratios of doxorubicin at 1 and 4h, compared to Oatp1a/1b$^{-/-}$ mice, albeit not up to the WT levels. Collectively, the data suggest that transgenic OATP1A2 fully reverses the effects of the Oatp1a/1b knockout on plasma levels and liver-to-plasma ratios of doxorubicin, whereas transgenic OATP1B1 and -1B3 do so partially, and only after 0.5 h after drug administration.

This conclusion was further borne out by the intestinal content doxorubicin levels in the humanized strains (Figure 4C). At 0.5 and 1 h, transgenic OATP1A2 fully reversed the reduced intestinal content of the Oatp1a/1b knockout back to WT levels. The 4 h time point was not informative, as any effect of the Oatp1a/1b knockout had already faded out by this time. However, the OATP1B1 and OATP1B3 transgenic strains did show a highly significant ($P < 0.001$) but partial reversal towards the WT doxorubicin levels in the intestinal content at 1 h, but not at 0.5 h, consistent with the delayed onset of noticeable effects on doxorubicin disposition in these two strains (Figure 4C).

### Expression of Oct6 influx and ABC efflux transporters in the liver of WT and Oatp1a/1b$^{-/-}$ mice

Doxorubicin has been shown to be a substrate of the drug uptake transporter OCT6 *(SLC22A16)* [31]. OCT6 expression was detected in human testis, fetal liver, bone marrow, peripheral blood leukocytes, in leukemias and in some cancer cell lines, but not in liver, kidney, or placenta [39]. We therefore analyzed the expression of Oct6 in our mouse strains and found that it was

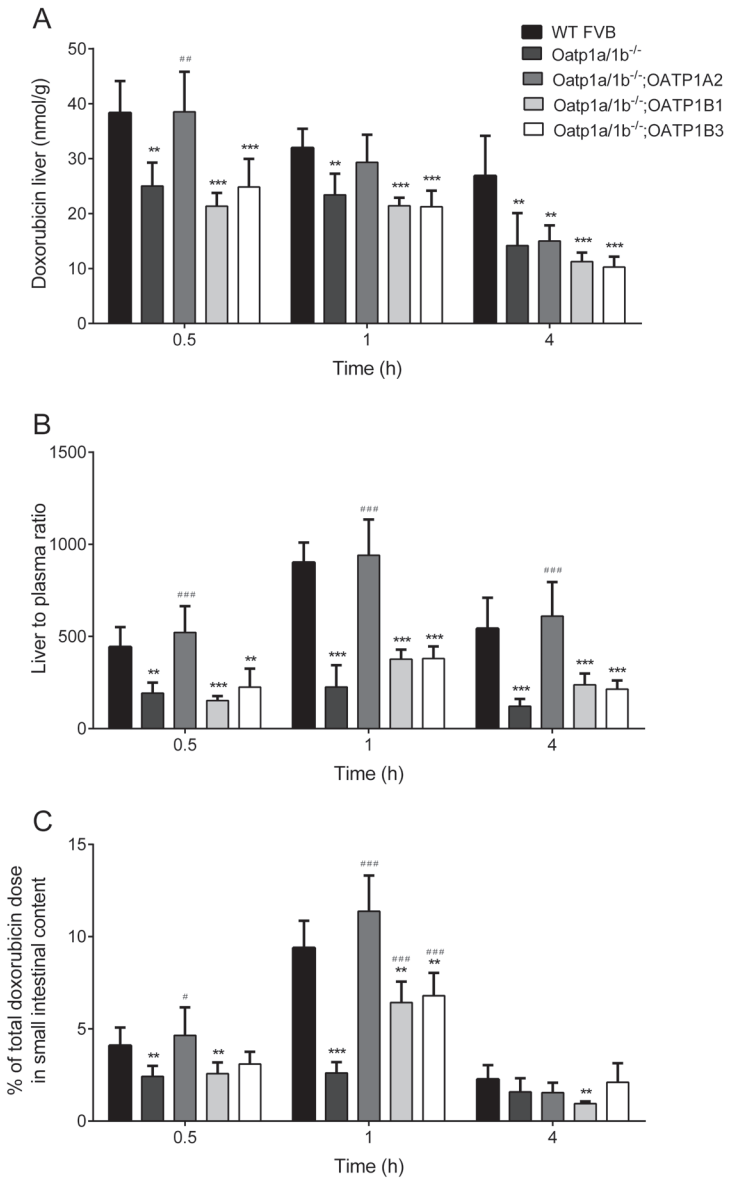


**Figure 4. Liver and small intestinal content levels of doxorubicin in female WT, Oatp1a/1b$^{-/-}$ and OATP1A2-, OATP1B1-, and OATP1B3-humanized transgenic mice at 0.5, 1 and 4 h after intravenous administration of 5 mg/kg doxorubicin.** Doxorubicin levels in liver as nmol/g (A), liver-to-plasma ratios (B) and small intestinal content levels as % of the total doxorubicin dose (C) are represented in the graphs. Averaged liver-to-plasma ratios were calculated from individual mouse data. Data are given as mean ± S.D. One-way Anova was applied to compare Oatp1a/1b$^{-/-}$ and either of the transgenic strains to WT and Student's t-test was applied to compare either of transgenic strain to Oatp1a/1b$^{-/-}$ mice. (n = 4-9, **, P < 0.01; ***, P < 0.001 when compared with WT, and #, P < 0.05; ##, P < 0.01; ###, P < 0.001 when compared with Oatp1a/1b$^{-/-}$ mice).

undetectable by RT-PCR in liver of WT, Oatp1a/1b$^{-/-}$ and OATP1A2-, OATP1B1- and OATP1B3-humanized transgenic mice (data not shown). These results exclude a possible contribution of Oct6 to the hepatic uptake of doxorubicin in our mouse strains. Furthermore, we analyzed the hepatic expression of Mdr1a, Mdr1b and Mrp2, as these are good doxorubicin transporters. We observed significant increases in the expression of Mdr1a ($P < 0.001$), Mdr1b ($P < 0.05$) and Mrp2 ($P < 0.05$) in OATP1A2-transgenic mice and a decrease of Mdr1a ($P < 0.05$) in OATP1B1-transgenic mice (Supplementary Table 1). However, shifts were generally modest, and unlikely to explain the observed changes in doxorubicin disposition. For instance, the increased expression of Mdr1a, Mdr1b, and Mrp2 in the OATP1A2 transgenic mice should reduce hepatic doxorubicin levels compared to the Oatp1a/1b knockout strain, whereas the opposite effect was observed. The other strains did not show significant changes in hepatic expression of any of the transporters tested.

Theoretically, changes in expression of drug transporters during the course of the experiment due to the drug administration itself might also affect the distribution of doxorubicin. However, the major pharmacokinetic differences between all the strains emerged quickly, being already clearly apparent between 3 (Figure 2) and 60 min (Figures 3 and 4) after doxorubicin administration. It seems unlikely that substantial shifts in protein levels of these quite stable and abundant transport proteins could have occurred over this short time span. In addition, the ApoE-hepatic control region promoter used in the OATP transgenic expression constructs is unlikely to be regulated by xenobiotics like doxorubicin.

**Expression of OATP1B1 and OATP1B3 in HEK293 cells, liver of transgenic mice and human liver**

Our *in vitro* uptake studies (Figure 1) showed no demonstrable transport of doxorubicin by OATP1B1 and OATP1B3 in HEK293 cells, whereas our *in vivo* experiments in transgenic mice showed clear effects of these transporters on plasma elimination of this drug and on liver-to-plasma ratios (Figure 3 and 4B). To investigate whether this discrepancy might be related to different protein levels in these systems, we compared OATP1B1 and OATP1B3 expression in the transfected HEK293 cells, livers of OATP1B1- and OATP1B3-humanized transgenic mice, and in human liver by Western blotting. We found that, when corrected for the endogenous β-actin signal, levels of OATP1B1 in transgenic mice were similar to those in the transfected HEK293 cells and in human liver, whereas levels of OATP1B3 were similar between all samples (Figure 5). Note that variable levels of N-glycosylation between different cell types result in multiple major bands representing the full-length OATP proteins. These results indicate that the absence of detectable transport of doxorubicin by OATP1B1 and OATP1B3 in the HEK293 cells cannot be explained by low OATP protein levels in these cells.

## DISCUSSION

We show here that OATP1A/1B transporters play a substantial role in the *in vivo* disposition of doxorubicin. *In vitro* in HEK293 cells, human OATP1A2, but not OATP1B1 and OATP1B3, transported doxorubicin noticeably. In mice, absence of the Oatp1a/1b transporters led to a substantial increase in the systemic exposure and a corresponding decrease in hepatic and

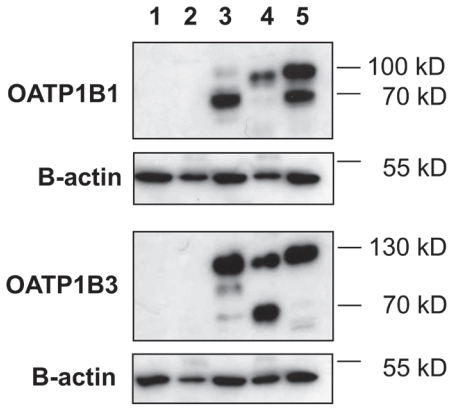


**Figure 5. Expression of human OATP1B1 and OATP1B3 in HEK293 cells, OATP1B1-, and OATP1B3-humanized transgenic mouse liver and human liver by Western blotting.** 1, HEK 293 vector control cells; 2, Oatp1a/1b$^{-/-}$ mouse liver lysate; 3, HEK 293 OATP1B1 or OATP1B3 expressing cells; 4, OATP1B1tg or OATP1B3tg mouse liver lysate; 5, Human crude liver lysate. Molecular masses of 55, 70, 100 and 130 kD are indicated. Western analysis of β-actin was used as a loading control.



small intestinal exposure of doxorubicin. Furthermore, using humanized transgenic mice with liver-specific expression of human OATP1A2, -1B1 and -1B3 in an Oatp1a/1b$^{-/-}$ background, we found that there was a substantial impact of mainly OATP1A2 and to a lesser extent of OATP1B1 and OATP1B3 transporters on systemic and intestinal exposure. In line with this, decreased hepatic uptake of doxorubicin in Oatp1a/1b$^{-/-}$ mice as judged by liver-to-plasma ratios was completely rescued by OATP1A2 (back to WT levels) and partially by OATP1B1 and OATP1B3. To the best of our knowledge, this is the first study demonstrating that the mouse Oatp1a/1b and human OATP1A2, -1B1 and -1B3 proteins transport doxorubicin *in vivo*. These findings implicate a potentially important role in doxorubicin distribution to normal and cancerous tissues. In mice, the systemic exposure of doxorubicin was markedly increased in the absence of Oatp1a/1b transporters, most likely primarily due to the reduced hepatic uptake of the drug. Interestingly, the impact of Oatp1a/1b transporters on doxorubicin disposition was virtually immediate, as already 3 minutes after intravenous injection of doxorubicin we found substantially increased plasma levels and reduced liver levels in Oatp1a/1b$^{-/-}$ mice compared to WT mice (Figure 2A-D). These findings suggest a high intrinsic clearance ($V_{max}/K_m$) capacity of Oatp1a/1b transporters for doxorubicin hepatic uptake. At the same time, it is also clear that there must still be additional hepatic doxorubicin uptake mechanisms, as the hepatic uptake was not much more than 2-fold reduced in Oatp1a/1b$^{-/-}$ mice (Figure 2B-D). While speculative, these might encompass passive diffusion, Oatp2b1 and possibly other sinusoidal organic cation or other transporters expressed in the liver.

We used transgenic mice expressing either human OATP1A2, -1B1 or -1B3 in liver to elucidate the individual *in vivo* effects of each human OATP. Our results show that OATP1A2, -1B1 and -1B3 could all at least partially reverse the increased plasma doxorubicin exposure in

Oatp1a/1b$^{-/-}$ mice at 1 and 4 h, and OATP1A2 also at 0.5 h (Figure 3). The impact of OATP1A2 on the hepatic uptake of doxorubicin was visible, albeit not very pronounced, from the liver levels, but that of OATP1B1 and OATP1B3 was not obvious when liver levels alone were analyzed (Figure 4A). However, consideration of the liver-to-plasma levels indicated a modest rescue effect of OATP1B1 and OATP1B3 on doxorubicin hepatic uptake at 1 and 4 h, versus a strong effect of OATP1A2 at all time points (Figure 4B). It is worth noting that we previously also found a minimal (if any) effect of the Oatp1a/1b knockout on the apparent liver concentrations of the drug rosuvastatin, whereas plasma clearance and liver-to-plasma ratios were strongly reduced [40]. This observation could be explained by a physiologically based pharmacokinetic model described by Watanabe *et al.* [41]. It is therefore not unexpected that a modestly altered hepatic uptake of a drug like doxorubicin (by OATP1B1 or OATP1B3) does not result in an obviously altered liver concentration of a drug. Moreover, the modest rescue effect of OATP1B1 and OATP1B3 (and strong effect of OATP1A2) was further supported by the intestinal content results as discussed below.

Doxorubicin levels in the small intestinal content of Oatp1a/1b$^{-/-}$ mice were reduced compared to those in the WT mice. We previously showed that biliary excretion of doxorubicin (output into the bile) in WT FVB mice over 1 h was ~9% of the dose, whereas the direct intestinal excretion of doxorubicin (i.e., transported directly from the systemic circulation across the intestinal wall) was only 1-2% of the dose after intravenous administration of doxorubicin at 5 mg/kg [27]. This suggests that in WT mice biliary excretion of doxorubicin is about 4-5 times more important for intestinal content levels than clearance by direct intestinal excretion. In our study we found ~10% of the total doxorubicin dose back in the small intestinal content of WT (and OATP1A2 transgenic) mice and 2.5% in that of Oatp1a/1b$^{-/-}$ mice after 1 h (Figure 4C). We therefore conclude that the decreased small intestinal content levels of doxorubicin in Oatp1a/1b$^{-/-}$ mice are mostly due to reduced hepatobiliary excretion of doxorubicin as a consequence of lower hepatic uptake levels. Conversely, the significant increases in intestinal content doxorubicin levels in OATP1A2, -1B1, and -1B3 transgenic mice compared to Oatp1a/1b$^{-/-}$ mice (Figure 4C) suggest increased hepatic throughput (and hence hepatic uptake) of doxorubicin in these strains, with again a more pronounced effect of OATP1A2 than of OATP1B1 or OATP1B3.

Collectively, our findings demonstrate a substantial *in vivo* activity of the human OATP1A2, -1B1 and -1B3 transporters in hepatocellular uptake of doxorubicin, directly affecting plasma and tissue pharmacokinetics. We note here that in human liver, OATP1A2 is not expressed in hepatocytes but in cholangiocytes. The data we obtained with OATP1A2 expressed in hepatocytes of our transgenic mice therefore do not model the physiological human situation. However, they do indicate that human OATP1A2 can mediate *in vivo* uptake of doxorubicin in cells and tissues in which it is expressed. It is further worth noting that, although the impact of human OATP1B1 and OATP1B3 on doxorubicin disposition in the transgenic mice is comparatively modest, in human liver both proteins are coexpressed in hepatocytes, which will likely result in an additive effect on doxorubicin disposition.

Cardiac toxicity is the primary dose-limiting factor for doxorubicin therapy. We found that both Oatp1a/1b$^{-/-}$ and WT mice had similar cardiac doxorubicin concentrations, even though the

plasma levels were somewhat higher in the Oatp1a/1b$^{-/-}$ mice (Figure 2F and G). We think that the modestly lower doxorubicin heart-to-plasma ratios compared to the WT strain at early time points are most likely a secondary effect of the higher plasma levels in the knockout mice, and not so much a result of altered uptake of doxorubicin into the heart. Likely the initial loading of the heart with doxorubicin occurs very early after the intravenous administration, when plasma concentrations are very high, and not yet different between the strains. Subsequent clearance from the heart is very slow. These findings may be relevant for the clinic, as they suggest that there may be no separate impact of OATP1A/1B proteins (independent of their effect on plasma levels of doxorubicin) on cardiac doxorubicin uptake, and thus toxicity. However, extrapolation of these mouse data to the human situation should be done with great caution, and obviously long-term altered plasma levels due to reduced OATP1A/1B activity may still strongly impact on cardiac toxicity of doxorubicin.

The significant *in vivo* transport of doxorubicin by human OATP1A2, -1B1 and -1B3 has potentially important implications for the clinic. It is possible that patients with polymorphic variants or pharmacological inhibition of these transporters (due to dietary compounds or other co-administered drugs) might have altered systemic clearance and/or distribution of doxorubicin to tissues (e.g., reduced hepatic uptake and thus less metabolism and clearance) where these transporters are expressed. This might lead to substantial pharmacological and toxicological consequences, including a decreased therapeutic index of doxorubicin and increased toxicity. For instance, unexpectedly decreased clearance of doxorubicin due to reduced liver uptake by a low-activity OATP1B1 polymorphism can increase long-term exposure of the heart, one of the most important dose-limiting organs for doxorubicin chemotherapy. Therefore, it will be important to investigate whether the activity of OATP1A/1B transporters has any impact on doxorubicin therapy response and toxicity in especially high-risk patients.

Another important implication of the demonstrated *in vivo* doxorubicin uptake by the human OATP1A/1B transporters is that tumors that have expression of these transporters might have increased uptake of doxorubicin, and hence enhanced therapy susceptibility. Several studies have reported expression of OATP1A/1B transporters in various malignant tissues including breast, prostate, ovarian, gastrointestinal and colon cancers [8, 11-15]. Moreover, expression of these transporters might also contribute to the pathogenesis of the disease. For instance, one study showed that OATP1A2 expression was increased in breast cancer compared to the normal healthy part of the tissue, and that it could mediate estrogen uptake into the malignant cells [11]. Therefore, we think that OATP1A/1B transporter expression in tumors might be a relevant factor in the response to doxorubicin-containing therapies. Clearly, further investigations are required to test this hypothesis.

Over the past years, consensus on the structural variation of OATP1A/1B substrates has been changing substantially. Several studies found that OATP1A/1B proteins can transport compounds with unexpectedly varied structures, including amphipathic organic anions, neutral compounds and even some cations [42]. Recently, we have also shown that several (anti-cancer) drugs with highly diverse structures are transported by OATP1A/1B proteins *in vivo*. Examples of these drugs include methotrexate (organic anion), fexofenadine (zwitterion), and paclitaxel (bulky hydrophobic). The present study shows that also doxorubicin, an amphipathic

weak base and cation at physiological pH [32, 33] is substantially transported by these proteins *in vivo*.

In conclusion, doxorubicin, a widely used anti-cancer drug, is shown to be transported by mouse and human OATP1A/1B transporters *in vivo*. In the clinic, great caution should be taken for toxicity risks when doxorubicin therapy is given to the patients with OATP1B1 and/or OATP1B3 (and possibly also OATP1A2) polymorphisms or when drug-drug interactions modulating activity of OATP1A/1B transporters might occur. Most importantly, the efficacy of doxorubicin-containing therapy might be influenced by tumoral expression of OATP1A2, -1B1 or -1B3. Further investigations in patients in order to assess the practical clinical relevance of our findings will therefore be of great interest.

## REFERENCE LIST


1. Hagenbuch B, Meier PJ. Organic anion transporting polypeptides of the OATP/ SLC21 family: phylogenetic classification as OATP/ SLCO superfamily, new nomenclature and molecular/functional properties. Pflug*ers Arch 2004;* 447:653-665.
2. Obaidat A, Roth M, Hagenbuch B. The expression and function of organic anion transporting polypeptides in normal tissues and in cancer. Annu Re*v Pharmacol Toxicol 2012;* 52:135-151.
3. Cheng X, Klaassen CD. Tissue distribution, ontogeny, and hormonal regulation of xenobiotic transporters in mouse kidneys. Drug M*etab Dispos 2009;* 37:2178-2185.
4. Cheng X, Maher J, Chen C, Klaassen CD. Tissue distribution and ontogeny of mouse organic anion transporting polypeptides (Oatps). Drug M*etab Dispos 2005;* 33:1062-1073.
5. Glaeser H, Bailey DG, Dresser GK, Gregor JC, Schwarz UI, McGrath JS et al. *Inte*stinal drug transporter expression and the impact of grapefruit juice in humans. Clin P*harmacol Ther 2007;* 81:362-370.
6. Lee W, Glaeser H, Smith LH, Roberts RL, Moeckel GW, Gervasini G et al. *Polym*orphisms in human organic anion-transporting polypeptide 1A2 (OATP1A2): implications for altered drug disposition and central nervous system drug entry. J Biol *Chem 2005;* 280:9610-9617.
7. Gao B, Hagenbuch B, Kullak-Ublick GA, Benke D, Aguzzi A, Meier PJ. Organic anion-transporting polypeptides mediate transport of opioid peptides across blood-brain barrier. J Phar*macol Exp Ther 2000;* 294:73-79.
8. Abe T, Unno M, Onogawa T, Tokui T, Kondo TN, Nakagomi R et al. *LST-2*, a human liver-specific organic anion transporter, determines methotrexate sensitivity in gastrointestinal cancers. Gastro*enterology 2001;* 120:1689-1699.
9. Konig J, Cui Y, Nies AT, Keppler D. A novel human organic anion transporting polypeptide localized to the basolateral hepatocyte membrane. Am J P*hysiol Gastrointest Liver Physiol 2000;* 278:G156-G164.
10. Tamai I, Nezu J, Uchino H, Sai Y, Oku A, Shimane M et al. *Molecu*lar identification and characterization of novel members of the human organic anion transporter (OATP) family. Biochem *Biophys Res Commun 2000;* 273:251-260.
11. Meyer zu Schwabedissen HE, Tirona RG, Yip CS, Ho RH, Kim RB. Interplay between the nuclear receptor pregnane X receptor and the uptake transporter organic anion transporter polypeptide 1A2 selectively enhances estrogen effects in breast cancer. Cancer *Res 2008;* 68:9338-9347.
12. Liedauer R, Svoboda M, Wlcek K, Arrich F, Ja W, Toma C et al. *Differe*nt expression patterns of organic anion transporting polypeptides in osteosarcomas, bone metastases and aneurysmal bone cysts. Oncol R*ep 2009;* 22:1485-1492.
13. Arakawa H, Nakanishi T, Yanagihara C, Nishimoto T, Wakayama T, Mizokami A et al. *Enhanc*ed expression of organic anion transporting polypeptides (OATPs) in androgen receptor-positive prostate cancer cells: possible role of OATP1A2 in adaptive cell growth under androgen-depleted conditions. Biochem *Pharmacol 2012;* 84:1070-1077.
14. Svoboda M, Wlcek K, Taferner B, Hering S, Stieger B, Tong D et al. *Expre*ssion of organic anion-transporting polypeptides 1B1 and 1B3 in ovarian

cancer cells: relevance for paclitaxel transport. Biomed *Pharmacother 2011;* 65:417-426.

15. Ballestero MR, Monte MJ, Briz O, Jimenez F, Gonzalez-San MF, Marin JJ. Expression of transporters potentially involved in the targeting of cytostatic bile acid derivatives to colon cancer and polyps. Biochem *Pharmacol 2006;* 72:729-738.
16. Konig J, Seithel A, Gradhand U, Fromm MF. Pharmacogenomics of human OATP transporters. Naunyn *Schmiedebergs Arch Pharmacol 2006;* 372:432-443.
17. Maeda K, Sugiyama Y. Impact of genetic polymorphisms of transporters on the pharmacokinetic, pharmacodynamic and toxicological properties of anionic drugs. Drug M*etab Pharmacokinet 2008;* 23:223-235.
18. Pasanen MK, Neuvonen PJ, Niemi M. Global analysis of genetic variation in SLCO1B1. Pharmaco*genomics 2008;* 9:19-33.
19. Laitinen A, Niemi M. Frequencies of single-nucleotide polymorphisms of SLCO1A2, SLCO1B3 and SLCO2B1 genes in a Finnish population. Basic C*lin Pharmacol Toxicol 2011;* 108:9-13.
20. Yamakawa Y, Hamada A, Shuto T, Yuki M, Uchida T, Kai H et al. *Pharma*cokinetic impact of SLCO1A2 polymorphisms on imatinib disposition in patients with chronic myeloid leukemia. Clin Ph*armacol Ther 2011;* 90:157-163.
21. Kalliokoski A, Niemi M. Impact of OATP transporters on pharmacokinetics. Br J Ph*armacol 2009;* 158:693-705.
22. Takane H, Kawamoto K, Sasaki T, Moriki K, Moriki K, Kitano H et al. *Life-t*hreatening toxicities in a patient with UGT1A1*6/*28 and SLCO1B1*15/*15 genotypes after irinotecan-based chemotherapy. Cancer *Chemother Pharmacol 2009;* 63:1165-1169.
23. Trevino LR, Shimasaki N, Yang W, Panetta JC, Cheng C, Pei D et al. G*erml*ine genetic variation in an organic anion transporter polypeptide associated with methotrexate pharmacokinetics and clinical effects. J Clin *Oncol 2009;* 27:5972-5978.
24. van de Steeg E, Stranecky V, Hartmannova H, Noskova L, Hrebicek M, Wagenaar E et al. *Compl*ete OATP1B1 and OATP1B3 deficiency causes human Rotor syndrome by interrupting conjugated bilirubin reuptake into the liver. J Clin *Invest 2012;* 122:519-528.
25. Weiss RB, Sarosy G, Clagett-Carr K, Russo M, Leyland-Jones B. Anthracycline analogs: the past, present, and future. Cancer *Chemother Pharmacol 1986;* 18:185-197.
26. Gewirtz DA. A critical evaluation of the mechanisms of action proposed for the antitumor effects of the anthracycline antibiotics adriamycin and daunorubicin. Biochem *Pharmacol 1999;* 57:727-741.
27. Vlaming ML, Mohrmann K, Wagenaar E, de Waart DR, Elferink RP, Lagas JS et al. *Carcino*gen and anticancer drug transport by Mrp2 in vivo: studies using Mrp2 (Abcc2) knockout mice. J Pharma*col Exp Ther 2006;* 318:319-327.
28. van Asperen J, van Tellingen O, Beijnen JH. The role of mdr1a P-glycoprotein in the biliary and intestinal secretion of doxorubicin and vinblastine in mice. Drug M*etab Dispos 2000;* 28:264-267.
29. van Asperen J, van Tellingen O, Tijssen F, Schinkel AH, Beijnen JH. Increased accumulation of doxorubicin and doxorubicinol in cardiac tissue of mice lacking mdr1a P-glycoprotein. Br J C*ancer 1999;* 79:108-113.
30. Allen JD, Brinkhuis RF, Wijnholds J, Schinkel AH. The mouse Bcrp1/Mxr/Abcp gene: amplification and overexpression in cell lines selected for resistance to topotecan, mitoxantrone, or doxorubicin. Cancer *Res 1999;* 59:4237-4241.
31. Okabe M, Unno M, Harigae H, Kaku M, Okitsu Y, Sasaki T et al. *Chara*cterization of the organic cation transporter SLC22A16: a doxorubicin importer. Biochem *Biophys Res Commun 2005;* 333:754-762.
32. van de Steeg E, Wagenaar E, van der Kruijssen CM, Burggraaff JE, de Waart DR, Elferink RP et al. *Organi*c anion transporting polypeptide 1a/1b-knockout mice provide insights into hepatic handling of bilirubin, bile acids, and drugs. J Clin *Invest 2010;* 120:2942-2952.
33. van de Steeg E, van EA, Wagenaar E, van der Kruijssen CM, van TO, Kenworthy KE et al. *High i*mpact of Oatp1a/1b transporters on in vivo disposition of the hydrophobic anticancer drug paclitaxel. Clin C*ancer Res 2011;* 17:294-301.
34. Peters J, Eggers K, Oswald S, Block W, Lutjohann D, Lammer M et al. *Clari*thromycin is absorbed by an intestinal uptake mechanism that is sensitive to major inhibition by rifampicin: results of a short-term drug interaction study in foals. Drug M*etab Dispos 2012;* 40:522-528.
35. Hirano M, Maeda K, Shitara Y, Sugiyama Y. Contribution of OATP2 (OATP1B1) and OATP8 (OATP1B3) to the hepatic uptake of pitavastatin in humans. J Pharma*col Exp Ther 2004;* 311:139-146.
36. van de Steeg E, van der Kruijssen CM, Wagenaar E, Burggraaff JE, Mesman E, Kenworthy KE et al. *Metho*trexate pharmacokinetics in transgenic mice with liver-specific expression of human organic anion-transporting polypeptide 1B1 (SLCO1B1). Drug M*etab Dispos 2009;* 37:277-281.

37. van Asperen J, van Tellingen O, Beijnen JH. Determination of doxorubicin and metabolites in murine specimens by high-performance liquid chromatography. J Chroma*togr B Biomed Sci Appl 1998;* 712:129-143.

38. de Graan AJ, Lancaster CS, Obaidat A, Hagenbuch B, Elens L, Friberg LE et al. *Influ*ence of polymorphic OATP1B-type carriers on the disposition of docetaxel. Clin C*ancer Res 2012;* 18:4433-4440.

39. Gong S, Lu X, Xu Y, Swiderski CF, Jordan CT, Moscow JA. Identification of OCT6 as a novel organic cation transporter preferentially expressed in hematopoietic cells and leukemias. Exp Hem*atol 2002;* 30:1162-1169.

40. Iusuf D, van EA, Hobbs M, Taylor M, Kenworthy KE, van de Steeg E et al. *Murine* Oatp1a/1b uptake transporters control rosuvastatin systemic exposure without affecting its apparent liver exposure. Mol Pha*rmacol 2013;* 83:919-929.

41. Watanabe T, Kusuhara H, Maeda K, Shitara Y, Sugiyama Y. Physiologically based pharmacokinetic modeling to predict transporter-mediated clearance and distribution of pravastatin in humans. J Pharm*acol Exp Ther 2009;* 328:652-662.

42. Hagenbuch B, Gui C. Xenobiotic transporters of the human organic anion transporting polypeptides (OATP) family. Xenobio*tica 2008;* 38:778-801.

## SUPPLEMENTARY DATA

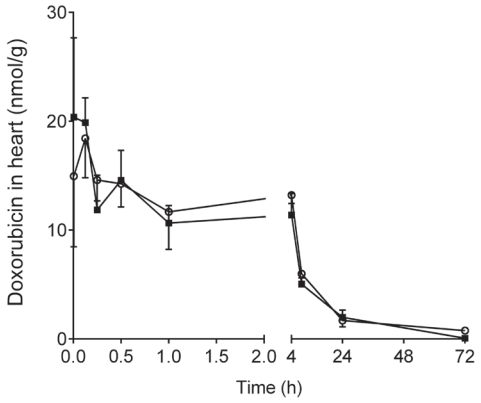


**Supplementary Figure 1. Doxorubicin concentration (nmol/g) in heart of female WT and Oatp1a/1b$^{-/-}$ mice after intravenous administration of 5 mg/kg doxorubicin.** Data are given as mean ± S.D. (n = 4-8).

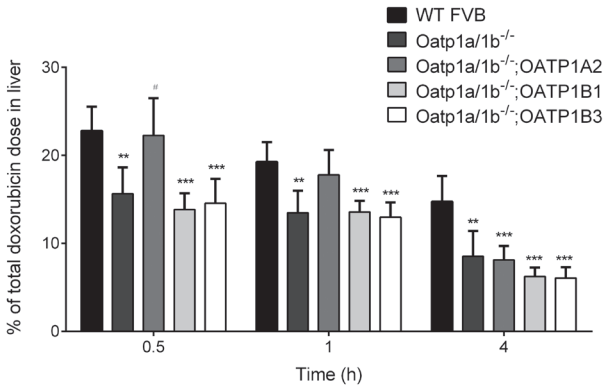


**Supplementary Figure 2. Percentage of the total doxorubicin dose in liver of female WT, Oatp1a/1b$^{-/-}$ and OATP1A2-, OATP1B1-, and OATP1B3-humanized transgenic mice at 0.5, 1 and 4 h after intravenous administration of 5 mg/kg doxorubicin.** Data are given as mean ± S.D. One-way Anova test was applied to compare Oatp1a/1b$^{-/-}$ and either of the transgenic strains to WT and Student's t-test was applied to compare either of transgenic strain to Oatp1a/1b$^{-/-}$ mice. (n = 4-9, **, P < 0.01; ***, P < 0.001 when compared with WT, and #, P < 0.05 when compared with Oatp1a/1b$^{-/-}$ mice).

**Supplementary Table 1.** Overview of the ΔCt values of the RT-PCR analysis to investigate expression of Mdr1a, Mdr1b and Mrp2 drug efflux transporters in liver of female WT, Oatp1a/1b-/- and OATP1A2, OATP1B1, and OATP1B3 humanized transgenic mice (n = 3, each sample was assayed in duplicate. *, $P < 0.05$; ***, $P < 0.001$ when compared with expression levels in WT mice). Analysis of the results was done by comparative Ct method. Quantification of the target cDNAs in all samples was normalized against the endogenous control Gapdh (Ctarget - CGapdh = ΔCt). Note that lower ΔCt values indicate higher expression levels.

| | **WT** | **Oatp1a/1b$^{-/-}$** | **Oatp1a/1b$^{-/-}$;1A2** | **Oatp1a/1b$^{-/-}$;1B1** | **Oatp1a/1b$^{-/-}$;1B3** |
|---|---|---|---|---|---|
| Mdr1a | 10.76 ± 0.09 | 10.67 ± 0.32 | 9.58 ± 0.22*** | 12.24 ± 0.60* | 10.35 ± 0.50 |
| Mdr1b | 14.45 ± 0.31 | 15.35 ± 0.84 | 13.15 ± 0.49* | 14.18 ± 0.47 | 14.09 ± 2.32 |
| Mrp2 | 3.39 ± 0.22 | 3.95 ± 0.28 | 2.85 ± 0.12* | 3.58 ± 0.23 | 3.65 ± 0.08 |

# CHAPTER 4

## PRECLINICAL MODELS TO ASSESS OATP-MEDIATED DRUG-DRUG INTERACTIONS *IN VIVO*

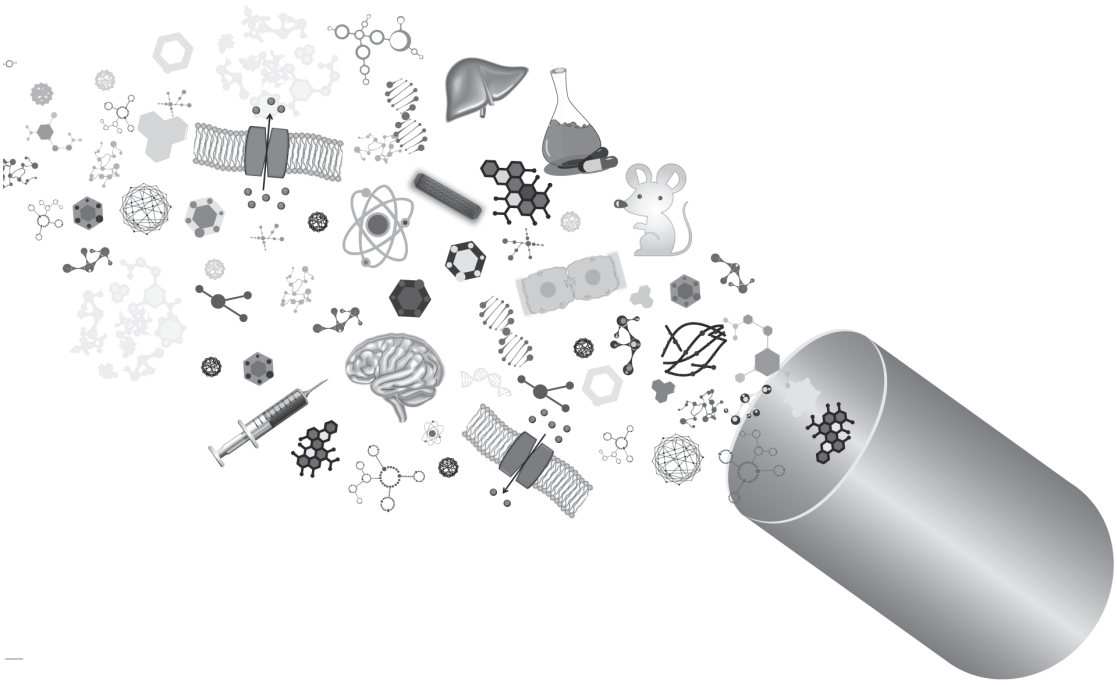

# CHAPTER 4.1

## PRECLINICAL MOUSE MODELS TO STUDY HUMAN OATP1B1- AND OATP1B3-MEDIATED DRUG-DRUG INTERACTIONS *IN VIVO*

Selvi Durmus[1], Gloria Lozano-Mena[1, 2], Anita van Esch[1], Els Wagenaar[1], Olaf van Tellingen[3], Alfred H. Schinkel[1]

[1]Division of Molecular Oncology, The Netherlands Cancer Institute, Amsterdam, The Netherlands,
[2]Department of Physiology and Nutrition and Food Safety Research Institute (INSA-UB), Universitat de Barcelona, Barcelona, Spain
[3]Department of Clinical Chemistry, The Netherlands Cancer Institute, Amsterdam, The Netherlands

*To be submitted*

## ABSTRACT

The impact of OATP drug uptake transporters in drug-drug interactions (DDIs) is increasingly recognized, especially during new drug discovery. OATP1B1 and -1B3 are human hepatic uptake transporters that can mediate liver uptake of a wide variety of drugs. Recently, transgenic mice with liver-specific expression of human OATP1B1/1B3 were generated in a knockout background for the mouse Oatp1a/1b transporters. Here, we investigated the applicability of these transgenic mice for studying DDIs mediated by human OATP1B1 or -1B3 using the prototypic OATP inhibitor rifampicin and a good OATP substrate, methotrexate (MTX). We next assessed the possibility of OATP-mediated interactions between telmisartan and MTX, a clinically relevant drug combination. Using HEK293 cells overexpressing OATP1B1,-1B3 or -1A2, we demonstrated that both rifampicin and telmisartan can inhibit OATP-mediated MTX uptake at low IC50 concentrations (1 - 11 μM) *in vitro*. Using WT, Oatp1a/1b-/- and OATP1B1 or -1B3 transgenic mice, we showed that rifampicin inhibits hepatic uptake of MTX mediated by the mouse Oatp1a/1b and human OATP1B1 and -1B3 transporters, at clinically effective concentrations, highlighting the applicability of these mouse models in DDI studies. Next, we demonstrated that telmisartan was a weak inhibitor of OATP1B1-mediated and not an inhibitor of mouse Oatp1a/1b or human OATP1B3-mediated hepatic uptake of MTX at concentrations higher than those used in the clinic; therefore risks for OATP-mediated clinical DDIs for this combination are low at best. Overall, we show here that OATP1B1/1B3 humanized mice can be used as proper *in vivo* tools to assess and predict clinical DDIs.



## NOVELTY & IMPACT STATEMENTS

We show that humanized OATP1B transgenic mice can be used as reliable preclinical models to predict DDIs. Using these models, here we demonstrated that rifampicin and methotrexate interact at the level of hepatic OATPs, leading to increased plasma and decreased liver levels of MTX at clinically relevant concentrations, whereas telmisartan and MTX do not show an obvious risk of clinical interactions mediated by OATPs. DDIs may lead to toxicity or altered therapeutic efficacy of at least one of the coadministered drugs. Extra caution should be taken for patients with polymorphic variants of OATP transporters, as they might be more susceptible to clinical outcomes of the DDIs. Therefore, proper preclinical models are highly relevant for clinical DDI predictions, since such predictions are currently largely based on *in vitro* and *in silico* models.

## INTRODUCTION

Organic anion-transporting polypeptides (OATP/Oatp) are sodium-independent transmembrane uptake transporters that are encoded by *SLCO/Slco* genes. OATPs are expressed in several organs including liver, kidney and small intestine where they mediate the tissue uptake of substrate compounds [1]. The pharmacological importance of OATPs is increasingly recognized as more and more studies show that OATPs are important players in disposition of a wide range of drugs including statins, cardiac glycosides, antibiotics, and chemotherapeutics [2]. OATP1B1 and -1B3 are selectively expressed in the sinusoidal membrane of hepatocytes where they have key roles in hepatic uptake and/or plasma clearance of many drugs with a broad range of structures such as methotrexate (MTX), paclitaxel, docetaxel, pravastatin, fexofenadine and doxorubicin [3-7]. Therefore, alterations in the OATP1B activity or drug-drug interactions (DDIs) mediated by inhibition of OATP1B transporters might have important clinical consequences for the pharmacokinetics, efficacy and toxicity of these therapeutics [2, 8-10]. For example, genetic variants of OATP1B1 showed significant changes in the disposition and toxicity of pravastatin, valsartan, MTX and SN-38 [9, 11, 12]. Deficiency of OATP1B1 and -1B3 has been shown to result in the disruption of the hepatic re-uptake and consequently increased plasma levels of conjugated bilirubin, causing a syndrome called Rotor-type hyperbilirubinemia [13].

Our knowledge of the involvement of the OATPs in DDIs is limited but growing rapidly, and the clinical importance of such interactions is becoming more and more evident [14]. FDA and EMA strongly recommend investigation of DDIs mediated by OATP1B1 and -1B3 for new molecular entities (NMEs) during drug development since 2012 [15]. Recently, Shitara *et al*. [2] reported examples of DDIs that are caused by inhibition of OATP1B transporters via potent inhibitors, and which affected the pharmacokinetics of victim drugs. The inhibitor drugs tested were antibiotics, antiviral drugs and the immunosuppressant cyclosporin A, and victim drugs were widely used statins, antidiabetic and hypertension drugs. Among the inhibitors, cyclosporin A and rifampicin appeared to be particularly strong inhibitors of OATP1B1 which caused increases in the plasma levels of several statins of 2.2- to 23-fold as a result of DDIs [2]. There are only few recent studies on OATP-mediated DDIs with anticancer drugs, although these are widely used and often substrates of OATPs. Hu *et al*. [16] recently published a study which investigated whether inhibition of OATP1B1 by tyrosine kinase inhibitors could explain a decreased docetaxel clearance. Sorafenib was selected as a potent inhibitor of OATP1B1 based on the *in vitro* assays, however single or multiple dose of sorafenib did not affect docetaxel plasma levels *in vivo* using Oatp1b2 knockout and hOATP1B1-expressing transgenic mice [16]. Another recent study by Nieuweboer *et al*. [17] showed that use of polysorbate 80 or Kolliphor (Cremophor) EL in the drug formulation can inhibit OATP1B2-mediated hepatic elimination of paclitaxel. Clearly, DDI studies involving interactions between widely used medicines and anticancer drugs are urgently needed, as such interactions may lead to unexpected toxicities and changed efficacy in the treatment of cancers, and anticancer drugs are usually administered at high dosages and have a narrow therapeutic window. The antifolate MTX is a widely used anticancer andantirheumatic drug that is a transported substrate of mouse Oatp1a/1b and human OATP1B1 and -1B3 transporters *in vivo* [7]. The likelihood of undesired DDIs and thus

altered pharmacokinetics of MTX might be substantial, when prescribed with other commonly used drugs such as antibiotics, hypertension drugs and antidiabetics that are inhibitors/substrates of OATPs. Thus, MTX is of great interest for assessment of such interactions and prediction of clinical outcomes.

In order to predict clinical DDIs, many studies utilize *in vitro* cellular uptake assays and *in silico* [18-22] and preclinical models [2, 23]. However, it remains challenging to translate *in vitro* data to the human *in vivo* situation and use of preclinical wild-type and knockout animal models does not necessarily result in optimal prediction due to species differences [24, 25]. Accordingly, we have generated humanized mouse models with liver-specific expression of OATP1B1 or -1B3 [7]. In this study, we wanted to investigate whether these transgenic mouse models could be used as a tool to assess human OATP1B1 and -1B3-mediated DDIs *in vivo*. For this aim, we used the antibiotic rifampicin as a model inhibitor of OATP1B transporters and MTX as a victim drug. Secondly, we tested OATP1B-mediated DDIs between the antihypertensive drug telmisartan and MTX which has a higher chance for co-prescription in the clinic.





## MATERIALS AND METHODS

### Chemicals

Methotrexate (100 mg/ml, Pharmachemie, the Netherlands) and cyclosporin A (CsA, 50 mg/ml, Novartis, Switzerland) were obtained as parenteral formulations from the pharmacy department of the Slotervaart Hospital, the Netherlands. Rifampicin was purchased from Sigma-Aldrich (USA) and telmisartan was purchased from Sequoia Research Chemicals (UK), both inpowder forms. 7-OH-MTX, rifampicin-d3 and telmisartan-d7 were purchased from Toronto Research Chemicals (Canada). All of the chemicals used for HPLC-UV and HPLC-MS analysis were from Sigma-Aldrich (USA) or Merck, Germany.

### Drug solutions

*In vitro experiments*

MTX stock solution (100 mg/ml = 220.1 mM) and cyclosporin A (50 mg/ml = 41.6 mM) were diluted in Krebs-Henseleit buffer to yield 50 µM MTX and 0.5 µM CsA solution, respectively. Rifampicin (50 mM) and telmisartan (10 mM) were prepared in DMSO and dimethyl formamide (DMF), respectively, and were further diluted in Krebs-Henseleit buffer to yield the desired concentrations.

*In vivo experiments*

MTX stock solution (100 mg/ml) was diluted 50 or 250-fold with 0.9% NaCl to yield a concentration of 2 or 0.4 mg/ml. Rifampicin was dissolved in DMSO (at 80 mg/ml) and further diluted in 0.9% NaCl to yield a concentration of 4 mg/ml. Telmisartan was dissolved in DMF (7 mg/ml, maximum solubility) and further diluted in PBS to yield a concentration of 1.4 mg/ml. All drugs were administered intravenously, using a volume of 5 µl/g body weight. All working solutions were prepared on the day of experiment.

**Cell culture**

HEK293 cells transduced with vector control, hSLCO1A2, hSLCO1B1 and hSLCO1B3 cDNAs were a kind gift from Prof. Werner Siegmund and Dr. Markus Keiser, (University of Greifswald, Greifswald, Germany) [26]. All cells were grown in Dulbecco's modified Eagle's medium low glucose (Invitrogen) supplemented with 10% fetal bovine serum (Sigma), 100 U/ml penicillin, 100 µg/ml streptomycin and 0.25 µg/ml amphotericin B at 37°C with 5% CO2 and 95% humidity.

**Cellular uptake experiments**

Cellular uptake experiments were performed according to previously described methods [3, 27] and modified as required. Krebs-Henseleit buffer at pH 7.4, which was adjusted before the experiment was started, was used in all the steps of the experiment including dilutions of the drug stock solutions. Briefly, cells were preincubated with 1 ml pre-warmed buffer for 15 min at 37°C. Uptake experiments were started by aspirating the preincubation buffer and adding 600 µl of pre-warmed buffer containing (inhibitor) drugs; MTX (50 µM) alone or together with rifampicin (0, 1, 2.5, 5, 15, 25, 50 or 100 µM) or telmisartan (0, 1, 2.5, 5, 25, 50 or 100 µM) or CsA (0.5 µM). CsA was used as a positive control for the uptake inhibition; therefore it was also added in the pre-incubation buffer as an OATP inhibitor. At designated time points (2.5, 5, 10, 15, 30, 60 or 120 min) experiments were terminated by removing the incubation buffer and immediately adding 1 ml ice-cold buffer. After twice washing with ice-cold buffer, cells were lysed with 150 µl of 0.2 N NaOH for a minimum of 15 min. 10 µl of the cell lysate was used to determine the cellular protein amount by the Bradford method using bovine serum albumin as a standard. 60 µl of the cell lysates were used to determine MTX levels by HPLC.

**Animals**

Mice were housed and handled according to institutional guidelines complying with Dutch legislation. Male WT, Oatp1a/1b-/-, Oatp1a/1b-/-;1B1tg and Oatp1a/1b-/-;1B3tg with liver-specific expression of human SLCO genes, all of a >99% FVB genetic background, were used between 8 and 14 weeks of age. Animals were kept in a temperature-controlled environment with a 12 hr light/12 hr dark cycle and received a standard diet (AM-II, Hope Farms) and acidified water ad libitum.

**Plasma and liver pharmacokinetic experiments**

Dosages of MTX were 10 and 2 mg/kg body weight, that of rifampicin was 20 mg/kg and that of telmisartan was 7 mg/kg body weight. Rifampicin, telmisartan or vehicles (0.9% NaCl or PBS) were injected into the tail vein of mice 3 minutes before MTX administration. For all experiments, mice were sacrificed at 5 or 15 min after MTX administration by terminal bleeding through cardiac puncture under isoflurane anesthesia and organs were rapidly removed. Plasma was isolated from blood samples after centrifugation at 2,100 g for 6 min at 4°C, livers were homogenized in 1% bovine serum albumin and all the samples were stored at −30°C until analysis.

After drug analysis, results were presented as concentrations in the organs (nmol/g), % of the total dose (dose corrected for the body weight of each individual mouse being equivalent to 100%) and/or organ-to-plasma ratios. Organ-to-plasma ratios were calculated by dividing

organ concentration expressed as nmol/g by plasma concentration expressed as nmol/ml, assuming 1 ml of plasma is roughly equivalent to 1 g of tissue.

**Drug analyses**

*Determination of MTX and 7-OH-MTX*

Levels of MTX and 7OH-MTX in plasma and liver homogenates were determined by HPLC-UV detection as described previously [28]. For the *in vitro* experiments, cell lysates in 0.2 N NaOH were pretreated with 1.5 M $HClO_4$ in a ratio of 1:1.6 v/v. After vortexing 5 s and centrifugation at 16,873 g for 5 min at 4°C, supernatants were injected into the HPLC system directly. Standard curve (4,4 – 2201 nM) and quality control (22.01, 220.1 and 2201 nM) samples were prepared using blank cell lysates as matrix.

*Sample pre-treatment for rifampicin and telmisartan*

Plasma and liver homogenates were thawed at room temperature and diluted 1:50 or 1:100 (for rifampicin or telmisartan determinations, respectively) in blank human plasma. A volume of 100 µl of plasma or liver homogenate was pipetted into 2 ml polypropylene vials (Eppendorf, Hamburg, Germany). Next, volumes of 50 µl of IS working solution (rifampicin-d3 or telmisartan-d3; 1 µg/ml in acetonitrile:water 30:70; v/v) and 1000 µl of ethyl acetate were added. After automatic shaking for 15 min at 480 rpm, the samples were centrifuged for 1 min at 14,000 rpm (20,000g). The aqueous layer was snap frozen in dry ice/ethanol and the upper organic layer was decanted into a 1.5 ml vial (Brand, Wertheim, Germany). The solvent was evaporated to dryness in Speed-Vac SC210A (Savant, Farmingdale, Ny, USA) and the residue was reconstituted with 100 µl of acetonitrile:water (30:70, v/v) by sonicating for 5 min and vortex-mixing for 5 s. Finally, samples were centrifuged for 5 min at 14,000 rpm (20,000 g) prior to analysis.

*Instrumentation for rifampicin and telmisartan*

The levels of rifampicin and telmisartan in plasma and liver homogenates were quantified by means of HPLC coupled to tandem mass spectrometry (HPLC-MS/MS).

The chromatographic system included a solvent rack with in-line degasser (SRD-3600, Dionex, Sunnyvale, CA, USA), a dual low-pressure gradient pump (DGP-3600A, Dionex) and an autosampler with refrigerated plate (WPS-3000TSL, Dionex). The instrument was coupled to a triple quadrupole mass spectrometer (API3000 MS/MS, ABSciex, Framingham, MA, USA) equipped with an electrospray ionization source (ABSciex). Data acquisition and analysis were performed using the Analyst v1.5.1 software package (ABSciex).

For both drugs, chromatographic separations were carried out using a stainless steel analytical Zorbax Extend C-18 column (2.1 x 100 mm) (Agilent Technologies, Palo Alto, CA, USA) at ambient temperature. The mobile phase consisted of 0.1% formic acid in water (A) and methanol (B) and was delivered at a flow rate of 0.2 ml/min in gradient elution. For rifampicin, the gradient was: 0-3 min 30-95% B; 3-5 min 95% B; 5-5.2 min 95-30% B; 5.2-13 min 30% B. For telmisartan, the gradient was: 0-2 min 40-95% B; 2-4 min 95% B; 4-4.2 min 95-40% B; 5.2-13 min 40% B. The sample compartment of the autosampler was maintained at 10ºC and the injection volumes were 50 µl and 10 µl for rifampicin and telmisartan, respectively.

Mass spectrometric analyses of both rifampicin and telmisartan were performed in positive ion mode with ionization voltage set at 5500 V and a temperature of 300ºC. Nebulizer gas and curtain gas (both nitrogen) were delivered at 12 and 8 L/min, respectively. Other ESI-MS/MS operating parameters were optimized for each drug. Declustering potential (DP), focusing potential (FP), entrance potential (EP), collision energy (CE) and collision cell exit potential (CXP) were 50 V, 200 V, 10 V, 35 V and 16 V, respectively, for rifampicin, and 60 V, 190 V, 10 V, 47 V and 16 V for telmisartan. For quantification, the multiple reaction monitoring (MRM) mode was used and the following transitions were monitored: 823.7 → 399.2 for rifampicin, 826.7 → 402.3 for rifampicin-d3 (I.S.); 515.4 → 497.4 for telmisartan, 519.4 → 501.4 for telmisartan-d3 (I.S.).

*Quantification*

The concentrations of rifampicin and telmisartan in plasma and liver homogenates were determined by means of the internal standard (I.S.) method, employing the corresponding stable isotope labeled drugs (rifampicin-d3 and telmisartan-d3).

Stock solutions of rifampicin and telmisartan were prepared in DMSO at 10 mM and stored at -20ºC. For each analytical run, these solutions were diluted in DMSO to obtain working solutions ranging from 100 nM to 100 µM) for the preparation of the above-mentioned calibration standards. A set of calibration standards in either blank plasma or liver homogenate was prepared using 100- fold dilution of the DMSO stock in blank biological matrix. Final calibration samples contained 1, 3, 10, 30, 100, 300 and 1000 nM.

**Statistical analysis**

IC50 values for rifampicin and telmisartan for inhibition of MTX uptake were determined using non-linear regression (curve fit) analysis in GraphPad Prism 6.01 software. The 2-sided Student's t-test or one-way analysis of variance (ANOVA) with post-hoc tests employing Tukey's corrections were used to determine statistical significance either between two or multiple groups, respectively. Results were presented as the mean ± standard deviation (SD). Differences were considered to be statistically significant when $p \leq 0.05$.

## RESULTS

### *In vitro* MTX uptake by OATP1A/1B transporters

In order to establish time-dependent uptake of MTX by OATP1A/1B transporters, we performed cellular uptake experiments with MTX (50 µM) using control and OATP1B1, -1B3 or -1A2-expressing HEK293 cells for various time periods between 2.5 and 120 min. The uptake of MTX by all three OATPs was significantly greater than that in control cells at all time points and remained linear until 30 min (Figure 1A-C). After 30 min, MTX uptake by all three OATPs appeared saturated to various degrees. Uptake in HEK-OATP1A2 cells was high, and that in HEK-OATP1B1 cells was intermediate. Despite low MTX uptake in OATP1B3-expressing cells (< LLOQ for control cells up to 15 min and for OATP1B3 cells at 2.5 min) which also correlated with a somewhat erratic uptake linearity, there was a clear difference between these cells and controls (Figure 1B). To stay in the linear phase of MTX uptake, 15 min time points were chosen for the subsequent inhibition studies. Furthermore, the uptake of MTX in all OATP-expressing cells

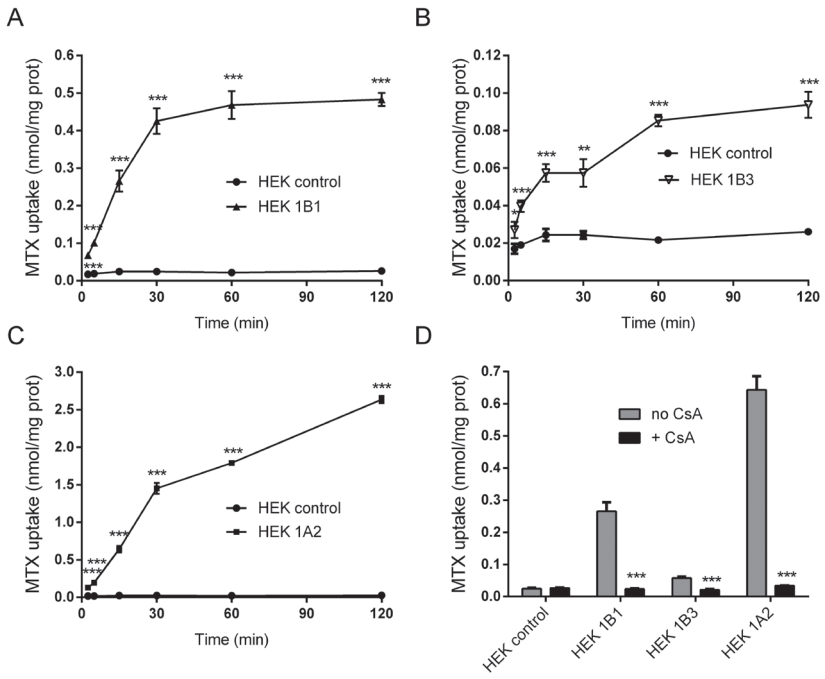


**Figure 1. Time-dependent in vitro uptake of MTX by OATP1B1 (A), OATP1B3 (B) and OATP1A2 (C), and its inhibition by CsA (D).** Uptake of 50 µM MTX was measured between 2.5 to 120 min incubation using vector-transfected (control) or OATP1B1-, OATP1B3- or OATP1A2- overexpressing HEK293 cells. Inhibition of MTX uptake by 0.5 µM Cyclosporin A (CsA), an OATP inhibitor, was assessed for 15 min. Data are given as mean ± S.D. Student's t-test was applied to compare transporter expressing cells to controls. (n = 3, *, $P < 0.05$; **, $P < 0.01$; ***, $P < 0.001$ when compared with HEK control cells).



could be inhibited completely by 0.5 µM CsA, an OATP inhibitor, at 15 min (Figure 1D), further supporting the conclusion that MTX uptake in these cells was OATP-mediated.

### Effect of rifampicin on OATP-mediated MTX uptake *in vitro*

To determine whether OATP-mediated MTX uptake could be inhibited by the OATP inhibitor rifampicin, we determined the IC50 of rifampicin for each OATP-expressing cell type using a concentration range between 1 to 100 µM. As indicated in Figure 2, IC50 concentrations of rifampicin were 0.9, 1.1 and 6.1 µM for OATP1B1, -1B3 and -1A2-mediated MTX uptake, respectively. These IC50 levels suggest that rifampicin is a fairly strong inhibitor of MTX uptake mediated by these three OATPs (strong = µM range).

### Effect of rifampicin on OATP-mediated MTX and 7-OH-MTX disposition *in vivo*

In order to investigate whether rifampicin can also inhibit OATP-mediated MTX transport *in vivo*, we administered 20 mg/kg rifampicin or vehicle (i.v.) 3 min before 10 mg/kg MTX dosing (i.v.) to WT, Oatp1a/1b knockout mice as well as to transgenic mice with liver-specific expression of OATP1B1 and -1B3 in view of their physiological relevance to human drug disposition.

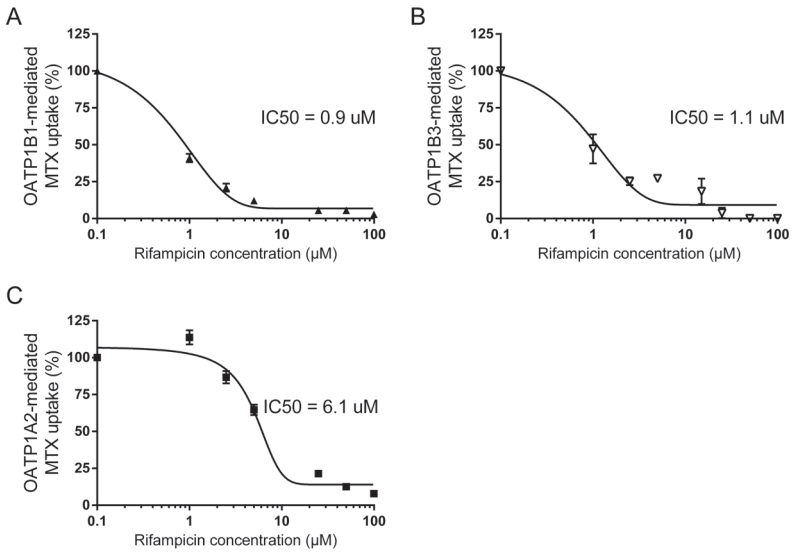


**Figure 2. Inhibition of OATP-mediated MTX uptake by rifampicin.** Inhibition of 50 μM MTX uptake by different concentrations of rifampicin (1 - 100 μM) was assessed at 15 min using OATP1B1 (A), OATP1B3 (B) or OATP1A2 (C) over expressing HEK293 cells. MTX uptake in OATP-expressing clones was not corrected for the background in the control cells. IC50 values were calculated from generated data using non-linear regression (curve fit) analysis. Data are given as mean ± S.D. (n = 3).



In groups receiving vehicle, MTX disposition results were similar to those described previously by van de Steeg *et al*. [7]. Plasma MTX levels were increased in Oatp1a/1b-/-, Oatp1a/1b-/-;1B1tg and Oatp1a/1b-/-;1B3tg mice compared to WT strains both at 5 and 15 min after MTX administration (Figure 3A and B). Liver levels of MTX and liver-to-plasma ratios were profoundly decreased by removal of the Oatp1a/1b transporters, and expression of human OATP1B1 or -1B3 in these livers led to substantial, albeit not complete, rescue of the impaired liver uptake of MTX (Figure 3), showing that MTX hepatic uptake is primarily mediated by OATPs.

In rifampicin-treated groups, plasma levels of MTX were significantly increased by 4.2-, 1.5- and 1.9-fold in WT, Oatp1a/1b-/- and Oatp1a/1b-/-;1B3tg mice 5 min after MTX administration, whereas no increase was observed in plasma of Oatp1a/1b-/-;1B1tg mice (Figure 3A). Of note, the increased plasma MTX levels in WT mice after rifampicin pretreatment reached the same levels as in vehicle-treated Oatp1a/1b-/- mice, and those in Oatp1a/1b-/-;1B3tg mice reached the same levels as rifampicin-treated Oatp1a/1b-/- mice, suggesting strong inhibition of OATP-mediated MTX uptake by rifampicin. Accordingly, rifampicin treatment led to significant decreases in liver MTX levels in all strains except the Oatp1a/1b-/- mice (Figure 3C and Supplementary Figure 1A). When corrected for plasma levels, substantial decreases were observed in liver-to-plasma ratios after rifampicin treatment. Although not reaching the level of knockout mice, WT mice showed a highly significant decrease by 8-fold ($P < 0.001$, Figure 3E), suggesting a very strong inhibiton of Oatp1a/1b-mediated hepatic uptake of MTX in this strain. Liver-to-plasma ratios of MTX in Oatp1a/1b-/-;1B1tg and Oatp1a/1b-/-;1B3tg mice were also decreased by 3.5- and 11.4-fold, respectively, and more or less

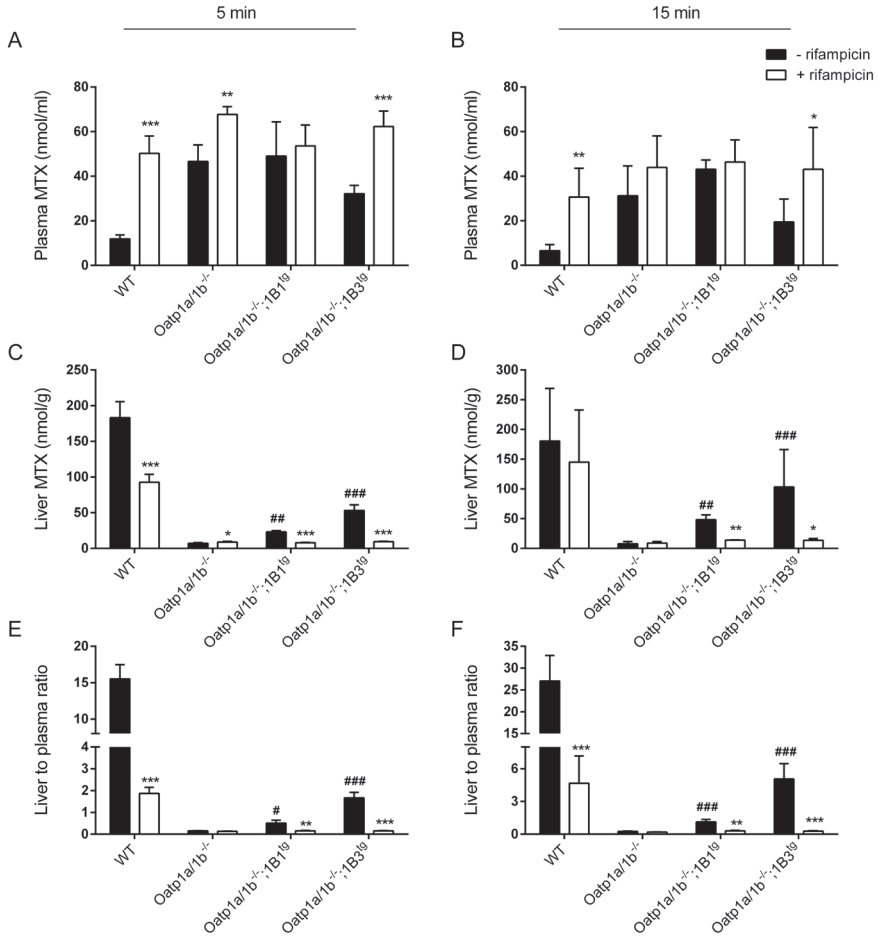


**Figure 3. Effect of rifampicin on OATP-mediated MTX disposition in male WT, Oatp1a/1b$^{-/-}$ and OATP1B1-, and OATP1B3-humanized transgenic mice.** MTX plasma concentrations in nmol/ml (A,B), liver concentrations in nmol/g (C,D) and liver-to-plasma ratios (E,F) 5 and 15 min after i.v. administration of 10 mg/kg MTX ± 20 mg/kg rifampicin are presented. Vehicle (0.9% NaCl) or rifampicin was administered i.v. 3 min before MTX dosing. Data are given as mean ± S.D. Student's t-test was applied to compare rifampicin-treated with vehicle-treated groups. (n = 4 for 5 min and n = 3 - 5 for 15 min experiments, *, $P$ < 0.05; **, $P$ < 0.01; ***, $P$ < 0.001 when compared with vehicle treatment. $^{\#}$, $P$ < 0.05; $^{\#\#}$, $P$ < 0.01; $^{\#\#\#}$, $P$ < 0.001 when compared with vehicle-treated Oatp1a/1b$^{-/-}$ mice).

back to the levels in knockout mice (Figure 3E). Furthermore, Oatp1a/1b-/- mice did not show any difference in liver-to-plasma ratios of MTX upon rifampicin treatment, indicating that the hepatic uptake of MTX that was inhibited by rifampicin was OATP-specific.

In order to assess whether the rifampicin effect also applied at a later time point, we also tested the disposition of MTX at 15 min. The disposition of MTX followed more or less the same trend as observed at 5 min, yet the plasma, but not the liver levels of MTX were overall reduced

due to distribution and clearance kinetics. Briefly, plasma levels of MTX were increased in WT (4.7-fold, $P < 0.01$) and Oatp1a/1b-/-;1B3tg (2.2-fold, $P < 0.05$) mice by rifampicin treatment but not in Oatp1a/1b-/- and Oatp1a/1b-/-;1B1tg mice (Figure 3B). Decreases in liver MTX levels were significant in Oatp1a/1b-/-;1B1tg (~3.5-fold, $P < 0.01$) and Oatp1a/1b-/-;1B3tg (~7.6-fold, $P < 0.01$) mice (Figure 3D and Supplementary Figure 1B). Liver-to-plasma ratios clearly showed that hepatic uptake of MTX was decreased highly in WT mice (5.8-fold, $P < 0.001$), substantially in Oatp1a/1b-/-;1B1tg (3.7-fold, $P < 0.01$) and profoundly in Oatp1a/1b-/-;1B3tg mice (17.9-fold, $P < 0.001$), but not in Oatp1a/1b-/- mice (Figure 3F). Overall, these results suggest that rifampicin can inhibit hepatic uptake of MTX mediated by mouse Oatp1a/1b transporters to a great extent, and uptake mediated by transgenic human OATP1B1 or 1B3 completely.

In line with the MTX data, the liver levels of the active metabolite 7-OH-MTX were decreased in WT and both transgenic strains at 5 ($P < 0.01$) and 15 min ($P < 0.01$ for transgenic mice) upon rifampicin treatment; however levels in Oatp1a/1b-/- mice did not change (Supplementary Figure 2). This is likely to reflect the hepatic availability of MTX, and is not due to changes in the expression levels of aldehyde oxidases (AOX), the enzymes required for conversion of MTX to 7-OH-MTX, since we previously showed that expression of *Aox1* and *2* were similar between all the strains [13]. These findings further support the conclusion that rifampicin inhibits the hepatic uptake of MTX mediated by OATPs, and that lower levels of the parent MTX molecule lead to reduction in the hepatic metabolism and thus lower formation of 7-OH-MTX.

**Plasma and liver levels of rifampicin**

In order to assess whether the disposition of rifampicin itself was noticeably affected by OATPs *in vivo*, we measured the levels in plasma and liver. Albeit not always significantly, rifampicin levels were increased in plasma and were decreased in liver of Oatp1a/1b-/-, Oatp1a/1b-/-;1B1tg and Oatp1a/1b-/-;1B3tg strains compared to WT mice at both 5 and 15 min (Figure 4A). The changes in plasma and liver MTX levels were similar between knockout and transgenic strains with the exception that liver levels in Oatp1a/1b-/-;1B3tg mice were significantly higher than those in Oatp1a/1b-/-;1B1tg mice (Figure 4B and D). Liver-to-plasma ratios showed significant decreases in all the strains relative to WT mice, but there were no differences between Oatp1a/1b-/- and Oatp1a/1b-/-;1B1tg or Oatp1a/1b-/-;1B3tg mice (Figure 4C). These results suggest that rifampicin can be substantially transported by mouse Oatp1a/1b transporters, but not by human OATP1B1 or -1B3 *in vivo*. The very limited differences in plasma concentration of rifampicin between the strains make it unlikely that this substantially affected the DDI experiments.

**Effect of telmisartan on OATP-mediated MTX uptake *in vitro***

Next, we assessed whether OATP-mediated MTX uptake (50 μM) could be inhibited by telmisartan *in vitro*. We used a concentration range of telmisartan between 1 to 100 μM for each OATP-expressing cell type and calulated its IC50 values for MTX uptake. IC50 concentrations of telmisartan were 6.8, 11.1 and 2.8 μM for OATP1B1, -1B3 and -1A2-mediated MTX uptake, respectively. These IC50 values were about 10-fold higher than what we had found for rifampicin for OATP1B1 and 1B3, but lower for OATP1A2. This suggests that telmisartan is a less strong inhibitor for MTX uptake mediated by the tested human OATPs occuring in the sinusoidal membrane of the human liver.

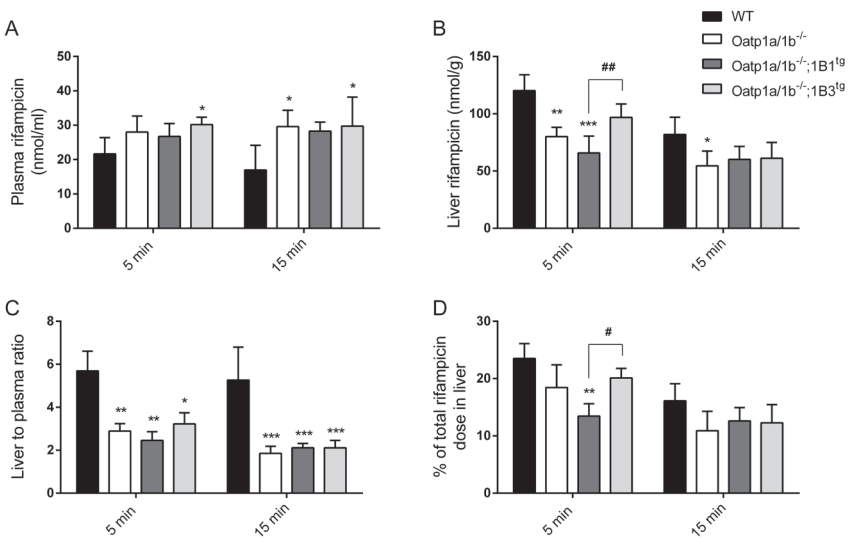


**Figure 4. Plasma and liver disposition of rifampicin in male WT, Oatp1a/1b$^{-/-}$ and OATP1B1-, and OATP1B3-humanized transgenic mice predosed with rifampicin.** Rifampicin plasma concentrations in nmol/ml (A), liver concentrations in nmol/g (B), liver-to-plasma ratios (C) and % of the total rifampicin dose in liver (D) 5 and 15 min after i.v. administration of 10 mg/kg MTX and 20 mg/kg rifampicin are presented. Data are given as mean ± S.D. One-way ANOVA was applied to compare Oatp1a/1b$^{-/-}$ and either of the transgenic strains to WT mice. (n = 4 for 5 min and n = 3 - 5 for 15 min experiments, *, $P < 0.05$; **, $P < 0.01$; ***, $P < 0.001$ when compared with WT mice and $^{\#}$, $P < 0.05$; $^{\#\#}$, $P < 0.01$ when transgenic mice were compared to each other).



### Effect of telmisartan on OATP-mediated MTX disposition *in vivo*

We initially assessed the inhibition efficacy of telmisartan on OATP-mediated MTX transport *in vivo* by predosing WT, Oatp1a/1b-/-, Oatp1a/1b-/-;1B1tg and Oatp1a/1b-/-;1B3tg mice with 7 mg/kg telmisartan or vehicle (i.v.) 3 min before 10 mg/kg MTX (i.v.) administration. 7 mg/kg telmisartan was chosen as it was the highest practically feasible dose. Higher doses were prohibited by formulation problems.

In telmisartan-treated groups, plasma levels of MTX were slightly, but significantly increased by 1.4-fold in WT and 1.3-fold in Oatp1a/1b-/- or Oatp1a/1b-/-;1B3tg mice 15 min after 10 mg/kg MTX administration (Figure 6B). MTX levels in liver were slightly increased in WT by 1.2- ($P < 0.05$) and in Oatp1a/1b-/- mice by 1.1-fold ($P < 0.01$), whereas this was decreased in Oatp1a/1b-/-;1B1tg mice by 1.5-fold ($P < 0.01$) (Figure 6D and Supplementary Figure 3B). Liver-to-plasma ratios were decreased in Oatp1a/1b-/- mice by 1.2-fold ($P < 0.05$) but in Oatp1a/1b-/-;1B1tg mice by 1.9-fold ($P < 0.001$) (Figure 6F), whereas they remained unchanged in WT and Oatp1a/1b-/-;1B3tg mice. These results suggest that the inhibitory effect of telmisartan at the plasma concentrations achieved on hepatic uptake of MTX mediated by OATPs is negligible, except for the human OATP1B1. Telmisartan does not seem to inhibit mouse Oatp1a/1b-mediated MTX transport into the liver at this plasma drug concentrations. Furthermore, a slight, but significant decrease in hepatic uptake of MTX in Oatp1a/1b-/- mice suggests a contribution of other factor(s) mediating hepatic uptake of MTX, albeit very minor, which can be inhibited by telmisartan.

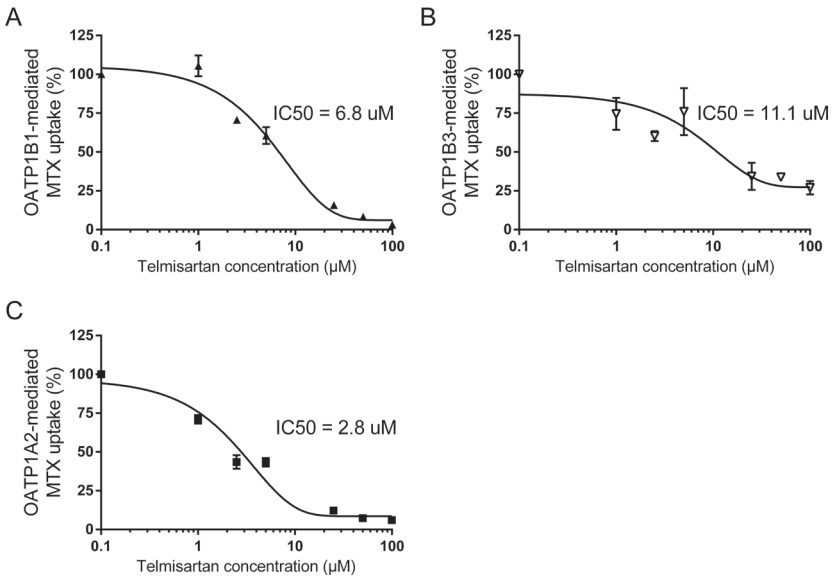


**Figure 5. Inhibition of OATP-mediated MTX uptake by telmisartan.** Inhibition of 50 μM MTX uptake by different concentrations of telmisartan (1 - 100 μM) was assessed at 15 min using OATP1B1- (A), OATP1B3- (B) or OATP1A2- (C) overexpressing HEK293 cells. MTX uptake in OATP-expressing clones was not corrected for the background in control cells. IC50 values were calculated from generated data using using non-linear regression (curve fit) analysis. Data are given as mean ± S.D. (n = 3).



In order to assess how the achieved *in vivo* telmisartan levels related to the *in vitro* IC50 values, we determined telmisartan concentrations in plasma and liver. We observed that plasma telmisartan levels were often below 10 μM in all strains, i.e. comparable to or below the IC50 concentrations (Figure 7B). As this could be a reason for the low inhibition efficacy of telmisartan for OATP-mediated MTX transport and as increasing the telmisartan dose was not technically feasible, we performed a separate experiment to assess the plasma and liver levels at an earlier time point (5 min) after the same i.v. dose of telmisartan. We assumed that telmisartan plasma levels would be higher at this earlier time point. In order to reach higher plasma levels of telmisartan, but similar MTX concentrations compared to the 15 min experiment, we lowered the MTX dose from 10 to 2 mg/kg. This experiment resulted in similar plasma concentrations of MTX in all strains, except for WT which showed a 1.4-fold increase ($P < 0.05$) upon telmisartan treatment (Figure 6A). Significant differences were observed by telmisartan treatment in liver levels of each strain (Figure 6C and Supplementary Figure 3A). However, liver-to-plasma ratios of telmisartan-treated groups were decreased compared to nontreated groups (Figure 6E). Liver-to-plasma ratios were decreased by 1.5-fold in WT ($P < 0.05$) and Oatp1a/1b-/- ($P < 0.01$) mice, and by 1.6-fold in Oatp1a/1b-/-;1B1tg ($P < 0.001$) mice when predosed with telmisartan. In addition, liver concentrations of the active metabolite 7-OH-MTX were also decreased in telmisartan-treated Oatp1a/1b-/-;1B1tg mice at 15 min, probably reflecting reduced liver availability of MTX (Supplementary Figure 4). Altogether, these results suggest that hepatic uptake of MTX mediated by human OATP1B1 is partly inhibited

by telmisartan, but this inhibition is not complete. Moreover, although minor, other transporters that can be inhibited by telmisartan may also contribute to hepatic uptake of MTX.

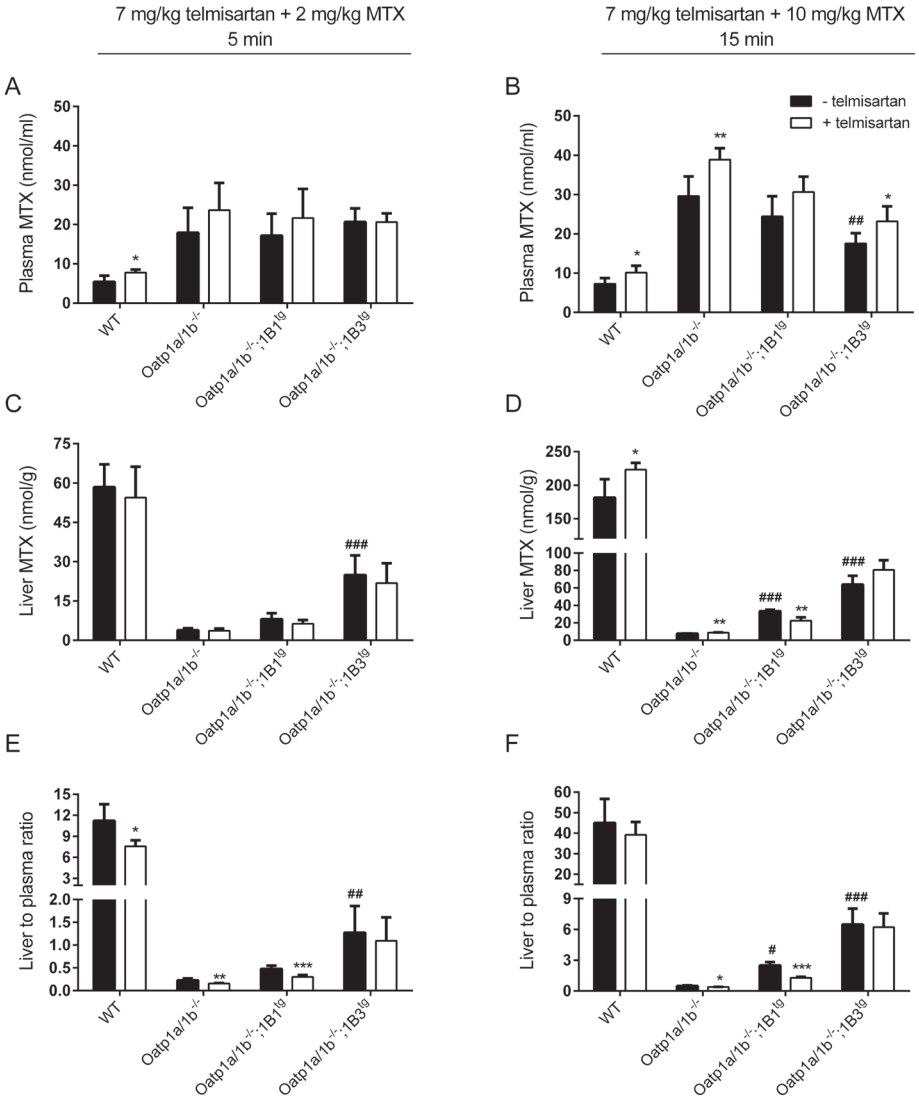


**Figure 6. Effect of telmisartan on OATP-mediated MTX disposition in male WT, Oatp1a/1b$^{-/-}$ and OATP1B1-, and OATP1B3-humanized transgenic mice.** MTX plasma concentrations in nmol/ml (A,B), liver concentrations in nmol/g (C,D) and liver-to-plasma ratios (E,F) 5 and 15 min after i.v. administration of 2 or 10 mg/kg MTX and 7 mg/kg telmisartan are presented. Vehicle (PBS) or telmisartan were administered i.v. 3 min before MTX dosing. Data are given as mean ± S.D. Student's t-test was applied to compare telmisartan-treated with vehicle-treated groups. (n = 4 - 6 for 5 min and n = 4 for 15 min experiments, *, $P < 0.05$; **, $P < 0.01$; ***, $P < 0.001$ when compared with vehicle treatment. $^{\#}$, $P < 0.05$; $^{\#\#}$, $P < 0.01$; $^{\#\#\#}$, $P < 0.001$ when compared with vehicle-treated Oatp1a/1b$^{-/-}$ mice).

**Plasma and liver levels of telmisartan**

*In vivo* assessment of telmisartan concentrations showed that plasma telmisartan levels remained similar between 5 and 15 min, suggesting very slow liver elimination of this drug. Moreover, there were no clear differences between the groups in plasma telmisartan levels at both time points, except for a 1.9-fold decrease ($P < 0.05$) in Oatp1a/1b-/- mice compared to the WT strain at 15 min (Figure 7A and B). There were also no clear differences between all strains in either liver levels or liver-to-plasma ratios of telmisartan at 5 or 15 min (Figure 7 C-H). These findings suggest that telmisartan is not a substrate of mouse Oatp1a/1b, or human OATP1B1 or OATP1B3 transporters *in vivo*.

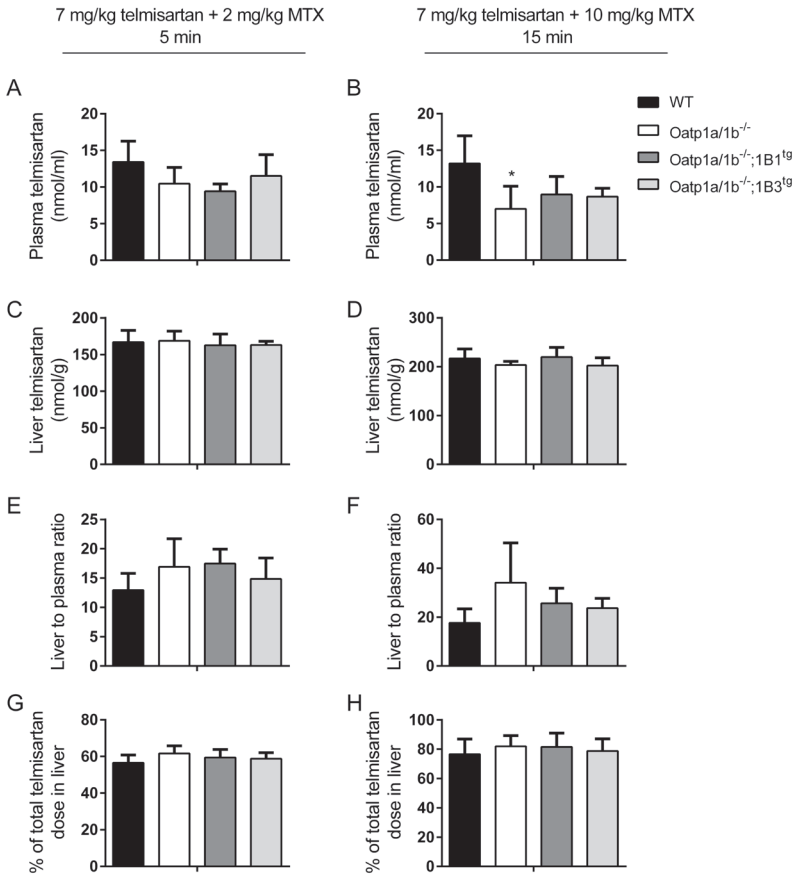


**Figure 7. Plasma and liver disposition of telmisartan in male WT, Oatp1a/1b$^{-/-}$ and OATP1B1-, and OATP1B3-humanized transgenic mice dosed with 7 mg/kg telmisartan.** Telmisartan plasma concentrations in nmol/ml (A), liver concentrations in nmol/g (B), liver-to-plasma ratios (C) and % of the total telmisartan dose in liver (D) 5 and 15 min after i.v. administration of 2 or 10 mg/kg MTX ± 7 mg/kg telmisartan are presented. Data are given as mean ± S.D. One-way ANOVA was applied to compare Oatp1a/1b$^{-/-}$ and either of the transgenic strains to WT mice. (n = 4 for 5 min and n = 3 - 5 for 15 min experiments, *, $P < 0.05$ when compared with WT mice).

## DISCUSSION

In this study, we show that transgenic mice expressing human OATP1B1 or OATP1B3 can be useful tools to assess clinically relevant DDIs that are mediated by human OATPs. We assessed the potential of these mouse models using the prototypical OATP inhibitor rifampicin as a perpetrator drug and a very good OATP substrate, the anticancer drug MTX, as a victim drug. We showed that *in vitro*, rifampicin inhibited OATP1A2-, -1B1- and -1B3-mediated MTX uptake at low μM concentrations that are easily achievable in the clinic. *In vivo*, rifampicin showed strong inhibition efficacy for mouse Oatp1a/1b and human OATP1B-mediated hepatic uptake of MTX at clinically relevant plasma concentrations. These results suggest a possible clinical DDI risk when rifampicin and MTX are coadministered and therefore illustrated that humanized OATP1B1- and OATP1B3-transgenic mice can be a useful model to study DDI *in vivo*. In addition to the existing *in vitro* and *in silico* models, these mice may provide a reliable *in vivo* method to predict clinical DDIs.

Using the abovementioned models, we tested the possibility of DDIs between a commonly used antihypertensive drug telmisartan and the anticancer drug MTX. In spite of fairly low IC50 concentrations (< 11 μM) for OATP1B1, -1B3 and -1A2 *in vitro*, telmisartan was only a weak inhibitor of human OTP1B1-mediated hepatic uptake of MTX *in vivo*. Neither mouse Oatp1a/1b nor human OATP1B3-mediated MTX transport were noticeably inhibited by telmisartan. Moreover, telmisartan was not substantially transported by any of the tested OATPs *in vivo*; thus we think that its inhibition of MTX transport is due to inhibition of OATP1B1 activity, and not related to competition with MTX in the transport process.

The slight, but significant inhibition by telmisartan of hepatic uptake of MTX in Oatp1a/1b-/- mice suggests inhibition of another alternative transporter that can transport MTX into the liver. Of course, the very low hepatic levels of MTX in non-treated Oatp1a/1b-/- mice show that the contribution of this unknown transporter is small compared to that of the Oatp1a/1b transporters. A possible candidate for this alternative transporter is the reduced folate carrier, RCF-1 (gene name: *SLC19A)*. RCF1 is known as a high capacity, bi-directional folate transporter, which can mediate transport of the antifolate drug MTX [29, 30]. Furthermore, patients with a c.80AA polymorphism in their *SLC19A1* gene were associated with the occurrence of higher serum MTX concentrations [31, 32].

The discrepancy between our *in vitro* and *in vivo* findings on the inhibitory effect of telmisartan on MTX transport via OATPs may be explained by the modest plasma telmisartan concentrations achieved, and by the available free fraction of telmisartan. It is known that free concentrations of the perpetrator drug are an important factor in DDI in addition to the inhibition capacity and specificity of the perpetrator drug for the transporter. Availability of the free drug molecule is inversely related to its plasma protein binding capacity, meaning that high plasma protein binding results in low free drug concentration. As soon as the effective free drug concentration is lower than its Km or IC50, the risk of inhibition of transporter- or enzyme-mediated processes becomes small. The plasma protein binding capacity of telmisartan is known to be very high, ~99.5% [33]. With a simple estimation, free telmisartan levels in plasma of mice in our experiments were thus only ~0.5% of the *in vitro* IC50 concentrations, explaining why there were no strong interactions observed. On the other hand, rifampicin, with ~80% plasma protein binding capacity [34], shows

comparable free drug concentrations in plasma of mice as the IC50 levels found *in vitro*. Actually, it is surprising that we could still observe a mild interaction at the OATP1B1 level with the low free telmisartan concentrations, which were far below the IC50 values.

Our findings may be a good basis for the clinic. For the rifampicin part of this study, our results suggest a risk of DDI for rifampicin and MTX via OATP1B transporters at clinically administered dosages. The plasma rifampicin levels in all of the mice strains were in a similar range with previously reported serum levels in patients who are treated for tuberculosis [35]. In addition, the plasma levels of MTX in our mice were in the same range as seen in cancer patients receiving high-dose MTX intravenously [36]. These are of particular importance, as the interaction between rifampicin and MTX mediated by both mouse and human OATP1A/1B transporters that we found in this study strongly argues that this interaction may well happen in patients receiving both of these drugs concomitantly. It should be noted though that combined administration of rifampicin (for tuberculosis treatment) and high-dose MTX (for cancer treatment) will be rare. Interactions between rifampicin and MTX at the OATP level for the lower doses of MTX should be investigated for the risk of DDI in other groups of patients receiving lower doses of MTX.

On the other hand, the telmisartan part of our study suggests that combination treatment of telmisartan and MTX is likely to be safe in patients. In the clinic, hypertension patients receive a daily dose of 40 or 80 mg telmisartan and show effective plasma exposure of ~40 to 200 nM with high intersubject variability at a steady state level [33]. On the other hand, the concentration range that we achieved in mouse plasma (7 - 13 μM) was far higher than what is achieved in the serum levels in hypertension patients treated with telmisartan. Considering the lack of substantial interactions even at relatively high telmisartan concentrations in humanized mice, we think that the risk of DDI between telmisartan and MTX at the level of hepatic OATP1B transporters in patients are low. These results are positive for the clinic, as telmisartan and MTX is a clinically realistic combination for the treatment of cancer patients who are at the same time suffering from hypertension.

Variants in the *SLCO1B* genes are found in many people around the world [37]. As these patients have altered activity of their OATP proteins, they might be more sensitive to DDIs and show drug toxicities or altered efficacy due to altered pharmacokinetics such as disposition and clearance. Therefore, extra caution should be taken when two OATP substrate or inhibitor drugs are administered to patients with polymorphic OATPs.

In conclusion, this study demonstrates the usefulness of humanized mouse strains as proper preclinical models to predict clinical DDIs mediated by OATP1B transporters. Using these preclinical models, we demonstrated that rifampicin and MTX interact at the level of hepatic OATPs, causing increased plasma and decreased liver levels of MTX at clinically relevant doses, whereas telmisartan and MTX do not show a visible risk of interaction involving OATPs at clinical dose levels.



## ACKNOWLEDGEMENTS

We thank Levi Buil for technical assistance during experimental phase, and Anita Kort and Stephanie van Hoppe for critical reading of this manuscript.

## REFERENCE LIST


1. Klaassen CD, Aleksunes LM. Xenobiotic, bile acid, and cholesterol transporters: function and regulation. Pharmac*ol Rev 2010;* 62:1-96.
2. Shitara Y, Maeda K, Ikejiri K, Yoshida K, Horie T, Sugiyama Y. Clinical significance of organic anion transporting polypeptides (OATPs) in drug disposition: their roles in the hepatic clearance and intestinal absorption. Biopha*rm Drug Dispos 2012*.
3. Durmus S, Naik J, Buil L, Wagenaar E, van TO, Schinkel AH. In vivo disposition of doxorubicin is affected by mouse Oatp1a/1b and human OATP1A/1B transporters. Int J *Cancer 2014*.
4. Iusuf D, Sparidans RW, van Esch A, Hobbs M, Kenworthy KE, van de Steeg E et al. *Organi*c anion-transporting polypeptides 1a/1b control the hepatic uptake of pravastatin in mice. Mol Ph*arm 2012;* 9:2497-2504.
5. Iusuf D, Hendrikx JJ, van EA, van de Steeg E, Wagenaar E, Rosing H et al. *Human* OATP1B1, OATP1B3 and OATP1A2 can mediate the in vivo uptake and clearance of docetaxel. Int J *Cancer 2014*.
6. van de Steeg E, Wagenaar E, van der Kruijssen CM, Burggraaff JE, de Waart DR, Elferink RP et al. *Organi*c anion transporting polypeptide 1a/1b-knockout mice provide insights into hepatic handling of bilirubin, bile acids, and drugs. J Clin *Invest 2010;* 120:2942-2952.
7. van de Steeg E, van Esch A, Wagenaar E, Kenworthy KE, Schinkel AH. Influence of human OATP1B1, OATP1B3, and OATP1A2 on the pharmacokinetics of methotrexate and paclitaxel in humanized transgenic mice. Clin C*ancer Res 2013;* 19:821-832.
8. Ieiri I, Higuchi S, Sugiyama Y. Genetic polymorphisms of uptake (OATP1B1, 1B3) and efflux (MRP2, BCRP) transporters: implications for inter-individual differences in the pharmacokinetics and pharmacodynamics of statins and other clinically relevant drugs. Expert *Opin Drug Metab Toxicol 2009;* 5:703-729.
9. Kalliokoski A, Niemi M. Impact of OATP transporters on pharmacokinetics. Br J P*harmacol 2009;* 158:693-705.
10. Yoshida K, Maeda K, Sugiyama Y. Transporter-mediated drug--drug interactions involving OATP substrates: predictions based on in vitro inhibition studies. Clin Ph*armacol Ther 2012;* 91:1053-1064.
11. Takane H, Kawamoto K, Sasaki T, Moriki K, Moriki K, Kitano H et al. *Life*-threatening toxicities in a patient with UGT1A1*6/*28 and SLCO1B1*15/*15 genotypes after irinotecan-based chemotherapy. Cancer *Chemother Pharmacol 2009;* 63:1165-1169.
12. Trevino LR, Shimasaki N, Yang W, Panetta JC, Cheng C, Pei D et al. *Germli*ne genetic variation in an organic anion transporter polypeptide associated with methotrexate pharmacokinetics and clinical effects. J Clin *Oncol 2009;* 27:5972-5978.
13. van de Steeg E, Stranecky V, Hartmannova H, Noskova L, Hrebicek M, Wagenaar E et al. *Comple*te OATP1B1 and OATP1B3 deficiency causes human Rotor syndrome by interrupting conjugated bilirubin reuptake into the liver. J Clin *Invest 2012;* 122:519-528.
14. Giacomini KM, Huang SM, Tweedie DJ, Benet LZ, Brouwer KL, Chu X et al. *Membra*ne transporters in drug development. Nat Rev *Drug Discov 2010;* 9:215-236.
15. Prueksaritanont T, Chu X, Gibson C, Cui D, Yee KL, Ballard J et al. *Drug-d*rug interaction studies: regulatory guidance and an industry perspective. AAPS J *2013;* 15:629-645.
16. Hu S, Mathijssen RH, de BP, Baker SD, Sparreboom A. Inhibition of OATP1B1 by tyrosine kinase inhibitors: in vitro-in vivo correlations. Br J C*ancer 2014;* 110:894-898.
17. Nieuweboer AJ, Hu S, Gui C, Hagenbuch B, Ghobadi Moghaddam-Helmantel IM, Gibson AA et al. *Influ*ence of Drug Formulation on OATP1B-Mediated Transport of Paclitaxel. Cancer *Res 2014;* 74:3137-3145.
18. Hirano M, Maeda K, Shitara Y, Sugiyama Y. Drug-drug interaction between pitavastatin and various drugs via OATP1B1. Drug Me*tab Dispos 2006;* 34:1229-1236.
19. Karlgren M, Ahlin G, Bergstrom CA, Svensson R, Palm J, Artursson P. In vitro and in silico strategies to identify OATP1B1 inhibitors and predict clinical drug-drug interactions. Pharm R*es 2012;* 29:411-426.
20. Kindla J, Muller F, Mieth M, Fromm MF, Konig J. Influence of non-steroidal anti-inflammatory drugs on organic anion transporting polypeptide (OATP) 1B1- and OATP1B3-mediated drug transport. Drug Me*tab Dispos 2011;* 39:1047-1053.
21. Noe J, Portmann R, Brun ME, Funk C. Substrate-dependent drug-drug interactions between gemfibrozil, fluvastatin and other organic anion-transporting peptide (OATP) substrates on OATP1B1, OATP2B1, and OATP1B3. Drug Me*tab Dispos 2007;* 35:1308-1314.
22. Yoshida K, Maeda K, Sugiyama Y. Transporter-mediated drug--drug interactions involving OATP substrates: predictions based on in vitro

inhibition studies. Clin Pharmacol Ther 2012; 91:1053-1064.

23. Chang JH, Ly J, Plise E, Zhang X, Messick K, Wright M et al. Differential Effects of Rifampin and Ketoconazole on the Blood and Liver Concentration of Atorvastatin in Wild-Type and Cyp3a and Oatp1a/b Knockout Mice. Drug Metab Dispos 2014; 42:1067-1073.
24. Chu X, Bleasby K, Evers R. Species differences in drug transporters and implications for translating preclinical findings to humans. Expert Opin Drug Metab Toxicol 2012.
25. Grime K, Paine SW. Species differences in biliary clearance and possible relevance of hepatic uptake and efflux transporters involvement. Drug Metab Dispos 2013; 41:372-378.
26. Peters J, Eggers K, Oswald S, Block W, Lutjohann D, Lammer M et al. Clarithromycin is absorbed by an intestinal uptake mechanism that is sensitive to major inhibition by rifampicin: results of a short-term drug interaction study in foals. Drug Metab Dispos 2012; 40:522-528.
27. Hirano M, Maeda K, Shitara Y, Sugiyama Y. Contribution of OATP2 (OATP1B1) and OATP8 (OATP1B3) to the hepatic uptake of pitavastatin in humans. J Pharmacol Exp Ther 2004; 311:139-146.
28. van TO, van der Woude HR, Beijnen JH, van Beers CJ, Nooyen WJ. Stable and sensitive method for the simultaneous determination of N5-methyltetrahydrofolate, leucovorin, methotrexate and 7-hydroxymethotrexate in biological fluids. J Chromatogr 1989; 488:379-388.
29. Ganapathy V, Smith SB, Prasad PD. SLC19: the folate/thiamine transporter family. Pflugers Arch 2004; 447:641-646.
30. Zhao R, Diop-Bove N, Visentin M, Goldman ID. Mechanisms of membrane transport of folates into cells and across epithelia. Annu Rev Nutr 2011; 31:177-201.
31. Dervieux T, Furst D, Lein DO, Capps R, Smith K, Walsh M et al. Polyglutamation of methotrexate with common polymorphisms in reduced folate carrier, aminoimidazole carboxamide ribonucleotide transformylase, and thymidylate synthase are associated with methotrexate effects in rheumatoid arthritis. Arthritis Rheum 2004; 50:2766-2774.
32. Laverdiere C, Chiasson S, Costea I, Moghrabi A, Krajinovic M. Polymorphism G80A in the reduced folate carrier gene and its relationship to methotrexate plasma levels and outcome of childhood acute lymphoblastic leukemia. Blood 2002; 100:3832-3834.
33. Stangier J, Su CA, Roth W. Pharmacokinetics of orally and intravenously administered telmisartan in healthy young and elderly volunteers and in hypertensive patients. J Int Med Res 2000; 28:149-167.
34. Acocella G. Clinical pharmacokinetics of rifampicin. Clin Pharmacokinet 1978; 3:108-127.
35. van IJ, Aarnoutse RE, Donald PR, Diacon AH, Dawson R, Plemper van BG et al. Why Do We Use 600 mg of Rifampicin in Tuberculosis Treatment? Clin Infect Dis 2011; 52:e194-e199.
36. Holmboe L, Andersen AM, Morkrid L, Slordal L, Hall KS. High dose methotrexate chemotherapy: pharmacokinetics, folate and toxicity in osteosarcoma patients. Br J Clin Pharmacol 2012; 73:106-114.
37. Nakanishi T, Tamai I. Genetic polymorphisms of OATP transporters and their impact on intestinal absorption and hepatic disposition of drugs. Drug Metab Pharmacokinet 2012; 27:106-121.

## SUPPLEMENTARY MATERIALS

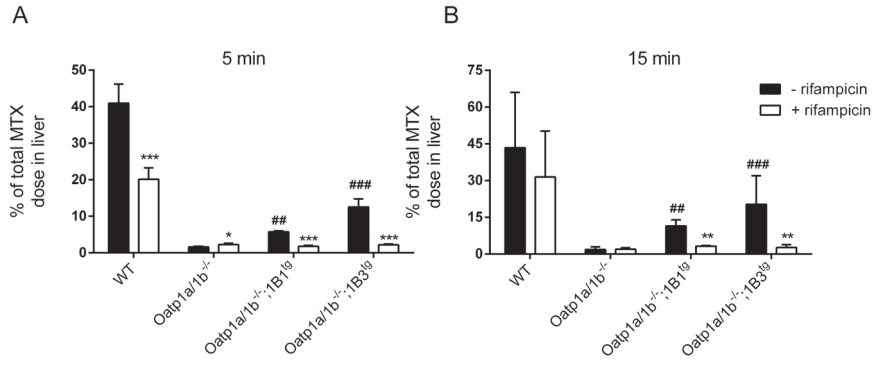


**Supplementary Figure 1. Effect of rifampicin on OATP-mediated MTX disposition in male WT, Oatp1a/1b$^{-/-}$ and OATP1B1-, and OATP1B3-humanized transgenic mice.** % of the total MTX dose in liver 5 (A) and 15 (B) min after i.v. administration of 10 mg/kg MTX ± 20 mg/kg rifampicin are presented. Data are given as mean ± S.D. Student's t-test was applied to compare telmisartan-treated with vehicle-treated groups. (n = 4, *, $P < 0.05$; ** when compared with vehicle treatment. $^{\#}$, $P < 0.05$; $^{\#\#}$, $P < 0.01$; $^{\#\#\#}$, $P < 0.001$ when compared with vehicle-treated Oatp1a/1b$^{-/-}$ mice).

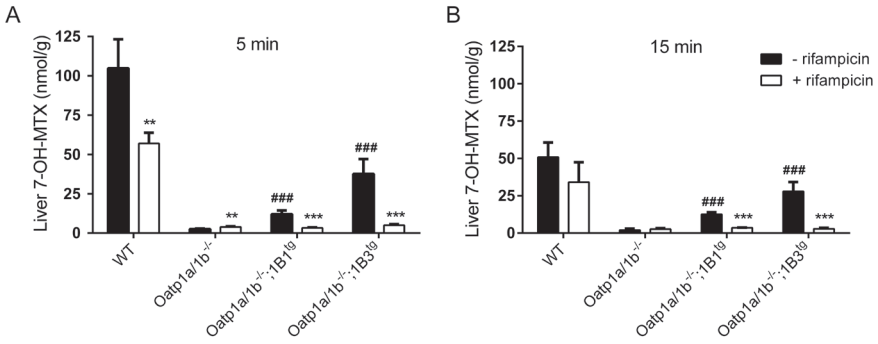


**Supplementary Figure 2. Effect of rifampicin on liver levels of 7-OH-MTX in male WT, Oatp1a/1b$^{-/-}$ and OATP1B1-, and OATP1B3-humanized transgenic mice.** 7-OH-MTX liver concentrations in nmol/g 5 (A) and 15 (B) min after i.v. administration of 10 mg/kg MTX ± 20 mg/kg rifampicin are presented. Vehicle (0.9% NaCl) or rifampicin was administered i.v. 3 min before MTX dosing. Data are given as mean ± S.D. Student's t-test was applied to compare rifampicin-treated with vehicle-treated groups. (n = 4 for 5 min and n = 3 - 5 for 15 min experiments, **, $P < 0.01$; ***, $P < 0.001$ when compared with vehicle treatment. $^{\#}$, $P < 0.05$; $^{\#\#}$, $P < 0.01$; $^{\#\#\#}$, $P < 0.001$ when compared with vehicle-treated Oatp1a/1b$^{-/-}$ mice).

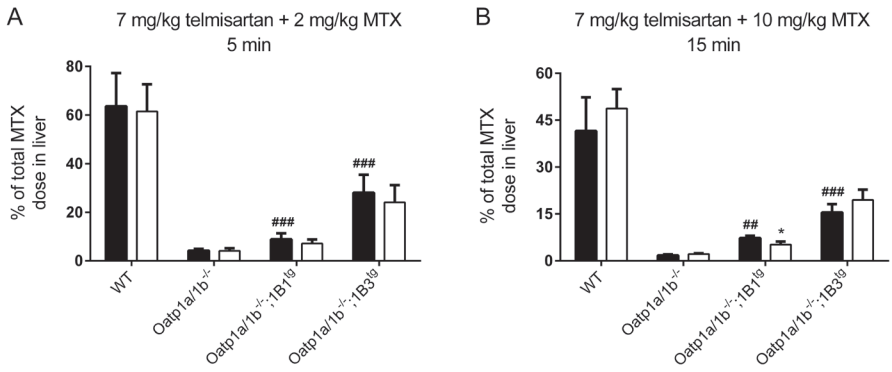


**Supplementary Figure 3. Effect of telmisartan on OATP-mediated MTX disposition in male WT, Oatp1a/1b$^{-/-}$ and OATP1B1-, and OATP1B3-humanized transgenic mice.** % of the total MTX dose in liver 5 (A) and 15 (B) min after i.v. administration of 2 or 10 mg/kg MTX ± 7 mg/kg telmisartan are presented. Data are given as mean ± S.D. Student's t-test was applied to compare telmisartan-treated with vehicle-treated groups. (n = 4, *, $P < 0.05$; ** when compared with vehicle treatment. #, $P < 0.05$; ##, $P < 0.01$; ###, $P < 0.001$ when compared with vehicle-treated Oatp1a/1b$^{-/-}$ mice).

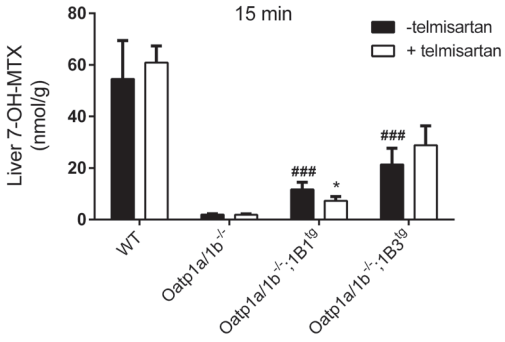


**Supplementary Figure 4. Effect of telmisartan on liver levels of 7-OH-MTX in male WT, Oatp1a/1b$^{-/-}$ and OATP1B1-, and OATP1B3-humanized transgenic mice.** 7-OH-MTX liver concentrations in nmol/g 15 min after i.v. administration of 10 mg/kg MTX ± 7 mg/kg telmisartan are presented. Vehicle (PBS) or telmisartan were administered i.v. 3 min before MTX dosing. Data are given as mean ± S.D. Student's t-test was applied to compare telmisartan-treated with vehicle-treated groups. (n = 4, *, $P < 0.05$; ** when compared with vehicle treatment. #, $P < 0.05$; ##, $P < 0.01$; ###, $P < 0.001$ when compared with vehicle-treated Oatp1a/1b$^{-/-}$ mice).

# CHAPTER 5

## HEPATOCYTE HOPPING OF EXOGENOUS COMPOUNDS

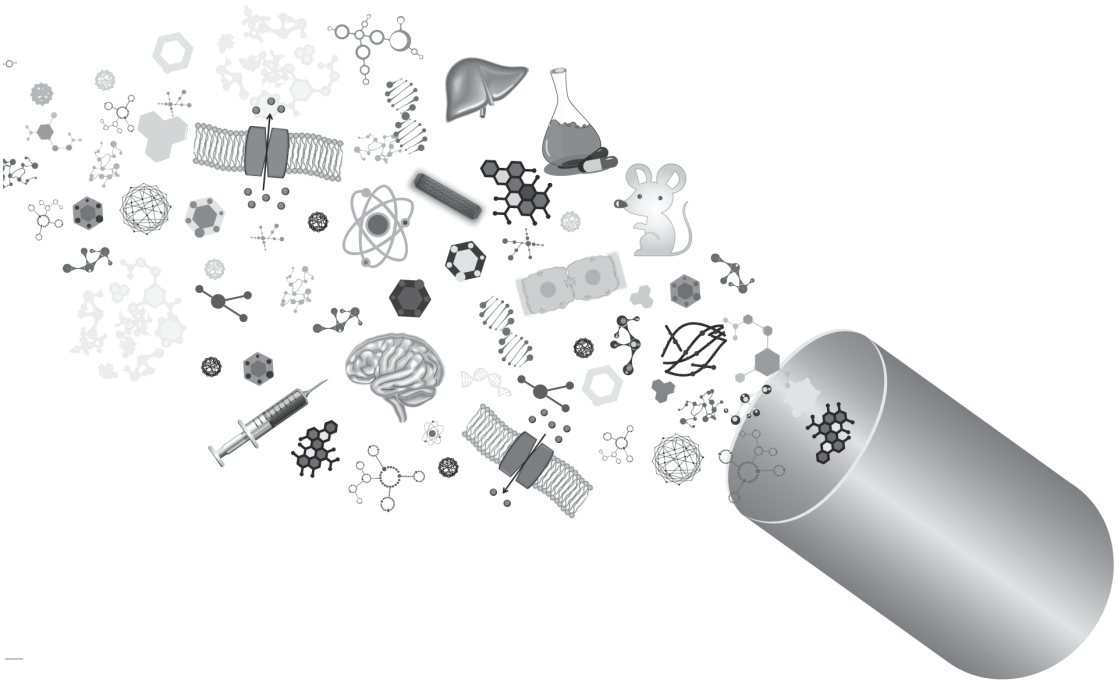

# CHAPTER 5.1

## SLCO1A/1B AND ABCC3 CONTRIBUTE TO HEPATOCYTE HOPPING OF SORAFENIB GLUCURONIDE

Selvi Durmus[1], Aksana Vasilyeva[2], Lie Li[2], Els Wagenaar[1], Sharyn Baker[2], Alfred H. Schinkel[1]

[1]Division of Molecular Oncology, the Netherlands Cancer Institute, Amsterdam, the Netherlands,
[2]Department of Pharmaceutical Sciences, St. Jude Children's Research Hospital, Memphis, USA

*In preparation*

## ABSTRACT

Recently, an efficient liver detoxification process dubbed 'hepatocyte hopping' was proposed based on findings with an endogenous substrate, bilirubin glucuronide (BG). According to this model, hepatocytic BG can follow a liver-to-blood shuttling loop via Abcc3 transporter-mediated efflux and subsequent Slco1a/1b-mediated liver uptake. Compounds taken up, possibly conjugated, and accumulating in an upstream hepatocyte can 'hop' to a downstream hepatocyte via this sinusoidal liver-to-blood shuttle. This process reduces the risk of saturation of detoxifying metabolic or hepatobiliary excretion capacity of the upstream hepatocytes in the liver lobule. We here tested whether conjugates of exogenous compounds like drugs can also undergo the hepatocyte hopping process, analyzing glucuronide conjugates of the anti-cancer drug sorafenib. Using various knockout mouse models, we showed that sorafenib glucuronide can be substantially extruded from hepatocytes into the blood circulation by Abcc3, but also by other unknown sinusoidal efflux transporters and that it can be taken up efficiently again into hepatocytes by Slco1a/1b transporters. This liver-to-blood shuttling of sorafenib glucuronide through Slco1a/1b and Abcc3 occurred even in the presence of very efficient, Abcc2-mediated biliary excretion. In the absence of Abcc2 activity, the role of Abcc3 was not clearly demonstrable anymore, presumably due to saturation of Abcc3 and functional takeover by the other sinusoidal efflux transporter(s), since impaired biliary excretion led to extremely high plasma levels of sorafenib glucuronide. In conclusion, we here demonstrate for the first time that hepatic detoxification of a glucuronide conjugate of an exogenous compound and drug is subject to hepatocyte hopping. These findings imply a much broader relevance of the hepatocyte hopping process for detoxification of drugs and other compounds conjugated in the liver.

## INTRODUCTION

The liver is the major elimination site for a broad range of endogenous and exogenous compounds including drugs, generally involving metabolism and biliary excretion. There are several uptake and efflux transporters in the liver that contribute to this disposition and clearance of such compounds. These hepatic transporters can play a vital role in the pharmacokinetics, toxicity and efficacy of their substrate drugs.

Organic anion-transporting polypeptides (OATP/Oatp; genes: *SLCO/Slco*) are important sodium-independent drug uptake transporters that can transport a wide range of endogenous substrates including bile acids, steroid and thyroid hormones and bilirubin glucuronide, but also many exogenous substrates including many drugs and toxins and their conjugates [1-3]. Mouse Oatp1a/1b and human OATP1B1 and -1B3 transporters are prominently expressed in the sinusoidal (basolateral) membrane of the hepatocytes where they can mediate hepatic uptake of many of the above-mentioned compounds [4-6].

Several polymorphisms found in the OATP1B1 gene have been shown to be clinically important, as they cause decreased transport activity and hence altered plasma and tissue distribution of a wide range of drug substrates (pravastatin, valsartan, methotrexate and SN-38), leading to a high risk for toxicities [7-10]. Moreover, we recently showed that a full deficiency in the OATP1B1 and OATP1B3 genes causes Rotor syndrome, a disorder mainly characterized by conjugated hyperbilirubinemia [11].

ABC transporters are important efflux transporters expressed in either the apical or the basolateral membrane of hepatocytes [12]. ABCC2, ABCG2 and ABCB1 are important apically located transporters, mediating biliary excretion of a wide range of endogenous and exogenous substrates [13-15]. Hepatic ABCC3 and ABCC4 are basolaterally located transporters, mediating transport of their substrates from hepatocytes into the systemic circulation [14].

Under normal physiological conditions, substrates of OATP1B1 and -1B3 are taken up into the hepatocytes, where they often undergo conjugation via glucuronidation, sulfation, or glutathionylation and get subsequently eliminated via excretion into the bile, mostly by ABCC2 and ABCG2 or other canalicular efflux transporters. However, there may also be secretion back into the systemic circulation, for instance by ABCC3 [16]. There is an extensive overlap in the substrates of OATP and ABC transporters, which includes bilirubin glucuronides (BGs) [17, 18]. We recently showed in mice that Slco1a/1b transporters work together with the basolaterally located efflux transporter Abcc3 to mediate substantial hepatic secretion and subsequent reuptake of bilirubin glucuronide into hepatocytes and called this phenomenon 'hepatocyte hopping' [16, 19]. We demonstrated that not only under pathological, but also normal physiological conditions, a substantial amount of the hepatocyte bilirubin monoglucuronide (BMG) is not immediately excreted into the bile, but transported back into the blood by Abcc3. This BMG is then efficiently taken up again in downstream hepatocytes by Slco1a/1b activity, affording another chance of being excreted into bile (illustrated in Figure 1). This liver-to-blood shuttling loop allows management of situations in which the biliary excretion in upstream hepatocytes is saturated, for example by bilirubin overload or incidental Abcc2 inhibition. With this efficient and flexible process, BG can then be easily transferred to downstream hepatocytes via Abcc3-mediated secretion and Slco1a/1b-mediated reuptake and then get eliminated by

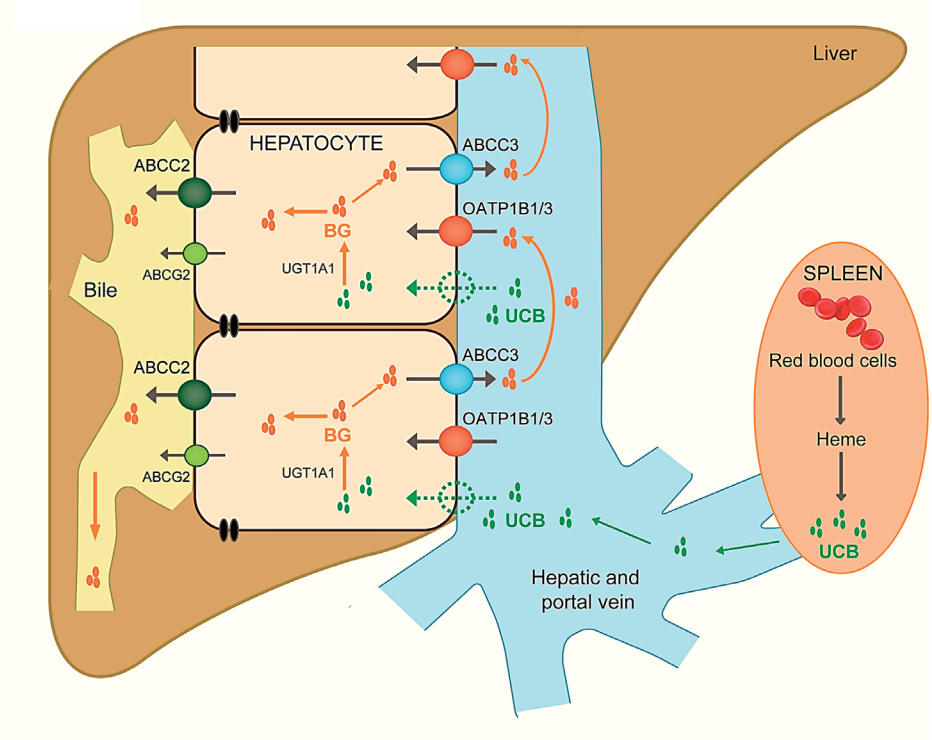


**Figure 1. Hepatocyte hopping of bilirubin glucuronide.** Unconjugated bilirubin (UCB) is formed in the spleen as a degradation product of heme resulting from spent red blood cells, and then travels (tightly bound to albumin) to the liver via the hepatic artery and portal vein. In the liver, UCB enters the hepatocytes via passive diffusion and/or incompletely defined transporters. After conjugation with glucuronic acid by (UDP)-glucuronosyltransferase 1A1 to bilirubin glucuronides (BGs), BGs are secreted into the bile. This secretion is mediated mainly by ATP binding cassette (ABC) transporter ABCC2, although ABCG2 can also contribute to this process. Under physiological conditions, a substantial fraction of the intracellular BGs is secreted by ABCC3 to the blood, from where they can be taken up again into downstream hepatocytes via organic anion–transporting polypeptides (OATP)1B1 and OATP1B3 (Oatp1a and Oatp1b in mice). This secretion-and-reuptake loop may prevent the saturation of biliary excretion in the upstream hepatocytes, thereby ensuring efficient biliary elimination and hepatocyte detoxification. It is likely that an analogous process applies for many of the drugs conjugated in the liver. The figure and the explanation is taken from Iusuf *et al.*, Clinical Pharmacology & Therapeutics (2012); 92 5, 559–562.

excretion into bile safely, instead of being trapped in the upstream hepatocytes. Thus, a more evenly distributed biliary excretion of substrates over the entire liver lobule can be achieved, leading to a more flexible and safer hepatic detoxification of the substrates.

This hepatocyte-hopping process likely applies equally in humans through OATP1B1 and -1B3 (and ABCC3), as Rotor patients with full deficiency in the genes of both uptake transporters show highly increased conjugated bilirubin levels in their serum [11]. Accumulation of glucuronidated compounds in hepatocytes may pose a substantial hepatic toxicity risk [20]. Albeit demonstrated so far only for an endogenous substrate, BG, based on the broad substrate specificity of the

transporters involved, we foresee that many drugs and their conjugates will be subject to the same hepatocyte hopping process, thus allowing more efficient hepatic detoxification. We wanted to test this hypothesis also with a drug substrate, sorafenib glucuronide, a conjugated metabolite of the anti-cancer drug sorafenib. Sorafenib glucuronide was recently shown to be a transported substrate of OATP1B transporters [21]. Moreover, Vasilyeva and coworkers recently established that Abcc2 is most likely an essential player in the biliary excretion of sorafenib glucuronide, with Abcc2 deficiency in mice resulting in dramatically increased plasma levels of this metabolite (*in preparation*). In the current study we assessed whether, analogous to the situation for BG, the hepatocyte hopping process also applies for sorafenib glucuronide which is primarily formed in the liver [21]. For this purpose, we used single and combination knockout mouse models for the most important liver transporters involved in this process.

## MATERIALS AND METHODS

### Chemicals

Sorafenib tosylate was purchased from Sequoia Research Products (Berkshire, UK).

### Animals

Mice were housed and handled according to institutional guidelines complying with Dutch legislation. Male WT, *Slco1a/1b(-/-), Slco1a/1b;Abcc2(-/-), Slco1a/1b;Abcc3(-/-), Slco1a/1b;Abcc2(-/-); Abcc3(-/-), Abcc4(-/-) and Abcc3;Abcc4(-/-),* all of a >99% FVB genetic background, were used between 8 and 14 weeks of age. Animals were kept in a temperature-controlled environment with a 12 h light / 12 h dark cycle and received a standard diet (AM-II, Hope Farms) and acidified water *ad libitum*.

### Real-Time-PCR Analysis

RNA isolation from mouse livers, subsequent cDNA synthesis, and real-time (RT)-PCR using specific primers (QIAGEN, Hilden, Germany) for various mouse drug transporters were performed as described previously [22].

### Drug solutions

Sorafenib was administered orally at 10 mg/kg body weight. First, 8 mg/ml sorafenib was dissolved in 1:1 Cremophor EL and absolute EtOH (v/v) mixture. In order to reach 8 mg pure sorafenib, 10.96 mg sorafenib tosylate was dissolved in each ml of solution (Mw sorafenib tosylate / Mw sorafenib = 1.37). A clear sorafenib solution was achieved after incubation at 60°C for ~5 min and 10 min of sonication. 8 mg/ml solution was then diluted 4 times in water to yield a concentration of 2 mg/ml and administered to mice orally using a volume of 5 µl/g body weight. The injection and 4x stock solutions were prepared freshly on the day of experiment and/or the day before, respectively.

### Plasma and organ pharmacokinetic experiments

Mice were fasted about 2-3 h before sorafenib was orally administered in order to minimize the variation in absorption. For plasma pharmacokinetic studies, multiple blood samples (50 µl) were collected from the tail vein at 0.25, 0.5, 1, 2 and 4 h using heparinized capillary

tubes (Sarstedt, Germany). At 2 (in a separate experiment) or 8 h, mice were anesthetized with isoflurane and heparin-blood samples were collected via cardiac puncture. Mice were sacrificed immediately thereafter by cervical dislocation, and livers and a set of organs were rapidly removed. Organs were homogenized on ice using water or 1% bovine serum albumin, and stored at -30°C until analysis. Blood samples were centrifuged at 2,100 g for 6 min at 4°C immediately after collection; the plasma fraction was collected and stored at -30°C until analysis. After LC-MS analyses, results are presented as concentrations in the organs (nmol/g), % of the total dose (with 5 mg/kg dose corrected for the body weight of each individual mouse being equivalent to 100%), and/or liver-to-plasma ratios. Liver-to-plasma ratios are calculated by dividing organ concentration expressed as nmol/g by plasma concentration expressed as nmol/ml, assuming 1 µl of plasma is roughly equivalent to 1 µg of tissue.

### Drug analysis

Sorafenib and sorafenib glucuronide concentrations in plasma samples and organ homogenates were analyzed using a sensitive and specific liquid chromatography coupled with tandem mass spectrometry (LC-MS/MS) assay as described previously [21]. 10 µL of plasma was extracted with 60 µL acetonitrile containing internal standards. Liver was homogenized with 10 times volume of water or 1% BSA and 20 µL homogenate was extracted with 80 µL acetonitrile containing internal standards. Samples were centrifuged as above, and 2 µL supernatant was injected for analysis. Calibrators and QCs were made using blank plasma or liver homogenate from the same mouse strains in which the pharmacokinetic studies were conducted. The measured concentration range of sorafenib was between 0.02 and 25.1 nmol/ml, and that of sorafenib N-oxide and sorafenib glucuronide was between 0.016 and 7.8 nmol/ml.



### Pharmacokinetic calculations and statistical analysis

Pharmacokinetic parameters were calculated by non-compartmental methods using the software package PK Solutions 2.0.2 (Summit Research Services, Ashland, OH). The area under the plasma concentration-time curve was calculated using the trapezoidal rule, without extrapolating to infinity. Student's t-test or one-way analysis of variance (ANOVA) was used to determine significance of differences between two or more groups, respectively. After ANOVA, post-hoc tests with Tukey correction were performed for comparison between individual groups. When variances were not homogeneous, data were log-transformed before statistical tests were applied. Differences were considered statistically significant when $P < 0.05$. Data are presented as means ± SD.

## RESULTS

### Disposition of parent sorafenib in knockout mouse strains

Oral sorafenib pharmacokinetics was tested in WT, Slco1a/1b(-/-), Slco1a/1b;Abcc2(-/-), Slco1a/1b;Abcc3(-/-), Slco1a/1b;Abcc2;Abcc3(-/-), Abcc3(-/-), Abcc4(-/-) and Abcc3;Abcc4(-/-) mice. Plasma exposure of sorafenib over 8 h was not significantly altered in any of the strains (Figure 2A and B). When plasma exposure of parent sorafenib was highest ($T_{max}$ = 2 h), liver levels of sorafenib were similar between all Slco1a/1b-related knockouts and WT strains (Figure 2C)

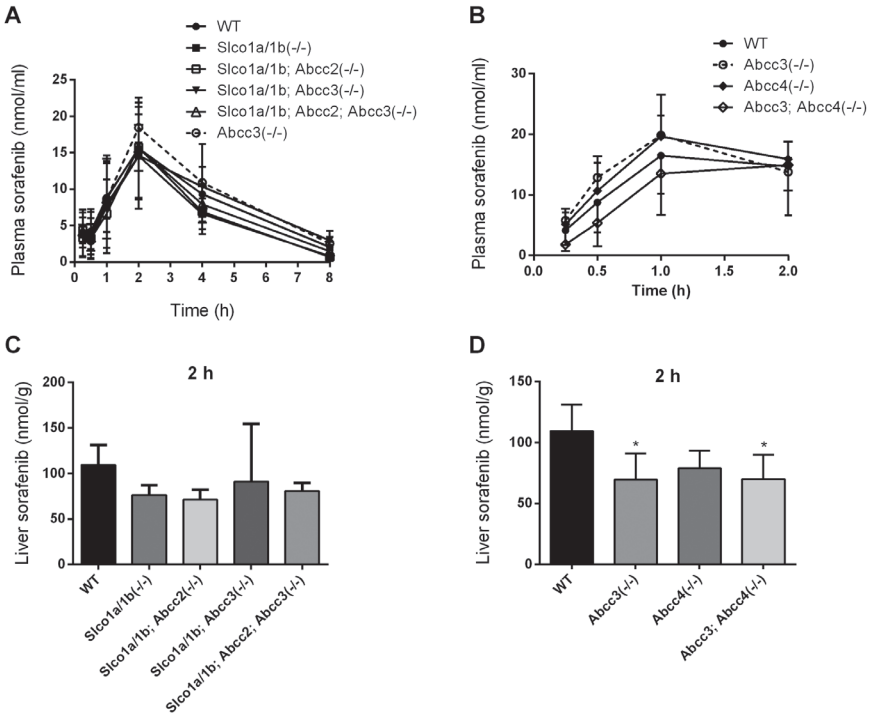


**Figure 2. Plasma and liver levels of sorafenib in male WT, Slco1a/1b(-/-), Slco1a/1b;Abcc2(-/-), Slco1a/1b;Abcc3(-/-), Slco1a/1b;Abcc2;Abcc3(-/-), Abcc3(-/-), Abcc4(-/-) and Abcc3,Abcc4(-/-) mice after oral administration of 10 mg/kg sorafenib.** Sorafenib plasma concentrations as nmol/ml (A and B) and liver concentrations as nmol/g (C and D) are represented in the graphs. Average liver-to-plasma ratios were calculated from individual mouse data. Data are given as mean ± S.D. One-way ANOVA was applied to calculate the statistical significance, unless stated otherwise. (n = 4-9, *, $P < 0.05$; **, $P < 0.01$; ***, $P < 0.001$ when compared with WT).

whereas they were slightly lower in Abcc3-related knockouts compared to WT mice (Figure 2D). These findings indicate that the differences between the strains were marginal for plasma and liver sorafenib levels, suggesting that changes in parent sorafenib levels are unlikely to be a confounder for the interpretation of the sorafenib glucuronide experiments.

### Slco1a/1b (*Slco1a/1b*) and Abcc3 transporters work together to eliminate sorafenib glucuronide from liver

As shown previously [21], the impact of Slco1a/1b transporters on the disposition of sorafenib glucuronide was far higher than that for sorafenib. Absence of the Slco1a/1b transporters resulted in a 60.2-fold increase in the plasma $AUC_{0-8}$ of sorafenib glucuronide relative to that in WT mice (20.1 ± 7.8 and 0.34 ± 0.06 nmol/ml•h, respectively, $P < 0.001$) (Figure 3A). Importantly, this increase was partially reversed by 1.9-fold in Slco1a/1b;Abcc3(-/-) mice ($AUC_{0-8}$: 10.7 ± 3.9 nmol/ml•h, $P <$ 0.05), suggesting that Abcc3 activity contributed substantially to the plasma increase of sorafenib

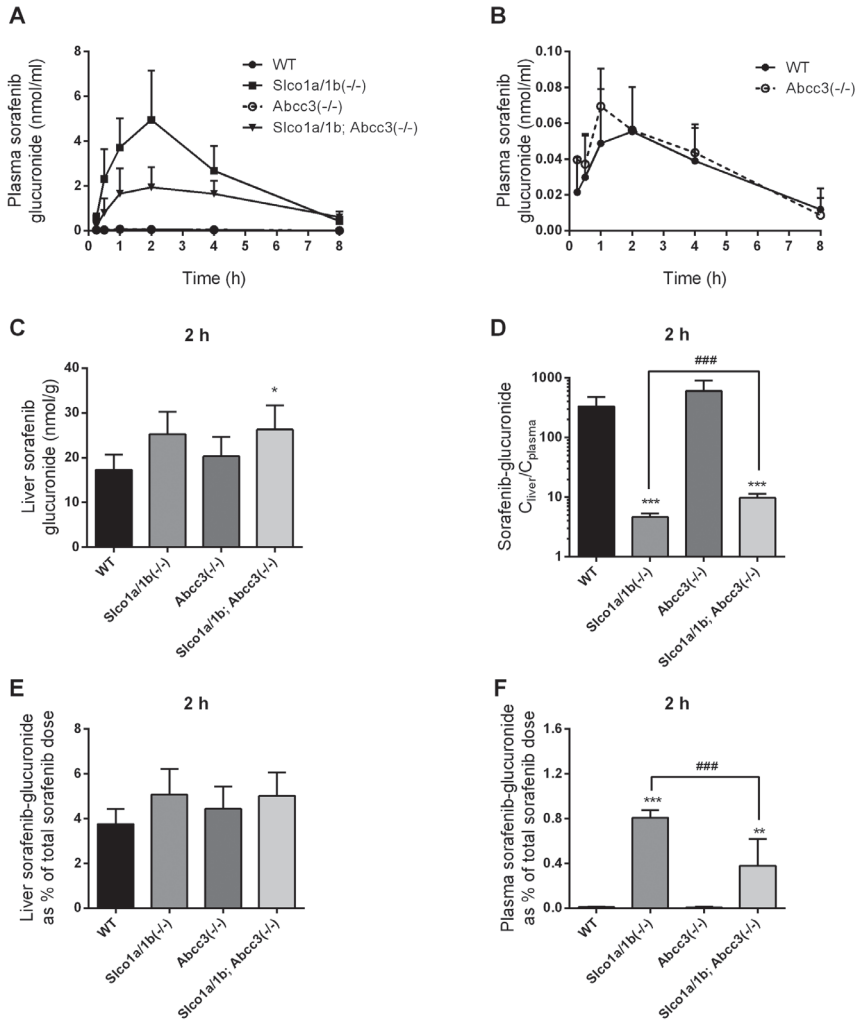


**Figure 3. Plasma and liver levels of sorafenib glucuronide in male WT, Slco1a/1b(-/-), Abcc3(-/-) and Slco1a/1b;Abcc3(-/-) mice after oral administration of 10 mg/kg sorafenib.** Sorafenib glucuronide plasma concentrations as nmol/ml (A and B), liver concentrations as nmol/g (C) and liver-to-plasma ratios (D) are represented in the graphs. Liver (E) and plasma (F) sorafenib glucuronide levels as % of total sorafenib dose are also shown in the figure. Average liver-to-plasma ratios were calculated from individual mouse data. Note the log-scale in the Y axis of the liver-to-plasma graph. Data were log-transformed when necessary and were given as mean ± S.D. One-way ANOVA was applied to calculate the statistical significance, unless stated otherwise. (n = 4-9, *, $P < 0.05$; ***, $P < 0.001$ when compared with WT; ###, $P < 0.001$ when compared with Slco1a/1b(-/-) using Student's-t-test).

glucuronide. In contrast, in single Abcc3(-/-) mice plasma sorafenib glucuronide levels were similar to those in WT mice, indicating that the impact of Abcc3 does not come to the fore in the presence of Slco1a/1b transporters (Figure 3B). Very similar results were obtained in a separate

experiment terminated at 2 h (i.e., at the $T_{max}$ for plasma sorafenib glucuronide), showing 115- and 51-fold increased plasma $AUC_{0-2}$ in Slco1a/1b(-/-) and Slco1a/1b;Abcc3(-/-) mice (7.60 ± 0.88 nmol/ml•h and 3.36 ± 1.19 nmol/ml•h, $P < 0.001$) compared to WT mice, respectively (Supplementary Figure 1A and B). In liver, there was a slight and similar increase in sorafenib glucuronide levels at 2 h ($T_{max}$) in both Slco1a/1b(-/-) (1.46-fold, $P = 0.0617$) and Slco1a/1b;Abcc3(-/-) mice (1.52-fold, $P < 0.05$), but not in Abcc3(-/-) mice compared to the WT strain (Figure 3C). Interestingly, liver-to-plasma ratios of sorafenib glucuronide were highly decreased by 71.9-fold in Slco1a/1b(-/-) and by 34.2-fold in Slco1a/1b;Abcc3(-/-) mice compared to WT, and the difference between these two strains was 2.1-fold ($P < 0.001$) (Figure 3D). To put these results in a quantitative context, the sorafenib glucuronide % of dose in plasma in these strains ranged from 0.01% to 0.8%; whereas the liver accounted for 3.8% to 5.1% of the dose at 2h (Figure 3E and F). These data suggest a major role of Slco1a/1b transporters in hepatic uptake and a clear impact of Abcc3 on sinusoidal extrusion of sorafenib glucuronide. However, there must be other efflux transporter(s) located at the sinusoidal membrane of hepatocytes that can mostly compensate for the loss of Abcc3 in the hepatic elimination of sorafenib glucuronide to the plasma.

**Abcc4 does not contribute noticeably to sorafenib glucuronide elimination from liver**

We next tried to assess whether Abcc4 could be the alternative transporter mediating sinusoidal secretion of sorafenib glucuronide to the systemic circulation, using Abcc4(-/-) and Abcc3;Abcc4(-/-) mice. Plasma $AUC_{0-2}$ of sorafenib glucuronide in Abcc4(-/-) mice was slightly higher than that of Abcc3(-/-) and Abcc3;Abcc4(-/-) mice, but a significant difference was only seen with the WT mice (0.13 ± 0.04 vs. 0.07 ± 0.03 nmol/ml•h, $P < 0.05$) (Figure 4A). Liver levels were similar in all the strains whereas liver-to-plasma ratios in Abcc3(-/-) and Abcc3;Abcc4(-/-) mice appeared higher than those in WT mice, but this didn't reach significance (Figure 4B and C). Abcc4(-/-) liver-to-plasma ratios were not significantly different from those in WT mice, but significantly lower than those in Abcc3(-/-) or Abcc3;Abcc4(-/-) strains (2.3-fold, $P < 0.05$ for both comparisons, Figure 4C). This overall pattern likely again reflects the modest but noticeable impact of Abcc3 (but not Abcc4) on sorafenib-glucuronide liver-to-plasma ratios. These findings suggest that a possible contribution of Abcc4 in sinusoidal extrusion of sorafenib glucuronide is not detectable under these circumstances, in contrast to that for Abcc3. It might be masked by functional compensation via other (non-Abcc3 or -Abcc4) efflux transporter(s) present in the sinusoidal membrane of the hepatocytes.

**Abcc2 has an important role in the hepatic elimination of sorafenib glucuronide**

Following up on, and in line with, previous studies by Vasilyeva *et al*. (in preparation), we found that deletion of Abcc2 in combination with Slco1a/1b in mice led to a very large increase in plasma exposure of sorafenib glucuronide compared to WT, but also compared to Slco1a/1b(-/-) mice (Figure 5A and B). Plasma $AUC_{0-8}$ of sorafenib glucuronide in Slco1a/1b;Abcc2(-/-) mice (255.5 ± 42.9 nmol/ml•h) were 763.5- and 12.7-fold increased compared to that in WT (0.34 ± 0.06 nmol/ml•h, $P < 0.001$) and Slco1a/1b(-/-) (20.1 ± 7.8 nmol/ml•h, $P < 0.001$) strains, respectively (Figure 5A). 2 h after sorafenib administration, liver levels of sorafenib glucuronide were 1.8-fold increased by removal of Abcc2 on Slco1a/1b(-/-) background compared to WT mice ($P < 0.01$, Figure 5C). However, the increase in liver levels (Figure 5C) compared to the increase

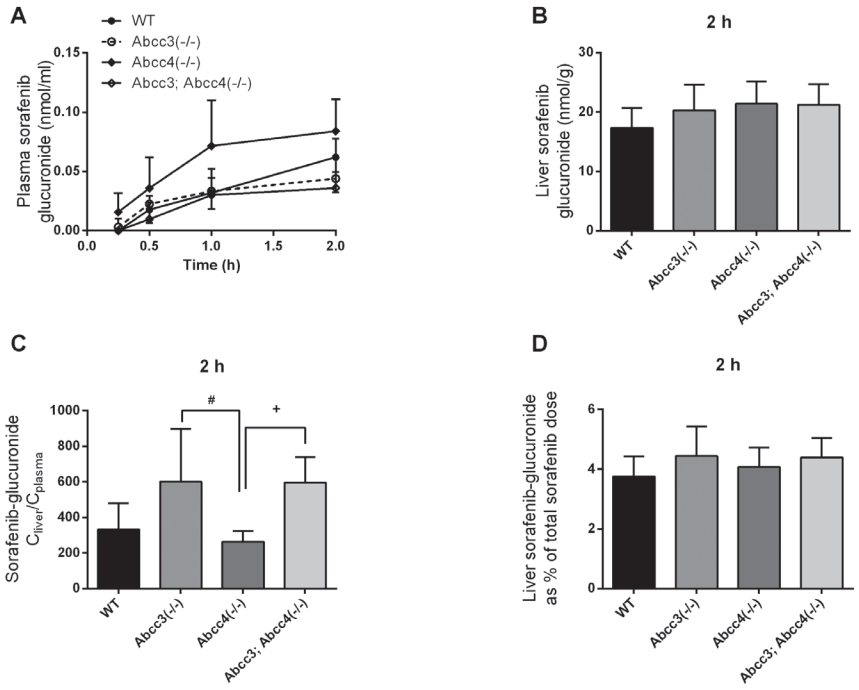


**Figure 4. Plasma and liver levels of sorafenib glucuronide in male WT, Abcc3(-/-), Abcc4(-/-) and Abcc3,Abcc4(-/-) mice after oral administration of 10 mg/kg sorafenib.** Sorafenib glucuronide plasma concentrations as nmol/ml (A), liver concentrations as nmol/g (B), liver-to-plasma ratios (C) and liver levels as % of total sorafenib dose (D) are represented in the graphs. Average liver-to-plasma ratios were calculated from individual mouse data. Data are given as mean ± S.D. One-way ANOVA was applied to calculate the statistical significance, unless stated otherwise. (n = 4-5, #, $P < 0.05$ when compared with Abcc3(-/-) mice and +, $P < 0.05$ when compared with Abcc4(-/-) mice).



in plasma exposure (Figure 5A and B) due to Abcc2 deletion was far smaller in these mice. As a result of the highly increased plasma levels of sorafenib glucuronide, liver-to-plasma ratios were decreased by 6.2-fold by additional removal of Abcc2 on top of the Slco1a/1b knockout ($P < 0.001$, Figure 5D). Of note, the % of sorafenib glucuronide at 2h ranged from 0.01% to 8.5% in plasma and from 3.8% to 14.4% in liver of these strains (Figure 5E and F). These findings suggest an important role for Abcc2 in biliary excretion of sorafenib glucuronide, and that deletion of Abcc2 on top of the Oatp1a/1b transporter deficiency leads to a major increase in the sinusoidal extrusion of this metabolite into the plasma.

On the other hand, we found no significant difference between Slco1a/1b;Abcc2(-/-) and Slco1a/1b;Abcc2;Abcc3(-/-) in plasma exposure of sorafenib glucuronide over 2 h in an independent experiment (Figure 5B), although the % of sorafenib glucuronide dose in plasma compared to the total administered sorafenib dose was increased by 1.4-fold ($P < 0.05$, Figure 5F). These results suggest that the impact of additional deletion of Abcc3 on plasma exposure of sorafenib glucuronide is not substantial, if present. Of note, the role of Abcc3 in

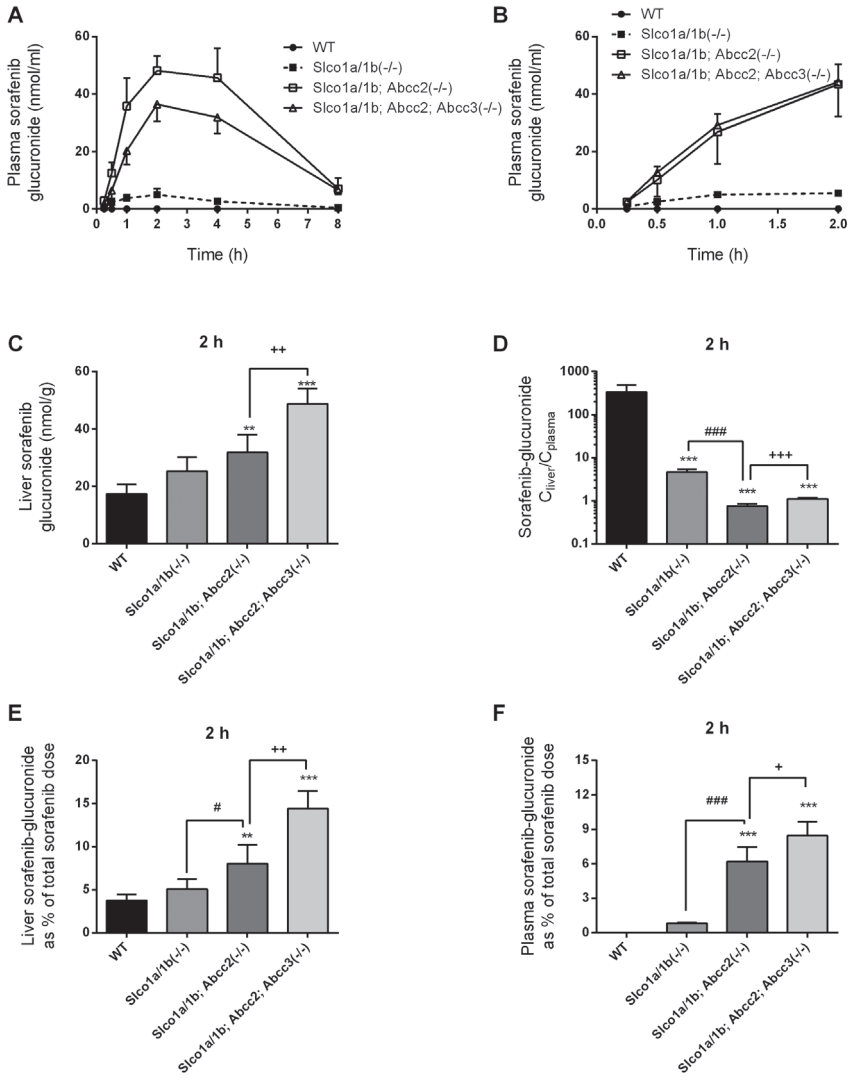


**Figure 5. Plasma and liver levels of sorafenib glucuronide in male WT, Slco1a/1b(-/-), Slco1a/1b;Abcc2(-/-) and Slco1a/1b;Abcc2;Abcc3(-/-) mice after oral administration of 10 mg/kg sorafenib.** Sorafenib glucuronide plasma concentrations as nmol/ml (A and B), liver concentrations as nmol/g (C) and liver-to-plasma ratios (D) are represented in the graphs. Average liver-to-plasma ratios were calculated from individual mouse data. Liver (E) and plasma (F) sorafenib glucuronide levels as % of total sorafenib dose are also shown in the figure. Note the log-scale in the Y axis of the liver-to-plasma graph. Data were log-transformed when necessary and were given as mean ± S.D. One-way ANOVA was applied to calculate the statistical significance, unless stated otherwise. (n = 4-9, *, $P < 0.05$; **, $P < 0.01$; ***, $P < 0.001$ when compared with WT mice; ###, $P < 0.001$ when compared with Slco1a/1b(-/-) mice. ++, $P < 0.01$ and +++, $P < 0.001$ when compared with Slco1a/1b;Abcc2(-/-) mice using Student's-t-test).

plasma distribution of sorafenib glucuronide in the absence of Abcc2 is less clear compared to the findings in the presence of Abcc2 (Figure 3A), which may be due to saturation of Abcc3 at these extremely high plasma concentrations. However, the impact of Abcc3 in liver remained noticeable, with a 1.5-fold increase in both hepatic sorafenib glucuronide concentrations ($P < 0.001$, Figure 5C) and liver-to-plasma ratios ($P < 0.001$, Figure 5D) of Slco1a/1b;Abcc2;Abcc3(-/-) strains compared to Slco1a/1b;Abcc2(-/-) mice. These findings suggest that Abcc3 has a modest, but clear impact on sinusodial secretion of sorafenib glucuronide even at very high plasma sorafenib glucuronide concentrations. This modest effect might be due to the saturation of Abcc3 and/or the existence of alternative sinusoidal sorafenib glucuronide efflux systems operating at the very high sorafenib glucuronide concentrations caused by the impaired biliary excretion via Abcc2.

## DISCUSSION

In this study we provide evidence that a glucuronidated metabolite of an exogenous compound, the anti-cancer drug sorafenib, is subject to the same 'hepatocyte hopping' process described recently for an endogenous glucuronidated Slco1a/1b substrate, bilirubin glucuronide [5, 11, 16]. This process is thought to be especially useful when the canalicular excretion process of glucuronidated substrates in upstream hepatocytes in liver lobules is saturated. Substrates can then be transferred to downstream hepatocytes via Abcc3 and Slco1a/1b to distribute the biliary excretion load over all hepatocytes in the liver lobule and thus provide more flexible detoxification by the liver.

Our results suggest that the plasma and liver disposition of sorafenib glucuronide is controlled by Slco1a/1b uptake transporters, by Abcc2 and Abcc3 and by other sinusoidal efflux transporters that are yet to be identified. Based on our findings, we think that under normal physiologic conditions, a large fraction of sorafenib glucuronide formed in hepatocytes is excreted into bile mainly by Abcc2. Still, a significant fraction, possibly due to partly saturated biliary excretion, is transported back into the blood in part by Abcc3, but also by one or more other transporters. Sorafenib glucuronide that reaches the bloodstream is then efficiently taken up again into downstream hepatocytes by Slco1a/1b activity, affording another possibility to be excreted into the bile.

We have considered the option that the expression of transporters might be substantially altered in the knockout strains and thus alter the disposition of sorafenib glucuronide. This would of course lead to the need of an adapted interpretation of our data. However, our real-time PCR analyses showed that the expression of most transporters did not display substantial changes (Table 1 and 2) in the relevant knockout strains. Therefore, the possibility of major compensatory changes in transporter expression affecting interpretation of results in the knockout strains was all but ruled out in this study.

Zimmerman *et al.* [21] previously showed that hepatic uptake of sorafenib-glucuronide is mediated by the Slco1b2 transporter and also that the majority of sorafenib glucuronide is likely formed in the liver. In line with this earlier study, our results showing a large increase in the plasma sorafenib glucuronide levels in Slco1a/1b(-/-) mice confirm that in these mice hepatocyte reuptake of sorafenib glucuronide was impaired.

**Table 1.** Overview of ΔCt values of the real-time RT-PCR analysis to investigate expression of several endogenous uptake and efflux transporters in livers of male wild-type and various knockout strains (n = 3; each sample was assayed in duplicate). Analysis of the results was done by the comparative Ct method. Quantification of the target cDNAs in all samples was normalized against the endogenous control β-actin ($Ct_{target}$ – $Ct\beta_{-actin}$ = ΔCt). Accordingly, the lower the value, the higher the expression level.

| | ***WT*** | ***Abcc3(-/-)*** | ***Slco1a/1b(-/-)*** | ***Slco1a/1b;Abcc3(-/-)*** |
|---|---|---|---|---|
| *Abcc2* (Abcc2) | -3.30 ± 0.23 | -3.04 ± 0.40 | -2.64 ± 0.05* | -2.43 ± 0.28* |
| *Abcc3* (Abcc3) | -1.82 ± 0.14 | - | -2.68 ± 0.06* | - |
| *Abcc4* (Abcc4) | -8.67 ± 0.35 | -8.17 ± 0.46 | -8.78 ± 0.40 | -8.21 ± 0.49 |
| *Abcg2* (Bcrp1) | -0.31 ± 0.26 | -0.22 ± 0.41 | -0.35 ± 0.05 | -0.14 ± 0.39 |
| *Abcb1a* (Mdr1a) | -5.19 ± 0.33 | -6.63 ± 0.90 | -6.10 ± 0.86 | -6.96 ± 1.28 |
| *Abcb1b* (Mdr1b) | -7.39 ± 0.51 | -6.98 ± 1.05 | -7.95 ± 0.05 | -7.74 ± 0.69 |
| *Slco1a1* (Slco1a1) | -2.10 ± 0.15 | -1.66 ± 0.49 | - | - |
| *Slco1a4* (Slco1a4) | -0.30 ± 0.39 | -0.90 ± 0.65* | - | - |
| *Slco1b2* (Slco1b2) | -4.76 ± 0.16 | -4.38 ± 0.34 | - | - |

**Table 2.** Overview of ΔCt values of the real-time RT-PCR analysis to investigate expression of Abcc2 and Abcc3 efflux transporters in livers of male WT, *Abcc4(-/-)* and *Abcc3;Abcc4(-/-)* strains (n = 3; each sample was assayed in duplicate). Analysis of the results was done by the comparative Ct method. Quantification of the target cDNAs in all samples was normalized against the endogenous control β-actin ($Ct_{target}$ – $Ct\beta_{-actin}$ = ΔCt). Accordingly, the lower the value, the higher the expression level.

| | ***WT*** | ***Abcc4(-/-)*** | ***Abcc3;Abcc4(-/-)*** |
|---|---|---|---|
| *Abcc2* (Abcc2) | -0.75 ± 0.12 | -0.22 ± 0.16** | -0.67 ± 0.33 |
| *Abcc3* (Abcc3) | 3.91 ± 0.47 | 3.39 ± 0.37 | - |

Following up on previous observations by Vasilyeva *et al*. (*in preparation*) suggesting an important role of Abcc2 in biliary excretion of sorafenib glucuronide and hence overall plasma clearance, our results further emphasized that Abcc2 plays an important role in sorafenib glucuronide disposition, even when the hepatic reuptake of this metabolite was impaired due to the absence of Slco1a/1b transporters. The very large increase in plasma and moderate increase in liver levels of sorafenib glucuronide in Slco1a/1b;Abcc2(-/-) and Slco1a/1b;Abcc2;Abcc3(-/-) mice compared to Slco1a/1b(-/-) strains suggest that Abcc2 is an important contributor of the liver clearance of this metabolite by extrusion into the bile. As a result of Abcc2 absence, the biliary excretion of sorafenib glucuronide is disrupted and what is formed in the liver is primarily secreted into the systemic circulation by sinusoidal efflux transporters, including Abcc3.

We think that the impact of Abcc3 on sinusoidal efflux of sorafenib glucuronide can be easily underestimated. First of all, Abcc2, which mediates efficient biliary excretion of sorafenib glucuronide, was still present in the WT and several of the knockout strains (*Slco1a/1b*-, *Abcc3*- and *Slco1a/1b;Abcc3*-null mice) used in this study. One possibility is that, in Abcc2-proficient mice, high-affinity biliary excretion of sorafenib glucuronide might completely

compensate for the loss of Abcc3, thereby preventing any substantial increase in liver levels of sorafenib glucuronide. Indeed, when Abcc2 was absent, plasma sorafenib glucuronide levels were dramatically increased and the impact of Abcc3 became obvious also in the liver levels, suggesting the importance of Abcc3 for sorafenib liver to blood extrusion. Altogether, these findings suggest that, despite not being as important as Abcc2, Abcc3 works with Slco1a/1b to mediate hepatic clearance of sorafenib glucuronide, especially when Abcc2 is absent (or possibly saturated).

In conclusion, our study shows that a sinusoidal liver-to-blood shuttling loop for sorafenib glucuronide is formed by Slco1a/1b, Abcc3 and likely other sinusoidal efflux transporters. These findings contribute to our current knowledge by showing that in addition to endogenous molecules, exogenous compounds that are glucuronidated in the liver can also be subject to the hepatocyte hopping process, depending on the relative affinity of these compounds for the sinusoidal and canalicular efflux and uptake transporters. The existence of the Rotor syndrome shows that hepatocyte hopping for BG also occurs in humans. Given the broad substrate specificity of human OATP1B1, -1B3 and -2B1, as well as ABCC3, we expect that our findings for glucuronidated exogenous sorafenib in mice will very likely apply in humans as well, and encompass many more glucuronidated xenobiotics.





## ACKNOWLEDGEMENTS

We thank Anita van Esch for technical help during experimental phase of this project.

## REFERENCE LIST

1. Hagenbuch B, Meier PJ. Organic anion transporting polypeptides of the OATP/ SLC21 family: phylogenetic classification as OATP/ SLCO superfamily, new nomenclature and molecular/functional properties. Pflüger*s Arch 2004;* 447:653-665.
2. Hagenbuch B, Gui C. Xenobiotic transporters of the human organic anion transporting polypeptides (OATP) family. Xenobio*tica 2008;* 38:778-801.
3. Klaassen CD, Aleksunes LM. Xenobiotic, bile acid, and cholesterol transporters: function and regulation. Pharmac*ol Rev 2010;* 62:1-96.
4. Konig J, Cui Y, Nies AT, Keppler D. Localization and genomic organization of a new hepatocellular organic anion transporting polypeptide. J Biol *Chem 2000;* 275:23161-23168.
5. van de Steeg E, Wagenaar E, van der Kruijssen CM, Burggraaff JE, de Waart DR, Elferink RP et al. *Organ*ic anion transporting polypeptide 1a/1b-knockout mice provide insights into hepatic handling of bilirubin, bile acids, and drugs. J Clin *Invest 2010;* 120:2942-2952.
6. van de Steeg E, van Esch A, Wagenaar E, Kenworthy KE, Schinkel AH. Influence of human OATP1B1, OATP1B3, and OATP1A2 on the pharmacokinetics of methotrexate and paclitaxel in humanized transgenic mice. Clin C*ancer Res 2013;* 19:821-832.
7. Kalliokoski A, Niemi M. Impact of OATP transporters on pharmacokinetics. Br J P*harmacol 2009;* 158:693-705.
8. Konig J, Seithel A, Gradhand U, Fromm MF. Pharmacogenomics of human OATP transporters. Naunyn *Schmiedebergs Arch Pharmacol 2006;* 372:432-443.
9. Takane H, Kawamoto K, Sasaki T, Moriki K, Moriki K, Kitano H et al. *Life*-threatening toxicities in a patient with UGT1A1*6/*28 and SLCO1B1*15/*15 genotypes after irinotecan-based chemotherapy. Cancer *Chemother Pharmacol 2009;* 63:1165-1169.
10. Trevino LR, Shimasaki N, Yang W, Panetta JC, Cheng C, Pei D et al. *Germlin*e genetic variation in an organic anion transporter polypeptide associated with methotrexate pharmacokinetics and clinical effects. J Clin *Oncol 2009;* 27:5972-5978.
11. van de Steeg E, Stranecky V, Hartmannova H, Noskova L, Hrebicek M, Wagenaar E et al.

*Comple*te OATP1B1 and OATP1B3 deficiency causes human Rotor syndrome by interrupting conjugated bilirubin reuptake into the liver. J Clin *Invest 2012;* 122:519-528.

12. Schinkel AH, Jonker JW. Mammalian drug efflux transporters of the ATP binding cassette (ABC) family: an overview. Adv Drug *Deliv Rev 2003;* 55:3-29.
13. Vlaming ML, Lagas JS, Schinkel AH. Physiological and pharmacological roles of ABCG2 (BCRP): recent findings in Abcg2 knockout mice. Adv Drug *Deliv Rev 2009;* 61:14-25.
14. Lagas JS, Vlaming ML, Schinkel AH. Pharmacokinetic assessment of multiple ATP-binding cassette transporters: the power of combination knockout mice. Mol Int*erv 2009;* 9:136-145.
15. Kouzuki H, Suzuki H, Sugiyama Y. Pharmacokinetic study of the hepatobiliary transport of indomethacin. Pharm Res *2000;* 17:432-438.
16. Iusuf D, van de Steeg E, Schinkel AH. Hepatocyte hopping of OATP1B substrates contributes to efficient hepatic detoxification. Clin Ph*armacol Ther 2012;* 92:559-562.
17. Zamek-Gliszczynski MJ, Hoffmaster KA, Nezasa K, Tallman MN, Brouwer KL. Integration of hepatic drug transporters and phase II metabolizing enzymes: mechanisms of hepatic excretion of sulfate, glucuronide, and glutathione metabolites. Eur J P*harm Sci 2006;* 27:447-486.
18. Iusuf D, van de Steeg E, Schinkel AH. Functions of OATP1A and 1B transporters in vivo: insights from mouse models. Trends *Pharmacol Sci 2012;* 33:100-108.
19. van de Steeg E, Stranecky V, Hartmannova H, Noskova L, Hrebicek M, Wagenaar E et al. *Comple*te OATP1B1 and OATP1B3 deficiency causes human Rotor syndrome by interrupting conjugated bilirubin reuptake into the liver. J Clin *Invest 2012;* 122:519-528.
20. Zhou S, Chan E, Duan W, Huang M, Chen YZ. Drug bioactivation, covalent binding to target proteins and toxicity relevance. Drug Me*tab Rev 2005;* 37:41-213.
21. Zimmerman EI, Hu S, Roberts JL, Gibson AA, Orwick SJ, Li L et al. C*ontri*bution of OATP1B1 and OATP1B3 to the disposition of sorafenib and sorafenib-glucuronide. Clin C*ancer Res 2013;* 19:1458-1466.
22. van Waterschoot RA, van Herwaarden AE, Lagas JS, Sparidans RW, Wagenaar E, van der Kruijssen CM et al. *Midazo*lam metabolism in cytochrome P450 3A knockout mice can be attributed to up-regulated CYP2C enzymes. Mol Ph*armacol 2008;* 73:1029-1036.

## SUPPLEMENTARY MATERIAL

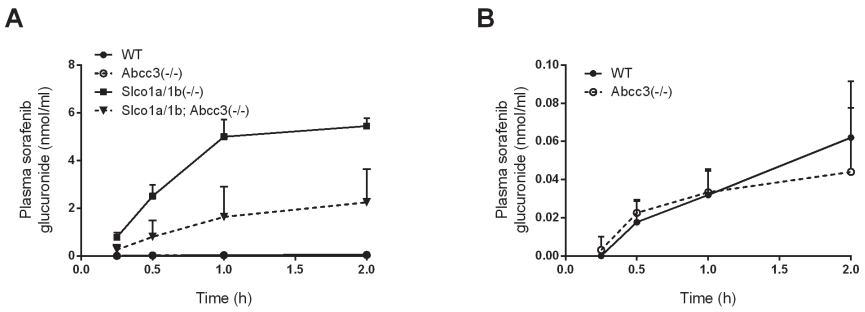


**Supplementary Figure 1. Plasma levels of sorafenib glucuronide in male WT, Slco1a/1b(-/-), Abcc3(-/-) and Slco1a/1b;Abcc3(-/-) mice after oral administration of 10 mg/kg sorafenib over 2 h.** Sorafenib glucuronide plasma concentrations (A and B) are represented in the graphs as nmol/ml. Data are given as mean ± S.D. (n = 4-5).

# CHAPTER 6

## CONCLUSIONS & FUTURE PERSPECTIVES

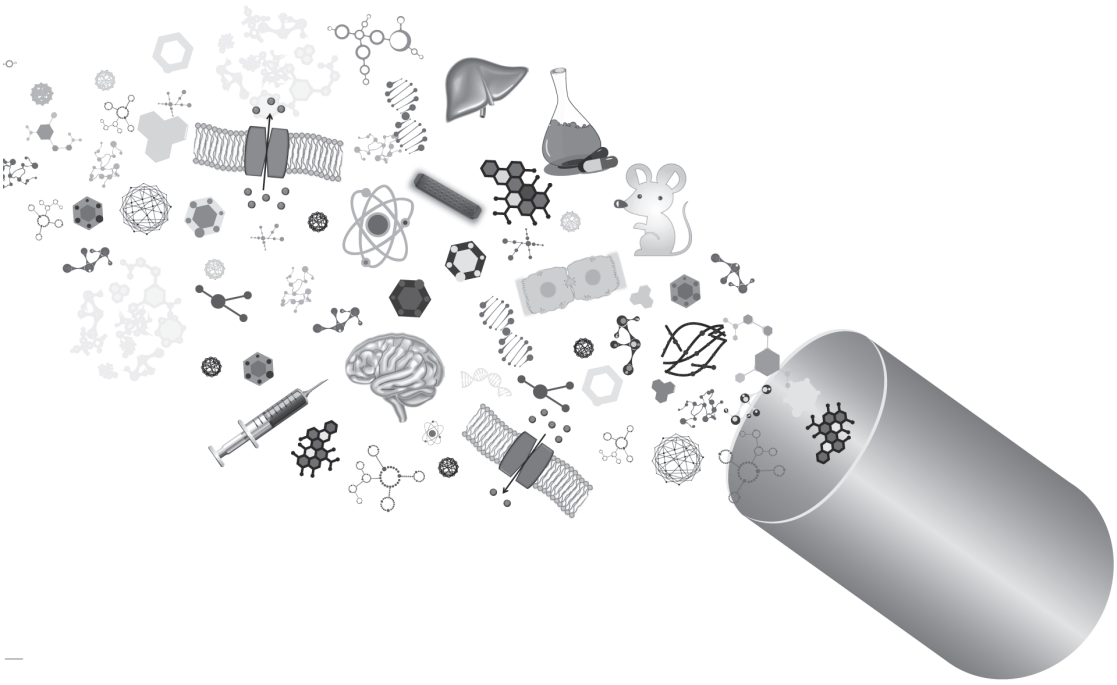

In this thesis, we investigated the pharmacological functions of ABC efflux and OATP uptake transporters *in vitro* using different cellular systems and *in vivo* using several knockout and humanized transgenic mice with specific liver expression of human OATP1A2, OATP1B1 or OATP1B3. Our findings can be divided in three major sections as explained below.

Firstly, we have demonstrated that the ABC transporters Abcb1a/1b and Abcg2 restrict the oral absorption and/or brain disposition of several novel targeted anti-cancer drugs including tyrosine kinase inhibitors (TKIs) and an inhibitor of the poly ADP-ribose polymerase (PARP). Although several studies including ours showed that pharmacological inhibition of these transporters could increase brain accumulation of anti-cancer drugs, whether this will be clinically plausible and effective to treat patients with brain tumors or (micro) metastases remains to be further investigated.

Secondly, we have shown that mouse and human OATP1A/1B transporters can have major roles in the hepatic uptake and/or plasma clearance of a wide range of structurally different compounds. They can also be involved in drug-drug interactions (DDIs) when more than one OATP substrate is administered. There is increasing evidence for a wider pharmacological/clinical relevance of OATPs than anticipated, including our own findings on the surprisingly broad structural diversity of OATP substrates. This simply means that factors altering the activity OATPs, such as pharmacological inhibition (i.e. by DDIs, food-drug interactions or other OATP inhibitors) or genetic polymorphisms in the genes encoding OATP proteins can strongly influence the pharmacokinetics, efficacy and toxicity profile of substrate drugs. Within this thesis, we have also demonstrated that humanized transgenic mouse models are useful tools to assess the importance of the human OATP1B1 and -1B3 in pharmacokinetics and DDIs. We think that these transgenic models have more relevance to the human situation compared to the other available systems such as OATP-expressing cell lines, *in silico* prediction tools and wild-type and knockout mouse strains. Of course, these humanized mouse models can also be used to assess other types of questions (i.e. food-drug interactions, chemical inhibitors and tissue-specific toxicities) involving the human OATP1B transporters.

Characterization of pharmacological functions of human OATPs is also particularly interesting from the perspective of tumor cell uptake as expression of OATP1A/1B transporters has been detected in several types of tumors. Moreover, overexpression of these transporters in cell lines caused increased sensitivity to anti-cancer drug treatments. As we already identified several anti-cancer drugs (methotrexate, paclitaxel, SN-38, docetaxel and doxorubicin) being *in vivo* substrates of one or more of the human OATP1A/1B transporters, and we also expect this list to expand in the near future, it is likely that OATP1A/1B transporters mediate the tumor uptake of many anti-cancer drugs that are substrates, and therefore modulate chemotherapy response. Nevertheless, to establish their exact contribution in this process, systematic assessments should be performed in a number of reliable preclinical and clinical studies.

Lastly, we here validated a broader relevance for a recently described liver detoxification process, 'hepatocyte hopping', using a glucuronidated conjugate of the anti-cancer drug sorafenib. Using various knockout mouse strains, we previously demonstrated that the endogenous substrate bilirubin glucuronide (BG), which can reach high intrahepatic levels, can be secreted into blood via Abcc3 and be reabsorbed into downstream hepatocytes via

Oatp1a/1b transporters. This allows a more flexible, efficient and safe liver detoxification of this metabolite throughout the whole liver lobule, as it will prevent saturation of biliary excretion and toxicity. We have subsequently shown that this is likely to happen in humans as well, as there are people with a full deficiency in the OATP1B1 and OATP1B3 genes who suffer from conjugated hyperbilirubinemia due to interrupted hepatic reuptake of bilirubin glucuronide (a disorder called Rotor syndrome). Our study is therefore particularly relevant as we demonstrate for the first time that an exogenous compound is subject to the same hepatocyte hopping process, suggesting a broader pharmacological relevance of this process also in humans. One could study the involvement of the human OATP transporters by using the humanized transgenic mice as an intermediate step to assess whether a compound is subjected to hepatocyte hopping in human liver as well. Nevertheless, the assessment of the involvement of sinusoidal human efflux transporters in this process will be limited as proper tools are not yet available. Obviously, whether hepatocyte hopping applies to exogenous compounds in humans should eventually be rigorously assessed in the clinic. For that purpose people with polymorphisms or deficiencies in their OATPs or in ABCC3 or other sinusodial efflux transporter genes who are treated with drugs and other compounds that are conjugated in the liver may be studied.

All in all, we have gained important insights into the functions of both ABC and OATP drug transporters using various *in vitro* cellular systems and *in vivo* knockout and transgenic mouse strains, which can be used as a solid translational basis for clinical studies in several cases.

# CHAPTER 7

## SUMMARY

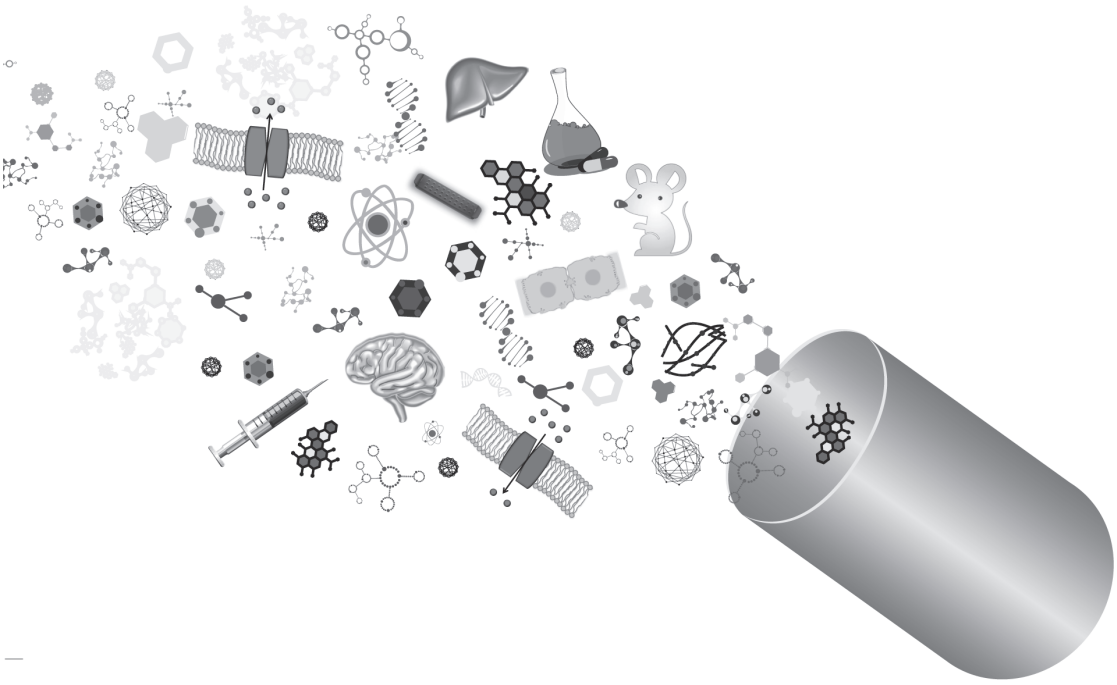

Membrane transporters have major roles in the absorption, disposition, elimination and toxicity of drugs. ATP-binding cassette (ABC) drug efflux and Organic Anion-Transporting Polypeptide (OATP) drug uptake transporters are two major transporter superfamilies that are widely expressed in several pharmacokinetically relevant organs (liver, small intestine, brain, kidney etc.). Members of these transporter families have been shown to be clinically important in drug absorption and disposition. ABC transporters such as P-GP (MDR1, ABCB1) and BCRP (ABCG2) are particularly important in modulating the oral absorption and tissue distribution, whereas OATP transporters such as those of the OATP1A/1B family are important in systemic exposure and liver uptake of a broad range of drugs, including many chemotherapeutics. In this thesis, we have investigated the *in vitro* and *in vivo* pharmacological functions of ABC and OATP transporters for several anti-cancer drugs using various cell systems, and knockout and transgenic mouse models.

In **Chapter 1** of this thesis, we provide an introduction to the ABC and OATP transporters together with their expression, tissue localization and roles in disposition of substrates with a special focus on pharmacological, rather than physiological functions. **Chapter 1.1** gives an overview of new insights into the roles of ABC transporters in drug disposition, especially of chemotherapeutics. Furthermore, we also review new findings from preclinical research aiming to improve the systemic and tissue availability of chemotherapeutics by inhibiting these transporters. **Chapter 1.2** gives an overview of the physiological and pharmacological functions of the mouse and human OATP1A/1B transporters with respect to their tissue localization. The current knowledge on their involvement in the plasma and liver disposition of a broad range of substrates, obtained using the available knockout and humanized transgenic mouse models is also reviewed in this chapter. This includes an efficient liver detoxification process, dubbed "hepatocyte hopping". Furthermore, clinical insights obtained from genetic variants (i.e. increased toxicity upon drug treatment) or full deficiencies (Rotor syndrome; a genetic disorder causing hyperbilirubinemia) of the OATP1A/1B transporters are presented. Lastly, the importance of OATPs with respect to drug-drug interactions (DDIs) and the mouse models to study these interactions are also discussed.

**Chapter 2** focuses on the role of ABC transporters in the oral availability and/or tissue disposition of a number of targeted anti-cancer drugs. In **Chapter 2.1,** we show that Abcb1a/1b (P-gp) and Abcg2 (Bcrp1) restrict the oral availability and brain accumulation of the tyrosine kinase inhibitor (TKI) vemurafenib. We also show that coadministration of elacridar, a dual inhibitor of ABCB1 and ABCG2, improves both the systemic and brain levels of vemurafenib, suggesting a possible route for enhancing efficacy of vemurafenib in cancer patients with brain metastases. **Chapter 2.2** and **2.3** demonstrate the importance of these transporters in the brain accumulation of the two more TKIs, CYT387 and regorafenib. **Chapter 2.4** describes that these transporters are also important in restricting the oral availability and brain accumulation of an inhibitor of the enzyme poly ADP ribose polymerase (*PARP)*, rucaparib.

**Chapter 3** shows that mouse and human OATP1A/1B transporters are important determinants of the plasma clearance and liver uptake of the anti-cancer drug doxorubicin. As the fairly hydrophobic weak base doxorubicin is an atypical OATP1A/1B substrate, this study was particularly important as it adds diversity to the known OATP substrate structures. We believe

that together with a number of other recent studies, this chapter contributed to the perception that the substrate specificity of OATPs is much wider than initially anticipated.

In **chapter 4,** we investigated the involvement of the mouse and human OATP1A/1B transporters in drug-drug interactions (DDIs). Using the antibiotic rifampicin and anti-cancer drug methotrexate, we have shown that transgenic mouse models with liver-specific expression of the human OATP1B1 and -1B3 can be useful as tools to assess and predict clinically relevant DDIs. Using these models, we studied a novel and clinically feasible combination of a hypertension and an anti-cancer drug (telmisartan and methotrexate), and found that there is a low risk at best for possible interactions between these drugs at the OATP level.

In **Chapter 5,** we investigated whether the hepatocyte hopping process also applies to exogenous substrates, such as drug conjugates. Using knockout mice, we showed that Oatp1a/1b uptake and Abcc2 and Abcc3 efflux transporters cooperate at the hepatocyte level to eliminate a glucuronide conjugate of an exogenous compound, the anti-cancer drug sorafenib from the liver, in a safe, efficient and robust way. With this study, we demonstrate for the first time that liver detoxification of an exogenous compound can also be subject to hepatocyte hopping, like that of the previously studied endogenous metabolite, bilirubin glucuronide. These findings are of interest as they suggest a much broader relevance of the hepatocyte hopping process for detoxification of drugs and other exogenous compounds conjugated in the liver.

Taken together, studies presented in this thesis contribute to the current knowledge on the pharmacological functions of ABC efflux and OATP uptake transporters. On the one hand, we have demonstrated that ABCB1 and ABCG2 restrict the oral absorption and brain accumulation of several novel targeted anti-cancer drugs, and that this may be reversed by pharmacological inhibition of these transporters. On the other hand, we have shown that the substrate specificity of OATPs is wider than initially anticipated, and that transgenic mouse models can be used as *in vivo* tools to assess and predict clinically relevant DDIs. Lastly, demonstrating the cooperation between Oatp1a/1b uptake and Abcc3 efflux transporters in liver-to-blood shuttling of sorafenib-glucuronide, we have experimentally shown that hepatocyte hopping applies not only to endogenous, but also exogenous substrates. Considering the findings described in this thesis, we believe that there is still much to be discovered in the field of transporters in terms of pharmacological, but also physiological functions of these and other families of drug transporters.

# APPENDICES &

**NEDERLANDSTALIGE SAMENVATTING**

**LIST OF ABBREVIATIONS**

**CIRRICULUM VITAE**

**ÖZGEÇMIŞ**

**LIST OF PUBLICATIONS**

**ACKNOWLEDGEMENTS**

## NEDERLANDSTALIGE SAMENVATTING

Eiwitten die stoffen over de membraan transporteren ("transmembraan transporteurs") hebben belangrijke functies in de opname, eliminatie en toxiciteit van geneesmiddelen. De ATP-bindings cassette (ABC) geneesmiddel efflux transporteurs, en de "Organic Anion-Transporting Polypeptide" (OATP) geneesmiddel opname transporteurs vormen twee belangrijke superfamilies, die hoog tot expressie komen in verschillende farmacokinetisch relevante organen (bijvoorbeeld lever, dunne darm, hersen en nier). Van leden van deze transporteurfamilies is aangetoond dat ze klinisch van belang zijn in de opname en weefselverdeling van geneesmiddelen. ABC transporteurs zoals P-GP (MDR1, ABCB1) en BCRP (ABCG2) zijn vooral belangrijk in het moduleren van de orale opname en weefselverdeling, terwijl OATP transporteurs zoals die van de OATP1A/1B familie vooral belangrijk zijn voor de systemische blootstelling en leveropname van een breed scala aan geneesmiddelen, waaronder veel chemotherapeutica. In dit proefschrift hebben we de *in vitro* en *in vivo* farmacologische functies onderzocht van ABC en OATP transporteurs voor verscheidene antikankermiddelen, gebruikmakend van diverse celsystemen, en knockout en transgene muizen.

In **Hoofdstuk 1** van dit proefschrift geven we een inleiding over de ABC en OATP transporteurs, met hun expressie, weefselverdeling, en functies in dispositie van substraten, met speciale focus op hun farmacologische functies. **Hoofdstuk 1.1** geeft een overzicht van nieuwe inzichten in de functies van ABC transporteurs in geneesmiddeldispositie, met name die van chemotherapeutica. Verder behandelen we nieuwe bevindingen in preklinisch onderzoek dat erop gericht is om de systemische- en weefselbeschikbaarheid van chemotherapeutica te verbeteren door het remmen van deze transporteurs. **Hoofdstuk 1.2** geeft een overzicht van de fysiologische en farmacologische functies van de muis- en humane OATP1A/1B transporteurs in het licht van hun weefseldistributie. De huidige kennis over hun betrokkenheid bij de plasma- en weefselverdeling van een brede reeks substraten, verkregen met behulp van de beschikbare knockout en gehumaniseerde transgene muismodellen, wordt ook behandeld in dit hoofdstuk. Dit behandelt tevens een efficiënt leverdetoxificatie proces, genaamd "hepatocyte hopping". Verder worden klinische inzichten verkregen met behulp van genetische varianten in de OATP1A/1B transporteurs (bijvoorbeeld toegenomen toxiciteit na geneesmiddelbehandeling) of volledige genetische deficiënties (Rotor syndroom, een genetische afwijking die leidt tot hyperbilirubinemie) gepresenteerd. Tenslotte wordt het belang van OATP's met betrekking tot geneesmiddel-geneesmiddel interacties (GGI), en de muismodellen om deze interacties te bestuderen, besproken.

**Hoofdstuk 2** concentreert zich op de rol van ABC transporteurs in de orale biologische beschikbaarheid en weefselverdeling van een aantal rationeel ontwikkelde antikankermiddelen. In **Hoofdstuk 2.1** laten we zien dat Abcb1a/1b (P-gp) en Abcg2 (Bcrp1) de orale biologische beschikbaarheid en hersenaccumulatie van de tyrosine kinase remmer (TKI) vemurafenib beperken. We tonen verder aan dat gelijktijdige toediening van elacridar, een duale remmer van ABCB1 en ABCG2, zowel de systemische blootstelling als de hersenaccumulatie van vemurafenib verbetert. Dit suggereert een mogelijke benadering voor het verbeteren van de werkzaamheid van vemurafenib in patiënten met hersenmetastasen.

**Hoofstukken 2.2** en **2.3** demonstreren het belang van deze transporteurs bij de hersenaccumulatie van twee andere TKI's, CYT387 en regorafenib. **Hoofdstuk 2.4** beschrijft dat deze transporteurs ook van belang zijn voor de orale beschikbaarheid en de hersenaccumulatie van een remmer van het "poly ADP ribose polymerase" (PARP), rucaparib.

**Hoofdstuk 3** laat zien dat de muis en humane OATP1A/1B transporteurs belangrijke determinanten zijn van de plasmaklaring en leveropname van het antikanker geneesmiddel doxorubicine. Aangezien de tamelijk hydrofobe zwakke base doxorubicine geen typisch OATP1A/1B substraat is, is het belang van deze studie vooral dat deze de al bekende brede diversiteit van OATP substraten nog verder uitbreidt. Wij denken dat, tezamen met een aantal andere recente studies, dit hoofdstuk bijdraagt aan het inzicht dat de substraatspecificiteit van OATP's veel breder is dan oorspronkelijk is onderkend.

In **Hoofdstuk 4** hebben we de betrokkenheid onderzocht van de muis en humane OATP1A/1B transporteurs aan geneesmiddel-geneesmiddel interacties (GGIs). Gebruikmakend van het antibioticum rifampicine en het antikankermiddel methotrexaat hebben we laten zien dat transgene muismodellen met leverspecifieke expressie van het humane OATP1B1 en -1B3 bruikbaar kunnen zijn als hulpmiddelen om klinisch relevante GGI's te beoordelen en voorspellen. Gebruikmakend van deze modellen hebben we een nieuwe en klinisch realistische combinatie van een bloeddrukverlagend- en een antikanker-middel bestudeerd (telmisartan en methotrexaat), en gevonden dat er op z'n hoogst een gering risico is voor interacties tussen deze middelen op het niveau van OATP's.

In **Hoofdstuk 5** onderzochten we of het zogenaamde "hepatocyte hopping" proces ook van toepassing is op exogene substraten, zoals geneesmiddel conjugaten. Met behulp van knockout muizen hebben we laten zien dat de Oatp1a/1b opname transporteurs en de Abcc2 en Abcc3 efflux transporteurs samenwerken op het niveau van de hepatociet om het glucuronide conjugaat van een exogene stof, het antikankermiddel sorafenib, te elimineren uit de lever op een veilige, efficiënte en betrouwbare manier. Met deze studie laten we voor het eerst zien dat de leverontgifting van een exogene stof ook onderhevig kan zijn aan het "hepatocyte hopping" proces, net zoals dat van de eerder bestudeerde endogene metaboliet bilirubine glucuronide. Deze bevindingen zijn interessant omdat ze een veel breder belang illustreren van het "hepatocyte hopping" proces voor de ontgifting van geneesmiddelen en andere exogene stoffen die in de lever geconjugeerd worden.

Alles bij elkaar dragen de studies beschreven in dit proefschrift bij aan de huidige kennis over de farmacologische functies van ABC efflux en OATP opname transporteurs. Aan de ene kant hebben we aangetoond dat ABCB1 en ABCG2 de orale absorptie en de hersenaccumulatie van verschillende nieuwe, rationeel ontwikkelde antikankermiddelen beperken, en dat dit proces omgekeerd kan worden door farmacologische remming van deze transporteurs. Aan de andere kant hebben we laten zien dat de substraat specificiteit van OATP's breder is dan oorspronkelijk voorzien, en dat transgene muismodellen gebruikt kunnen worden als *in vivo* hulpmiddelen om klinisch relevante geneesmiddel-geneesmiddel interacties te beoordelen en voorspellen. Tenslotte, door het aantonen van de samenwerking tussen Oatp1a/1b opname transporteurs en de Abcc3 efflux transporteur in het "shuttlen" van lever naar bloed en terug van sorafenib-glucuronide, hebben we experimenteel aangetoond dat "hepatocyte hopping"

niet alleen relevant is voor endogene, maar ook voor exogene substraten. De bevindingen in dit proefschrift in aanschouw genomen, denken we dat er nog veel te ontdekken valt over de farmacologische, maar ook de fysiologische functies van deze en andere families van geneesmiddel transporteurs.

## ABBREVIATIONS

| | |
|---|---|
| ABC | ATP-binding cassette |
| ANOVA | Analysis of variance |
| AUC | Area under the plasma concentration-time curve |
| BBB | Blood-brain barrier |
| BG | Bilirubin glucuronide |
| BCRP | Breast cancer resistance protein |
| BTB | Blood-testis barrier |
| Cmax | Maximum drug concentration in plasma |
| DDI | Drug-drug interaction |
| $E_2$17B-G | Estradiol 17β-D-glucuronide |
| EGFR | Epidermal growth factor receptor |
| FGF | Fibroblast growth factor |
| HEK | Human embryonic kidney |
| IC50 | The half maximal inhibitory concentration required for inhibiting biological or biochemical function |
| i.v. | Intravenous |
| JAK | Janus kinase |
| LLQ | Lower level of quantitation |
| LOD | Lower level of detection |
| MDCK | Madin-Darby canine kidney |
| MDR | Multidrug resistance |
| MDR1 | Multidrug resistance protein 1 |
| mTOR | Mammalian target of rapamycin |
| MTX | Methotrexate |
| 7-OH-MTX | 7-hydroxymethotrexate |
| OATP | Organic anion-transporting polypeptide |
| PDGF | Platelet-derived growth factor |
| P-gp | P-glycoprotein |
| SD | Standard deviation |
| *SLCO/Slco* | Organic anion-transporting polypeptide encoding gene name |
| Tmax | The time after administration of a drug when the maximum plasma concentration is reached |
| VEGF | Vascular endothelial growth factor |
| WT | Wild-type |

## CIRRICULUM VITAE

Selvi Durmus Erim was born on September 6th, 1985 in Ankara, Turkey. After obtaining her high school degree in 2003, she started her bachelor studies in Molecular Biology and Genetics at Istanbul University, Turkey. In 2005, she attended the Erasmus ex-change studentship program and studied at the University of Groningen (the Netherlands) for a year. Right after graduating from her bachelor in 2007, she joined the Topmaster program "Medical and Pharmaceutical Drug Innovation' at the Medical Faculty of University of Groningen. During this master's program, she completed two internships. During her first internship in the laboratory of Prof. Dr. Gerald de Haan, she investigated the feasibility of a retroviral barcoding system to track the progeny of hematopoietic stem cells under the supervision of Dr. Leonid V. Bystrykh and Dr. Brad Dykstra. She has completed her second internship in the laboratory of Dr. Jan-Willem Kok, where she assessed the role of cytoskeleton-lipid raft associations in modulating the localization and activity of ABC transporters under his direct supervision. In 2009, Selvi received her MSc degree (*cum laude*) and soon after she started her PhD studies in the group of Dr. Alfred H. Schinkel at the Netherlands Cancer Institute (the Netherlands). During her PhD, she studied pharmacological functions of ABC efflux and OATP uptake transporters in the disposition of anti-cancer drugs *in vitro* and *in vivo*. These projects were conducted in collaboration with the research laboratory of Prof. Dr. Jos H. Beijnen at the Netherlands Cancer Institute/Slotervaart Hospital and Utrecht University (the Netherlands). The results obtained during her PhD study are described in this thesis.

## ÖZGEÇMİŞ

Selvi Durmuş Erim, 6 Eylül 1985 tarihinde Ankara'da doğdu. 2003 yılında Gölbaşı Anadolu Lisesi'nden mezun olduktan sonra, lisans öğrenimine İstanbul Üniversitesi, Moleküler Biyoloji ve Genetik bölümü'nde başladı. 2005 yılında, Erasmus öğrenci değişim programına katılarak bir yıl süre ile Hollanda'da bulunan Groningen Üniversitesi'nde eğitim aldı. 2007 yılında mezun olduktan sonra, Groningen Üniversitesi Tıp Fakültesi tarafından "Medical and Pharmaceutical Drug Innovation" adli yüksek lisans programına katılmak için burs kazandı. Yüksek lisans eğitimi süresince üniversite hastanesinde iki araştırma projesinde rol aldı. İlk projesini Prof. Dr. Gerald de Haan'ın laboratuvarında yürüttü. Burada, Dr. Leonid V. Bystrykh and Dr. Brad Dykstra'nın danışmanlığında hematopoetik kök hücre ve progenitörlerinin retroviral barkod sistemi ile takip edilmesi üzerinde çalıştı. Dr. Jan-Willem Kok'un laboratuvarında ve danışmanlığında yürüttüğü ikinci projesinde ise nöroblastoma hücrelerinde lipid raft alanlarının ABC Tasiyici proteinleri ve hücre iskeleti ile karşılıklı etkileşimleri üzerinde çalıştı. 2009 yılında yüksek lisansını onur derecesi ile bitirdikten hemen sonra, Hollanda Kanser Enstitüsü, Dr. Alfred H. Schinkel'in laboratuvarında doktora eğitimine başladı. Doktora eğitimi süresince ABC ve OATP ilaç taşıyıcı proteinlerinin anti-kanser ilaçların dağılımındaki farmakolojik etkileri üzerinde birçok proje yürüttü. Bu projeler Hollanda Kanser Enstitüsü/Slotervaart Hastanesi ve Utrecht Üniversitesi, Prof. Dr. Jos H. Beijnen'in araştırma laboratuvarı ile işbirliği içinde yürütülmüştür ve elde edilen sonuçlar bu tezde yer almaktadır.

## LIST OF PUBLICATIONS

1. **Durmus S**, Hendrikx JJ, Schinkel AH. ABC transporters and cancer: Chemotherapeutic drug disposition. *To be submitted*
2. **Durmus S***, Vasilyeva A*, Li L, Wagenaar E, Baker S, Sparreboom A, Schinkel AH. Slco1a/1b and Abcc3 contribute to hepatocyte hopping of sorafenib glucuronide. * contributed equally. *To be submitted*
3. **Durmus S**, Lozano-Mena G, van Esch A, Wagenaar E, van Tellingen O, Schinkel AH. Preclinical mouse models to study human OATP1B1- and OATP1B3-mediated drug-drug interactions in vivo. *To be submitted*
4. **Durmus S***, Kort A*, Sparidans RW, Wagenaar E, Beijnen JH, Schinkel AH. Brain and testis accumulation of regorafenib is restricted by breast cancer resistance protein (BCRP/ABCG2) and P-glycoprotein (P-GP/ABCB1). * contributed equally. *To be submitted*
5. **Durmus S**, Sparidans RW, van Esch A, Wagenaar E, Beijnen JH, Schinkel AH. Breast Cancer Resistance Protein (BCRP/ABCG2) and P-glycoprotein (P-GP/ABCB1) Restrict Oral Availability and Brain Accumulation of the PARP Inhibitor Rucaparib (AG-014699). Pharm Res. 2014 Jun 25. [Epub ahead of print]
6. Tang SC, Sparidans RW, Cheung KL, Fukami T, **Durmus S**, Wagenaar E, Yokoi T, van Vlijmen BJ, Beijnen JH, Schinkel AH. P-Glycoprotein, CYP3A, and Plasma Carboxylesterase Determine Brain and Blood Disposition of the mTOR Inhibitor Everolimus (Afinitor) in Mice. Clin Cancer Res. 2014 Jun 15;20(12):3133-45.
7. Luethi D, **Durmus S**, Schinkel AH, Schellens JH, Beijnen JH, Sparidans RW. Liquid chromatography-tandem mass spectrometric assay for the multikinase inhibitor regorafenib in plasma. Biomed Chromatogr. 2014 Mar 12. [Epub ahead of print]
8. **Durmus S**, Naik J, Buil L, Wagenaar E, van Tellingen O, Schinkel AH. In vivo disposition of doxorubicin is affected by mouse Oatp1a/1b and human OATP1A/1B transporters. Int J Cancer. 2014 Feb 19. [Epub ahead of print]
9. Sparidans RW, **Durmus S**, Schinkel AH, Schellens JH, Beijnen JH. Liquid chromatography-tandem mass spectrometric assay for the PARP inhibitor rucaparib in plasma. J Pharm Biomed Anal. 2014 Jan;88:626-9.
10. Luethi D, **Durmus S**, Schinkel AH, Schellens JH, Beijnen JH, Sparidans RW. Liquid chromatography-tandem mass spectrometry assay for the EGFR inhibitor pelitinib in plasma. J Chromatogr B Analyt Technol Biomed Life Sci. 2013 Sep 1;934:22-5.
11. **Durmus S**, Xu N, Sparidans RW, Wagenaar E, Beijnen JH, Schinkel AH. P-glycoprotein (MDR1/ABCB1) and breast cancer resistance protein (BCRP/ABCG2) restrict brain accumulation of the JAK1/2 inhibitor, CYT387. Pharmacol Res. 2013 Oct;76:9-16.

12. Sparidans RW, **Durmus S**, Schinkel AH, Schellens JH, Beijnen JH. Liquid chromatography-tandem mass spectrometric assay for the mutated BRAF inhibitor dabrafenib in mouse plasma. J Chromatogr B Analyt Technol Biomed Life Sci. 2013 Apr 15;925:124-8.

13. **Durmus S**, Sparidans RW, Wagenaar E, Beijnen JH, Schinkel AH. Oral availability and brain penetration of the B-RAFV600E inhibitor vemurafenib can be enhanced by the P-GLYCOprotein (ABCB1) and breast cancer resistance protein (ABCG2) inhibitor elacridar. Mol Pharm. 2012 Nov 5;9(11):3236-45.

14. Sparidans RW, **Durmus S**, Xu N, Schinkel AH, Schellens JH, Beijnen JH. Liquid chromatography-tandem mass spectrometric assay for the VEGFR inhibitor cediranib and its primary human metabolite cediranib-$N^+$-glucuronide in plasma. J Chromatogr B Analyt Technol Biomed Life Sci. 2012 May 1;895-896:169-73.

15. Sparidans RW, **Durmus S**, Xu N, Schinkel AH, Schellens JH, Beijnen JH. Liquid chromatography-tandem mass spectrometric assay for the JAK2 inhibitor CYT387 in plasma. J Chromatogr B Analyt Technol Biomed Life Sci. 2012 May 1;895-896:174-7.

16. Sparidans RW, **Durmus S**, Schinkel AH, Schellens JH, Beijnen JH. Liquid chromatography-tandem mass spectrometric assay for the mutated BRAF inhibitor vemurafenib in human and mouse plasma. J Chromatogr B Analyt Technol Biomed Life Sci. 2012 Mar 15;889-890:144-7.

17. Slezak-Prochazka I, **Durmus S**, Kroesen BJ, van den Berg A. MicroRNAs, macrocontrol: regulation of miRNA processing. RNA. 2010 Jun;16(6):1087-95.

## ACKNOWLEDGEMENTS

Here comes the most emotional part of my thesis. I want to say that I am very happy to be at this stage; almost defending my PhD! I guess this is the most visited section of this book. No doubt this attention is well deserved as I would not be having these pages without the ones mentioned here.

As a start, I would like to express my greatest appreciation to my co-promoter and daily supervisor, **Alfred**. I have learned a lot from you that have contributed to my scientific career, but also to my personality. After all these years, I became much more organized, responsible and respectful. I am not sure whether it is possible to get another supervisor/colleague who can be as good as you; I just hope it is. You have such an elegant balance of giving your students independence, yet being there whenever support is needed, and letting them grow in their career confidently. Like all others, I have benefitted this style of yours a lot and tried to learn how you do this, but I am not sure of my success in the latter one...It seems to me some traits are just not easy to learn. Thank you very much for all of your contributions and giving me chance to work in your group.

**Jos**, being my promoter, you have been my example for how much efficient a person can be... Although we have met occasionally, I felt your encouragement continuously via your emails. I should say I enjoyed your short, yet positive reactions that motivated me for diving in a new project after each publication.

Dear **Piet**, I have always been amazed by the lively atmosphere you provided to our department, your kindness and great experience. I am very happy that you have attended to most of my presentations and gave challenging critics that kept me thinking about my work continuously. I wish I could have learned from you a lot more. I hope other people do this more efficiently than me.

**Olaf**, although your name is not on my promoter list, your contributions to my PhD projects cannot be underestimated. I learned from you how good a collaborator could be... Thank you for being very generous all the time and for letting us benefit from your lab, high-tech instruments and your instructive supervision.

**Rolf**, you have been a super-efficient collaborator. Thanks to sharing several projects, we could generate a mass amount of interesting data within those few years. Your short and to-the-point emails have helped me to learn how to keep focused and be fast.

Special thanks to my dear paranymphs, **Anita** and **Stephanie**. I am very glad that you will be my special angels on the day of defense, being with me to enjoy those special moments. Thanks helping me out during the preparation of this thesis. Since you two are around, I have been enjoying the funny jokes that you keep making and feeling less stressed. Thank you very much for the 'gezellig' atmosphere in the office that was often couple with chocolate J Anita, besides your admirable enthusiasm and supportive friendship, you have such a great talent in baking cakes with a wide variety, which we surely enjoyed eating. Stephanie, thank you for being amusing and introducing us to the world of the nerds and weekly spams to keep our minds positive. Your journey of PhD had just started, but I have the impression that you will manage it well with your hardworking attitude.

**Dilek** and **Seng**, my mates for the most of my PhD, it was a lot of fun to have you as friends, but also as mentors many times. Looking back, we have accumulated lots of vivid memories together which I will mention only a part due to space problem. I have enjoyed the PhD retreats in Texel and in Glasgow, parties and dinners we had together, our visit to Birk in Basel and our banters during the long hours of computer work in the office. I am grateful for your continuous support and explanations to my countless questions at work. **Dilek,** you have been social and travel guru of our group. I was always amazed by your talent on getting aware of every*thing* what was happening around. Thank you for being a helpful colleague, calming me down when I was stressed and our personal talks. I wish you a great life with your family. **Seng,** it didn't take long to realize how good hearted you are. Thank you for being not only a great colleague, but also such a good friend outside the work. I am grateful for your patience in answering my questions, listening to my frustrations and happy stories all those years, inviting us for nice dinners and being a great host in Malaysia. I wish you a great life with Zheng, and am looking forward to keeping our friendship in the future, who knows maybe between different continents.

**Els**, thank you very much for your invaluable support during my presence, providing me with mice whenever I needed and being open of what you think. I always felt that I could count on you, no matter what kind of matter it was. Without you, things would have been differently, and I would not be able to handle those large-scale experiments. Thank you for saving my Sunday's during the long-term in vivo experiments which helped me to stay fresh in mind and motivated. Also, I always felt grateful to you for listening to my problems and trying to help me in my difficult moments outside of work. Thanks for spoiling us with stroopwafels and making efforts to keep us healthy during winter with all kinds of fruits.

**Anita (van Esch),** thank you for making things easier in the lab and office by having a proper working system and perfect memory. You have been a great help in a few of my projects in the last year of your stay at NKI. Your early start of the day helped me a lot as you could prepare mice and other things for the experiments, so we could proceed quickly. You reminded me the motto of 'Impossible is possible' by managing to have large family and work. I wish you a happy family and job life in the future.

Special thanks to **Jyoti, Ning** and **Gloria** whom I have worked together throughout my PhD and managed to have publishable stories. **Jyoti**, it was nice to work with such a hardworking and positive student like you. You were more than a student to me after your long internship, we became friends. I am happy that you have started your PhD in the end. **Ning**, no doubt that your stay in our group has brought another color to our life. Thank you teaching us how to make dumplings and sushi, and also sharing your stories from China, but also from many cities in Europe that you managed to travel in short time. **Gloria**, you have been a great match, as a project partner, but also as a friend. Despite your short stay, you managed to contribute a lot to the project you were involved in. I enjoyed your positive and supportive personality a lot. I wish you stayed longer, so we could share more time.

I would like to thank to my other group members, **Jeroen**, **Birk** and **Luan**. **Jeroen**, you are such an efficient, focused and kind colleague. I am happy that we could collaborate on a review manuscript to get a feeling of how good you are on planning. **Birk**, it was nice to work together

in my first year. You are a very good colleague and also a great host! Thank you very much for the nice moments we have shared in Amsterdam and during our visit to you in Basel. Thanks to **Evita**, **Marijn** and **Robert** for your friendly and collaborative attitude towards me.

**Lin**, I am happy to have your and Ester's friendship. I should say I really enjoyed being your paranymph in your graduation, which was a unique experience. In addition to our good times in Amsterdam, you have been a great host to us in Singapore. Thank you for insightful discussions about science and careers, showing us around and making us feeling at home at the other side of the world. Till next time, maybe in another country!

**Levi**, you have been a great person to work with in the lab, helping us whenever we needed, and to share the joy of preparing a nice day for Lin. **Mark**, although we could not work with you, I felt positive whenever I saw or talk to you. **Margaritha**, thanks for the helpful attitude for the few times we worked.

Dear **Koen** and **Sven**, thanks for the suggestions you gave to my studies from time to time. **Charlotte**, sharing office with you for about two years have thought me a lot about French culture and your handicraft talents. You are such a lovely, responsible and thoughtful colleague who I enjoyed talking a lot. I hope you will find a niche in science where you are happiest in the near future.

Dear **Alex** and **Sharyn**, thank you for the successful collaboration, warm interaction during your visit to NKI and friendly emails.

**Henri,** thank you very much for arranging many things very efficiently. **Tom**, thank you for the great helps in organizing things sending away packages immediately and being a friendly colleague.

**Sedef**, you are a great friend and a colleague. We have shared a lot through the PhD journey of us. Thank you very much for being there when I needed to talk, connecting me to many other Turkish friends and of course supplying us with Nespresso. **Judith**, **Patricia**, **Johanna** and **Gozde**, thank you for your warm interaction from the moment we have met. It is lots of fun and very comfortable to have colleagues like you around.

**Marijn**, **Krijn** and **Brigitte**, it hasn't been long that you have come to our office, but surely you brought colors into the environment. **Marijn** and **Brigitte**, thank you for your care and advices on how to deal with the up and downs of the thesis production. Special thanks to **Sunny, Asli, Ariena, Wendy, Guotai, Janneke, Robert, Petra, Marcel, Ewa, Banu, Zeliha, Inge, Vera, Andreas, Zheng**, **Cesare**, **Jelle, Jorma** and **Marta**, and all other members of the old P2, H5 and other floors for the nice atmosphere you provided. **Romy**, thank you very much for your efficiency in arranging any type of requests that I have come to you.

Thanks to all of the people, **Martin, Sjoerd, Ji-Ying**, **Maaike, Roel, Marco, Jan, Adrie, Marissa, Yvonne, Klaas, Juriaan, Desiree, Sido, Natalie, Bjorn, Tanja** and others who have been involved in planning, managing and executing my *in vivo* experiments and taking care of our mice and in the animal facility... **Martin and Sjoerd,** special thanks to you for your important contributions in reviewing hundreds of pathology slides and your instructive discussions.

**Baukje, Nienke** and **Lieke**... As your names come together with a nice rhyme, our friendship had a beautiful connection. I have enjoyed very much to grow with you during last seven years... Thank you for the nice time and dinners, listening to my stories, being interested in my culture

and teaching me yours, being there in all of many special moments... I am looking forward to keeping in touch. Special thanks to my masters superviors **Lenya, Brad** and **Jan-Willem**, MPDI buddies and other Groningen friends **Balaji, Christiaan, Maroleijn, Matthieu, Marta, Anil, Marta, Alice, Peter, Loes** and **Luigi** for making life a lot nicer during my stay in Groningen.

**Secil**, you have been a great housemate, close friend and a sister to me since then. Thank you very much for your endless support, understanding and patience which resulted in our home to be a peaceful nest for us. **Chris**, I am happy to have met you and enjoyed your presence every time. **Gozde and Yorgos**, thank you for your vibrant, sharing and entertaining friendship during our stay in the Netherlands. **Cigdem**, you have been there whenever I needed a friend. Thank you very much for sharing lots of time together. My other friends, **Elena, Beatriz, Carlos, Esengul, Funda, Erdinc** abi, **Buket, Gurbet, Fatih, Fatma and Tugba** thank you very much for your good friendships and being always there independent of the distance we have. Also, thanks to the many others that I could not mention here...

**Engin** ve **Avni** hocalarım başta olmak üzere değerli hocalarım, bana olan güveniniz, verdiğiniz yüksek motivasyon ve beraber çalışma ortamlarınız için çok teşekkür ediyorum. Engin hocam, beraber yapacağımız projeleri sabırsızlıkla bekliyorum. Bilime beraber katkı sağlamak benim için gurur kaynağı olacak.

Sevgili **anneciğim** ve **babacığım**, bana verdiğiniz limitsiz sevginiz, güveniniz ve koşulsuz desteğiniz için edebileceğim teşekkürler yetmez. Bir anne babanın yaşadığı zorlukları, duyduğu özlem ve endişeyi hissettirmeden, ne kadar destekleyici olabileceğini gösterdiniz bana. Mutluluğum mutluluğunuz, derdim derdiniz, hastalığım hastalığınız oldu, bu yüzden başarım da başarınızdır. **Kardeşim**, canımdan parça, her ne kadar bütün hayatın boyunca önüne gelen zor bir örnek olsam da, sevgini ve başarımdan duyduğun mutluluğunu ve destegini her zaman hissettim. Hayatıma yakın zamanda giren yeni **ailem**, o güzel kapleriniz, iyi niyetiniz, bana hissettirdiğiniz sıcaklığınız ve sevginiz için çok teşekkür ederim. **Nermin**, sayende ne kız kardeşin, ne de gerçek dostun eksikliğini hissettim. Hayatımdaki önemli hiçbir anda yokluğunu hatırlamıyorum, hatta varlığın olabilecek en fazla şekilde oldu. **Yeter**, **Yasemin** ve diğer bütün aile üyelerim sizlerle olan hatıralarım yüzüme hep tebessüm getirdi. Güzel varlığınız için hepinize teşekkür ederim.

Sevgilim, hayat arkadaşım, diğer yarım **Fatih**. Bu mezuniyet sadece benim değil, bizim mezuniyetimiz. Bunca yıldır verdiğin sınırsız desteğin, zor günlerimde ve yoğun çalışma tempomda hep yanımda olduğun, bitmeyen sevgin ve anlayışın için ne kadar teşekkür etsem de yetmiyor; bu kelimeler beni bile tatmin etmiyor... Paylaştığımız bu özel hayatın hep devam etmesi, güçlü sevgi bağımızın hiç kopmaması ve o hep hayalini kurduğumuz sade ve anlamlı hayatımızı beraber yaşayabilmek dileğiyle...

*Selvi*